UNIVERSITY OF SOUTHAMPTON

FACULTY OF MEDICINE

Academic Unit of Clinical and Experimental Sciences

The Potential Health Effects of Transition Metals in Particulate Air Pollution

by

Matthew Loxham

Thesis for the degree of Doctor of Philosophy

October 2013

UNIVERSITY OF SOUTHAMPTON

ABSTRACT

FACULTY OF MEDICINE

Respiratory Toxicology

Thesis for the degree of Doctor of Philosophy

THE POTENTIAL HEALTH EFFECTS OF TRANSITION METALS IN PARTICULATE AIR POLLUTION

Matthew Loxham

Background: Inhaled air contains myriad potential toxicants, which vary by source and site. These may include particulate matter (PM) containing transition metals, polyaromatic hydrocarbons and soot, aeroallergens, and pathogens. Different toxicants exert their deleterious effects *via* a variety of mechanisms, and may also differentially affect individuals depending on other factors such as the presence of disease.

Methods: Size-fractionated airborne particulate matter (10-2.5 μm, <2.5 μm, <0.18 μm) was collected at a busy mainline underground railway station. PM composition was analysed by inductively-coupled plasma mass spectrometry alongside comparator PM samples from a woodstove, roadwear simulator, and road tunnel. Underground railway PM-mediated generation of reactive oxygen species (ROS) was measured using dichlorofluorescein. Primary bronchial epithelial cells (PBECs) were cultured as monolayers and differentiated air-liquid interface (ALI) cultures before exposure to underground railway PM for 24 h. IL-8 release, barrier integrity, and antioxidant gene expression were assayed. Intracellular PM was studied by transmission EM. As a separate PM type, the effects of the allergenic fungus *Alternaria alternata* on PBECs were similarly examined, and interactions with underground railway PM were studied.

Results: Underground PM was metal-rich, especially iron, and generated ROS in a concentration-, size-, and iron-dependent manner. PBEC monolayer cultures showed a moderate PM concentration-dependent increase in IL-8 release without LDH release, but this was absent in ALI cultures. There was observable intracellular PM 24 h post-challenge in ALI cultures, and an upregulation of antioxidant genes (HO-1, NQO1) which could be diminished by DFX and NAC. *Alternaria* extract induced a significant and marked concentration-dependent increase in IL-8 release and a drop in transepithelial electrical resistance (TER), predominantly due to a heat-labile serine protease. *Alternaria* extract appeared to have more pronounced effects on cells pre-treated with underground railway PM, but this was independent of a heat-labile component.

Conclusion: Metal-rich underground railway PM potently generates ROS, with modest pro-inflammatory effects and a marked induction of antioxidant defences. The potential effects of PM entry into cells merits further study. The novel metal-rich nature of such an environmental ultrafine PM warrants further work in light of its high surface area/volume ratio and potential ability to penetrate into the alveoli and possibly the systemic circulation. Additionally, the ability of underground railway PM to generate ROS potently suggests that individuals with defective antioxidant defences, such as seen in asthmatic airways, may be at heightened risk of the effects of metal-rich PM, as may those concomitantly exposed to airborne fungi.

Contents

List of Figures

List of Tables

Declaration of Authorship

I, Matthew Loxham, declare that this thesis and the work presented in it are my own and have been generated by me as the result of my own original research.

The Potential Health Effects of Transition Metals in Particulate Air Pollution

I confirm that:

This work was done wholly or mainly while in candidature for a research degree at this University;

Where any part of this thesis has previously been submitted for a degree or any other qualification at this University or any other institution, this has been clearly stated;

Where I have consulted the published work of others, this is always clearly attributed;

Where I have quoted from the work of others, the source is always given. With the exception of such quotations, this thesis is entirely my own work;

I have acknowledged all main sources of help;

Where the thesis is based on work done by myself jointly with others, I have made clear exactly what was done by others and what I have contributed myself;

Parts of this work have been published as:

Papers (included at the end of the thesis)

Loxham, M., M. J. Cooper, M. E. Gerlofs-Nijland, F. R. Cassee, D. E. Davies, M. R. Palmer, and D. A. H. Teagle. 2013. Physicochemical Characterization of Airborne Particulate Matter at a Mainline Underground Railway Station. *Environmental Science & Technology* 47: 3614-3622.

Leino, M. S.*, M. Loxham*, C. Blume, E. J. Swindle, N. P. Jayasekera, P. W. Dennison, B. W. Shamji, M. J. Edwards, S. T. Holgate, P. H. Howarth, and D. E. Davies. 2013. Barrier disrupting effects of alternaria alternata extract on bronchial epithelium from asthmatic donors. *Plos One* 8: e71278.

Poster

"The Physicochemical And Inflammogenic Properties Of Metal-Rich Airborne Particulates Collected At An Underground Railway Station", Conference of the American Thoracic Society, San Francisco, USA, May 2012.

Further publicity gained as a result of the work contained herein:

Invited Speaker: 3rd International Conference of Health Status of Transit Workers. Brighton, UK. 21st-22nd June 2013.

Interviewee: BBC World Service, "Health Check", first broadcast 5th May 2013 http://www.bbc.co.uk/programmes/p017k0dl (piece at 19.50)

Interviewed by Sky News Radio (supplying news coverage to almost every commercial radio station in the UK, a network of over 280 stations with a combined audience of 34 million)

Featured on LBC Radio.

English Language Press

SeparationsNOW.com, 8th April 2013
http://www.separationsnow.com/details/ezine/13dd5d06644/Going-underground-Toxic-particles-in-an-underground-station.html?tzcheck=1

London Evening Standard, 24th April 2013 (also in print copy)
http://www.standard.co.uk/news/transport/health-fears-over-tiny-particles-of-metal-in-tube-dust-which-can-get-into-your-liver-brain-and-kidneys-8586001.html

Metro, 24th April 2013 (also in print copy)
http://metro.co.uk/2013/04/24/travelling-on-tube-could-be-bad-for-your-health-scientists-say-3664947/

Daily Mail, 24th April 2013
http://www.dailymail.co.uk/health/article-2314123/Travelling-Tube-bad-health-air-rich-toxic-dust.html?ito=feeds-newsxml

Huffington Post, 24th April 2013
http://www.huffingtonpost.co.uk/2013/04/24/tube-travel-is-bad-for-yo_n_3145363.html?utm_hp_ref=uk

Science Daily, 24th April 2013
http://www.sciencedaily.com/releases/2013/04/130424081330.htm

Railway-Techology.com, 29th April 2013
http://www.railway-technology.com/news/newsdust-underground-railways-may-damage-health/

Air Quality News, 29th April 2013
http://www.airqualitynews.com/2013/04/29/underground-railway-dust-may-pose-a-risk-to-health/

Times Higher Education, 2nd May 2013 (also in print copy)
http://www.timeshighereducation.co.uk/news/campus-round-up-2-may-2013/2003512.article

BBC News, 3rd May 2013
http://www.bbc.co.uk/news/health-22404446

The Guardian, 9th May 2013
http://www.theguardian.com/higher-education-network/2013/may/09/research-in-brief-universities-may

WorldHealth.net, 24th May 2013
http://www.worldhealth.net/news/underground-railway-stations-may-compromise-health/

Railway-Technology.com, 25th July 2013 (commissioned piece, written after direct contact with author)
http://www.railway-technology.com/features/feature-air-in-underground-subways-harming-health/

European Lung Foundation News
http://www.european-lung-foundation.org/18269-.htm

Foreign Language Coverage

News Medical, 25th April 2013 (Spanish, also in Dutch, Italian, Chinese)
http://www.news-medical.net/news/20130424/5182/Spanish.aspx

Orthopaedie der Klinikfuehrer, 25th April 2013 (German)
http://orthopaedie.der-klinikfuehrer.de/fachbereiche/pneumologie/medizin-forschung/belastung-u-bahn-hoeher-auf-strasse

Argumenty Fakty, 27th April 2013 (Russian; the leading publication in Russian with a circulation of around 2 million, including the business community, politicians, and researchers)
http://www.aif.ru/health/news/361860

Money Journal, 28th April 2013 (Russian)
http://www.moneyjournal.ru/bizness/transport/uchenie-britanii-chastoe-ispolzovanie-metro-mozhet-bit-opasnim-dlya-zdorovya-8838.html

Le Figaro, 3rd May 2013 (French)
http://sante.lefigaro.fr/actualite/2013/05/03/20468-lair-metro-trop-riche-particules-metalliques

International Chronicle, 3rd May 2013
http://www.internationalchronicle.com/2013/05/03/underground-air-quality-health-risk/

Shia International News, 4th May 2013 (covers Turkey, Lebanon, Afghanistan, Pakistan, Bahrain)
http://en.shafaqna.com/component/k2/item/16405.html

Top Santé, 6th May 2013 (French)
http://www.topsante.com/forme-et-bien-etre/environnement/risques-sante/metro-source-de-particules-metalliques-toxiques-32329

Signed:

Date:

Contributors

All experiments and data analysis were performed by the author in the Brooke Laboratory, Academic Unit of Clinical and Experimental Sciences, Faculty of Medicine, Southampton University Hospital, University of Southampton, with the following exceptions:

Section 3.2.1.

Particulate matter was collected by the Inhalation Toxicology Group at the National Institute for Public Health and the Environment, Bilthoven, Netherlands. Permission for sampling, and the sampling itself, was carried out by a team led by Professor Flemming Cassee, and including John Boere, Paul Fokkens, and Miriam Gerlofs-Nijland. The author participated in underground railway particulate matter collection on one day in July 2010.

Particle digestion and metal analysis was performed at the National Oceanography Centre, Southampton, by the author, under the supervision of Dr Matthew Cooper, who also configured the ICP-MS apparatus.

Section 3.2.2

Preparation of samples for anion analysis was performed by the author. Samples were run at the National Oceanography Centre, Southampton, by Darryl Green and Catriona Menzies.

Section 3.2.3

Limulus amoebocyte lysate assay sample preparation was performed by the author. The assay itself was performed by Zofi McKenzie in the Faculty of Medicine, Southampton General Hospital.

Section 3.2.5

Sample preparation and scanning electron microscopy was performed by the author, under the supervision of Dr Richard Pearce, National Oceanography Centre, Southampton.

Chapters 4 and 5

Primary bronchial epithelial cells were obtained from healthy and severely asthmatic donors by clinicians including Drs Paddy Dennison, Chris Grainge, Nivenka Jayasekera, Valia Kehagia, and David Sammut. Epithelial cells were cultured by the author with routine assistance from Emma-Jane Goode, Maria Zarcone, Dr Robert Ridley, and Dr Natalie Smithers.

Section 4.2.1

Particle irradiation was performed by Ian Mockridge within the Cancer Sciences Division, Faculty of Medicine, University of Southampton.

Section 4.2.7

Fixing, embedding, and sectioning of cell cultures for transmission electron microscopy was performed by the author, under the supervision of Dr Anton Page and Patricia Goggin in the Biomedical Imaging Unit, University of Southampton. Transmission electron microscopy was performed by the author with guidance from Patricia Goggin and Dr Elizabeth Angus. X-ray analysis of intracellular particle composition was performed by the author under the supervision of Patricia Goggin.

Chapter 5

Experiments were performed by the author (IL-8, TNFα, TER, FITC-dextran passage, fluorescent protease assay, TSLP, IL-33, IL-18) and Dr Marina Leino (IL-8, TNFα, TER, FITC-dextran). All data were analysed by the author.

Acknowledgements

Over the course of my PhD studies and the preceding Master of Research, I have been helped and supported by several people. It is not possible to list all those who have helped me in one way or another, but there are nonetheless several people whose help I would like to acknowledge.

I am grateful to Dr Peter Lackie who supervised me during the first part of my MRes year, introduced me to the importance of the epithelium, and who first showed me how to perform transmission electron microscopy. I would also like to thank Dr Anton Page and Patricia Goggin in the Biomedical Imaging Unit, Southampton General Hospital, whose kind willingness to help at a moment's notice made microscopy far simpler than it would have been without their assistance. I also wish to thank Dr Jane Collins for her supervision in the first year, and subsequent guidance on matters science- and career-related. I am also thankful to Dr Peter Peachell at the University of Sheffield Medical School, whose lectures on immunopharmacology during my undergraduate degree, and subsequent supervision of my final year research project and post-degree year introduced me to immunology, airways biology, and the world of "real" science.

Most importantly of all, I am keen to thank those with whom I worked for extended periods. The great majority of techniques I have learned or become accustomed to were hitherto unknown to me, and that I was able to grasp them is attributable to the help and assistance of various members of the Brooke Laboratory during my time in Southampton. To that end, I would particularly like to thank Dr Cornelia Blume and Dr Emily Swindle for teaching me how to culture cells, perform ELISAs, and for being available to discuss all aspects of epithelial cell work. Whenever I had questions about the clinical aspect of the field, I was able to discuss these with Dr Patrick Dennison, Dr Mark Jones, Dr Nivenka Jayasekera, and Dr Valia Kehagia. Primary cell culture is very time consuming, and also requires excellent technique, and to this end I am hugely grateful to Camelia Molnar, Maria Zarcone, Emma Goode, Dr Natalie

Smithers, and Dr Robert Ridley for performing the work which allowed me to utilise with primary bronchial epithelial cells. I am also grateful to Dr Rebecca Morgan-Walsh for her helpful suggestions regarding ROS detection assays, and Dr David Smart, who has been on hand with useful advice about almost everything involved in my work.

I am very grateful indeed to the assistance of Dr Matthew Cooper, who showed great patience in his supervision of me while performing particle analysis at the National Oceanography Centre, Southampton, especially in his understanding of my trepidation at dealing with highly concentrated acids, and repeated questioning regarding ICP-MS data analysis. I am also grateful to Professor Flemming Cassee and his team at RIVM, Netherlands, without whom there would have been no particulate matter to analyse. Finally, I am most grateful to Professor Donna Davies, Professor Martin Palmer, and Professor Damon Teagle, who were always on hand with comments, advice, guidance, and readiness to review manuscripts, but who always allowed me to express my opinions, and who helped me develop hugely during the course of my PhD.

There are also people I wish to thank from a non-academic standpoint. I would like to thank Lizzie Davies and Jess Donaldson, with whom I have shared an office for the latter half of the PhD, and also Angela Tait and Gemma Bashevoy, for discussions about science and PhDs, but more importantly for breaks from science. I would also like to thank Lizzie Angus, Lawrence Andrews, Matt Brown, Gerry Cole, Claire Heath, Megan Jarman, Romana Mikes, Emma Reeves, Annie Tocheva, Annette West, and Emily Wilkinson, for their chats, advice, and willingness to engage in mutual grumbling.

There are two more people I would like to thank. First, James Robards, whose discussions on academia, current affairs, and all manner of other subjects, all while consuming far too much caffeine, were a major source of inspiration over the past four years. Finally, I would like to thank Agnieszka Janeczek, whose support and patience over the latter half of my PhD helped me through times when I was losing focus of the light at the end of the tunnel.

Very last of all, I would like to thank my family – my dad David, my mum Carolyn, and my sister Angela. The unending support of my parents, from their persistence in teaching me to read, teaching me to enquire, and teaching me the value of learning, to organising day long trips to London to visit the Science and Natural History Museums when I was very young, and providing for me vast quantities of books, for their support through difficult times at school and since, supporting my seemingly endless indecisiveness, their belief in a positive long-term outcome, and most of all for their love. This work would not have been possible without them.

Abbreviations

8-oxodG	8-Oxo-2'-deoxyguanosine
AC	Alternating current
AEBSF	4-(2-Aminoethyl)benzenesulphonyl fluoride hydrochloride
AJC	Apical junction complex
ALI	Air-liquid interface
AP-1	Activator protein 1
ApoE	Apolipoprotein E
ARE	Antioxidant response element
ATI/ATII	Alveolar type 1/type 2 cell
ATP	Adenosine 5'-triphosphate
BALF	Bronchoalveolar lavage fluid
BEBM	Bronchial epithelial basal medium
BEGM	Bronchial epithelial growth medium
BET	Brunauer Emmett Teller
BSA	Bovine serum albumin
CD	Cluster of differentiation
cDNA	Complementary DNA
COPD	Chronic obstructive pulmonary disease
COSHH	Control of Substances Hazardous to Health
CYP	Cytochrome P450
DC	Direct current
DCF	Dichlorofluorescein
DCF-DA	Dichlorofluorescein diacetate
DEP	Diesel exhaust particulate
DFX	Desferrioxamine
DMEM	Dulbecco's modified Eagle's medium
DMSO	Dimethyl sulphoxide
DNA	Deoxyribonucleic acid
DTPA	Diethylene triamine pentaacetic acid

E-64	*Trans*-epoxysuccinyl-L-leucylamido-(4-guanidino)butane
EDAX	Energy dispersive x-ray analysis
EDTA	Ethylenediaminetetraacetic acid
EGF	Epidermal growth factor
EGFR	Epidermal growth factor receptor
ELISA	Enzyme-linked immunosorbent assay
eGPx	Extracellular glutathione peroxidase
ERK	Extracellular signal-related kinase
FEV_1	Forced expiratory volume in 1 second
FITC	Fluorescein isothiocyanate
FVC	Forced vital capacity
GPx	Glutathione peroxidase
GSH	Glutathione (reduced form)
GSSG	Glutathione (oxidised form)
GST	Glutathione S-transferase
HBSS	Hanks' balanced salt solution
HDM	House dust mite
hs-CRP	High-sensitivity C-reactive protein
HO-1	Haem oxygenase-1
HRP	Horseradish peroxidase
HUVEC	Human umbilical vein endothelial cell
HVCI	High volume cascade impactor
ICP-MS	Inductively coupled plasma mass spectrometry
IκB	Inhibitor of NF-κB
IL	Interleukin
Keap1	Kelch-like ECH-associated protein 1
LBP	LPS-binding protein
LDH	Lactate dehydrogenase
LPS	Lipopolysaccharide
MAPK	Mitogen-activated protein kinase
MCP	Monocyte chemotactic protein
MEM	Minimum Essential Medium
MIP-2	Macrophage inflammatory protein 2

MMLV	Moloney murine leukaemia virus
mRNA	Messenger RNA
MTT	Methylthiazolyldiphenyltetrazolium bromide
NAC	N-acetylcysteine
NAD(P)H	Nicotinamide adenine dinucleotide (phosphate)
NF-κB	Nuclear factor κB
NOAEL	No observed adverse effect level
Nrf2	Nuclear factor (erythroid-derived 2)-like 2
NQO1	NAD(P)H quinone oxidoreductase 1
NUDT1	7,8-dihydro-8-oxoguanine triphosphatase
OGG1	8-Oxoguanine glycosylase
PAH	Polyaromatic hydrocarbon
PAI-1	Plasminogen activator inhibitor 1
PAR	Protease-activated receptor
PARP-1	Poly(ADP-ribose) polymerase 1
PBS	Phosphate buffered saline
PCR	Polymerase chain reaction
PEG	Polyethylene glycol
PIPES	1,4-Piperazinediethanesulphonic acid
PM	Particulate matter
PT	Permeability transition
qPCR	Quantitative polymerase chain reaction
RANTES	Regulated upon activation, normal T-cell expressed and secreted
RAPTES	Risk of Airborne Particles, a Toxicological-Epidemiological hybrid Study
RNA	Ribonucleic acid
RNS	Reactive nitrogen species
ROFA	Residual oil fly ash
ROS	Reactive oxygen species
RT	Reverse transcription
RT-qPCR	Reverse transcription qPCR
SA	Surface area
SB203580	4-(4-Fluorophenyl)-2-(4-methylsulphinylphenyl)-5-(4-pyridyl)-1H-

	imidazole
SEM	Scanning electron microscope/microscopy
SOD	Superoxide dismutase
TBARS	Thiobarbituric acid reactive substances
TBS	Tris-buffered saline
TEM	Transmission electron microscope/microscopy
TER	Transepithelial electrical resistance
Th2	T-helper cell type 2
TLR	Toll-like receptor
TMB	3,3',5,5'-tetramethylbenzidine
TNF	Tumour necrosis factor
TMTU	Tetramethylthiourea
TSLP	Thymic stromal lymphopoietin
VACES	Versatile aerosol concentration enrichment system
VOC	Volatile organic compound
WHO	World Health Organisation
XTT	2,3-Bis(2-methoxy-4-nitro-5-sulfophenyl)-2H-tetrazolium-5-carboxanilide inner salt

1 Introduction

1.1 The Structure of the Respiratory System

The respiratory system comprises a network of tubes with 23 generations of branches, leading from the mouth and nostrils to the lungs. The lungs are the organs of the body whose alveoli are specialised for gas exchange, allowing inhaled oxygen to enter the blood and waste gases to leave and be exhaled. The average adult male inhales approximately 23 m^3 of air per day (1). This air contains nitrogen, oxygen, argon, carbon dioxide, and other trace gases, but also pollutant gases such as sulphur dioxide and nitrogen oxides. The air also carries particles, either biological such as bacteria, viruses, and fungal spores, or anthropogenic such as soot, oily fly ash, or roadwear particles. It is these anthropogenic particles which will form the basis of the majority of the work presented within this thesis.

The airways can be divided into three stages – the upper airways, the lower airways, and the alveoli. The upper airways are composed of the nasal passage, the trachea, and the bronchi. Air passing through the upper airways is humidified and warmed as it passes over the nasal turbinates to avoid cooling or drying the lower parts of the airways. The upper airways are lined with pseudostratified epithelium, in which all epithelial cells are in contact with the *lamina reticularis* which underlies the epithelium, but not all protrude to the lumen. In this way, the columnar epithelial cells which form the epithelium have the appearance of a stratified epithelium (2). The epithelial cells of the upper airways are lined with hair-like projections which extend into the airway lumen. These cilia, by way of their internal structure, are motile and beat synchronously as part of the process of mucociliary clearance (3). The mucus lining the upper airways is secreted by goblet cells which are interspersed between the ciliated columnar epithelial cells.

The lower airways of the lung are formed by the bronchioles. In contrast to the upper airways, the epithelial lining of the bronchioles is flatter, being formed of cuboidal epithelium. The bronchiolar epithelium is generally not ciliated, and there is a much lower population of goblet cells compared to the upper airways. However, a layer of surfactant is secreted by Clara cells (4). Surfactant is a fluid of lower viscosity than the mucus found in the upper airways, and contains surfactant proteins, which have important antiviral properties, and surfactant lipids, which reduce surface tension, and in so doing are vital in keeping the terminal airways and alveoli patent so that they do not collapse on themselves.

The lowest section of the lungs is the alveoli, where gas exchange takes place. The alveolar epithelium is composed of two types of cells. Alveolar type 1 (ATI) cells are extremely thin squamous epithelial cells which form a thin barrier to allow for optimal diffusion of gases from the air spaces to the underlying capillaries. Alveolar type 2 (ATII) cells are cuboidal epithelial cells which secrete surfactants and are also able to transform into ATI cells to replace other ATI cells which have become damaged (5) . Due to their thickness, ATII cells are not involved in gas exchange.

Whereas the alveolar epithelium has a primary function in forming a barrier which is able to facilitate gas exchange, the epithelium of the upper conducting airways is crucial in providing a selectively permeable barrier between the outside environment, as found in the airway lumen, and the subepithelial tissue (6). Airway mucus is a complex mixture of glycosylated proteins forming a gel which also contains antibacterials, antivirals, antiproteases, and antioxidants, whose composition can be altered by certain stimuli (7-9). Together, the particle trapping effect of the mucus and the upward sweeping motion of the cilia comprise the mucociliary escalator (10). In addition to the chemical barrier formed by the mucus, tight junctions and adherens junctions in the apical junction complex (AJC) are key in the regulation of paracellular flux, while desmosomes and hemidesmosomes in the lateral and basolateral sections of the epithelial layer secure epithelial cells to adjacent cells and the *lamina reticularis* respectively (2, 11) (Figure 1.1). The leakiness of this barrier can be increased by cytokines (12, 13), viral infection (14), and inhaled allergens (15) amongst others. However, the barrier is also able to be disrupted intentionally, for example to enable

the diapedesis of immune cells into the airway lumen. One example of this is the migration of neutrophils into the airways. Another cell type commonly found in the airway lumen is dendritic cells, which sample the external environment and act as antigen presenting cells by transporting antigenic material to the lymph nodes (16). Macrophages – "professional" phagocytic cells – are found in the airway lumen where they are able to ingest pathogens and particulate matter. However, they more commonly perform this role in the alveoli, which are not protected by a layer of mucus, and can then either translocate to the lymph nodes or move up the airways to the mucociliary escalator, by which they can be cleared from the respiratory tract altogether (17).

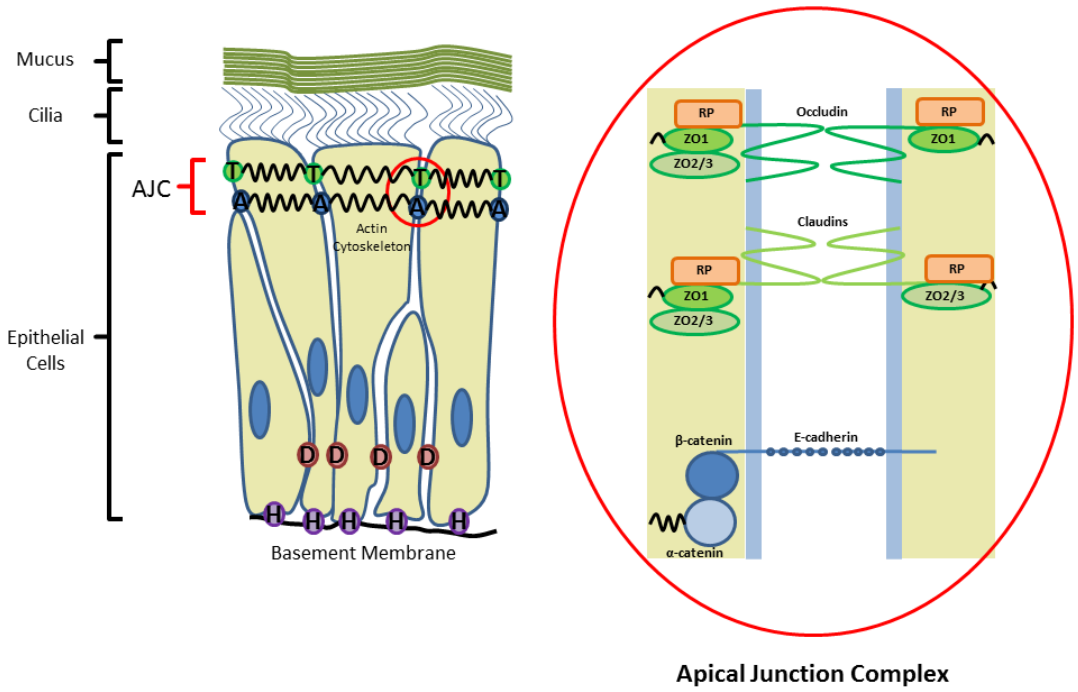

Figure 1.1. The structure of the bronchial epithelium.

The pseudostratified epithelium of the bronchi is able to form a tight barrier between the external and internal environments by virtue of its cell-cell junctions. The apicobasal junction complex (AJC) is comprised of tight junctions (T) and adherens junctions (A), with adaptor proteins such as ZO-1 in tight junctions (modified by regulatory proteins (RP)) and catenins in adherens junctions connecting the junctional complex to the actin cytoskeleton. Desmosomes on the lateral surface of the cells provide further cell-cell contacts, and hemidesmosomes bind the basal surface of the cell to the basement membrane.

Although macrophages are one mode of particle clearance from the lungs, the airways possess a number of mechanisms by which the passage of inhaled particulate matter can be impeded. In normal breathing at rest, air is predominantly taken in through the nasal passages, which are lined with hairs and mucus to trap particulate matter suspended in the inhaled air. Furthermore, the crooked path of the nose and the eddying airflows produced by the turbinates increase the deposition of particles in this uppermost section of the respiratory tract. However, if breathing becomes predominantly oral rather than nasal, for example during periods of exercise or certain diseases, these filtration mechanisms become relatively redundant. Further down the airways, particles can be trapped by mucus, as previously described, and swept upwards by the wafting motion of airway cilia, and aided by the cough reflex. Once this has been accomplished, particle-laden mucus may be expelled through the mouth or swallowed, where it may go on to exert effects in the gastrointestinal tract. In the lower airway, clearance becomes predominantly macrophage-mediated.

These defences, in combination with the diameter of the airways, create a size-selective gradient for the distribution of particles deposited throughout the airways (Figure 1.2). Particles of greater than 10 μm aerodynamic diameter are generally unable to pass the defences of the nasal passages and upper airways, and are classed as non-respirable, although in circumstances where there is an exceptionally high airborne particulate matter (PM) load, this may not be the case. Conversely, particles of an aerodynamic diameter ≤ 10 μm are classed as respirable due to their ability to enter the respiratory tract. Of these respirable particles, those of approximately 2.5-10 μm aerodynamic diameter, termed coarse particles, are deposited in the extrathoracic region and upper airways, particles of between 0.1 μm and 2.5 μm, the fine particles, are deposited in the bronchi and bronchioles, and particles of an aerodynamic diameter smaller than 0.1 μm, the ultrafine particles, generally deposit in the alveoli (18, 19). As particle size decreases, the major mechanism of sedimentation changes from impaction to sedimentation (gravitational settling) and, for the smallest particles, diffusion (20).

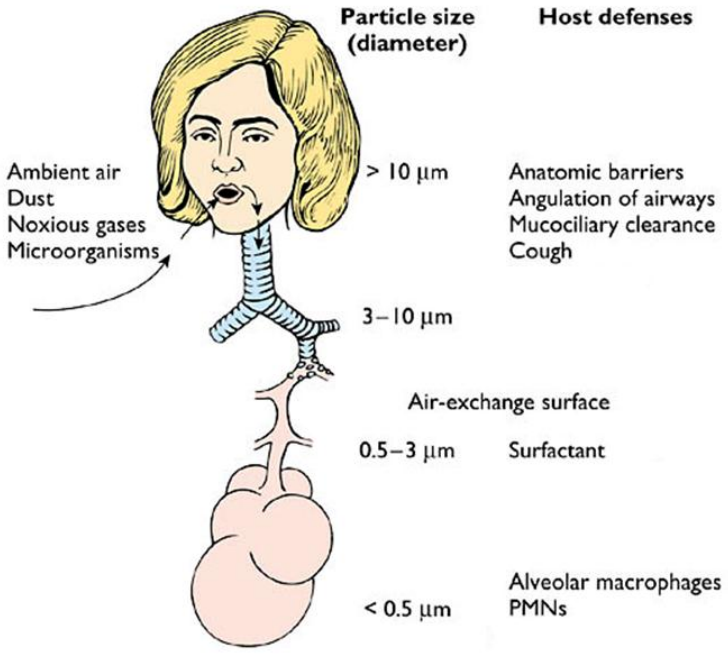

Figure 1.2. Particle deposition in the airways.

Particles suspended in inhaled air deposit in different regions of the airways depending on their size, with coarse particles depositing in the extrathoracic airways, fine particles in the bronchi and bronchioles, and ultrafine particles in the terminal bronchioles and alveoli. Defences to trap particles in the upper airways are predominantly mechanical, whereas those in the lower airways are more cell-mediated. Adapted from (21).

The airways can also be affected by disease. Asthma is a disease of the upper and lower (conducting) airways, characterised by airflow obstruction which is reversible with time or medication, airways inflammation, hyperresponsiveness of the bronchi to stimuli such as allergens, virus, and low temperatures, a progressive decline in lung function over time (22), and airways remodelling (23) (Figure 1.3).

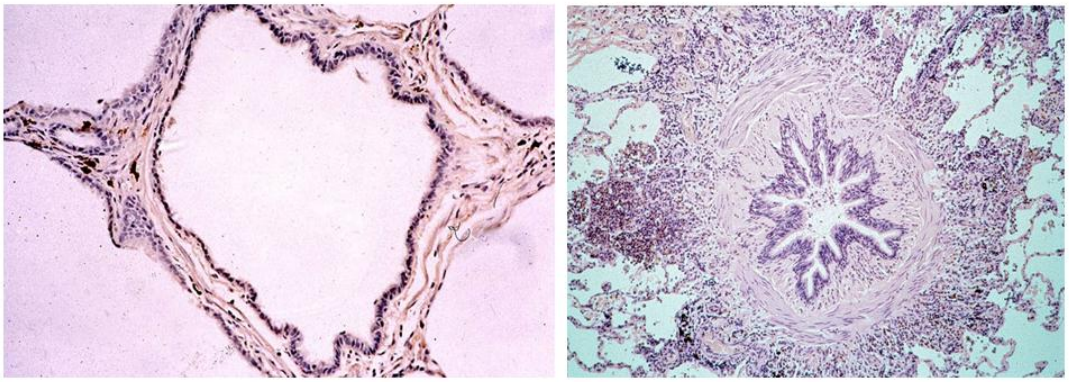

Figure 1.3. Airway remodelling in asthma.

The airway epithelium in asthma appears to be locked into a cycle of damage and incomplete repair. The healthy airway is a has a patent lumen lined by a layer of ciliated pseudostratified epithelium attached to the *lamina reticularis*, underneath which are found fibroblasts and a layer of smooth muscle. In asthmatic airways, there is occlusion of the airways due to smooth muscle hyperplasia along with thickening of the *lamina reticularis* and mucus hypersecretion. There is also bronchial hyperresponsiveness, resulting in the potential for further closing of the lumen by contraction of the smooth muscle.

Asthma may have an allergic or non-allergic basis, and is thought to involve a genetic component (24), although its causes and treatment are not fully understood because of the range of different symptom groups into which patients can be classified. Conversely, chronic obstructive pulmonary disease (COPD) is a disease of the small airways and alveoli, characterised by an irreversible shortness of breath with airway obstruction, cough, and mucus hypersecretion (25). As with asthma, there is a progressive decline in lung function. The predominant causative factor in the aetiology of COPD is smoking, although there may also be occupational and genetic components. Although both asthma and COPD involve reduced airflow, differential diagnosis on the basis of spirometry can be made in that the reduced airflow in asthma is reducible on administration of the β_2-adrenergic agonist salbutamol, further inducible on administration of the M_3 cholinergic agonist methacholine, and may exhibit diurnal variation. Furthermore, gas exchange as measured by carbon monoxide uptake into the blood may be impaired in COPD compared to asthma.

Therefore, airways diseases can, to an extent, be caused by materials suspended within inhaled air and, in turn, the response to inhaled particles can be influenced by the presence of these diseases, both in terms of particle deposition within the lungs and the biochemical responses to particulates.

1.2 The Potential Risk to Public Health Posed by Particulate Matter

There have been a number of fatal air pollution incidents over the past century, generally attributed to industrialisation and increased fossil fuel combustion. The first scientifically investigated incident was the Meuse Valley fog in 1930, when over 60 people died as a result of temperature inversion-induced pollution build-up in a valley close to the industrial city of Liege, Belgium. The fatalities were attributed to release of sulphur dioxide and fine soot particles from domestic and industrial coal burning (26, 27). Subsequent pollution incidents have been reported, notably the London fog of 1952 (28). Indeed, there were further reports of subsequent episodes of pollution-linked fog in London in January 1955, where there was a trend of worsening of symptoms in patients previously diagnosed with chronic bronchitis and emphysema when increased smoke and SO_2 concentrations were noted (29), and similar observations were drawn over a longer period in the winter of late 1955 and early 1956 (30). A subsequent ten-year study suggested that mean smoke concentrations in London began to fall from 1954, but that spikes still occurred where favoured by the prevailing weather conditions (31).

Airborne PM, in size fractions termed coarse (PM_{10}), fine ($PM_{2.5}$), or ultrafine ($PM_{0.1}$), has long been recognised as presenting a risk to health and mortality (32-35), its size permitting it to penetrate into the bronchial tree and beyond. There is interest in each of these size fractions as potential toxicants, with each fraction having different properties, mechanisms of action, and sites of action. While larger particles are suggested to exert their effects by virtue of their chemical composition, smaller particles are more often noted to exert effects by way of their vastly increased surface area, and different effects may be related to size fractions as well as source processes

(36). However, opinion varies as to which is the more toxic fraction (37, 38), and this may depend on site of sampling, as the relative proportions of each fraction in the air may differ depending on the sampling location and the processes which generate the particulates, as well as whether toxicity is measured in terms of particle mass, number, or surface area. Larger particulates are generally the result of friction processes, while ultrafine particles are more commonly a result of secondary reactions between gaseous components in the environment, including photochemical reactions catalysed by sunlight (39, 40). Generally, $PM_{2.5}$ is the predominant fraction on a mass basis, while in terms of particle number $PM_{0.1}$ is the predominant fraction (41).

In 1993, a seminal paper looking at the effect on mortality of air pollution showed increased mortality rates for PM_{10} (odds ratio 1.27), and $PM_{2.5}$ (odds ratio 1.26), with significant correlation with lung cancer and cardiopulmonary disease (42). Another important study was published in 2002 by Pope and colleagues, which involved assessing the link between fine particulate air pollution and mortality in half a million Americans. They found a significant link between $PM_{2.5}$ levels and mortality from all causes (a 4% increase in risk per 10 $\mu g/m^3$ elevation in $PM_{2.5}$ levels), and also specifically from lung cancer (6% increase) and cardiopulmonary causes (8% increase) (43), while a recent European study found PM_{10} to be a contributor to adenocarcinoma cases more than was $PM_{2.5}$, and these links persisted even at PM levels below European Union recommended limits (44). Indeed, up to 52,000 deaths per year in the USA have been attributed to PM_{10} (45), and a further study observing a link between concentrations of PM_{10} and $PM_{2.5}$ and heart failure suggested that a USA-wide reduction in $PM_{2.5}$ of 3.9 $\mu g/m^3$ would reduce heart failure hospitalisations by almost 8,000, saving over $300 million per annum (46). Cardiovascular mortality was also linked to $PM_{2.5}$, but not PM_{10} in a recent study which also found links for both PM fractions with respiratory mortality even in those with no history of asthma or COPD (47). Particles with a median aerodynamic diameter of less than 0.03 μm were linked to hospital asthma presentation in children and the elderly (48), while a similar connection was made between $PM_{2.5}$ and PM_1 and asthma (49, 50), and recently for PM_{10} and asthma- and COPD-associated emergency room visits (51). Despite occasional attempts at refuting a link between air pollution (52), the link between

particulate matter and adverse health effects is becoming more evident and better defined.

There is much evidence that the physiochemical properties of particulate matter and by association, the biological effects of such material, are dependent on a wide variety of factors, such as processes involved in generation of the material, chemistry of the "source material" from which the particles derive, fuel combustion processes in the area whether related to power stations or traffic, and even season of collection of particulates (33, 53-55). To this end, work has been carried out to examine the effects of particulate matter from specific sources and in specific environments, the aim being to characterise the source of deleterious activity of particulate matter, and also to determine whether the effects are due to the particulate matter itself, rather than levels of other pollutants which may correlate with particulate matter levels (56). Steel mills and smelting works are of particular interest in this respect, because of their reliance on processes involving the use of transition metals. Such studies can be difficult to conduct due to the number of confounding factors and the lack of control over exposures. However, a number of authors have successfully demonstrated a deleterious effect of this type of pollution. One such study utilised the abnormally low smoking rate in the Utah Valley, ascribed to religious teachings, coupled with a period of closure and reopening of a local steel mill, to show an increase in hospital admissions for respiratory reasons, increased two-fold for children and by 47% for adults when PM_{10} exceeded 50 $\mu g/m^3$, while PM_{10} decreased when the steel mill closed (57). Ambient PM samples from the local area taken when the steel mill was open were also more able to cause apoptosis, increased BAL fluid cell count, and airways hyperresponsiveness when instilled in rat airways compared to PM samples collected when the mill was closed (58). Moreover, a recent randomised cross-over study has shown decreased lung function when subjects spent eight hours per day for five consecutive days in the vicinity of a steel mill, linked to increased SO_2, NO_2, $PM_{2.5}$ and ultrafine PM (59). When PM was collected from a site in Tuxedo, NY, and instilled intratracheally into apolipoprotein E- (ApoE)-deficient mice, there was an increase in heart rate, marking cardiac stress, when the PM was collected on days where the prevailing wind came from the direction of a local nickel smelting plant, but not when the wind direction was different, implicating inhaled nickel in cardiac toxicity (60).

The World Health Organisation (WHO) has set maximum 24-hour exposure limits of 50 μg/m^3 and 25 μg/m^3 for PM_{10} and $PM_{2.5}$ respectively (61). These limits are generally applicable only outdoors, and do not apply to workplace environments. The UK Health and Safety Executive has set out additional limits as part of their Control of Substances Hazardous to Health (COSHH) regulations, which state that total airborne dust concentrations should not exceed 10 mg/m^3 averaged over an 8 h period, and respirable dust concentrations should not exceed 4 mg/m^3 over an 8 h period (62). However, specific dusts also have their own, generally lower, limits set, for example iron oxide respirable dust concentrations should not exceed 5 mg/m^3 over an 8 h period or 10 mg/m^3 in any fifteen min period (62). Interestingly, there has been no limit set for ultrafine particles ($PM_{0.1}$) either in terms of public exposure or workplace exposure, probably due to the paucity of research on the sources and effects of particles in this fraction. Indeed, the discipline of nanotoxicology, investigating the effects of particulates in the nanometre size range, is still in relative infancy.

Underground railway systems are widely used mass transit systems in many large cities. According to London Transport, over 1.2 billion individual journeys were made on the London Underground in the financial year 2012/13 (63). The presence of large mass concentrations of suspended particulate matter of a respirable size (10 μm median aerodynamic diameter or below) is of concern, both in terms of acute effects and the effects of prolonged exposure to such particulates. This exposure is compounded by the lack of ventilation in the tunnels and stations, resulting in a greater build-up of particulates than would be seen at surface level. Such particulates are known to contain a significant proportion of transition metals, especially iron, but also manganese, chromium, and copper, which may be capable of catalysing the generation of reactive oxygen species (ROS) (64).

Underground railway particulate mass concentrations have been found to be far in excess of the WHO limits, at 470 μg/m^3 and 260 μg/m^3 for PM_{10} and $PM_{2.5}$ on the Stockholm underground (five- and ten-fold greater than the above ground levels respectively) (65), with similar levels being found on the London Underground (66),

and PM_5 levels of almost 900 $\mu g/m^3$ in one study (67). This has been picked up on by the media, with sensationalist stories being published in widely-read newspapers (68). Exposure to $PM_{2.5}$ can be eight- to ten-fold higher on journeys made underground rather than overground (69, 70). Notably, the distribution of particle sizes underground has been suggested to be more uniform than above ground, with a greater level of PM_{10} but a reduced load of smaller particles (67) compared to ambient urban PM. These high levels of particulate matter persist in spite of improvements to braking systems and the banning of smoking in many underground train systems (71). Although the majority of underground particles are thought to derive from processes occurring in the underground railway system, and levels are closely correlated to train traffic levels (65), the contribution of particles from ambient, above ground sources is a matter of debate (72, 73), adding complexity to the make-up of underground air PM. Table 1.1 shows particulate matter concentrations from a variety of underground environments, with comparison to above-ground levels if these were measured as part of the same study.

Site	*Fraction*	*Conc μg/m³*	*Author*
Berlin Underground	PM_{10}	153 (summer); 141 (winter)	(74)
Guangzhou Underground	PM_{10}	67	(75)
	$PM_{2.5}$	44	"
Helsinki Underground Station	$PM_{2.5}$	47 (Rautatientori station); 60 (Sörnäinen station)	(76)
Helsinki Overground Station	$PM_{2.5}$	19	"
Helsinki Underground Train	$PM_{2.5}$	21	"
Helsinki Urban	$PM_{2.5}$	10	"
London Underground	$PM_{2.5}$	246.0±52.49	(70)
London Underground	PM_5	708.6-892.8	(67)
London cyclist exposure	PM_5	14.00-88.54	"
London Underground	$PM_{2.5}$ (mean) underground journey	247.2 (summer); 157.3 (winter)	(69)
	$PM_{2.5}$ (mean) overground journey	29.3 (summer)	"
London Underground	$PM_{2.5}$	130-480	(77)
London Underground	$PM_{2.5}$	270-480 (platform); 130-200(driver's cab)	(66)
Mexico City Underground	$PM_{2.5}$	61	(78)
Mexico City Bus	$PM_{2.5}$	71	"
New York City Underground	$PM_{2.5}$	62	(79)
Paris RER	PM_{10}	360.9	(80)
Paris Metro	PM_{10}	67.5	"
Prague Underground Train	PM_{10}	82.3 (summer); 125.5 (winter)	(72)
Prague Underground Station	PM_{10}	71.1 (summer); 120.2 (winter)	"
Prague street	PM_{10}	51.4 (summer); 84.9 (winter)	"

Rome Underground	PM_{10}	348-479 (varying stations)	(81)
Seoul Underground Platform	PM_{10}	359.0	(82)
	$PM_{2.5}$	129.0	"
Seoul Underground Platforms	PM_{10}	129.3	(83)
	$PM_{2.5}$	105.4	"
Seoul Underground Trains	PM_{10}	145.3	"
	$PM_{2.5}$	116.6	"
Stockholm Underground (Mariatorget platform)	PM_{10}	469 (max 722)	(65)
	$PM_{2.5}$	258 (388)	"
Hornsgatan urban street (traffic-dense)	PM_{10}	98 (max 454)	
	$PM_{2.5}$	23.1 (88.5)	"
Stockholm Underground (Odenplan)	PM_{10}	242±40	(64)
	$PM_{2.5}$	77±10	"
Stockholm Underground	$PM_{2.5}$	63 (platform workers); 19 (underground train drivers); 10 (ticket sellers)	(84)

Table 1.1. Airborne PM concentrations in underground railways.

This table shows variation in airborne PM levels between different underground railway locations, and also between sites in close proximity to each other, whether underground or above ground. While sampling equipment is generally certified as accurate, there is evidence of disparity between values from different sets of sampling equipment in the same environment, and therefore some degree of care should be taken when comparing between studies (72, 85).

While the risk to occasional underground train passengers may be low, regular exposure to airborne particulates over a prolonged period may pose a risk, not only to the respiratory system, but also to the cardiovascular system (86). The cardiovascular effects which may manifest themselves are suggested to be due to either (1) airway inflammation which then results in distribution of inflammatory mediators in the systemic circulation, (2) autonomic nerve activation in the airway which results in effects on the cardiovascular system, or (3) passage of ultrafine PM across the blood-lung barrier, allowing interaction with the vascular endothelium and also distribution of these ultrafine particulates to distal locations (87, 88).

A study of Stockholm underground train drivers showed increased plasminogen activator inhibitor-1 (PAI-1) and high-sensitivity C-reactive protein (hs-CRP), markers of coagulation and inflammation (89, 90), mirrored by particulate matter-induced increases PAI-1 and coagulation in mice (91), although a further report by the same authors found no increased risk of lung cancer in underground train drivers (92). Conversely, assessment of plasma and urinary markers of oxidative damage in groups of workers in New York City found that plasma deoxyribonucleic acid (DNA)-protein crosslinks were in a greater concentration in underground railway workers than in bus drivers, but no different to those in office workers, and the increase in urinary isoprostane concentrations in underground workers was not statistically significant, although it did correlate with the number of years of underground railway work (93). In support of increased markers of coagulation with high PM loads, an earlier study found increased plasma fibrinogen levels in healthy London office workers associated with PM_{10} levels, although only during the spring/summer period (94). However, it could be argued that temperature and humidity levels in underground railway systems are more akin to those found on the surface during the summer, although this seasonality could also be associated with increased photochemical formation of secondary sulphate particles. This could lead to increased hydroxyl-generating capability of particulate iron on account of the increased bioavailability of iron sulphate (95). Platform level workers, such as tickets collectors and cleaners, may be exposed to even greater levels of airborne particulates (66, 89), and so studies into prolonged exposure are certainly warranted. However, recent research by the same Swedish group responsible for much of the above work has indicated that, at least for

acute exposure, there may be no significant inflammation or effect on lung function, although this does not rule out effects of chronic exposure (84).

Increased particle deposition is also seen in the lungs and airways of smokers and subjects with COPD, possibly due to increased minute ventilation in COPD or altered airway geometry in COPD increasing airflow turbulence (56, 96-98). Pertinent to this, PM_{10} levels have been linked to increased hospital admissions among COPD patients, with lags dependent on both age and gender (99), although a controlled exposure study showed that aspects of COPD may actually confer some protection against the effects of particulate matter, possibly due to impaired airway airflow in COPD, resulting in reduction of carriage of airborne PM to the smaller airways (100). The risk posed to asthmatics by PM is discussed later in this chapter.

1.3 The Sampling of Particulate Matter

In order to obtain airborne particulate matter, whether purely to determine ambient concentrations, or to perform physicochemical analyses and *in vitro* or *in vivo* tests, efficient sampling methods have been devised and are subject to regular improvement. The ideal sampling system should be able to extract and collect particulate matter from the air in a manner such that its morphology and chemistry are maintained, able to separate particles into size fractions as required, and able to obtain sufficient quantities of particles to be used in both *in vivo* and *in vitro* laboratory tests. Two subtly different methods for particle separation exist – impaction and virtual impaction. While it is beyond the scope of this review to illustrate the complex mathematics of fluid mechanics, the principles of which underlie the design of such samplers, it is still possible to discuss the basic premises behind their workings.

The impactor was first developed in 1945 as a means of sampling a variety of airborne substances, including dusts, pollen, and insecticides (101). The basic premise of the impactor is that the airborne moiety is carried in a stream of air directed towards a plate. When the stream hits the plate, the stream is deflected, but particles of a sufficient size, depending on air flow rate, have too great a momentum to change

direction and thus impact the plate (microscope slides have been used for this purpose). However, an inherent design flaw with this apparatus was the rate at which the particle collection surface became overloaded (102). Furthermore, the problem of particle bounce on the impaction plate, followed by re-entrainment in the airstream and subsequent contamination of smaller fractions, could only be solved by the use of mineral oil/grease or adhesive to coat the collection plates, for example fluorocarbon grease-coated Tedlar (polyvinyl fluoride) sheets (103), dibutyl phthalate- or oleic acid-coated Teflon filters (104), or Vaseline (petroleum jelly)-coated mylar films (105).

This problem of particle bounce-off was overcome by the use of a virtual impactor, which does not use an impaction plate, and thus avoids bounce and re-entrainment (106). First devised in 1965 (102), and subject to many modifications in the intervening period (107, 108), virtual impaction involves the carriage of particulate matter in a stream of air entering the virtual impactor. Inside the virtual impactor, a major air flow diverts at an angle, while a minor air flow continues in the same direction as the entrant air stream (Figure 1.4). Particles above a certain size have enough momentum to resist the change in direction encouraged by the major air flow, and thus continue in the minor air flow, from which they can be collected. Particles of an aerodynamic diameter below the cutpoint of the virtual impactor are diverted in the major airflow, from which they can either be retrieved from the apparatus or, in the case of a cascade device, moved to another impactor stage with a smaller cutpoint (102). Recent advances in cascade impactors mean that particles can now be adsorbed to, and collected in, inert polyurethane foam, enabling the collection of sufficient quantities of particulate matter for laboratory studies (approximately 2.15g per cm^2 foam with an air intake of 900 l/min), this being the most common impaction material in high volume cascade impactors (HVCI). However, the problem of extraction of particulates from the foam remains, especially if it is necessary to preserve the chemistry of the particulates (109). Indeed, it has been suggested that the oxidative activity of particles may be lost when they are extracted from a filter, as opposed to collected as a slurry (110, 111). As such, the "gold standard" of sampling would still appear to be virtual impaction, from which particulate matter can be collected as a suspension in ultrapure MilliQ water, allowing relatively easy use and reducing the risk of chemical modification in extraction of PM from the impaction material. However,

the collection of PM as a suspension may result in the leaching of water soluble components of PM. Even though such solutes may be present in *in vitro* and *in vivo* experiments, this will not be the same as them being part of the particle until contact with the airway. The most significant drawbacks of virtual impaction are the possibility of the minor flow becoming contaminated with a small proportion of particles smaller than the cutpoint (102, 108), and also internal losses of particulates between intake and collection (108).

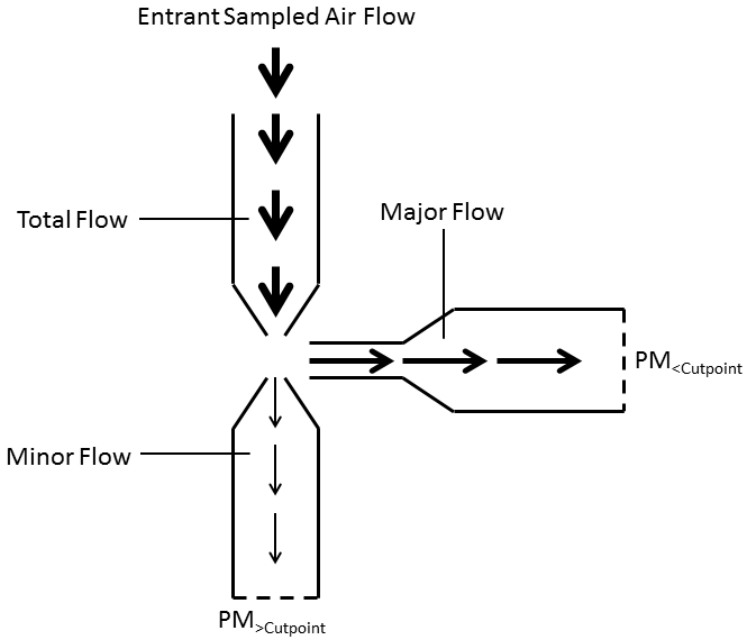

Figure 1.4. The internal structure of a virtual impactor.

Particles entering the virtual impactor are carried through a slit into a perpendicular major air flow. Those particles with an aerodynamic diameter smaller than the filter cutpoint, which can be altered by adjusting the slit sizes and airflows, enter the major airflow, while those particles with an aerodynamic diameter larger than the cutpoint are unable to be deflected by the perpendicular major airflow, and leave the virtual impactor *via* the minor airflow (which replaces the impaction plate of a traditional impactor). Diagram adapted from (106-108).

The versatile aerosol concentration and enrichment system (VACES) was recently developed and evaluated at the University of California, Los Angeles (112, 113). Instead of being a cascade device with impactors in series, the VACES is composed of three separate intake and virtual impaction systems, one with a cutpoint of 10 μm (coarse), one with a cutpoint of 2.5 μm (fine and ultrafine) and one with a cutpoint of

0.18 μm (ultrafine). Particles enter the apparatus in the entrant airflow, which is then passed through a humidification chamber maintained at 37°C and saturated with water vapour (Figure 1.5). The air stream then passes through a refrigeration chamber, which forces water vapour out of the gas phase and into the liquid phase. The particles in the air provide nucleation sites for this condensation, and thus become individually encapsulated within water droplets. Particles are then sorted by size fraction in virtual impactors, and particles of the correct size enter Biosampler vials where they are collected as a water suspension. Parallel collection of particulate matter on Teflon filters is performed so that the dry mass of PM collected can be calculated, and silica gel columns are used absorb moisture in this part of the apparatus. Air flow meters monitor the volume of air being drawn into the VACES system, allowing the total volume of air sampled during the collection period to be calculated. The parallel filters can be used to measure the total mass particles of each size fraction collected and therefore, in conjunction with the air flow meter readings, the mean mass concentration of each PM size fraction during the sampling period.

Although the VACES possesses the function to expose cells to collected particulate matter *in situ*, this is severely limited by the culture apparatus which can be used, the difficulty in applying a metered dose of particulate matter to the cells, and the high risk of infection of cells, as the cells have to be moved to the site of sampling. Therefore, the standard procedure is for the particles to be collected as a suspension in ultrapure MilliQ water for subsequent use in the laboratory.

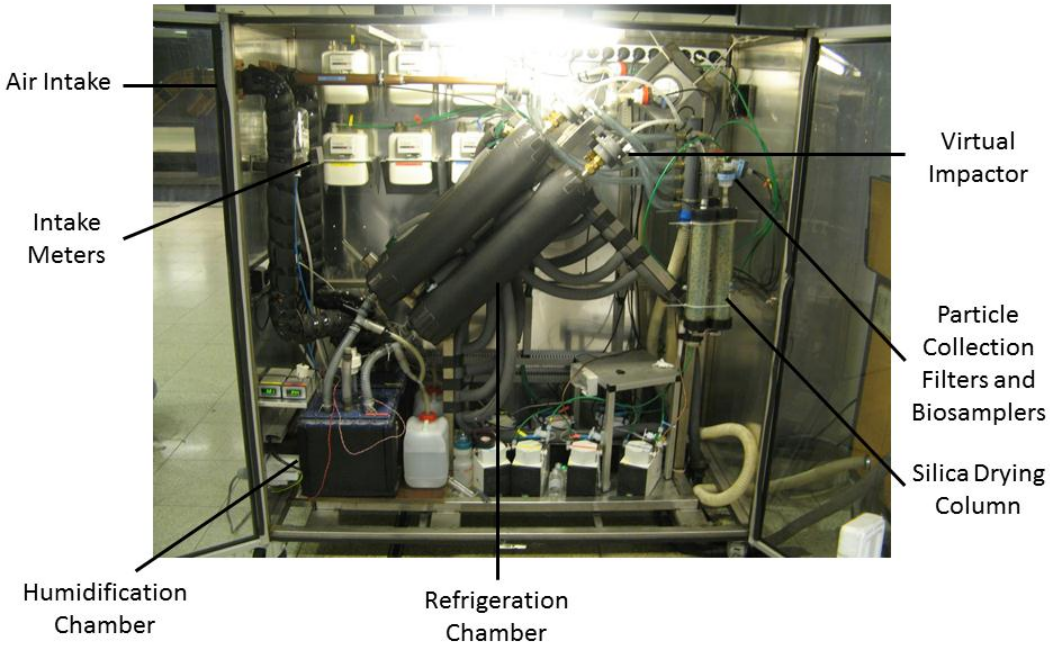

Figure 1.5. The versatile aerosol concentration and enrichment system (VACES). Particle-laden air is drawn in through the air intake pipes, with the total volume sampled being monitored by the intake meters. After passing through a humidification chamber, with water-saturated air at 37 °C, the air is cooled in the refrigeration chamber, where water vapour condenses around the individual particles. Particles then enter the virtual impactors, where they are size-fractionated according to the relevant cutpoint. A parallel dry Teflon filter is used to collect particles for measurement of airborne PM load. The remaining moisture in the air is then removed in the silica drying columns.

1.4 Components of Particulate Matter

Airborne particulate matter is composed of a variety of components, dependent on source, location, and size fraction. The main components found in ambient air are elemental carbon, organic compounds (often found with diesel exhaust particles (DEP)), metals, bacteria and bacterial endotoxins, and allergens which may be adsorbed to particulate surfaces.

1.4.1 Lipopolysaccharide (LPS)

Lipopolysaccharide is a component of gram negative bacterial cell walls which is predominantly found in the coarse fraction of airborne particulate matter, in which it can contribute to the particle's ability to activate macrophages and thus initiate an inflammatory response (36, 114). The effects of endotoxin inhalation *in vivo* include wheeze, asthma symptoms, and airway inflammation (115). LPS binds CD14 and LPS-binding protein (LBP) to form a trimer which activates Toll-like receptor 4 (TLR4), promoting an inflammatory response *via* MyD88-dependent or -independent signalling pathways (see review by Lu e*t al* (116)). CD14 can exist either as an insoluble, membrane-anchored moiety, tethered by glycerophosphatidylinositol, such as found in macrophage membranes, or as a soluble component of blood serum. Both LBP and CD14 are vital in mediating a response to LPS, and thus lack of CD14, such as in culture medium, can abrogate the response of cells such as bronchial epithelial cells or human umbilical vein endothelial cells (HUVECs) to LPS (117). Therefore, care must be taken to avoid ascribing lack of pro-inflammatory effect *in vitro* to the absence of LPS.

In one study, urban air particles induced an increase in release of tumour necrosis factor alpha (TNFα) from rat alveolar macrophages, which could be blocked with polymyxin B, but not with antioxidants dimethylsulphoxide (DMSO) or trimethylthiourea (TMTU) (118). Polymyxin B is an antibiotic which binds the lipid A 2-keto-3-deoxyoctulosonate region of LPS and can be used to chelate LPS, thus negating its effects (119). Using either LPS or heat-treatment, a number of studies have shown that LPS is present in PM, and responsible for at least part of its inflammogenic effects. Soukup and Becker showed that polymyxin B can reduce the ability of the insoluble fraction of PM_{10} to induce inflammatory cytokine release from human alveolar macrophages, although other effects of the insoluble fraction, including reduced phagocytic activity and oxidant generation in response to yeast, were not endotoxin-dependent (120). In agreement with this, heat-treatment of $PM_{10-2.5}$ can, *in vivo*, abrogate the increase in TNFα messenger ribonucleic acid (mRNA) and eotaxin mRNA, the LPS receptor component mCD14, and phagocytic activity. However, this study showed no effect of heat treatment on neutrophil influx, suggesting that IL-8

release after PM exposure may be LPS-independent (121). Similarly, forest fire-related $PM_{2.5}$ was found to be relatively high in LPS, and this appeared to increase release of TNFα from rat alveolar macrophages (122), building on earlier observations that LPS may prime macrophages to release TNFα in response to particulate matter (123). Compared to macrophages, epithelial cells seem to respond less vigorously to LPS, and this may be due to varying levels of membrane CD14 expression between different cell types (124, 125), although a CD14-independent mechanism of TLR4 activation by LPS has also been proposed (126). Inhalation of LPS can increase epithelial expression of phosphorylated p38, and also translocation of this signalling molecule into the nucleus, and this is accompanied by increased IL-8 expression, suggesting a role for p38 mitogen-activated protein kinase (MAPK) in LPS-induced cytokine release (127). Other markers of inflammation, such as IL-6, IL-8, and monocyte chemotactic protein-1 (MCP-1), have been found at higher levels in bronchoalveolar lavage fluid (BALF) after exposure to LPS, with simultaneous observation of an increase in protein permeability of the epithelium, suggesting that LPS is able to injure the airway epithelium (128).

1.4.2 Aeroallergens

Particles are shed from almost all living organisms, and many of these are able to act as allergens. Living sources of airborne allergens include house dust mites (HDM), pollens, fungi, and animals (129), and there are various groups of allergens, including glycosidases, oxidative stress response proteins, and enzymes involved in protein and carbohydrate metabolism (130). House dust mite faecal pellets are one such source of allergens, and indeed contain allergens which exert their activity by different mechanisms. For example, the carbohydrate polymer β-glucan in house dust mite faeces has been shown to induce CCL20 (MIP3α) release from 16HBE cells *via* a dectin-1-like receptor (131). Interestingly, β-glucan is found in fungal cell walls, and it may be the case that the β-glucan in HDM faeces is ultimately derived from fungi, which have been ingested by the dust mites (132). Another interesting mechanism of action of aeroallergens is *via* TLR4. Hammad and co-workers showed that HDM extract is able to induce changes characteristic of allergic asthma in the airways of mice

in a manner dependent on airway epithelial expression of TLR4. This was ascribed in part to low but detectable level of LPS in the HDM extract, although differences in response compared to LPS alone implied roles for other components as well (133). Indeed, the work of another group in the same year suggested that the HDM allergen Der p 2 shared functional as well as structural homology with MD-2, the LPS-binding component of TLR4. As such, Der p 2 is able to promote a T-helper cell type 2 (Th2)-type response to LPS under conditions of exposure to very low levels of LPS, and so HDM faecal pellets may possess a "double hit" of low levels of LPS, and a mechanism to facilitate its interaction with, and activation of, TLR4 (134). However, particular interest has focused on particles with protease activity. Sources of such airborne proteases include fungi of genera *Alternaria*, *Aspergillus*, *Penicillium* (135-138), house dust mite faecal pellets (139), and German cockroach extract (140).

Exogenous proteases can be detected by cellular protease-activated receptors (PARs). These are receptors with seven transmembrane domains, coupled to an intracellular G-protein. The protease cleaves a section of the protein near the N-terminal, which then acts as a tethered ligand to activate the protein (141) (Figure 1.6). PARs are predominantly activated by serine proteases, although there is some heterogeneity between the activities of different serine proteases at different PARs, with PAR-2 being activated by trypsin-like proteases, while PARs -1. -3, and -4 are activated by thrombin (142). Additionally, there is debate over whether cysteine proteases play a role in activating PAR-2 (142, 143). Indeed, recent evidence also suggests a possible role for aspartate proteases in PAR-2 activation, although at the time of writing this has only been observed by one group (144, 145) – scant evidence compared to that which supports the role of serine proteases. Activation of these protease receptors has been seen to result in increased release, from epithelial cells, of pro-inflammatory cytokines such as IL-6, IL-8, GM-CSF, and also increased thymic stromal lymphopoietin (TSLP) release (135, 136, 142, 145-149). Furthermore, airborne proteases appear able to degrade tight junctions by virtue of direct proteolytic activity on tight junction proteins (150-152). This may then result in a loss of epithelial barrier function allowing permeation of allergen through the epithelium (15).

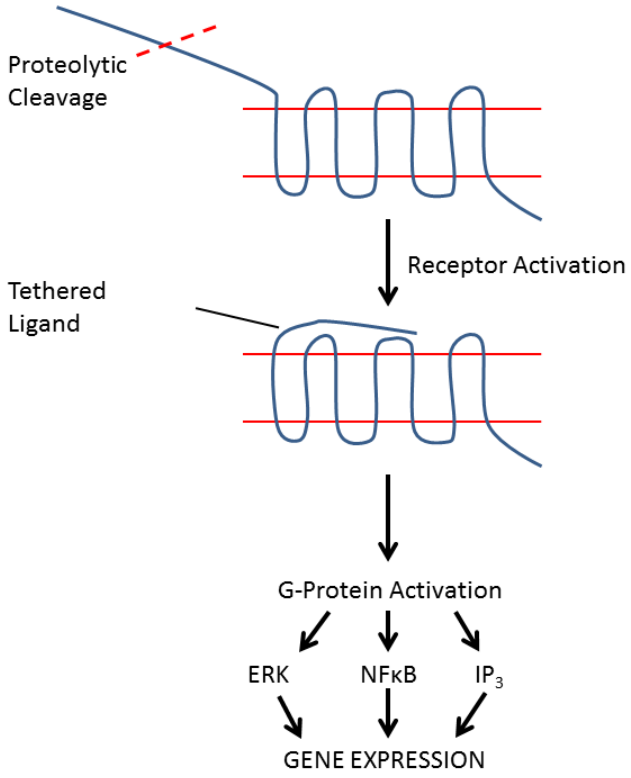

Figure 1.6. Cleavage of protease-activated receptors.

Protease-activated receptors possess a long extracellular N-terminal sequence. Proteases cleave this section of the peptide at a position which depends on the protease and the receptor being activated. The truncated N-terminal sequence is then able to bind its receptor which is located on one of the extracellular loops (varying between PAR family members). Activation of the receptor by the tethered ligand results in intracellular G-protein activation and modulation of gene expression by varying mechanisms. Adapted from (153, 154).

Several authors have noted that there is a significant link between sensitivity to *Alternaria* and asthma (155-158). At the cellular level, it has been suggested that activation of PAR-2, achieved in this instance by an activating peptide mimicking the tethered ligand of PAR-2, can sensitise mice to ovalbumin, resulting in an IgE response, in a sensitisation process involving TNFα (159). Conversely, a recent study suggested that the link between exposure to moulds and asthma was greater in non-atopic children than in those with atopy (160). Of further relevance to asthma, proteases from fungi of the genus *Alternaria* have been observed to stimulate human peripheral blood eosinophil degranulation, in a manner apparently involving PAR-2 which is, in eosinophils, the only functioning PAR (144, 161). Finally, mice exposed to

fungal spores (genera *Alternaria* or *Cladosporium*) after sensitisation exhibited a number of changes characteristic of asthmatic processes, such as increased mRNA expression of Th2-type cytokines, and also structural changes indicative of airways remodelling (162).

1.4.3 Diesel exhaust particulates (DEP) and Organic Species

In urban environments, up to 40% of the airborne PM_{10} may be DEP (163), although there may also be significant contribution from road wear and tyre wear (164-166). DEP are composed of an elemental carbon nucleus to which are adsorbed a wide range of organic compounds such as polyaromatic hydrocarbons (PAH), quinones, and aldehydes, and also transition metal-containing compounds, which may include iron, copper, nickel, vanadium, manganese, and chromium, in various oxidation states depending on the non-metal elements present (167-169). Because of the diverse nature of their constituents, DEP are able to exert a wide range of effects following inhalation, particularly involving redox-sensitive signalling pathways (170). The ability of DEP to induce production of the superoxide and hydroxyl radical ROS has been noted to be partly dependent on a fraction of the DEP which can be removed by washing with methanol, implicating organic solvent-extractable species in this part of the activity of DEP. There was also a significantly higher mortality after intratracheal installation of DEP in mice compared to methanol-washed DEP, accompanied by reduced activity of enzymes involved in the antioxidant defence. The increased mortality could be abrogated by pre-treatment with antioxidants (171). Further *in vivo* studies have suggested that DEP-induced mortality in mice may be *via* pulmonary oedema following endothelial cell damage (168, 171). DEP instillation in mice results in increased influx of neutrophils into the BAL fluid, with decreased levels of macrophages until 24h-post instillation, possibly due to deleterious effects of DEP on macrophages post-phagocytosis, and these effects were far more pronounced with DEP than with instillation of activated charcoal as a control (168). The same group subsequently showed that the pathogenic effects of DEP in mice, such as increased inflammatory cell infiltration, goblet cell hyperplasia with mucus hypersecretion, and airway hyperresponsiveness, symptoms similar to those of asthma, could be reduced

by administration of superoxide dismutase conjugated to polyethylene glycol (PEG-SOD), implicating DEP-derived superoxide radicals in the pathogenicity of DEP (167). Indeed, DEP has also been shown to deplete antioxidants in lung lining fluid *in vitro*, although without similar effects in humans *in vivo*, suggesting that healthy airways can cope with this level of oxidative attack (172). Indeed, at the same time an increase in the antioxidant glutathione is seen *in vivo*, most likely as a protective mechanism against oxidative attack (172, 173). Further evidence for the role of ROS comes from a study by Han and colleagues, using L-band electron spin resonance spectroscopy in conjunction with a nitroxyl radical probe to show that there is significant hydroxyl radical generation *in vivo* after intratracheal DEP instillation (169). In contrast to the results of Sagai and co-workers (171), this study showed that radical production was attributable to the presence of iron, although there was no analysis to determine whether this iron was endogenous or DEP-derived (169). However, other groups have also attributed a significant component of DEP-generated hydroxyl radical generation to the presence of iron (174). Therefore, research suggests that oxidative effects may derive from either the organic or transition metal components of DEP, or both. Volatile organic compounds (VOCs) and PAH have been noted as components of DEP, but are also found in urban particulates, where they have been suggested to exert toxicity toward A549 cells, possibly *via* metabolic activation by cytochromes P450 (CYPs) (175, 176).

In terms of the barrier function of the airway epithelium, a recent study has indicated that DEP can lead to a reduction in tight junction occludin levels in 16HBE cells, seemingly *via* redistribution rather than decreased expression levels, and that this is accompanied by a reduction in the transepithelial electrical resistance of the epithelial layer. However, a co-culture of 16HBE cells with macrophages and dendritic cells showed resistance to this effect of DEP, perhaps due to a combination of increased cell number in the co-culture, resulting in reduced DEP burden per cell, and the action of macrophages in clearing DEP before effects on epithelial cells become apparent (177).

In vivo, DEP exposure has been observed to result in decreased lung function and increased sputum neutrophil counts of mild and moderate asthmatics (178), although

this study was not powered to examine differences between healthy and asthmatic subjects. Furthermore, a similar neutrophilic response has been seen in the airways of healthy subjects after controlled exposure to diesel exhaust in a laboratory (173). A study comparing healthy and asthmatic airway responses found that neutrophilic inflammation, with airway neutrophilia and increased bronchial wash IL-6, was seen following DEP exposure only in healthy subjects, while this response was absent in mild-moderate asthmatic airways (179). While there is general agreement between these studies in terms of the ability of diesel exhaust to elicit a neutrophilic inflammatory response in healthy subjects, the discrepancy in asthmatic responses may relate either to phenotypic differences in the asthmatic subjects between studies or, perhaps more likely, differences in the diesel exhaust itself – while the study showing lack of response in asthmatics was laboratory-based and used exhaust direct from the exhaust pipe, with the engine operating in a regulated manner (179), the study showing neutrophilic inflammation was performed in a "real world" setting (Oxford Street, London), with engines of varying capacity, operating at different speeds and possibly with some idling (178). Furthermore, if the DEP are either re-entrained by traffic movement in roadside experiments, or have been aged for laboratory experiments, it is likely that they will have lost much of their VOC content. Therefore, there is likely to be some inter-study heterogeneity in the physicochemical properties of the exhaust to which subjects were exposed.

Although it is beyond the scope of this review to discuss the cardiovascular toxicity of DEP, which has been reviewed elsewhere (87, 180), research suggests that diesel exhaust can inhibit clot breakdown *via* reduced release of profibrinolytic tissue plasminogen activator in humans (181, 182). Furthermore the vasodilatory effect of a number of endothelial-dependent and -independent vasodilators is reduced by diesel exhaust exposure (181), while, at least in coronary heart disease subjects, diesel exhaust appears able to induce myocardial ischaemia (182). Therefore, diesel exhaust seems able to interfere with both vascular tone and endogenous anticoagulant mechanisms (183).

1.4.4 Transition Metals

Transition metals are of particular interest in particle toxicology as, due to their variable oxidation states, they are able to catalyse reactions involving electron transfer (184, 185), forming ROS, such as the superoxide anion $^{\bullet}O_2^-$, hydrogen peroxide H_2O_2, and hydroxyl radical $^{\bullet}OH$ (186), which can also be produced by PAH found in diesel particles and residual oil fly ash (ROFA) (187). Two properties of oxygen make it ideally suited to the formation of such species – molecular oxygen is abundant in the atmosphere, and it has a high affinity for electrons, allowing it to be relatively easily reduced (188).

The effects of transition metal-rich particulate matter has been studied using particles from a variety of specifically metal-rich sources, including steel mills and plants (58, 189, 190), smelting plants (60, 191), welding fume (192, 193), and fireworks (194).

ROFA is a metal-rich particulate generated by combustion of fossil fuels (53). The main transition metal components of ROFA are iron, nickel, and vanadium, but ROFA is remarkable for its vanadium content, which may constitute 4% of ROFA by mass, and may be the most predominant of all metals in ROFA (184, 195). Furthermore, the majority of metal content in ROFA is water soluble, and may constitute up to 10% of ROFA by mass in total (195, 196), and thus bioavailability of ROFA constituents may be greater than if the metal content was predominantly insoluble. Indeed, soluble components of ROFA have been suggested to be a crucial determinant of ROFA toxicity (53, 197-199). ROFA has been shown to elicit increased expression and release of several pro-inflammatory cytokines, an action which can generally be inhibited by metal chelators such as desferrioxamine (DFX), or free radical scavengers such as N-acetylcysteine (NAC) (200, 201). Vanadium has been suggested as being the constituent of ROFA which is primarily, although not solely, responsible for the inflammogenic and toxic effects of ROFA (202, 203).

Another source of transition metal-rich particulates is underground railway systems. Compared to particles in ambient air, underground railway particles contain high proportions of transition metals. Morphologically, underground particles are more

angular than those found above ground, suggesting that they derive from processes involving friction (67), either between wheel and rail, brake and wheel, or current collector and electrified third rail, including arcing of current (66, 70). The dominant transition metal in underground particles is iron, mainly in the form of magnetite (Fe_3O_4), as opposed to haematite (Fe_2O_3) in urban particles (204). However, copper, manganese, zinc, vanadium, and chromium have also been detected (79, 81, 205, 206). Iron is generally the focus of studies into transition metals in particulates, but there are several studies which also look at other transition metals, such as copper, nickel, vanadium, manganese, and tin. However, while studies have been performed on the constituents and physicochemical properties of underground PM, and also a limited number of epidemiological studies on underground staff and commuters, there has been little in-depth work performed *in vitro* to look at the biological effects of these particles, and this therefore validates the work contained in this thesis.

1.5 Nano-Sized Particles

The term "nanoparticle" is usually applied to particles measuring no more than 100 nm in at least one dimension (207). However, it is most commonly applied to particles of this size which are generated intentionally, that is to say those nanoparticles which are engineered. The use of such particles is increasing, examples being the use of titanium dioxide nanoparticles in sunscreen, paint, toothpaste, photocatalysis, and photovoltaic cells (208), carbon nanotubes, whose remarkable properties in terms of strength and thermal and electrical conduction give rise to many potential applications (209, 210), and quantum dots, whose size tends sufficiently towards that of individual molecules to allow them to exhibit quantum-state properties, giving rise to applications in electronics and computing (211). Conversely, particles fitting into this definition on account of their size but which are generated environmentally are more commonly referred to as "ultrafine particles". The term "nano-sized particle" is often used as a catch-all term to emphasise that a particle has at least one dimension of no more than 100 nm, without making reference to its mode of generation. The root cause of the concern over the potential effects of nano-sized particles is their size. Although nano-sized particles have miniscule surface areas when considered on an individual basis,

their surface area/volume ratio is such that the total surface area of a relatively small mass of nanoparticles may be remarkably large. For example, when considering spherical nanoparticles of unit mass (i.e. 1 g/cm^3), a reduction in diameter from 10 μm to 1 nm results in an increase in total surface area from 0.6 m^2 to 6,000 m^2, roughly the area of a football pitch (see Table 1.2).

Diameter (μm)	Radius (μm)	Sphere Volume (μm^3)	Spheres Formed	SA/Sphere (μm^2)	Total SA (m^2)
10	5	5.24×10^{2}	1.91×10^{9}	3.14×10^{2}	0.6
1	0.5	5.24×10^{-1}	1.91×10^{12}	3.14	6
0.1	0.05	5.24×10^{-4}	1.91×10^{15}	3.14×10^{-2}	60
0.01	0.005	5.24×10^{-7}	1.91×10^{18}	3.14×10^{-4}	600
0.001	0.0005	5.24×10^{-10}	1.91×10^{21}	3.14×10^{-6}	6000

Table 1.2. Surface area of particles of decreasing diameter.
As particle diameter decreases, as long as total particle mass is held constant, there is a corresponding increase in total particle surface area (SA), allowing relatively small masses of particles to exhibit very large surface areas.

The corollary of the increased surface area/volume ratio of nano-sized particles is that a much greater percentage of the constituent molecules of the particle are located on the surface of the particle, and thus able to interact with the surrounding environment (212). Indeed, particle surface area has been proposed as an accurate exposure metric in nanoparticle toxicity (213-216). Correspondingly, studies examining the effects of nano-sized *vs.* fine particles of the same chemistry frequently find more pronounced deleterious and toxic effects with the nano-sized particles (217, 218). Furthermore, nano-sized particles are able to penetrate more deeply into the lungs, avoiding the trapping mechanisms of the upper and middle airways which are responsible for arresting the passage of larger particles, and reaching the terminal airways and alveoli (219). Clearance of particles from the alveoli is much slower than from the upper airways (20), and it appears that macrophages are less able to clear nano-sized particles than they are larger particles, potentially increasing the persistence of such particles (220). Indeed, for particles such as fibres or graphene platelets, whose morphology deviates sufficiently from the spherical, there exists the risk of frustrated phagocytosis,

where phagocytic uptake of nano-sized particles by macrophages has commenced but cannot be completed due to the excessive size of the particle in other dimensions (221, 222).

Once deposited within the lungs, the nano-scale dimensions of such particles makes them susceptible to uptake by epithelial cells, and this has been proposed to be another reason for the toxicity of nano-sized particles. For instance, titanium dioxide and carbon black nanoparticles have been seen to be taken up by both 16HBE bronchial epithelial cells and MRC5 fibroblasts, although with differing time courses and concentration-response relationships (223), while A549 alveolar epithelial cells and LK004 fibroblasts have been reported to take up nanoparticles more readily than 16HBE or Calu-3 bronchial epithelial cells (224). Indeed, working groups have suggested that nano-sized particle internalisation may be a potential dose metric for monitoring particle toxicity (225). However, quantitative assessment of particle uptake by traditional transmission electron microscopy is extremely time-consuming, and measurement by the use of fluorescently-tagged nanoparticles or chemical analysis does not permit differentiation between particle uptake and particle adhesion to the exterior of the cell membrane. However, new techniques for faster throughput analysis of particle internalisation are being developed by integrating multiple outcome measures, such as FACS data and quantitative confocal laser scanning microscopy (226). Particle uptake may play a role in translocation of nanoparticles to the underlying tissue, and potentially to the circulation, possibly to a greater extent than mechanisms facilitating paracellular particle movement (227). Technetium-radiolabelled nanocolloids (representing nanoparticles) have been found to translocate to multiple organs, mainly the liver, but also the heart, kidneys, spleen and brain following intratracheal instillation in hamsters (228), although there has since been debate regarding the stability of the radiolabel. Furthermore, translocation of nanoparticles to the lymph nodes has been observed in rodent and rabbit models (222, 229-231).

Unlike PM_{10} and $PM_{2.5}$, nano-sized particles are often studied as single chemical particles, and there is therefore less capacity for debate about which component molecules are responsible for any observed effects. To this end, engineered

nanoparticles are often used for studies examining the fundamental aspects of particle-cell interactions or of single chemical species. Such studies have emphasised that responses to nanoparticles may differ according to composition of the nanoparticle, although different nanoparticles may cause varying changes in a range of markers of inflammation in terms of cytokine release, cell death, BALF protein, and neutrophilic/eosinophilic inflammation (232). Indeed, nanoparticle studies have shown that not only does assessment of inflammation depend on the endpoints examined, but that the observed effects can differ depending on the cell type examined (233). However, recent research using nanoparticles has attempted to determine the fundamental causes of toxicity, which would facilitate high throughput screening of nanoparticles for toxicity. For instance, contrary to the popular oxidative stress paradigm (234, 235), haemolysis, rather than the ROS-detecting dichlorofluorescein (DCF) assay or spin trapping with electron paramagenetic resonance (EPR) measurements, was the best predictor of metal oxide nanoparticle-induced inflammation in rats (236), while the same group have also suggested zeta-potential (the electrical potential between particle surface and the surrounding milieu) and particle solubility to be key determinants of metal and metal oxide nanoparticles (237). At a more fundamental level, analysis of the band gap in metal oxide nanoparticles (the energy gap between the valence band and conduction band of a material) has yielded promising results in predicting the inflammogenicity and oxidative stress generated by nanoparticles (238).

In spite of the aforementioned advances in knowledge, nanotoxicology is a relatively new field. Indeed, there is no consensus over the most relevant dose metric to use, termed the biologically effective dose (239, 240), nor which outcome measures are the most relevant. In the meantime, concern over the potential health risks associated with proliferation of engineered nanoparticles will mount, meriting extensive examination (241).

1.6 Free Radical Generation

Free radicals and ROS play important roles in normal physiology. For example, they are generated by, and are intrinsic to, the mitochondrial electron transport chain, part of oxidative phosphorylation (242), are produced by nicotinamide adenine dinucleotide (phosphate) (NAD(P)H) oxidases in phagocytes (188), and play important roles in cell signalling (243, 244). However, an excess of these species, which may arise from exposure to exogenous generators of ROS, can prove extremely damaging. In addition to ROS, reactive nitrogen species (RNS) such as nitric oxide ($NO^{\bullet}$) and peroxynitrite ($ONOO^{-}$) may be produced by reaction of ROS with nitrogen-containing species (185).

The superoxide anion can participate in the formation of the highly reactive hydroxyl radical, which owes its reactivity to a rate constant so high that reactions with biomolecules are limited only by rate of diffusion to the reaction site (174, 188). The hydroxyl radical is postulated to cause the majority of ROS-mediated damage, as shown below, and summarised by van Klaveren (245):

$$Fe^{2+} + O_2 \rightarrow Fe^{3+} + {}^{\bullet}O_2^{-}$$

$$Fe^{2+} + {}^{\bullet}O_2^{-} + 2H^{+} \rightarrow Fe^{3+} + H_2O_2$$

$$Fe^{2+} + H_2O_2 + H^{+} \rightarrow Fe^{3+} + H_2O + HO^{\bullet}$$

In the presence of hydrogen peroxide, the reactions follow a slightly different course according to the Haber-Weiss reaction, recycling the iron between oxidation states, and thus allowing a very small amount of iron to catalyse the formation of a much larger quantity of hydroxyl radicals (246):

$$Fe^{3+} + H_2O_2 \rightarrow Fe^{2+} + {}^{\bullet}O_2^{-} + 2H^{+}$$

$$Fe^{3+} + {}^{\bullet}O_2^{-} \rightarrow Fe^{2+} + O_2$$

$$Fe^{2+} + H_2O_2 + H^+ \rightarrow Fe^{3+} + H_2O + HO^{\bullet}$$

This last reaction is the so-called Fenton reaction, the crucial step in formation of the hydroxyl radical. Similar reactions can occur with other transition metals instead of iron, and thus airborne particulates with a significant transition metal component can generate ROS in the airways (247). However, these reactions may occur at different rates with different transition metals. For example, it has been postulated that copper is more efficient in the catalysis of hydrogen peroxide generation than is iron, whereas iron is most effects in catalysing the Fenton reaction, and so generation of hydroxyl radical from molecular oxygen is optimally achieved with a modest concentration of copper to form hydrogen peroxide, and a high concentration of iron to convert the hydrogen peroxide to hydroxyl radical, with synergy between the two metals (248, 249). Ironically, there is evidence that antioxidants, such as citrate and ascorbate, present in lung fluid, can increase ROS generation, by reducing transition metals to lower oxidation states (e.g. Fe(III) → Fe(II) and Cu(II) → Cu(I)), thus facilitating their continued participation in these reduction reactions (250). Indeed, superoxide dismutase (SOD) has been postulated to increase the generation of hydroxyl radicals *in vivo* under some circumstances, by facilitating dismutation of superoxide to hydrogen peroxide (169).

The ability of transition metals to participate in redox reactions depends upon solubility and redox state. For example, some of the iron found in particulate matter is in the form of insoluble iron (III) oxide, more commonly known as "rust", which is fully complexed and thus unable to take part in redox reactions (251). Conversely, underground railway PM iron may be predominantly magnetite (Fe_3O_4) or metallic iron (204, 252) Studies have also shown that the majority of soluble iron released by urban particulates is ferric rather than ferrous (251). Moreover, the solution in which the transition metals are found can affect oxidant production, with suggestions that oxidant production *in vitro* is significantly higher in phosphate buffered saline (PBS) than in Hanks' balanced salt solution (HBSS) or 1,4-piperazinediethanesulphonic acid (PIPES) buffers (253).

It is also postulated that inhaled particulate matter can cause increased levels of ROS *via* perturbation of intracellular, endogenous ROS production. There are two principle sources of endogenous ROS production – the mitochondrial electron transfer chain, and NAD(P)H oxidase systems, with those found in neutrophils and macrophages being especially relevant in the context of airway inflammation (254). Certainly there are reports that the ultrafine fraction of PM is able to penetrate into the mitochondria, causing mitochondrial injury, which may lead to escape of ROS into the cytosol (255). Titanium dioxide and zinc oxide nanoparticles have also been shown to exert deleterious effects upon mitochondria, including increased mitochondrial ROS generation, reduced mitochondrial mass, reduced mitochondrial transmembrane potential, and possibly uncoupling of the electron transport chain from adenosine 5'-triphosphate (ATP) synthase (256-258), with the potential for dysfunction to be displayed by first and second generation cells (256). Furthermore, mitochondrial haplotype may influence susceptibility to the effects of air pollution, since people of mitochondrial haplotype H (tightly coupled electron transport chain, greater ROS production) showed a greater response of plasma TNFα and IL-6 to traffic-related air pollutants and ultrafine PM than did people of mitochondrial haplotype U (looser electron transfer coupling, lesser ROS production) (259). Indeed, the cellular production of ROS has been cited as a source of underestimation of particulate ROS production when assayed in cell-free procedures (260).

In vitro, the standard method for measurement of ROS is dichlorofluorescein diacetate (DCF-DA). This reagent is taken up by cells into the cytosol, where cytosolic esterases cleave the two acetate groups, forming DCF, which reacts with intracellular peroxides to form a fluorescent product. This can then be quantified or detected using a fluorescence microscope. Other methods have been assessed, but none have superseded DCF-DA as the standard reagent (261).

Particulate matter has been shown to have varying capacity to generate ROS, which is dependent on both particulate size and particulate composition. In turn, these characteristics are specific to the source of, and processes involved in, the generation of, the particles. Ohyama and colleagues showed that, on an equivalent mass basis, diesel exhaust particulate generated more hydroxyl radicals in macrophages than did

ambient particulate matter. Furthermore, while carbon black was less able to generate hydroxyl radicals, nano-sized carbon black (average particle size 1.8 nm) generated a greater level of hydroxyl radicals than did fine carbon black (132.8 nm). However, while the ambient particulate matter caused increased chemiluminescence in macrophages, indicative of increased superoxide production, DEP did not. Similarity in size between DEP and ambient PM in this research suggests that the differences were due to differences in particle composition (262). On the other hand, conflicting evidence suggests that ultrafine carbon particles may have deleterious effects *in vivo*, despite the relatively inert nature of carbon (263). This may indicate that particulate matter can have effects *per se*, regardless of chemical composition, although this is possibly only relevant at the ultrafine level due to diminishing surface area/volume ratios in higher size fractions. In fact, with the emergence of nanotoxicology and a shift in focus towards materials in the nano-sized range, the relevance of surface area *vs.* composition has led some to propose that studies should dispense with the notion of particulate mass as a dose metric, and should instead use surface area or even oxidant activity (oxidative potential), as a dose metric (213, 235, 264). Indeed, it is apparent that the concentration of PM within a well *in vitro* does not necessarily represent the PM delivered to the cells (225), and determination of PM concentration as opposed to the concentration of PM components may also be complicated by the varying solubility of particles and PM components (265).

1.7 Oxidative Stress

The lung has a number of mechanisms to deal with oxidative stress, arranged in a hierarchy dependent on the levels of oxidative stress experienced. Initially, production of antioxidants such as glutathione (GSH) and ascorbic acid (172, 173), and enzymes involved in defence against oxidative stress such as HO-1, is induced *via* the nuclear factor (erythroid-derived 2)-like 2 (Nrf2) pathway and the antioxidant response element (ARE) (266). Exposure of murine macrophages to underground dust showed increased HO-1 expression compared to macrophages treated with carbon black (80), while mice exposed to urban particulate matter have exhibited a decreased GSH/GSSG ratio accompanied by increased levels of catalase, and also increased

markers of oxidative stress such as 8-isoprostane (a product of arachidonic acid oxidation) and thiobarbituric acid reactive substances (TBARS), both products of lipid peroxidation (267). At higher levels of oxidative stress, an inflammatory response is seen, co-ordinated by nuclear factor κB (NF-κB) and activator protein-1 (AP-1), resulting in the increased release of inflammatory cytokines and chemokines (170, 268). Indeed, a study of cigarette smoke-induced changes in gene expression by oxidative stress has found increased expression of a disproportionately high number of genes with NF-κB and activator protein 1 (AP-1) binding sites (70). These responses are vital as, if they are overwhelmed, cell death may occur as evidenced by increased activation of caspases in response to transition metal challenge in lung epithelial cells (269, 270). These levels of protection against oxidative stress are shown in Figure 1.7.

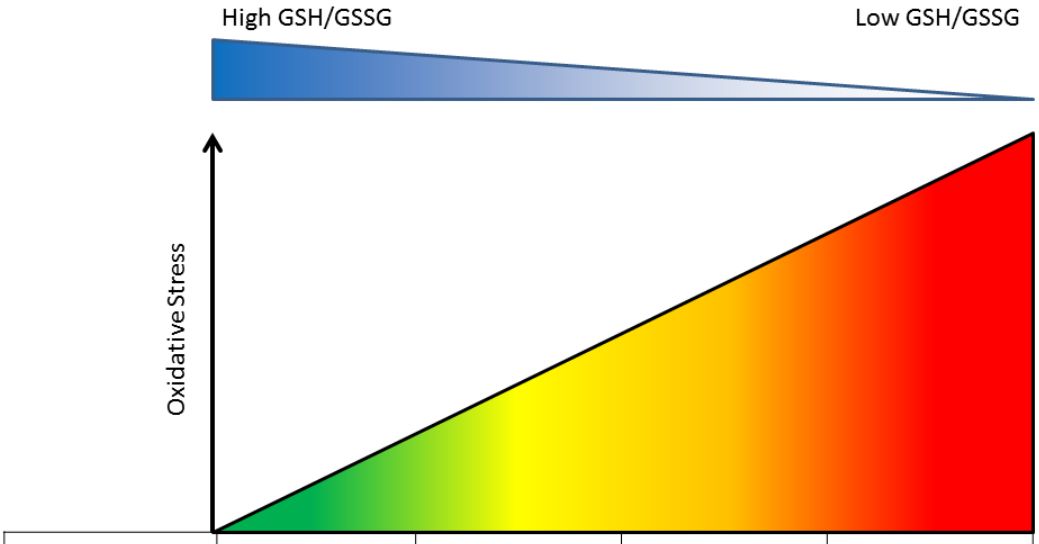

Response Type	None	Antioxidant	Inflammatory	Cytotoxic
Signalling		Nrf2	MAPK/NF-κB	Mitochondrial Electron Transfer
Outcome		Phase II Enzymes	Cytokines Chemokines	Apoptosis

Figure 1.7. The hierarchical response to oxidative stress.

At low levels of oxidative stress, the ratio of reduced/oxidised glutathione is high. The cell may respond with increased production of antioxidants, such as GSH and bilirubin, produced by the enzyme haemoxygenase-1 (HO-1). Such a response is regulated by the transcription factor Nrf2. At higher levels of oxidative stress, where the antioxidant mechanisms are overwhelmed, inflammatory processes such as cytokine release are activated by the MAPK and NF-κB signalling pathways, and lead to responses orchestrated by the transcription factors NF-κB and AP-1. At levels of oxidative stress above this, the majority of glutathione exists in the oxidised form (GSSG), mitochondrial membrane potential is perturbed, cytochrome c is released, and the permeability transition (PT) pore in the mitochondrial membrane is opened, resulting in cell death. Adapted from (271, 272).

1.7.1 Signalling Pathways Involved in the Response to Oxidative Stress

Nrf2 is thought to play a key role in the maintenance of intracellular redox status in the face of lower levels of oxidative stress. Nrf2 is a transcription factor which plays a role in regulation of the ARE (273). Nrf2 is normally localised to the cytosol, bound to Kelch-like ECH associated protein 1 (Keap1), which is attached to the cytoskeleton and targets Nrf2 for ubiquitination and subsequent degradation (274). A recent study has shown that Keap1 deletion, seemingly disinhibiting Nrf2, can increase expression of over 50 genes whose products are involved in antioxidant and detoxification processes. After Keap1 deletion *in vivo*, applied to Clara cells only, and H_2O_2 exposure, levels of H_2O_2-derived ROS were lower while the deletion of Keap1 ameliorated the effects of oxidative stress in mice after inhalation of cigarette smoke, observed as a blockage of cigarette smoke-induced increase in BAL macrophage numbers. *In vitro*, the same deletion applied to BEAS-2B cells also showed an abrogation in ROS levels after H_2O_2 exposure (274). These results suggest that Keap1 deletion upregulates the antioxidant response *in vivo*.

While not all antioxidant enzymes appear to be regulated by Nrf2, for example catalase, glutathione peroxidise, and SOD2, many others are, such as HO-1, SOD3, NAD(P)H-quinone oxidoreductase 1 (NQO1) and glutathione S-transferase (GST)-Ya (275). It has been found that, in the presence of DEP, RAW 264.7 macrophages exhibited activation of ARE, seen with an increase in translocation of Nrf2 to the nucleus. Furthermore, knockout of Nrf2 led to a significant drop in levels of HO-1 expression. Increased levels of Nrf2 were shown to be *via* post-transcriptional modification of Nrf2, whereby DEP increases Nrf2 half-life, resulting in increased antioxidant response element (ARE) activity (275). Nrf2-controlled genes are also upregulated by the Nrf2 activator sulforaphane (276), found naturally in cruciferous vegetables, and application of sulforaphane to primary bronchial epithelial cells reduced the ability of DEP to stimulate their increased release of IL-8, GM-CSF, and IL-1β (277). Another group extended these findings to an *in vivo* situation whereby Nrf2 knockout mice, following long-term exposure to DEP, showed increased airway

hyperresponsiveness, mucous cell hyperplasia, and reduced total cell and macrophage counts in BALF, but increased eosinophil counts, which may be linked to the observed increased IL-13 level which accompanied increased IL-12. Furthermore, a battery of antioxidant enzymes showed reduced mRNA levels in the Nrf2 knockout mice post-DEP (278)

The transcription factor NF-κB has been shown to play a major role in the increased synthesis and release of inflammatory cytokines and chemokines following exposure to particulates, and in the response to oxidative stress. Increased NF-κB-DNA binding activity has been observed in the airways of rats exposed to airborne iron when compared to the effects of airborne soot, but this only becomes significant when soot and iron are applied together, suggesting synergism *via* an unknown mechanism (279). Conversely, in PM_{10} from Provo, Utah, copper was found to be the component responsible for inflammation with NF-κB activation, underlining the variability in response, possibly due to interaction with cellular defence mechanisms such as ferritin, lactoferrin, and the copper chelator caeruloplasmin (190).

Similar effects on NF-κB were found in L132 cells exposed to $PM_{2.5}$ from Dunkirk, with concentration-dependent increases in cytosolic phosphorylated inhibitor of NF-κB-α (IκB-α) and cytosolic phosphorylated NF-κB p65, concomitant with increased DNA binding of p50 and p65 subunits of NF-κB (280). Iron and selenium have both been seen to elicit increased nuclear translocation of the p65 (RelA) subunit of NF-κB, accompanied by increased release of IL-8 and MIP-1 in A549 cells, which could be inhibited by the NF-κB inhibitor BMS345541 (281). Exposure of rat airway epithelial cells, in a tracheal explant model, to urban PM led to NF-κB activation which could be inhibited by TMTU, DFX, PP2 (a Src inhibitor), and an epidermal growth factor receptor (EGFR) inhibitor. Interestingly, particle uptake, but not NF-κB activation, was inhibited by colchicine, suggesting that particle uptake is not a prerequisite for NF-κB activation (282). The mechanism by which NF-κB-induced cytokine release is activated has been studied in HUVECs for chlorides of cobalt and nickel, with results suggesting that there is no intermediate cytokine pathway involved, and that activation involves ROS-dependent mechanisms in some form (283). A recent report has indicated that inhalation of ultrafine elemental carbon particles can increase NF-κB

activation in rats and also act as an adjuvant to ovalbumin (284). Furthermore, the adjuvant activity was sensitive to concomitant administration of the antioxidant N-acetylcysteine, suggesting that some of the effects of inhaled PM, at least for the ultrafine fraction, although dependent on redox mechanisms, may be independent of transition metal content (284).

The upstream mechanisms involved in NF-κB activation are the subject of current research, but appear to involve increased levels of intracellular calcium ions, due to both release from intracellular stores and influx from the extracellular milieu (285). This results in activation of NF-κB *via* a MAPK cascade. It should be noted, however, that there are other signalling pathways which can result in activation of phosphorylation of the inhibitor of NF-κB, IκB, and thus uncoupling, permitting nuclear translocation of NF-κB. There is much interconnectivity and interplay between some of these pathways, rendering isolation for study difficult (286). There may also be pathway redundancy, meaning that knockout of a pathway which is normally operational has no observable consequences when responses to certain challenges are assessed. In agreement with the argument favouring the involvement of several pathways, DEP has been found to activate extracellular signal-related kinase (ERK) 1/2 and p38 MAPK pathways in addition to NF-κB in 16HBE cells (287).

1.7.2 Antioxidant Defences Against ROS/RNS

Antioxidants have three roles – to prevent formation of pro-oxidant species, to scavenge ROS/RNS, and to repair or remove molecules damaged by oxidation. The most important enzymatic first line of defence against superoxide is SOD, of which various isoforms exist, including cytosolic Cu/Zn SOD, mitochondrial MnSOD, and extracellular SOD (288). Catalase degrades H_2O_2 at high concentrations and glutathione, while not an enzyme itself, is reliant on several inducible enzymes for its synthesis and action.

GSH is a thiol antioxidant tripeptide with the sequence gly-cys-glu, and plays a role in both antioxidant defence, particularly against low concentrations of H_2O_2, and

intracellular monitoring of redox status. ROS are able to oxidise the thiol group of the cysteine residue of GSH, and thus two oxidised thiol groups on separate GSH molecules can combine to form a disulphide bridge in the oxidised form of glutathione (GSSG), a reaction catalysed by glutathione peroxidase (GPx). GSSG can then be recycled back to GSH in a reaction catalysed by GSH reductase, or alternatively excreted from the cell (254). These reactions are illustrated in Figure 1.8. In the lungs, the first line of defence is extracellular GPx (eGPx), found in the epithelial lining fluid, whose function is to neutralise ROS before they reach the epithelial cell barrier (289)

A protective effect of GSH is supported by work showing that the increased release of TNFα by alveolar macrophages after exposure to ultrafine nickel is reduced by treatment of the cells with a monoethyl ester of glutathione, an effect also observed with another thiol antioxidant, NAC (263). The protective effect of GSH against DEP-induced lung injury has also been observed after inhalation of DEP by healthy volunteers. Bronchial inflammation was observed, as marked by increased IL-8 levels and neutrophil counts, but no such responses were seen in the alveolar compartment where, unlike in the airways, increased levels of reduced glutathione and urate were found, suggesting a reciprocal association between levels of these antioxidants and severity of inflammation (173).

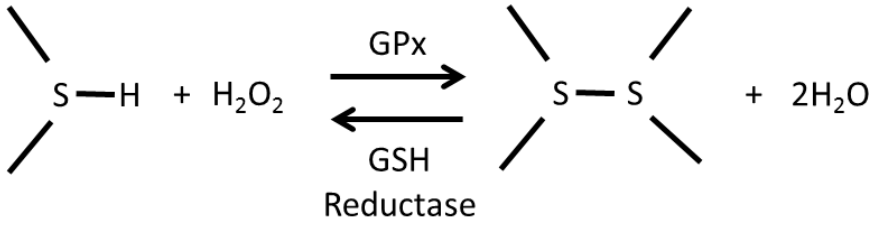

Figure 1.8. The reaction of the ROS hydrogen peroxide with the cysteine sulphydryl group of an antioxidant.

In the case of glutathione, as catalysed by glutathione peroxidase (GPx), this reaction results in the formation of GSSG – two glutathione molecules linked by a disulphide bridge after sulphydryl group oxidation, along with the production of two molecules of water. GSSG can then be recycled back to GSH by glutathione reductase. In this way, glutathione acts "sacrificially" to reduce oxidation of other intracellular species.

Another antioxidant of interest is HO-1, an inducible enzyme which catalyses the degradation of haemoglobin to biliverdin, a potent antioxidant. HO-1 expression is under the control of Nrf2, and can be induced in response to oxidative stress from numerous sources (275, 278, 290) and by cigarette smoke extract (291). This induction of Nrf2-activated HO-1 expression has been suggested to be controlled by ERK in BEAS-2B cells exposed to silica nanoparticles (292), while other authors have noted the role of PI3 kinase in controlling the Nrf2/HO-1 response in A549 cells exposed to roadside $PM_{2.5}$ (293). HO-1 is a quantifiable marker of oxidative stress, and it has been shown that ambient PM of the ultrafine fraction is more potent, than fine or coarse PM on a mass concentration basis, at inducing HO-1 expression in RAW 264.7 and BEAS-2B cells (255). However, contradictory results have shown oxidative damage to DNA without any corresponding increase in HO-1 expression (294).

It is therefore clear that there are a multitude of antioxidants involved in protection against oxidative stress. This multiplicity may be of some benefit in case of depletion of one or more of these antioxidants, but it has also been suggested that different antioxidants are involved in protecting the cell in the face of different reactive species (295).

1.8 Effects of PM on the Inflammatory Response

When cells mount an inflammatory response to inhaled particulate matter, a number of changes in cytokine release may be seen. Fujii and colleagues observed an increase in release from PM_{10}-challenged primary human bronchial epithelial cells of IL-8, IL-1β, and GM-CSF, with no change in release of IL-6, regulated upon activation, normal T-cell expressed and secreted (RANTES), TNFα, or MCP-1 (296). In accordance with this, Gilmour and co-workers found increased release of IL-8 from A549 epithelial cells treated with PM_{10} and hydrogen peroxide (297), while the same cell line exposed to $PM_{2.5}$ from Rome also caused time and concentration-dependent increases in IL-6 and TNFα (298). Lindbom and colleagues found that underground railway particles were more potent than particles generated by studded tyres on a granite pavement in eliciting release of TNFα from BEAS-2B epithelial cells, and that they increased TNFα

and IL-8 release from macrophages, although to a lesser extent than did the street particles, suggesting differences between cell types (299). Increased IL-8 release was also observed by Hetland and colleagues after exposure of A549 cells to urban particulate matter, with approximate equipotency between coarse, fine, and ultrafine fractions, and similar results for IL-6, although for this cytokine the fine fraction of particles were slightly more potent than the coarse fraction (300). This study also failed to find a significant increase in potency for mineral-rich road particulates over urban ambient PM (300).

Increased IL-8 has also been observed in BALF *in vivo* after exposure to diesel exhaust (173), while increased IL-6 and IL-8 expression at the mRNA and protein level have been seen after exposure of epithelial cells to ROFA *in vitro* (201), attributed to the presence of vanadium, but not iron or nickel. Indeed, the role of vanadium in eliciting an inflammatory response seems incontrovertible, and has been found by other researchers (301), and also tentatively associated with mortality *in vivo* by others (302), Other researchers claim that vanadium is toxic to the cardiovascular system but of lesser importance in respiratory toxicology (60).

Riley and co-workers found that vanadium chloride was the most toxic of a battery of metals chlorides tested in equimolar concentrations in a rat epithelial cell line, as measured by the methylthiazolyldiphenyltetrazolium bromide (MTT) assay (303). This was supported by a study showing that the inflammogenicity (by IL-6, TNFα, and macrophage inflammatory protein 2 (MIP-2)) of urban $PM_{2.5-0.2}$ was strongly correlated with vanadium, and also nickel content, with a weaker correlation for chromium, copper, and iron, and none for manganese or zinc, amongst others. However, the same study showed that $PM_{10-2.5}$-induced IL-6 release was strongly correlated with only manganese and zinc levels, illustrating the chemical heterogeneity of PM size fractions from the same source, although the variation in metal levels and the correlations with inflammation were greater for the urban $PM_{2.5-0.2}$ fraction, lending greater weight to the observations with this size fraction (304).

In addition to the aforementioned studies on ambient PM collected from the Utah Valley during periods of steel mill opening and closure, Schaumann and co-workers

found an increase in BAL fluid monocytes, IL-6, and TNFα, with no change in IL-8, after exposure of volunteers to particulate matter from an area with heavy smelting activity (191). These differing responses may be attributable to differing particle content. In support of this, a 2007 study found that underground railway PM elicited raised TNFα and MIP-2 release in murine macrophages, with an acute increase in BALF protein content, total cell, and neutrophil counts. Crucially, however, the study also showed differences between two sets of underground railway PM, with PM from a system using metal wheels and brakes being more able to induce MMP-12 from murine macrophages than PM from a system using wooden brakes and pneumatic tyres, with this difference being nullified by concomitant use of the iron chelator DFX (80). Zinc in fine PM from tyre wear and copper in coarse PM from brake wear have also been found to correlate with markers of cytotoxicity in rats (305).

Another study, using PM collected from three cities and subsequently assessed for transition metal content showed that transition metal-rich coarse PM caused an increase in many BALF markers of inflammation, including total cell, neutrophil, and macrophage count, and also BALF lactate dehydrogenase (LDH) and total protein levels, when compared to transition metal-poor coarse PM (306).

It has been postulated that, for coarse PM, the main determinant of toxicity is particulate composition, while for finer fractions composition becomes less important, possibly because the particle is able to penetrate further into the cell and cause chemistry-independent damage (255, 305, 306). Indeed, this would explain the apparent toxicity of ultrafine carbon black, which is able to cause obvious oxidative stress and inflammation while being chemically inert (41, 263, 307), although carbon black is generally less inflammogenic than airborne particulate matter (80, 262, 308).

Since many studies do not necessarily carry out elemental analysis of particulate composition, inter-study comparison is difficult. Indeed, it has even been suggested that the pro-inflammatory and oxidative stress responses may be caused by separate components of the particulate matter which may, in addition to metals, include VOCs and PAH, carbonaceous material, adsorbed allergens, and bacterial endotoxins such as LPS (306, 309).

There is also evidence to suggest that transition metals may interact with each other to modify their effects, and in this respect zinc has been seen to reduce the deleterious effects of vanadium and copper, while acting additively with nickel (303). Furthermore, there may be different responses observed depending on which cytokine is analysed, with different cytokines showing different responses to different metals – it is not the case that a single ROS-producing metal will necessarily induce a global increase in all inflammation-related species, and nor is it the case that all such metals will induce identical responses for a single cytokine (310, 311).

IL-6 may play an important role in lung injury mediated by airborne pollutants. Using aged and diluted cigarette smoke (ADCS) to represent PM from passive smoking, Yu and co-workers found that IL-6 knockout mice exhibited a lower increase in monocyte influx into the BALF and decreased BALF protein than did wild-type mice after ADSS exposure, also found with exposure to ozone, implicating oxidative stress. These effects could also be replicated by treating the mice with an antibody against IL-6. Furthermore, loss of Clara cell secretory protein following these exposures was seen in wild-type mice, but not in IL-6 knockout mice, suggesting that IL-6 may act as an intermediary in some of the detrimental effects of cigarette smoke (312).

Because of its effects on alveolar macrophages, it is possible that particulate matter may increase the susceptibility of an individual to infection or to the effects of other airborne particulate matter. In support of this assertion, a recent study indicated that pre-treatment of alveolar macrophages with DEP or urban PM reduced the subsequent release of inflammatory cytokines after exposure of alveolar macrophages to LPS, *via* either decreased production or increased retention of cytokine, or both, while DEP pre-treatment was also able to reduce cytokine release after exposure to a calcium ionophore or phorbol myristate acetate, a protein kinase C activator (313).

1.9 Genotoxicity

As well as induction of an inflammatory response, there is evidence that transition metals in particulate matter, or ultrafine particles with a very high surface area/volume ratio, can damage DNA (Figure 1.9), usually measured by formation of oxidised guanine, 8-oxo-7,8-dihydro-2'-deoxyguanosine (8-oxodG), or by DNA strand breakage as assessed by the Comet assay (176, 314). The hydroxyl radical has been identified as being of major importance in this process (315). Exposure to ambient particulate matter can induce DNA strand breakage and purine oxidation without concomitant increase in mRNA expression or activity of repair enzymes 8-oxoguanine glycosylase (OGG1) or 7,8-dihydro-8-oxoguanine triphosphatase (NUDT1) (294), although carbon black has been seen to cause an increase in rat lung mRNA expression for several genes involved in DNA repair, with the end result of no significant DNA damage (316). DNA damage may occur directly *via* attack from ROS, or indirectly *via* attack from ROS products, such as the lipid peroxidation product malondialdehyde, which has been demonstrated as being a reliable marker of air pollution exposure in asthmatic children (317, 318).

Interestingly, in light of the relevance to underground/transition-metal containing PM, a Swedish study found that underground railway PM_{10}, taking concentration into account, was eight times more genotoxic than street PM_{10} (204), ascribing the difference partially to the predominance of iron as magnetite (Fe_3O_4) in underground railway particles, compared to haematite (Fe_2O_3) in street particles. The authors also found that underground PM_{10} were four to five times more genotoxic than wood or roadwear particles per unit mass (319). Another study found that the organic extract of PM_{10} collected in the Seoul underground railway system was able to induce DNA strand breakage in the BEAS-2B cell line (320). DNA damage by ambient $PM_{2.5}$ has also been attributed to vanadium and chromium (321), while another study found that the reduced forms of vanadium and iron are more able to damage DNA than their higher oxidation state equivalents (322), the authors subsequently showing that nickel can also have genotoxic activity (323). It also seems that certain metal ions, including Ni^{2+}, Co^{2+}, and Cu^{2+} may interfere with DNA repair mechanisms, whereby nickel may

block recognition of DNA damage, cobalt may block incision and polymerisation post-repair, and all three may inhibit the zinc finger protein poly(adenosine disphosphate-ribose)polymerase 1 (PARP-1), which plays a role in the early stages of DNA repair (324)). Thus, the intriguing possibility is raised that transition metals in particulate matter may not only damage DNA, but may also simultaneously inhibit the repair of such damage.

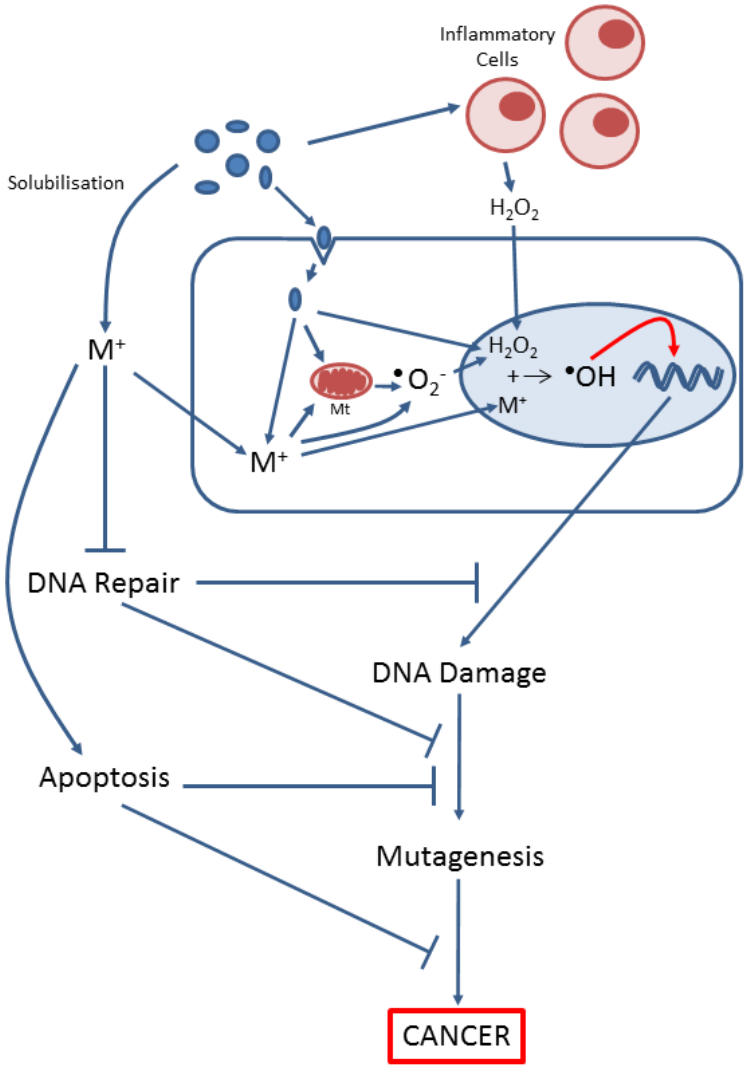

Figure 1.9. Transition metal-induced DNA damage and carcinogenesis.

Damage to DNA may be caused by both the insoluble and soluble metal fractions of particulate matter, and is caused by the hydroxyl radical ($^{\bullet}OH$), which is generated by reaction between the metal ion and hydrogen peroxide in the cell nucleus. In addition to generation by transition metals in solution or on the particle surface, hydrogen peroxide may be released from inflammatory cells in response to particulate matter, or liberated as a result of mitochondrial damage. Alternatively, reactions involving insoluble metal on the surface of the particulate may produce hydrogen peroxide. Soluble transition metal components of particles, such as iron, vanadium, or nickel, can diffuse into the nucleus and partake in the Fenton reaction with the hydrogen peroxide, generating hydroxyl radicals, which then oxidatively damage DNA. This damage to DNA, which may lead to mutagenesis, can be repaired by a variety of DNA repair processes, although these may themselves be impaired by certain transition metals. These mutations may ultimately result in dysregulation of cell cycle, cell death and, in the absence of transition metal-induced apoptosis, development of cancer. Adapted from (176, 325).

1.10 The Susceptibility of Asthmatics to the Effects of Airborne Particulates

A number of studies have examined whether there is a difference in susceptibility to the effects of particulate matter between various groups. For example, children and the elderly appear to be at greater risk, due to activity-induced increases in respiratory rate and greater exposure per body mass unit for children, and reduced clearance efficiency for the elderly, and individuals of a low socioeconomic status have also been identified as being potentially more susceptible (326). On the other hand, differences in susceptibility between genders and ethnicities seem to be small, if at all. However, pre-existing respiratory disease, particularly asthma and COPD, can significantly increase susceptibility to the effects of airborne PM (98, 326). Indeed, air pollution from a variety of sources can play a significant role in affecting allergic and non-allergic respiratory diseases, including asthma (48-50, 327).

First described by Henry Hyde Salter in 1860 as "paroxysmal dyspnoea of a peculiar character, generally periodic, with intervals of healthy respiration between the attacks" (328), asthma is classed as a disease of the conducting airways, characterised by recurrent, reversible airflow obstruction, airways inflammation, bronchial hyperresponsiveness, and a progressive decline in lung function (22). Recent estimates suggest that asthma affects at least 4.3% of the worldwide adult population (329). The UK National Health Service spends approximately £1 billion per annum treating asthma (330), with £850 million alone spent on drugs to control the disease (331). However, there is still a major shortfall in the understanding and management of asthma, with controversy over the aetiology, pathophysiological processes, and treatment of asthma (332), and it appears that the prevalence of the disease is on the rise (333).

The classification of asthma, ranging from intermittent through mild, moderate, and severe persistent forms is based upon frequency and severity of exacerbations, and forced expiratory volume in 1 second (FEV_1) (334). However, asthma severity has traditionally been determined while the patient is not using medication, and new

measures of asthma severity have been proposed, including the intensity of treatment required to bring asthma under control (335). Alternative classification methods, such as clinical and inflammatory phenotypes, endotype (pathophysiological mechanism), or trigger type, have been proposed with the aim of providing more targeted treatments (336-338). Recent research has suggested that patients can be separated into clusters based on a small number of factors including baseline and maximum FEV_1 and age of onset (339). It has also been suggested that clustering patients on the basis of age of onset and the extent of eosinophilic airway inflammation may enable more appropriate corticosteroid treatment, since non-eosinophilic asthma is more likely to be refractive to corticosteroids (340-342).

In addition to classification by phenotype, asthma can be subdivided into atopic and non-atopic asthma, with atopic asthma marked by increased Th2-type cytokines (e.g. IL-4, IL-5, IL-13). Although the majority of asthma cases are associated with atopy, a significant proportion are not (343). Allergens which may trigger asthma include house dust mite faeces (133, 344), fungal allergens (130, 345, 346), and pollen (347, 348). Non-allergenic triggers include respiratory viral infections (349-351), air pollution including cigarette smoke (273, 352), occupational exposures to a wide range of chemical and biological sensitising agents and irritants (353), exercise (354), aspirin (355), and lifestyle factors such as stress and obesity (356-359).

Treatment generally focuses on targeting the airways inflammation responsible for many of the symptoms. Currently used treatments fall into three classes. Inhaled β_2-adrenoceptor agonists, which may be short-acting (e.g. salbutamol) or long-acting (e.g. salmeterol), induce relaxation of bronchial smooth muscle thereby increasing airway patency, used as prophylaxis or "relievers" (360). Corticosteroids, which may be inhaled or orally administered, act *via* the nuclear glucocorticoid receptor to reduce the airway inflammation which underlies asthma (361). Cysteinyl leukotriene pathway antagonists (e.g. montelukast) block the effects of cysteinyl leukotrienes, lipid mediators with an emerging role in the pathogenesis of asthma (362). Finally, omalizumab is a humanised monoclonal antibody against IgE, levels of which are typically raised in atopic asthma. However, although omalizumab exhibits clear benefit

in the treatment of a subset of asthma patients, its use may be limited due to the cost of treatment (363, 364).

Despite much research, the causes of asthma are still incompletely understood. Asthma gene association studies are numerous, and genes positively associated with asthma fall into disparate groups. Studies have implicated genes coding for inflammatory cytokines and their receptors, including those involved in Th2-type responses such as the IL-4 gene cluster at chromosome 5q31 (365), TSLP (366, 367) and IL-33 (368, 369), and the IL-1 receptor gene cluster on chromosome 2q (370). Two genes at an asthma susceptibility locus on chromosome 17q21 including ORMDL3 (371), which may control release of calcium from the endoplasmic reticulum in epithelial cells and T-cells (372, 373) and GSDML (374) have also been linked to asthma. Furthermore, an association has been found between asthma and ADAM33, one of a subfamily of transmembrane metalloproteinases (375), which may play a role in airway remodelling (376). PCDH1, which may be involved in epithelial cell-cell adhesion (377) and, interestingly, the epidermal junction protein filaggrin FLG1, which has been strongly linked to development of atopic dermatitis (378), have also been linked to development of asthma (379, 380). However, although there is a clear genetic link in asthma, twin-studies have suggested that genetics alone cannot account for all or even most cases of asthma (381, 382), indicating that asthma is not determined purely by genetic factors, but rather by gene-environment interactions (383, 384). In addition, the involvement of genes coding for molecules with such varying functions lends weight to the assertion that asthma is a multi-factorial disease with a range of aetiologies.

Since many asthma-susceptibility genes are expressed in the airway epithelium, which is the first point of contact for any potential inhaled triggers, recent attention has focused on the airway epithelium as being crucial in the development and maintenance of an asthmatic phenotype (23, 385). On account of the large surface area of the respiratory system, and the fact that the airways are the predominant site of interaction with airborne particulate matter, there is much interest in the role particulate air pollution may play in asthma. Indeed, there is evidence that the effects of inhaled particulates may be more severe in asthma sufferers compared to healthy populations.

Severity of asthma has been correlated to reduction in forced vital capacity (FVC) following exposure to an environment with a large burden of diesel-powered vehicles (178). It has also been observed that asthmatic children living within 417 m of a major road showed increased wheezing, use of non-corticosteroid asthma medication, increasing risk of hospitalisation for asthma, reduced airflow, and decreased pH of exhaled breath condensate, all indicative of poorly controlled asthma (386), although another study found reduced pH and increased 8-isoprostane in exhaled breath condensate were linked to increased airborne black carbon levels in a study of schoolchildren irrespective of asthma status (387). Furthermore, wheeze, asthma, and bronchitis symptoms have been linked to increases in truck traffic, in a study which also found that the effects of the truck-related air pollution were more pronounced in children who also showed bronchial hyperresponsiveness or sensitisation to common allergens (388), suggesting effect modification by pre-existing conditions, with a sensitive population being more at risk of the effects of air pollution. Airborne pollutants are thought to skew the immune response to the Th2 phenotype, and have more generally been blamed for the frequency and severity of asthma cases (389, 390). Although particulate matter is not commonly studied in isolation, there appears to be evidence that it is one, but by no means the only, constituent of air pollution which can exert effects on asthma (388, 391), although the some studies find that gaseous components are solely responsible (392). Therefore, the majority of evidence suggests a role for particulate air pollution in case frequency and/or severity of asthma. However, the evidence of a role for particulate matter in the development of asthma is much less persuasive (see excellent recent reviews (393, 394)). Indeed, although a recent study found a synergy between past episodes of bronchiolitis and asthma development in children when looking at ozone as a causative factor, there was no link to particulate matter (395).

A number of reasons have been suggested for the discrepancy between asthmatic and normal responses to inhaled particulate matter. One possible reason for the increased risk posed to asthmatics is that the reduced, obstructed airflow in the airways of asthmatics results in a greater deposition of particulate matter in the airways of patients with asthma compared to healthy people (396), so that the effect may be due to increased exposure rather than intrinsic biological differences.

A key difference in the ability of asthmatic airways to overcome the challenge posed by inhaled particulate matter is that asthmatic airways appear to have a defective antioxidant response compared to healthy airways, and indeed there are suggestions that antioxidants may have a role in asthma therapy (397). The interplay between asthma and the formation and defence against ROS and RNS has been reviewed previously (389, 398). Baseline levels of SOD are lower in asthmatic lungs, and antigen challenge leads to a longer and more pronounced loss of SOD activity in asthmatic lungs than in healthy lungs, which is accompanied by a greater perturbation in the GSH/GSSG ratio (399). This defect in ability to dismutate superoxide has been shown to be instrumental in the increased levels of extracellular glutathione peroxidase (eGPx) found in the epithelial lining fluid of asthmatics. eGPx expression is induced by AP-1, but also requires the presence of ROS and GSH. By overexpressing either catalase or SOD, Comhair and colleagues showed that superoxide is the main ROS responsible for increased eGPx expression, thus explaining why epithelial lining fluid eGPx levels are higher in asthmatics than in healthy subjects (289). Another study looked at antioxidant levels in a variety of compartments in mild asthmatics, and found that while BALF and bronchial wash GSH levels were similar to those in healthy controls, these compartments contained significantly lower levels of ascorbate, urate, and α-tocopherol, although plasma levels of the latter were actually raised in the asthmatic group (400). Indeed, α-tocopherol and especially ascorbate are terminal antioxidants and as such, by virtue of their redox coupling, are able to repair other radicals and products of radical-antioxidant reactions (see reviews by Buettner and Jurkiewicz (401, 402)). Increased BALF and bronchial wash urate levels found in asthmatics were attributed to a mechanism compensating for the deficiency in ascorbate and α-tocopherol. Furthermore, while GSH levels were similar between groups, levels of GSSG were over three- (BALF) and six-times (bronchial wash) higher in asthmatics, this decreased GSH/GSSG ratio being a hallmark of increased oxidative stress in asthmatic lungs (400). Interestingly, asthmatic bronchial epithelium has also been observed as being more susceptible to oxidant-mediated apoptosis than epithelium from healthy volunteers (403), while oxidants can also deplete nitric oxide, a key signalling molecule involved in mediating bronchorelaxation (188).

In support of a role for deranged antioxidant mechanisms in asthma, polymorphisms of the enzymes glutathione S-transferase P1 (GSTP1) and glutathione S-transferase M1 (GSTM1), which are involved in mediating reactions between oxidants and glutathione, conferred an increased risk of asthma in Taiwanese schoolchildren (404), while single nucleotide polymorphisms (SNPs) in the glutathione synthase (GSS) gene appeared to increase the susceptibility to the effects of PM_{10} and $PM_{2.5}$ amongst others in growth of lung function (405). Similarly, expression of GSTPi, encoded by GSTP1, was seen to be reduced in nasal epithelial cells of asthmatic children compared to those without asthma, in work showing that HDM challenge in mice reduces mouse lung expression of GST genes (406). At the cellular level, knockdown of GSTM1 in BEAS-2B cells increases the ability of ozone to induce NF-κB activation and IL-8 production, as is also seen in GSTM1 null PBECs (407). While the main focus of antioxidant gene polymorphisms in asthma falls on GSTM1 and GSTP1, other genes whose products are involved in antioxidant processes, such as NQO1, have also been implicated (327).

The reasons for a defective antioxidant system are currently being investigated. One recently-published piece of research suggests that there is dysfunctionality in the activity of Nrf2 in severely asthmatic children, who were found to have significantly elevated levels of Nrf2 mRNA and protein compared to mild-to-moderate asthmatic children, but with no increase in levels of antioxidant enzymes which are targets of Nrf2 binding, although whether this is due to dysfunctional Keap1-Nrf2 interaction, post-translational modification of Nrf2, Nrf2 SNPs, or some other factor, is unknown (408).

Therefore, it appears that antioxidant processes are an important source of susceptibility to airborne pollutant-induced asthma exacerbations, and may even be the most important factor involved. It is, however, important to remember that other susceptible groups do not show defective antioxidant mechanisms, and thus antioxidant status may be neither sufficient, nor necessary, to determine absolutely whether an individual may be at a greater risk of the effects of particulate air pollution (196).

1.11 Hypotheses

The above review of the literature illustrates that airborne particulate matter may pose a risk to the respiratory system. Epidemiological evidence of the impact of air pollution upon respiratory health, and further studies showing the effects of PM both *in vivo* and *in vitro* suggest that there is an urgent need to further investigate the effects of PM at all levels, and in particular the relationships between particle source, size, composition, and effects. As detailed, transition metals have previously been found in particularly high levels in airborne dust from underground railway systems, and have been shown to exert deleterious effects on cells of the respiratory system *via* the formation of ROS. Epidemiological evidence suggesting an interaction between air pollution and asthma status, and findings that asthmatic lungs are deficient in antioxidant defences, provide grounds for investigation of the potentially different effects of underground railway PM on airway cells from healthy and asthmatic donors. Finally, since different components of particulate air pollution may interact to produce additive or synergistic effects where found together, the potential interaction of underground railway pollution with *Alternaria* species in exerting toxic effects on airway cells will be studied.

Therefore, there are five hypotheses to be tested herein:

1. Airborne particulate matter from an underground railway station has a greater transition metal content than particulate matter from other sources.

2. Underground particulates show pro-inflammatory activity in *in vitro* models of airway epithelium, as assessed by inflammatory cytokine release and antioxidant response.

3. The inflammogenic effects of the particle are more pronounced in *in vitro* models of asthmatic airways compared to equivalent models representing healthy bronchial epithelium.

4. This inflammogenicity is related to the transition metal content, and capacity for ROS generation, of the particulate matter.

5. Underground railway PM is able to prime a cell culture model of the airway epithelium to be more susceptible to the effects of *Alternaria* extract.

2 Materials and Methods

2.1 Materials

Reagent	Manufacturer	Code (if available)
2'7'-dichlorodihydrofluorescein diacetate	Sigma-Aldrich (Gillingham, UK)	D6883
3,3',5,5'-tetramethylbenzidine (TMB) ELISA substrate solution	eBioscience (Hatfield, UK)	00-4201-56
4-(2-Aminoethyl)benzenesulphonyl fluoride hydrochloride (AEBSF)	Sigma-Aldrich	A-8456
4-(4-fluorophenyl)-2-(4-methylsulphinylphenyl)-5-(4-pyridyl)-1H-imidazole (SB203580)	Sigma-Aldrich	S8307
Alternaria alternata extract (lyophilised)	Greer Laboratories (Lenoir, NC, USA)	XPM1D3A2.5
Bovine serum albumin (BSA; fraction V)	Sigma-Aldrich	A3059
Bronchial epithelial basal medium (BEBM)	Lonza (Slough, UK)	CC-3171
Bronchial epithelial growth medium (BEGM) Singlequots, added to BEBM to produce BEGM.	Lonza	CC-4175
Chloroform	Sigma-Aldrich	C2432

Reagent	Manufacturer	Code (if available)
Cladosporium herbarum extract (lyophilised)	Greer Laboratories	XPM9D3A25
CytoTox 96 lactate dehydrogenase assay kit	Promega (Southampton, UK)	G1780
Desferrioxamine mesylate salt (DFX)	Sigma-Aldrich	D9533
DNase kit	Life Technologies (Paisley, UK)	AM1906
Fluorescein isothiocyanate (FITC)-labelled dextran (4 kDa)	Sigma-Aldrich	FD4
Foetal bovine serum	Life Technologies	10500-064
Glycogen solution	Roche (Burgess Hill, West Sussex, UK)	10901393001
Hanks' Balanced Salt solution (HBSS) with Ca^{2+} and Mg^{2+}	Life Technologies	24020-091
Hanks' Balanced Salt solution without Ca^{2+} and Mg^{2+} ($HBSS^{-}$)	Life Technologies	14170-088
Hydrochloric acid 6 M, Primar Plus grade	Fisher Scientific (Loughborough, UK)	A466
Hydrofluoric acid 27 M, UpA grade	Romil (Cambridge, UK)	SS52
Hydrogen peroxide solution (30%)	Sigma-Aldrich	H1009
ICP-MS standards for Ag, Al, Ca, Cu, Fe, K, Mg, Na, Pb, Pd, Sr, Ti, Zn	Inorganic Ventures (Christiansburg, VA, USA)	Various
ICP-MS standards for As, B, Ba, Bi, Cd, Ce, Co, Cr(III), Cs, Ga, Hg, La, Li, Mn, Mo,	Romil	Various

Reagent	Manufacturer	Code (if available)
Nb, Ni, Pt, Rb, Rh, Sb, Sc, Se, Si, Sn, V, W, Y, Yb, Zr		
ICP-MS standard for Hf	Spex Certiprep (Metuchen, NJ, USA)	PLHF1-2Y
IL-8 (human) DuoSet ELISA kit	R&D Systems (Abingdon, UK)	DY208
IL-18 (human) ELISA kit	R&D Systems	7620
IL-33 (human) DuoSet ELISA kit	R&D Systems	DY3625
Isopropanol (propan-2-ol)	Sigma-Aldrich	I9516
ITS solution 100x (1mg/ml insulin, 550μg/ml transferrin, 500ng/ml sodium selenite)	Sigma-Aldrich	41400
MEM + GlutaMAX	Life Technologies	41090
N-acetylcysteine (NAC)	Sigma-Aldrich	A9165
Nitric acid 15 M, Primar Plus grade	Fisher Scientific	A467
Pepstatin A	Sigma-Aldrich	P5318
Precision reverse transcription kit	PrimerDesign (Southampton, UK)	RT-std
Prolong Gold antifade mounting reagent	Life Technologies	P36930
Protease fluorescent detection kit	Sigma-Aldrich	PF0100
PureCol collagen	Advanced BioMatrix (Tucson, AZ, USA)	5005-B
Quantitative polymerase chain reaction (qPCR) mastermix	PrimerDesign	PrecisionC PrecisionC-SY
qPCR primers (UBC/GAPDH, HO-1, IL-8, TNFα, TSLP)	PrimerDesign	PP-HU-600 SY-HU-600

Reagent	Manufacturer	Code (if available)
qPCR Primer NQO1	Applied Biosystems	4400291
Sulphuric acid	Sigma-Aldrich	00646
TNFα (human) DuoSet ELISA kit	R&D Systems	DY210
TNFα (human) Quantikine ELISA kit	R&D Systems	DTA00C
TSLP (human) ELISA kit	R&D Systems	DY1398
Trans-epoxysuccinyl-L-leucylamido-(4-guanido)butane (E-64)	Sigma-Aldrich	E3132
Triton X-100	Sigma-Aldrich	
Trizol lysis reagent	Life Technologies	15596-018
Trypan blue stain	Sigma-Aldrich	T8154
Trypsin-ethylenediaminetetraacetic acid (EDTA)	Life Technologies	15400054
Tween-20	Thermo Fisher Scientific (Waltham, MA, USA)	P1379

2.2 Reagent Compositions

PBS: 80.06 g NaCl
2.013 g KCl
11.5 g Na_2HPO_4
2.04 g KH_2PO4
pH to 7.2-7.4 if necessary

10x TBS: 80 g NaCl
24.2 g TRISbase
Make up to 1 L with ultrapure MilliQ water
pH to 7.6 with 37% HCl

2.3 Equipment

Equipment	Manufacturer
Adobe Photoshop CS5	Adobe Systems (San Jose, CA, USA)
Dionex ion chromatograph and constituent apparatus and Chromelon ion chromatography analysis software	Dionex (Sunnyvale, CA, USA)
Gammacell 1000 Cell Irradiator	Atomic Energy of Canada Ltd (Ontario, Canada)
GraphPad Prism 6	GraphPad Software (San Diego, CA, USA)
Hitachi H7000 Transmission Electron Microscope	Hitachi High-Technologies Europe GmbH (Maidenhead, UK)
Hummer VI A sputter coater	Anatech (Alexandria, VA, USA)
iCycler CFX96 Thermal Cycler	Biorad (Hemel Hempstead, UK)
Improved Neubauer bright-line haemocytometer	Marienfeld (Lauda-Königshofen, Germany)
Labsystems Fluoroskan FL fluorimeter	Thermo Fisher Scientific
Labsystems Multiskan Ascent plate reader	Thermo Fisher Scientific
Leica DMI6000B light microscope and software	Leica Microsystems GmbH (Wetzlar, Germany)
Leo 1540VP scanning electron microscope	LEO Electron Microscopy (Cambridge, UK) [now Carl Zeiss Nano Technology Systems (Welwyn Garden City, UK)]
Millicell ERS-2 epithelial volt-ohm meter	Millipore UK Ltd (Watford, UK)
Nanodrop ND-1000 spectrophotometer	Nanodrop (Wilmington, DE, USA)
Nunc cell culture plates	Nalge Nunc (Rochester, NY, USA)
Nunc MaxiSorp 96-well plates	Nalge Nunc
Savillex Teflon pots (3ml)	Savillex (Eden Prairie, MN, USA)
SigmaPlot 11.0 and 12.0	Systat Software (Chicago, IL, USA)
Soniclean Bath Sonicator	Soniclean (Thebarton, Australia)

Equipment	Manufacturer
T100 Thermal Cycler	BioRad
Thermo Fisher X-Series 2 inductively coupled plasma mass spectrometer	Thermo Fisher Scientific
Topmix vortexer	Fisher Scientific
Transwell culture apparatus	Thermo Fisher Scientific

2.4 Acquisition of Particulate Matter

Particulate matter was collected by the Inhalation Toxicology group at the Dutch National Institute for Public Health and the Environment (RIVM), led by Professor Flemming Cassee, as part of the RAPTES project. The author assisted in this process on one of the sampling days.

Particulate matter was collected at a mainline railway station located under the main departures and arrivals building of a major European airport. The railway station has six "island" platforms, each approximately 400 m long, running in a roughly north-easterly to south-westerly direction, and lies in the middle of a 5.1 km long tunnel. The station is used by approximately 60,000 passengers per day, although this can rise to 150,000 per day during holiday periods or at weekends. During the day 25-30 passenger trains per hour pass through the station, all of which are powered by electricity obtained *via* a pantograph from an overhead catenary. No electrified third rail is used. During the night there are occasional diesel-powered freight trains passing through the station. The station is cleaned regularly during daytime hours, principally using electrically powered ride-on machines to clean the floor of dirt and dust. There is no active ventilation system in operation, with air exchange driven solely by the "piston action" of train movement. Rail maintenance, in the form of rail grinding and polishing, takes place twice a year. There are three vans located in the upper part of the station, to be used in emergencies, but these are only turned on occasionally to check that they are still operational (Boere and Steenhof, personal communication).

Particulate matter was collected using a VACES (Versatile Aerosol Concentration and Enrichment System) unit, as detailed and validated previously (112, 113). The VACES unit was placed between platforms 3 and 4 of the station, approximately 50 m from the south-west end of the platform, approximately 3 m from the platform edge and 6 m from the centre of each pair of surrounding track, with air intakes approximately 3 m above the track levels and 4 m below the overhead catenaries (Figure 2.1). Sampling was performed between 08:30 and 17:30 on each of three sampling days, all of which were working weekdays in July 2010. Three virtual impactors, running in

parallel to each other, with cutpoints of 10-2.5 μm (coarse), 2.5 μm (fine and ultrafine, hereafter referred to as "fine"), and 0.18 μm (ultrafine) were used, with each fraction being collected separately as a suspension in ultrapure MilliQ water. When used in experiments, this suspension was kept in the original ultrapure MilliQ water instead of drying or filtering the PM, to ensure that water soluble components were retained. It is important to note that while the coarse fraction does not contain PM which would be expected to be found in other size fraction (i.e. PM aerodynamic diameter from 2.5-10 μm), fine and ultrafine fractions do not have a lower size limit, and therefore the fine fraction also contains particles of a size which would permit them to be present in the ultrafine fraction. The particulate mass concentration of each suspension was determined by calculating the mass of particulate matter on a parallel Teflon filter used for each particulate size fraction in the VACES unit. Filters were weighed before use and, following sampling, the pre-sampling weight of the filter was subtracted from the post-sampling weight to determine the mass of particulate matter collected. After collection, particle suspensions were kept on ice during transport, before being frozen and stored at -20°C.

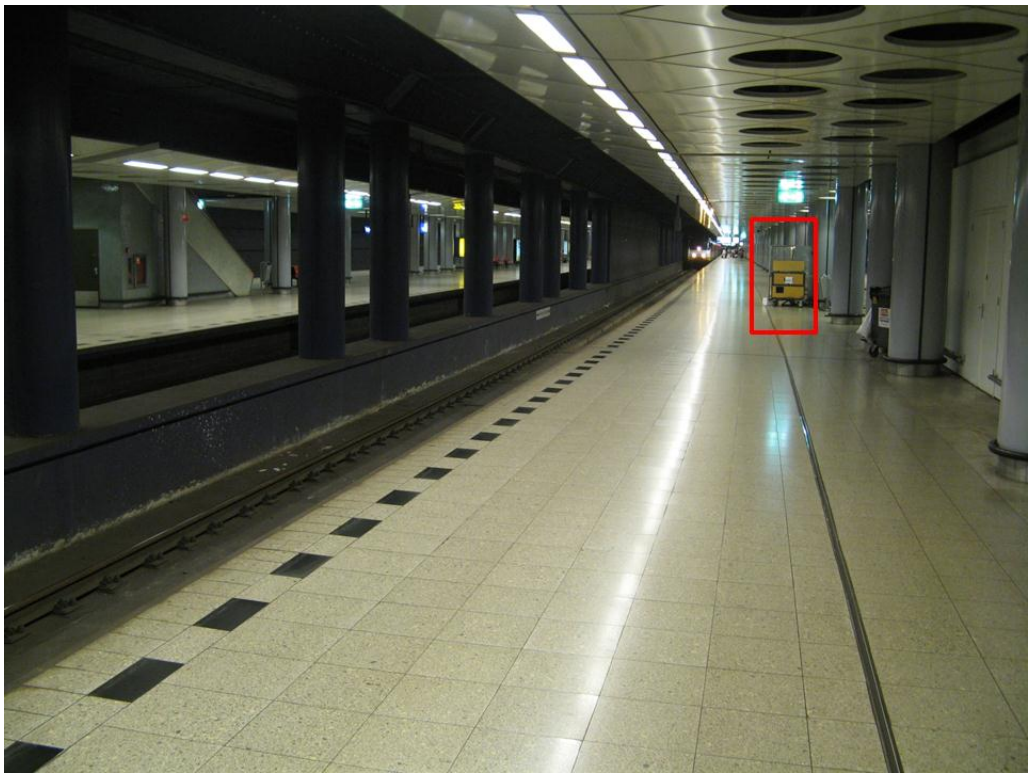

Figure 2.1. The location of the VACES unit for sampling underground railway particulate matter.

The location of the VACES unit is marked by the red rectangle.

As comparators for chemical analysis, particulate matter was collected from three further sources:

1. A woodstove. A portion of the woodstove exhaust was diluted with filtered air, and fed into a sealed sampling chamber sampling PM at a concentration of approximately 250 $\mu g/m^3$. Prior to operation, the chamber was flushed with filtered air.

2. A roadwear simulator, consisting of a circular road surface on which four wheels with studded tyres rotated. Prior to operation, the chamber was flushed with filtered air, and the PM concentration was allowed to build up to a steady state of approximately 5000 $\mu g/m^3$.

3. A heavily trafficked road tunnel in The Netherlands. Sampling was performed in a parking area immediately adjacent to the tunnel exit, with sampling performed during summer.

Additionally, four samples of diesel exhaust particulate matter were collected, these varying in terms of the composition of diesel and the exact mechanical location of their collection: DEP1 was collected from the outflow pipe of a diesel exhaust generator using cerium oxide as a diesel additive, DEP2 was collected from the roof of an inhalation chamber used for DEP exposure studies, DEP3 was collected from a diesel exhaust filter set, and DEP4 was collected from a diesel-powered generator.

2.5 Particulate Chemical Analysis by Inductively Coupled Plasma Mass Spectrometry (ICP-MS)

2.5.1 Principles

ICP-MS is an elemental analysis technique with sensitivity in at least the parts-per-trillion range, assuming completely uncontaminated reagents, with even greater sensitivity for detection of some elements depending on the specifics of the equipment used. The prepared sample is fed into a nebuliser which disperses the sample into micron-sized droplets, and these are then fed into the plasma, where the liquid is evaporated and atomised. A plasma is a gas made up of ions, rather than atoms or molecules. In the case of ICP-MS, the plasma is a stream of argon gas into which a spark gun emits electrons, argon being used due to its relative inexpensiveness, monatomic nature, inertness, and exhibition of a simple background spectrum. The electrons fired into the argon stream are shuttled by an electromagnetic coil with current direction oscillating at radio frequency, where they are able to ionise the argon gas to Ar^+ ions, which form the plasma. These processes cause the temperature of the plasma to reach approximately 5,000 K, and provide the high temperature ionising environment required for sample ionisation (409, 410).

Once the sample is atomised and ionised, generally forming monovalent ions, the ions are focused through ion lenses to a quadrupole filter. This consists of two opposing pairs of precisely-positioned rods, arranged as the points at the corner of a square, forming a tunnel-like structure through which the ions pass. These rods carry an alternating and a direct current (AC and DC respectively) superimposed onto each other, which allows the quadrupole to filter ions based on mass/charge (m/z) ratio. As the amplitude of the AC rises, ions with a low m/z ratio are more affected by the oscillations than are larger m/z ratio ions, and may end up colliding with the rods or leaving the ion beam. Thus the AC can remove ions below a certain m/z ratio. Conversely, as the magnitude of the DC increases, the deflection effect is more apparent on ions of a high m/z ratio, and so the DC portion is able to filter out ions

above a critical m/z ratio. As the ionised sample passes through the quadrupole, the amplitude and magnitude of the AC and DC currents can be varied, allowing the mass spectrometer to "scan" the range of desired elements (410). Once ions have passed through the quadrupole filter, they collide with a detector which, through a series of electron-releasing processes, allows a count to be taken for each element.

In the present research, a sweep of all elements to be analysed was performed 50 times and a mean taken to give a single count per element. This was then repeated two further times, to give three counts, and a further mean of these counts was taken to give a final count for each element in the sample.

2.5.2 Sample Digestion

Particles were supplied as suspensions in water or, in the case of diesel exhaust particulates, as dry powders. All particle samples were stored at -20 °C until required. All analysis steps were performed in a clean laboratory (class 100) environment in order to minimise the risk of contamination of particulate matter samples. For particulate matter in suspension, samples were thawed, followed by vortexing for 30 s and sonicating in a sonicating water bath at room temperature for 30 s. 100 µl suspension was removed for anion analysis, and the remaining volume was recorded and transferred to a clean 3 ml Savillex Teflon pot. The only exception to this was where the total mass of particulate matter in the remaining solution would have exceeded 1.5 mg, in which case a volume containing roughly 1.2 mg was dried down, and the remaining suspension returned to storage at -20 °C. Suspensions were then evaporated to dryness on a Teflon hotplate at 130 °C.

Dry diesel exhaust particulate matter was weighed and placed into a clean 3 ml Savillex Teflon pot. The dry weight of each sample of particulate was recorded (approximately 1.5 mg per pot). For some of the dry powder samples, 2 ml water was added to the vial of powder in order to create a suspension, since these particulate samples were difficult to handle in their dry state. These suspensions were vortexed, sonicated, and dried down as for the other suspensions. From this point onwards, all particles were

in dry form, and all were treated in the same manner. Digest blank samples, containing no particulate matter but subjected to the digestion procedure as for the particulates, were also used to verify lack of contamination in the digestion process.

Three overnight digestion steps were performed. For the first step, 1 ml concentrated nitric acid (15 M, Primar Plus grade) was added to each pot, followed by heating on a hot plate at 130 °C for approximately 30 min, and standing to cool for 15 min. 100 µl concentrated hydrofluoric acid (27 M, UpA grade) was then added to each pot, the lid reapplied, and the pots placed into individual Teflon bombes containing 4 ml ultrapure MilliQ water, to maintain pressure. Teflon bombs were then placed inside spring-sealed stainless steel bombs. These were incubated in an oven overnight at 180 °C before being removed from the oven to cool for approximately 60-90 min, and then evaporated to dryness on the hotplate at 130 °C. For the second step, approximately 1 ml 6 M hydrochloric acid (12 M, Primar Plus grade) was added to each pot, followed by a further overnight incubation on the hotplate at 130 °C, with the lids securely on each pot. After cooling, lids were removed, the contents of each pot was evaporated to dryness on a hotplate, and roughly 1 ml of 2% nitric acid spiked with beryllium (Be), indium (In), and rhenium (Re), was added to monitor instrument drift. Pots were then sealed and left to stand for at least 24 h.

2.5.3 Inductively Coupled Plasma Mass Spectrometry

Prior to analysis, digest solutions were transferred to scintillation vials, and further 2% nitric acid with Be/In/Re spike was added, so that the final mass of the solution was approximately 3 g, with the mass being recorded. To enable analysis by ICP-MS, three sets of standard solutions were made from individual element reference solutions. Set 1 (Standard 1) was comprised of elements expected to be relatively abundant in the particulates, while set 2 (Standard 2) was comprised of elements expected to be less abundant in the particulates. Set 3 (standard 3) contained elements which are harder to measure by ICP-MS. These elements are listed below, in alphabetical order.

Standard 1: aluminium (Al), antimony (Sb), arsenic (As), barium (Ba), boron (B), cadmium (Cd), calcium (Ca), chromium (III) (Cr), cobalt (Co), copper (Cu), gallium (Ga), iron (Fe), lead (Pb), magnesium (Mg), manganese (Mn), molybdenum (Mo), nickel (Ni), potassium (K), selenium (Se), sodium (Na), tin (Sn), titanium (Ti), tungsten (W), vanadium (V), zinc (Zn).

Standard 2: bismuth (Bi), caesium (Cs), cerium (Ce), hafnium (Hf), mercury (Hg), lanthanum (La), lithium (Li), niobium (Nb), palladium (Pd), platinum (Pt), rhodium (Rh), rubidium (Rb), scandium (Sc), strontium (Sr), ytterbium (Yb), yttrium (Y), zirconium (Zr).

Standard 3: silicon (Si), silver (Ag).

Standards were first made as 5 parts per million (ppm) w/w solutions. Each reference solution was supplied as approximately 1000 μg/ml, although the exact concentration and density are both stated in material data sheets for use in subsequent calculations. Therefore, 100 μl (approximately 100 μg) of each reference solution was weighed into a 20 ml scintillation vial, the mass for each individual solution being recorded, and made up to a final mass of approximately 20 g with 2% HNO_3. Serial dilutions of this 5 ppm solution were made into spiked 2% nitric acid, to give solutions of 1 ppm, 500 parts per billion (ppb), 250 ppb, 125 ppb, 25 ppb, 12.5 ppb, 5 ppb, 2.5 ppb, and 0.25 ppb. For Standard 2, only 125 ppb – 0.25 ppb solutions were used due to the expected paucity of these elements in the particulates, while for standard 3, the 1 ppm solution was serially diluted to give solutions of 200 ppb, 50 ppb, 10 ppb, and 2.5 ppb. Scintillation vials were then arranged into the autosampler component of the ICP-MS equipment, with standards running from low to high concentrations, followed by samples, and samples were then automatically analysed by the Thermofisher X-Series 2 mass spectrometer.

Analysis of samples yielded a "count" value for each element in each standard. Using the ppm/ppb concentrations, standard curves were plotted for each element, from which the elemental concentrations in each particulate digest sample could be read. For the majority of samples, certain elements produced counts which were too high to

be reliable in conjunction with the standard curves, due to the loss of linearity between actual concentration and measured counts at high levels. To remedy this, samples were further diluted in spiked 2% HNO_3 to bring all readings to a maximum of approximately 500 ppb.

Calculations were performed to correct for slightly different dilutions of each sample, and to correct for different starting masses of particulate in each sample, with the final derived value being a concentration of each element in the original particulate matter, expressed as milligrams of element per gram of particulate matter.

2.6 Anion Analysis by Ion Chromatography

Ion chromatography was used to determine the level of the anions sulphate (SO_4^{2-}), chloride (Cl^-), and nitrate (NO_3^-) in the particulate samples. 100 µl of each particulate suspension had been reserved for this purpose prior to sample digestion for ICP-MS. These aliquots were thawed, vortexed for 60 s, and sonicated for 60 min in order to ensure that a maximum possible amount of these anions entered solution from the particles. After sonication, suspensions were centrifuged at 20,000 x *g* for 10 minutes, before the supernatant was removed. Care was taken to ensure that particles were not disturbed or removed with the supernatant – this resulted in a final volume of supernatant of 80 µl being removed and retained for analysis. Individual supernatants were diluted in ultrapure MilliQ water to a volume of approximately 5 ml, before being analysed on a Dionex ICS2500 ion chromatograph, equipped with IP25 isocratic pump, CD25 conductivity detector, LC25 chromatography oven, and an automatic sampler. Standard solutions were prepared for SO_4^{2-}, Cl^-, and NO_3^- by serial dilution of commercially available stock standards, which were also used to monitor instrument drift. Peak analysis was performed using Dionex Chromeleon software, and results were adjusted to take into account variations in particulate mass concentration in the original suspension, and also variations in dilution factor of supernatants into ultrapure MilliQ water.

2.7 Scanning Electron Microscopy (SEM)

Particle suspensions were prepared for SEM by pipetting a small amount (roughly 50-100 μl) onto the surface of an aluminium stub. This was then placed in an oven at 50 °C overnight to evaporate the suspension to dryness.

After drying, the particulates were sputter coated with gold using a Hummer VI A sputter coater, operating at 7 kV for 4 min, to produce a gold coating of approximately 20 nm thickness. Gold was preferred to carbon as, while gold obscures detection of sulphur and phosphorus in elemental analysis, gold sputtering results in better imaging.

SEM was performed using a LEO 1450VP (variable pressure) scanning electron microscope operated at 20 kV.

2.8 Measurement of Particulate Matter LPS Concentration

The concentration of LPS in suspensions of underground railway particulate matter were determined using a commercially available chromogenic Limulus amoebocyte lysate (LAL) assay according to the manufacturer's instructions. Briefly, 50 μl samples of particulate matter (at a concentration of 25 μg/ml) were aliquotted into a 96-well plate. Similarly, 50 μl standard solutions for a 4-point standard curve with LPS concentrations of 1 EU/ml, 0.5 EU/ml, 0.25 EU/ml, and 0.125 EU/ml were dispensed into wells. 50 μl Limulus amoebocyte lysate was added to each well and incubated at 37 °C for 10 min. Subsequently, 50 μl chromogenic lyophilised substrate was added to each well, and incubated at 37 °C for 6 min. The reaction was arrested with the addition to each well of 100 μl 10% sodium dodecyl sulphate in LAL assay-grade water. Absorbance at 405 nm wavelength was measured immediately using a plate reader, and LPS concentrations of PM suspensions determined using the prepared standard curve.

2.9 Irradiation of Particulate Matter Samples

PM suspensions sorted by size fraction and aliquotted into vials of 2 ml each were stored at -20 °C until use. To prepare suspensions for cell culture, particles were gamma-irradiated to reduce the possibility of bacterial growth from bacteria collected during the sampling process. PM suspension vials were defrosted at room temperature and vortexed for 30 s at 40 Hz speed using a Topmix Vortexer. Following this, vials were sonicated for 15 s at ambient temperature in a Soniclean bath sonicator. Vials were then gamma-irradiated with a radiation dose of 1,250 Gy over a period of 10 h using a Gammacell 1000 cell irradiator with Cs137 source. While radiation doses of up to 25 kGy have been recommended for effective sterilisation of surgical equipment (411), the dose of 1,250 Gy was the maximum available in any continuous period due to constraints of time and equipment availability. For periods of carriage between these treatments, all vials were kept on ice. Immediately after irradiation, samples were returned to storage at -20 °C. Incubation of 10 µl of each particulate suspension in 500 µl medium confirmed that no fungal or bacterial growth could be observed in either starvation or complete media, although all subsequent experiments were monitored visually to verify lack of infection. This was in contrast to non-irradiated samples, which developed turbidity in culture medium after only 24 h incubation, suggesting contamination with viable organisms. To avoid repeated freeze-thawing, particulate suspensions were divided into aliquots of varying size and stored at -20 °C until required.

2.10 16HBE Epithelial Cell Culture

16HBE14o- cells, (hereafter referred to as 16HBE; a gift from Professor D.C. Gruenert, San Francisco, USA (412)), passage 48-60, were incubated at 37 °C, 5% CO_2 in Modified Eagle's medium (MEM) + GlutaMAX culture medium supplemented with 10% heat-inactivated foetal calf serum (FCS) and 1% penicillin and streptomycin mix (final concentrations of 50 units/ml and 50 µg/ml respectively). Starvation medium, applied 24 h prior to challenge, was Minimum Essential Medium (MEM)+

GlutaMAX medium without FCS or penicillin and streptomycin in the case of cells grown on Transwells (apical starvation only), and MEM + GlutaMAX medium with 0.1% bovine serum albumin (BSA) for monolayers. All culture reagents were warmed prior to use to avoid causing stress to cells.

2.10.1 Passaging and Seeding of 16HBE Cells

1% PureCol collagen in water (97% type I rat tail collagen, some type III collagen; final concentration 30 μg/ml) was prepared, and 5 ml added to a 75 cm^2 flask, 100 μl to the apical compartment of each apical Transwell (surface area 0.33 cm^2, pore size 0.4 μm), 500 μl to each well of a 24-well Nunc cell culture plate (surface area 1.8 cm^2), or 50 μl to each well of a 96-well Nunc cell culture plate (surface area 0.3 cm^2). Culture apparatus was then transferred to an incubator at 37 °C for 30-60 min. Cells ready for passaging in a 75 cm^2 flask were washed twice with 10 ml Hanks' balanced salt solution without calcium or magnesium ($HBSS^-$), and 1 ml 0.05% trypsin-EDTA in $HBSS^-$ was added to the flask. Cells were then incubated for 5-10 min to release from the culture surface. After release, 10 ml serum-containing culture medium was added to arrest trypsin activity, forming a cell suspension. This cell suspension was centrifuged at 300 x *g* for 5 min to pellet cells, and the pellet was then resuspended in 1 ml culture medium. 80 μl $HBSS^-$, 10 μl Trypan blue stain, and 10 μl cell suspension were mixed. 10 μl of the stained cell solution was pipetted into the chamber of an Improved Neubauer bright-line haemocytometer. Using a phase contrast microscope, cells in the four corner 1mm^2 squares were counted and a mean of the count per square calculated, with viable cell count calculated as below, using a volume scaling factor of 10,000 to convert the volume of suspension over the counting square at 0.1 mm^3 (1 mm x 1 mm x 0.1 mm) to 1 ml (1 cm^3 or 1,000 mm^3), and a correction factor of 10 to account for the cells being counted as a 1 in 10 dilution:

Cells/ml = cell count/mm^2 x 10,000 (volume scaling factor) x 10 (dilution factor)

The cell suspension was supplemented with complete medium to a concentration of 1 x 10^6 cells/ml. Collagen solution was removed from flasks, Transwells, and plates, and

culture apparatus seeded – 300,000 cells in 10 ml medium per 75cm^2 flask, 150,000 cells in 200 µl medium (undiluted cell suspension) per Transwell, 50,000 cells in 500 µl culture medium and 15,000 cells in 100 µl culture medium per well in a 24-well and 96-well plate respectively.

All cultures had their medium replaced with fresh complete medium every 2-3 days, 10 ml per 75cm^2 flask, 200 µl per apical compartment and 500 µl per basolateral compartment of each Transwell, and 500 µl per culture plate well. Transwells were used 7 days after seeding, and formation of a tight barrier was verified by measurement of a transepithelial electrical resistance (TER) of at least 330 Ωcm^2 (i.e. a reading of 1000 Ω). Monolayers were used when 85-90% confluent, as assessed by observation under light microscope.

2.11 Primary Bronchial Epithelial Cell Culture and Seeding

Primary bronchial epithelial cells (PBECs) were obtained as previously described *via* bronchial brushing during fibre optic bronchoscopy (403). Ethical approval had been obtained from the Southampton local research ethics committee under the description "Pathophysiology of Airway Diseases such as Asthma and COPD", Rec. No 05/Q1702/165, code MRC0268. All volunteers had provided their informed consent, and all samples were anonymous-linked, with access to patient-identifiable data only being available to those with prior ethical approval. PBECs were cultured and grown at air-liquid interface (ALI) according to a previously published method (413). Briefly, cells were cultured to confluence in collagen-coated culture flasks (25 cm^2 for passage 0, 25 cm^2 and 75 cm^2 for passage 1) in bronchial epithelial growth medium (BEGM) prepared from BEBM with Singlequots as supplied by the manufacturer (final concentration at 52 µg/ml bovine pituitary extract, 10 µg/ml transferrin, 5 µg/ml insulin, 1.5 µg/ml BSA, 0.5 µg/ml hydrocortisone, 0.5 µg/ml epinephrine, 6.5 ng/ml triiodothyronine, 0.5 ng/ml human epidermal growth factor, retinoic acid (concentration withheld by manufacturer), and 0.1% GA-1000 solution). After further growth, cells were seeded onto collagen coated Transwells at a density of 70,000 cells/well. Cells were grown in this configuration for 24 h, submerged in BEGM.

After 24 h, cells were grown further at air-liquid interface (ALI), with no medium in the apical compartment. The basolateral compartment contained 300 µl medium – equal volumes of Dulbecco's modified Eagle's medium (DMEM) and BEGM (containing twice the concentration of each added supplement compared to that used for passage 0 and 1 growth in flasks to account for dilution with DMEM, with GA-1000 omitted), with retinoic acid added to a final concentration of 50 nM. Basolateral medium was replaced with fresh medium on each weekday. TER was recorded on days 7, 14, and 21 post-seeding. Starvation medium, applied 24 h prior to challenge, was BEBM with 1% 100x ITS (to a final concentration of 10 µg/ml bovine insulin, 5.5 µg/ml transferrin, 5 ng/ml sodium selenite) and a final concentration of 1.5 µg/ml BSA.

For primary bronchial epithelial cell monolayers, after passage 1, cells were seeded in collagen-coated 24-well Nunclon cell culture plates at a density of 20,000 cells per well, in 1 ml BEGM (same composition as for passage 0 and 1 growth, minus GA-1000), or 5,000-8,000 cells in 200 µl BEGM for 96-well plates, and this medium was changed on alternate days. Cells were grown for 5-6 days until 80-90% confluent. 24 h prior to challenge, starvation medium of BEBM with 1% ITS and a final concentration of 1 mg/ml BSA was applied.

2.12 Challenge of Cells with Particulate Matter

For each experiment, stock solutions of each particulate fraction at 100 µg/ml were prepared by diluting stock suspensions in ultrapure MilliQ water, with 10% volume of 10x PBS, so that each suspension was at a concentration of 100 µg/ml. PBS was used due to the particulate suspensions being collected as different mass concentrations in water, so PBS was added to maintain overall osmolarity at the approximate level of starvation medium, regardless of the volume of aqueous particulate suspension used. Suspensions of the required concentration were prepared by diluting the prepared 100 µg/ml suspension with BEBM (primary cell cultures) or serum- and BSA-free medium (16HBE cultures). The total volume of PM suspension added was 400 µl per well in a 24-well plate or 75 µl per well for a 96-well plate or Transwell culture. To control for

the greater proportion of water/PBS and lesser proportion of culture medium in PM suspensions of a higher concentration, controls were run made up of PM-free ultrapure MilliQ water and PBS, diluted with culture medium in exactly the same proportions as were used for the PM suspensions.

Since particle suspensions were made up according to the mass of PM per volume of medium, but when applied to cells are often expressed as mass of PM per surface area of cells, both values are expressed in this thesis, depending on the circumstance. Interchange between the two values for each culture type is shown below (Table 2.1).

Plate	SA (cm^2)	Vol (µl)	PM Concentration Equivalents (µg/cm^2)					
			2.5 µg/ml	5 µg/ml	10 µg/ml	12.5 µg/ml	25 µg/ml	50 µg/ml
24-well	1.8	400	0.6	1.1	2.2	2.8	5.6	11.1
96-well	0.3	75	0.6	1.3	2.5	3.1	6.3	12.5
TW	0.3	75	0.6	1.1	2.2	2.8	5.6	11.1

Table 2.1. Transposition of PM concentrations between dose metrics.

Two methods of expressing PM concentration are as mass per volume of suspension (µg/ml) or mass per surface area of cell culture (µg/cm^2). Conversion from the volume metric to surface area metric was achieved by multiplying volume concentration (µg/ml) by volume (ml) to give PM mass, and then dividing by surface area (cm^2) to give surface area concentration (µg/cm^2). The procedure is reversed to convert from the surface area metric to volume concentration metric. SA – Surface area per well, Vol – Volume of suspension in challenge per well, TW – Transwell.

24 h post-challenge, supernatants were removed and centrifuged at 16,000 x *g* for 10 min at 4 °C to remove cellular debris and particulate matter. The supernatants were then transferred to new tubes and stored at -80 °C until needed.

2.13 Lactate Dehydrogenase (LDH) Assay

Cytotoxicity was measured using a Cytotox 96 lactate dehydrogenase assay kit, performed according to the manufacturer's instructions, except for the use of half volumes at each step, with samples being assayed in duplicate. The assay is a simple colorimetric assay based on a two-step reaction, the first of step of which is catalysed by LDH to produce nicotinamide adenine dinucleotide (NADH) (reaction 1), which then reacts with 2-(4-iodophenyl)-3-(4-nitrophenyl)-5-phenyl tetrazolium chloride (INT) to produce a red formazan product (reaction 2). The degree of colour change is proportional to LDH activity in the supernatant, as long as the extinction coefficient is not approached. These reactions are:

$$NAD^+ + \text{lactate} \rightarrow \text{pyruvate} + NADH \quad [1]$$

$$NADH + INT \rightarrow NAD^+ + \text{formazan} \quad [2]$$

To provide a measure of total cellular lactate dehydrogenase activity, one or more wells incubated with serum-free medium were supplemented with 400 µl starvation medium, containing 1% Triton X-100 to lyse cells. All solutions for LDH testing were stored at 4 °C and assayed within 24 h of removal. Freezing of samples was avoided due to considerable evidence that the process of freezing can dramatically reduce LDH activity in solutions which do not contain the high levels of protein found in serum or serum-supplemented medium, while LDH is largely unaffected by 24 h storage at 4 °C (414, 415). The reverse appears to be true for protein-rich samples, where levels of enzymes normally susceptible to degradation by the freeze-thaw process are better maintained by freezing rather than refrigeration (416).

To perform the assay, briefly, supernatants were diluted 1 in 4 in the same type of medium as used in the challenge (i.e. MEM or BEBM). 25 µl of this diluted supernatant was added to the well of an uncoated clear, flat-bottomed 96-well plate (Greiner Bio-One, Stonehouse, UK). To each well was added 25 µl reagent, reconstituted in reaction buffer according to the manufacturer's instructions, and the

plate left on a flat surface at room temperature, in the dark, for 30 min. Lysates were assayed similarly, but diluted 1 in 10 in serum- and BSA-free medium as used for the challenge, since this concentration had previously been found to lie on the liner part of a dilution curve. Blanks were run for the medium and also a positive control, included with the assay kit, diluted 1 in 5,000 in 1% BSA in PBS. After 30 min, the reaction was stopped by addition of 25 μl "stop" solution, and absorbance read at λ=492 nm using a Labsystems Multiskan Ascent plate reader. Total LDH activity was calculated as the sum of the LDH activities in the lysate and medium control samples, after correction for the 1 in 10 and 1 in 4 dilutions respectively. Cytotoxicity for each challenge was calculated as the LDH activity of the supernatant as a percentage of total LDH activity.

2.14 Cytokine Release Analysis

Cytokine release into culture supernatants was assessed using enzyme-linked immunosorbent assays (ELISA). Sandwich ELISA was used, the procedure being performed according to the manufacturer's instructions, except with the use of half volumes compared to those suggested. There are two principal forms of ELISA – sandwich ELISA and competition ELISA. Both are immunochemical methods exploiting antibody binding and colorimetric change, but differ in terms of the specifics of reagents used, and also in terms of colour change (in sandwich ELISA, colour change is proportional to concentration of the assayed species, while in competition ELISA colour change is inversely related to concentration of the assayed species). Only sandwich ELISA was used in these studies.

The principle of sandwich ELISA, described here for IL-8, involves the retention in the well of IL-8 by precoating a high-absorption plate with antibody specific to IL-8 (the capture antibody), followed by incubation with supernatant containing an unknown concentration of IL-8. Washing removes all unbound supernatant content, after which a detection antibody specific to IL-8 is added. Thus the IL-8 is "sandwiched" between the capture and detection antibodies. The detection antibody is pre-biotinylated, so subsequent incubation with a streptavidin-horseradish

peroxidase (HRP) conjugate permits retention of the HRP in the well, such that the greater the concentration of IL-8 in the supernatant, the greater the concentration of HRP retained in the well. After washing, a substrate solution mix of hydrogen peroxide (the substrate) and TMB (the chromogen) is incubated in each well. As the hydrogen peroxide component of the substrate solution is broken down by the horseradish peroxidase conjugated to the previously applied streptavidin, oxygen radicals are produced, which oxidise TMB to induce the development of a blue colour, in a manner which is initially proportional to HRP, and thus IL-8 concentration. Absorbance can then be read, and IL-8 concentration determined using a standard curve. This procedure is summarised diagrammatically in Figure 2.2.

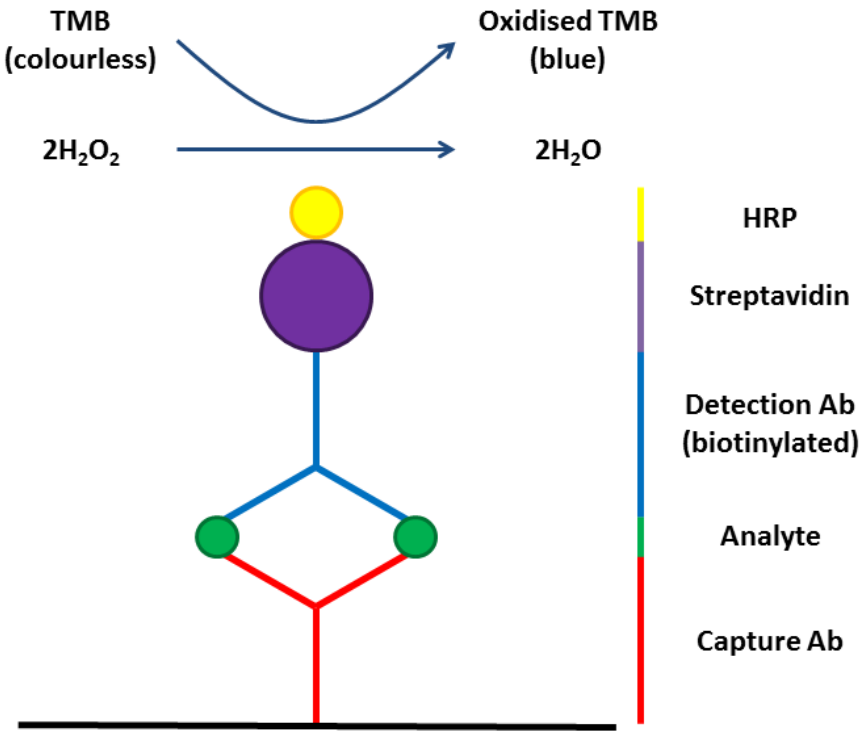

Figure 2.2. The principles of sandwich ELISA.

In this instance, for IL-8, 96-well Nunc Maxisorp plates were coated with capture antibody supplied with the kit, at a dilution of 1 in 180 in PBS, 50 µl per well (all reagent volumes were 50 µl per well unless stated otherwise). After overnight incubation at room temperature, plates were washed with wash buffer (0.05% Tween

20 in PBS), and blocked with 1% BSA in PBS, 150 µl per well, for 1 h at room temperature. Dilutions of supernatants were prepared at concentrations of 1 in 15 and 1 in 20 for 16HBE and primary cultures respectively, in reagent diluent (0.1% BSA and 0.05% Tween-20 in Tris-buffered saline (TBS)). After removal of the blocking buffer and three washes with wash buffer, diluted supernatants were added, each supernatant being assayed in duplicate. Standards were prepared from the supplied stock, diluted serially to form seven standards of 2000 pg/ml down to 31.25 pg/ml, and added to the plate in duplicate. Two wells were used as reagent blanks, containing reagent diluent without supernatant, and as such should be free of analyte. The plate was then incubated overnight in the dark at 4 °C.

After overnight incubation, plates were washed three times, incubated with a 1 in 180 dilution of detection antibody in reagent diluent for 2 h at room temperature, and washed as before. Streptavidin-HRP diluted 1 in 200 in reagent diluent was added and incubated at room temperature for 20 min, followed by further washing. Finally, substrate solution was added to each well and allowed to incubate at room temperature for approximately 20 min, making sure that a visible colour difference was seen between the lowest concentration standard and the reagent blank. The reaction was then arrested by the addition of 25 µl 1 M sulphuric acid (H_2SO_4) per well. Absorbance was measured using a Labsystems Multiskan Ascent plate reader at a wavelength of 450 nm, with absorbance at 570 nm also being measured and subtracted from the absorbance at 450 nm, as a measure of the absorbance of the plate itself. A standard curve was constructed using the software accompanying the plate reader, from which IL-8 levels in the supernatants were interpolated. The curve was plotted according to the "four parameter logistic" curve setting. An example of such a standard curve is shown in Figure 2.3. ELISA kits were tested for cross reactivity as indicated by Table 2.2 below.

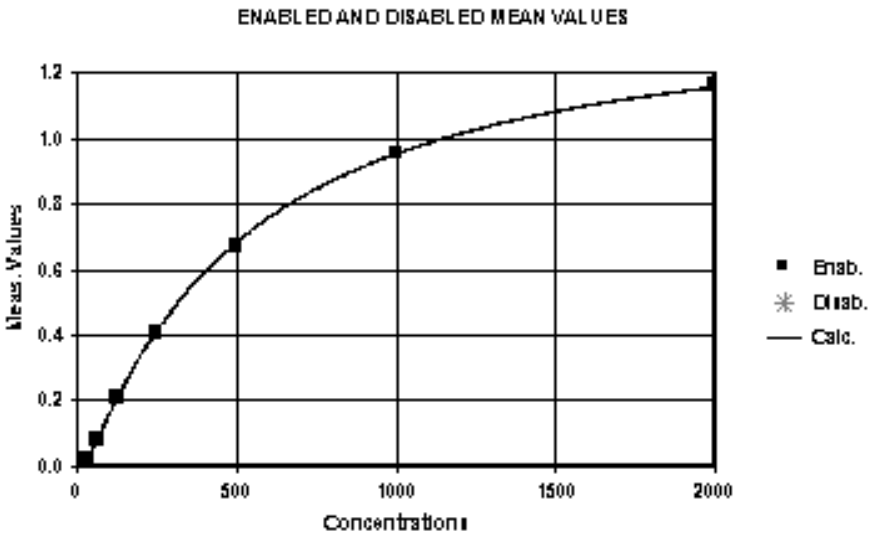

Figure 2.3. A typical standard curve for ELISA.

An example of a standard curve used to determine concentrations of cytokines and chemokines in culture supernatants assayed by ELISA.

Analyte	Lower Limit of Detection (pg/ml)	No Cross-Reactivity
IL-8	31	GROα, GROβ, GROγ, I-309, IP-10, MCP-1, MCP-2, MCP-3, MIP-1α, MIP-1β, RANTES
TNFα	16	TNFβ, sTNFRI, sTNFRII
TNFα (high sensitivity)	0.5	ANG, β-ECGF, EGF, FGF, FGF-4, G-CSF, GM-CSF, GROα, IGF-I, IGFI, IGFII, IFNγ, IL-1α, IL-1β, IL-1ra, IL-2, IL-3, IL-4, IL-5, IL-6, IL-6 sR, IL-7, IL-8, IL-9, IL-10, IL-11, LIF, M-CSF, MCP-1, MIP-1α, MIP-1β, OSM, PDGF, RANTES, SLPI, TGFα, TGF-β_1, TGF-β_2, TGF-β_3, TNFβ, sTNFRI, sTNFRII

TSLP (commercial)	31	IL-7, IL-7Rα, TSLPR
TSLP (in-house)	1	
IL-18	10	IFN-α, IFN-γ, IL-1β, IL-4, IL-5, IL-6, IL-10, IL-12, GM-CSF
IL-33	23	Pro-IL-33, ST2 (IL-1R4)

Table 2.2. ELISA kit detection limits and specificity.

Table shows lower limit of detection (lowest point on standard curve) and analytes which were stated in the product literature as being undetectable with the respective ELISA kit.

2.15 Detection of ROS Generation by Particulate Matter *in Vitro*

PBECs from healthy donors were cultured in 96-well plates as described above, until 85-90% confluent, before being starved for 24 h. Immediately prior to the experiment, starvation medium was removed, and cells were washed once with 150 µl/well HBSS. Following this wash, cells were incubated at 37 °C in the dark with 10 µM DCF-DA, 75 µl per well, from a pre-prepared 50 mM stock in DMSO, diluted to working concentration in HBSS. After 30 min loading, the DCF-DA solution was aspirated and the cells were washed twice with HBSS as for the initial wash. Subsequent steps were performed in a culture hood with the light turned off, in order to reduce photobleaching of the DCF or potential photochemical generation of ROS.

Underground railway PM challenges prepared as above were applied immediately in a volume of 75 µl per well, with each challenge being performed in duplicate. A pair of wells were also challenged with PM after being incubated with HBSS in the loading phase (i.e. no DCF-DA), to verify that there was no autofluorescence of either the cells or the medium confounding the results. As soon as challenges were applied, fluorescence was measured (λ_{exc} = 485nm, λ_{em} = 530nm) on a Labsystems Fluoroskan FL fluorimeter, this reading being regarded as t=0 h. Further readings were then taken at regular intervals.

To further explore the ability of PM to generate ROS, experiments were carried out with the addition of either DFX or N-acetylcysteine (NAC). DFX and NAC were each dissolved in MEM or BEBM at stock concentrations of 50 mM and 200 mM respectively and stored at -20 °C. Solutions for cell challenge were prepared in Eppendorf tubes as for the above experiments. DFX or NAC were prepared at seven concentrations of each, using 1 in 5 serial dilutions to achieve final concentrations from a high of 200 μM (DFX) and 25 mM (NAC). DFX and NAC solutions were then added to PM suspensions or controls to achieve the required final concentrations of all constituents. Immediately after addition of DFX or NAC, challenge solutions were applied to cells, and a fluorescence reading taken as above (t=0 h). No prolonged pre-incubation of PM with either DFX or NAC, nor of NAC with cells, was performed. As above, cells pre-incubated with HBSS and no DCF-DA were checked for fluorescence in the presence of DFX and NAC to verify the absence of fluorescence of either of these molecules.

2.16 The Effect of Underground Railway PM on Epithelial Permeability

In order to assess the effect of underground railway PM on epithelial barrier permeability after 24 h exposure, apical and basolateral supernatants of ALI cultures were removed, and the apical compartment washed once with 200 μl HBSS. 300 μl fresh starvation medium was added to the basolateral compartment, and 4 kDa FITC-labelled dextran (at a final concentration of 2 mg/ml in BEBM) was added to the apical compartment of ALI cultures. One Transwell with no cells was prepared identically in order to determine the extent of FITC-dextran passage when not impeded by the epithelial cell layer. A twelve-point standard curve with a top standard of 1 mg/ml FITC-dextran and subsequent points representing 1 in 2 serial dilutions was prepared in ALI starvation medium at the same time. Cultures and standards were incubated at 37 °C in the dark for 24 h, after which time the concentration of FITC-dextran in the basolateral compartment was determined against a standard curve using a Labsystems Fluoroskan FL fluorimeter, with λ_{exc}=485 nm and λ_{em}=530 nm for duplicate readings of 100 μl of basolateral medium from each well.

2.17 Effects of Ultrafine Underground Railway PM on Gene Expression

To examine changes in gene expression in healthy ALI cultures after exposure to ultrafine underground railway PM, ultrafine underground railway particulate matter (final concentration 5.6 μg/cm^2) was applied to the apical compartment of ALI cultures as above for 2, 4, 6, 8, 24, or 48 h. After the relevant time, supernatants were collected and total RNA was harvested by cell lysis using Trizol reagent according to the manufacturer's protocol. Briefly, apical and basolateral supernatants were removed from ALI-cultured PBECs, and 200 μl HBSS was applied to the apical side of the membrane and removed immediately, in order to wash the cells, removing cellular debris and residual particulate matter. 200 μl Trizol was then added to the apical compartment and left to incubate for approximately 10 minutes at room temperature. After scraping the membrane to remove any remaining cells, the lysate was transferred to a clean Eppendorf tube and stored at -80 °C until RNA extraction was performed. Further experiments were performed using the same concentration of ultrafine underground railway PM combined with either DFX (final concentration 200 μM) or NAC (final concentration 20 mM) to study the mechanism of any alterations in gene expression.

2.18 RNA Isolation and Real-Time PCR Challenge

2.18.1 RNA Extraction

RNA was extracted from cell lysates by means of a standard chloroform/ethanol precipitation protocol. After thawing of lysates, one fifth volume of chloroform was added, and the mixture was shaken vigorously for 15 s, followed by 10 min incubation at room temperature. The sample was then centrifuged at 13,800 x *g*, 4 °C for 15 min, producing two fractions – a colourless upper fraction containing RNA in chloroform and a pink lower fraction containing protein in phenol, separated by a well-defined turbid, viscous interphase containing DNA. The colourless upper phase was carefully removed and transferred to a new Eppendorf tube, and 1 µl of a 20 mg/ml glycogen solution was added to act as a nucleic acid co-precipitant, increasing the mass of the subsequently recovered RNA pellet. After briefly vortexing the mixture, an equal volume of ice-cold isopropanol was added, followed by further brief vortexing. RNA was then precipitated overnight at -80 °C.

2.18.2 RNA Precipitation

After overnight precipitation, samples were thawed and kept at room temperature for 15 min, before being centrifuged at 16,200 x *g*, 4 °C for 30 min. This resulted in formation of a small white pellet at the bottom of each tube. The isopropanol supernatant was carefully removed with a pipette, taking care not to disturb the pellet. Pellets were washed with 75% ethanol at the same volume as the original Trizol sample, and centrifuged again at 5,400 x *g*, 4 °C for 5 min. The ethanol was carefully removed, leaving a pellet which was air-dried in the tube for approximately 10 min.

2.18.3 Removal of DNA Contamination

In order to remove as much contaminating DNA as possible, a DNase kit was used. Pellets were resuspended in a mixture of 17 µl ultrapure MilliQ water, 1 µl DNase, and 2 µl 10x buffer, and incubated at 37°C for 45-60 min. DNase activity was arrested by addition of 5 µl neutralization buffer, and agitated twice at two min intervals. Samples were then centrifuged at 16,200 x *g* at room temperature for 2 min, and the resulting colourless supernatant transferred to a clean Eppendorf tube, while the slurry pellet was discarded. Samples were then stored at -80 °C.

2.18.4 RNA Quantification

RNA concentration of the solution was assayed using a NanoDrop 1000 spectrophotometer. RNA quantification was performed at 260nm absorbance, and DNA contamination was determined by the ratio of Abs_{260}:Abs_{280}, with 280nm being the peak absorption of DNA. A 260/280 ratio of 1.8-2.0 was considered sufficiently "pure". The volume of solution containing 1 µg RNA was calculated according to the formula:

Volume containing 1 µg RNA (µl) = (1 / RNA concentration (ng/µl)) x 1000

2.18.5 Reverse Transcription

RNA was reverse transcribed into complementary DNA (cDNA) using a Precision Reverse Transcription kit. In this two-step reverse transcription (RT) reaction, the RNA is heated to denature and remove secondary structures, followed by primers binding to the RNA strands (annealing step). Primers are then extended by a Moloney murine leukaemia virus (MMLV) reverse transcriptase enzyme (extension step).

For the annealing step, 1 μg of RNA (volume calculated as above) was made up to a final volume of 12 μl with ultrapure MilliQ water. To this was added 3 μl of annealing "mastermix" as below (Table 2.3).

Reagent	Volume for 1 Reaction
Oligo-dT Primers	1 μl
Random nonamer primers	1 μl
Deoxyribonucleotide triphosphate (dNTP) mix (10 mM each dNTP)	1 μl

Table 2.3. Reagents used in reverse transcription annealing mastermix.

Oligo-dT primers bind the polyA tail of mRNA, thus allowing the RT reaction to begin from the 3' end of the mRNA, (i.e. the 5' end of the newly synthesized cDNA). Random nonamer primers are random nonanucleotides which bind to the RNA prior to reverse transcription. The inclusion of dNTPs allows extension of the primers to synthesise full cDNA strands in the presence of reverse transcriptase enzyme. The 15 μl solution containing 1 μg RNA and RT kit components was incubated at 65 °C for 5 min in a T100 Thermal Cycler to denature secondary RNA structures, allowing primers and dNTPs to access and anneal to the full length of RNA strands (annealing step). Immediately after the incubation period, samples were snap-cooled using ice from a -80°C freezer to arrest annealing, the rapid cooling reducing the formation of further secondary structures.

The extension step was performed by the addition of 5 μl extension "mastermix" to each reaction tube (Table 2.4).

Reagent	Volume for 1 Reaction
MMLV-RT enzyme	0.8 μl
5x RT buffer	4.0 μl
Ultrapure MilliQ water	0.2 μl

Table 2.4. Reagents used in reverse transcription extension mastermix.

Extension was performed by incubation at 37 °C for 10 min, followed immediately by 42 °C for 60 min. After completion of the incubation, cDNA samples were diluted 1 in 10 in ultrapure MilliQ water (i.e. 180 µl water added to 20 µl reaction product), and stored at -80 °C until required for quantitative polymerase chain reaction (qPCR).

2.18.6 Quantitative Polymerase Chain Reaction

Polymerase chain reaction (PCR) is a method for the amplification of cDNA sequences. After heating of the cDNA to separate the two strands (denaturing, at approximately 95 °C), the mixture is cooled to approximately 50-65 °C and a strand of DNA usually 18-22 base pairs (bp) long, termed the primer, anneals to a complementary sequence in the cDNA. The forward primer anneals to part of the sense strand of cDNA, while the reverse primer anneals to the anti-sense strand. The mixture is then either maintained at this temperature or heated to approximately 70-75 °C so that dNTPs in the reaction mixture which have annealed to cDNA bases downstream of the primer can be joined together by a DNA polymerase enzyme. Such an enzyme must be able to maintain its tertiary structure and have optimum polymerisation rate at a temperature which would result in the denaturation of most other enzymes, and therefore such enzymes were originally extracted from thermophilic bacteria, such as Taq polymerase from *Thermophilus aquaticus*. However, such enzymes are now artificially produced. After this polymerisation step, the cycle is repeated, starting with the initial denaturation step to separate the original cDNA strand from the newly synthesised strand. Using primers which anneal specifically to sequences at different points within a certain gene means that only the RNA sequence between the forward and reverse primers is amplified. After one cycle, there is twice the original number of strands since each strand has been copied once. After two cycles, there is a further doubling. Therefore, the number of copies of the sequence to be amplified per original copy increases exponentially according to the series 2, 4, 8, 16, …2^n, where n represents the number of cycles of PCR performed.

Quantitative polymerase chain reaction (qPCR), sometimes known as reverse transcription quantitative polymerase chain reaction (RT-qPCR) is a technique using the principles of PCR as detailed above in order to measure the relative amounts of cDNA coding for the region being amplified. Each well of a white 96-well white plastic reaction plate contained a mastermix (containing nucleotides, a DNA polymerase enzyme and, for the SYBR Green system, the fluorophore), ultrapure MilliQ water, primers for the gene of interest (which also contain the fluorescently tagged probe if the Perfect Probe system is being used), and cDNA (Table 2.5). A mixture of Mastermix, water, and primer was prepared, and aliquotted into each well. cDNA was then added, with each sample being run in duplicate. The plate was centrifuged at 300 x *g* for 2 min to pull the reaction mixture to the bottom of the well. The plate was then run on an iCycler CFX96 thermal cycler.

Gene	Reagent	Volume per reaction
Housekeeping duplex (UBC/GAPDH)	Mastermix	12.5 µl
	H_2O	9 µl
	Primer	1 µl
	cDNA	2.5 µl
Gene of interest	Mastermix	5 µl
	H_2O	2 µl
	Primer	0.5 µl
	cDNA	2.5 µl

Table 2.5. Reagents used in qPCR.

Two systems were used – Perfect Probe and SYBR Green. In the Perfect Probe system, the primer mix also contains a probe – a short length of DNA complementary to a specific sequence within the amplified region. This probe is labelled with a fluorophore and a quencher so that under normal conditions fluorescence cannot be detected. However, when the extension step is performed, the exonuclease activity of the DNA polymerase enzyme cleaves the probe, separating the fluorophore and the quencher, which detaches from the probe, allowing fluorescence to be detected. As

such, the level of fluorescence indicates the number of amplified strands. The use of a probe which is complementary to a section of the amplified region ensures that only the amplification of the cDNA region of interest is measured, and not other sections such as mis-amplified regions or primer dimers. The SYBR Green system is simpler, whereby the fluorescent dye SYBR Green intercalates with the minor groove of double stranded DNA. This SYBR Green-DNA complex fluoresces with an emission wavelength of 520 nm (green). However, since there is no probe, it is possible that fluorescence comes from mis-amplified regions or primer dimers. Therefore, a melt curve is run at the end of the final qPCR cycle. The PCR products are heated incrementally, and a fluorescence reading is taken after each incremental heating step. If a single product has been amplified with no significant contamination, all SYBR Green-DNA complexes should have the same sequence, and thus the same melting temperature. Therefore, there should be a specific temperature point on the melt curve at which fluorescence drops markedly (Figure 2.4). Conversely, if there is a significant presence of primer dimers and mis-amplified fragments, there will be a variety of melting temperatures within a sample, and therefore the fluorescence will change over a range of temperatures. Inspection of the melting curve therefore verifies that the amplifications have produced a single product.

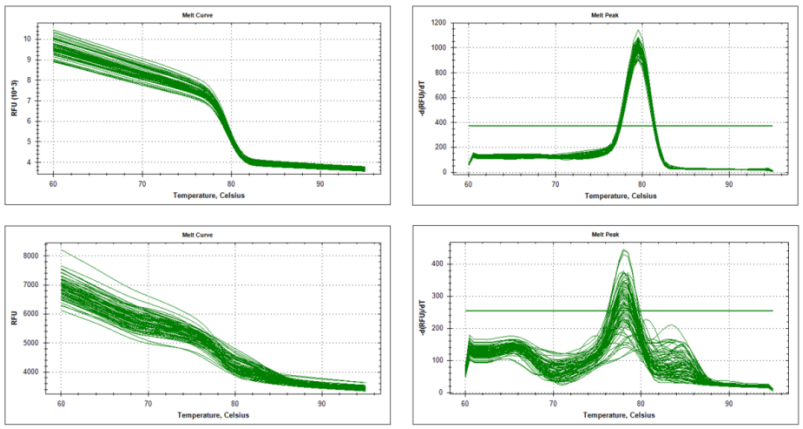

Figure 2.4. Melt curves after SYBR Green qPCR.

The melt curve for amplification of a single product should show a decrease in fluorescence at a single temperature (top left). The same data can also be represented as a change in fluorescence, rather than fluorescence intensity (top right). Conversely, wells containing multiple different amplification products will exhibit a range of temperatures at which fluorescence decreases, and thus Ct values for these reactions are unreliable (bottom left and bottom right).

For both detection systems, as amplification proceeds, there is an increasing fluorescence of the sample (Figure 2.5). A threshold for fluorescence is set on the liner ascending part of the curve which results when fluorescence is plotted on a logarithmic scale against amplification cycle number.

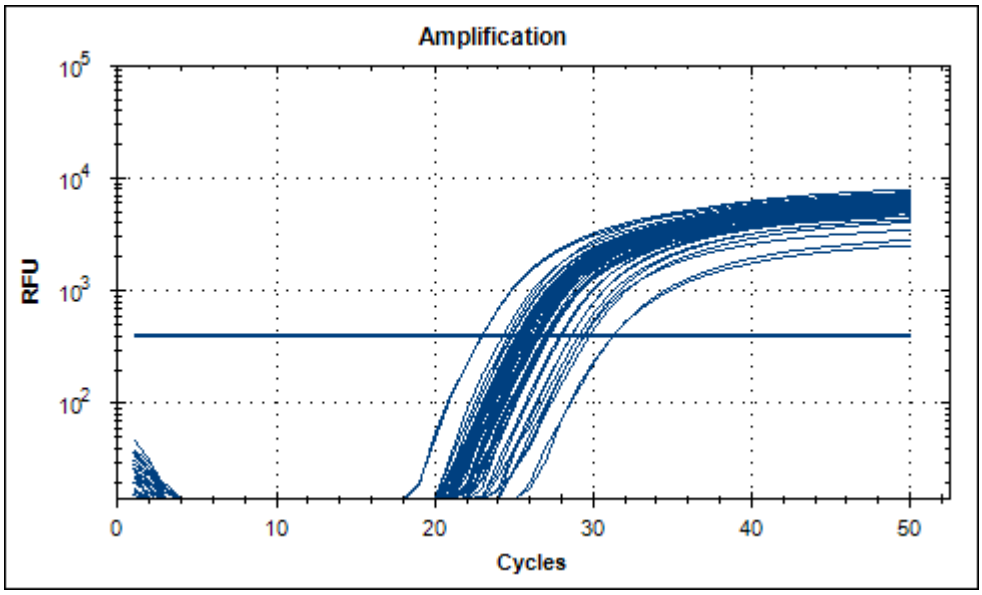

Figure 2.5. qPCR readout.

The relative fluorescence units (RFU) increase for each sample with increasing cycle number. The Ct value is the number of cycles requires for a sample's RFU value to exceed the threshold (blue horizontal line) suggested by the analysis software. Since this will occur after fewer cycles if there was a greater number of transcripts in the original sample, a low Ct value indicates a greater expression of the sequence of interest.

When the curve for a particular sample crosses this threshold, the cycle number is read off, termed the Ct value. Ct values are first calculated for both of the housekeeping genes (UBC (FAM fluorophore) and GAPDH (Cy5 fluorophore)), and a geometric mean of the two is calculated. The Ct value for the gene of interest is similarly calculated. The housekeeping gene geometric mean Ct is subtracted from the same sample, to give the ΔCt value (equation 1). The ΔCt value for the control sample is then subtracted from the ΔCt value for each treatment to give a ΔΔCt value for each treatment (equation 2). Fold change in gene expression is then calculated (equation 3):

$$\Delta Ct = Ct_{\text{gene of interest}} - Ct_{\text{housekeeping gene}} \quad [1]$$

$$\Delta\Delta Ct = \Delta Ct_{\text{treatment}} - \Delta Ct_{\text{control}} \quad [2]$$

$$\text{Fold change in gene expression} = 2^{-\Delta\Delta Ct} \quad [3]$$

qPCR was performed using primers for the genes HO-1, IL-8, IL-33, NQO1, and TSLP (Table 2.6), using the cycling conditions for the relevant system (Table 2.7).

Gene	Forward	Reverse	System
Housekeeping Genes UBC/GAPDH	Sequences not available from supplier. Assay code HK-PP-hu-900-d-UBC/GAPDH		Perfect Probe
HO-1	GGAAGCCCCCACTC AACA	GCATAAAGCCCTAC AGCAACT	Perfect Probe
IL-8	CAGAGACAGCAGA GCACAC	AGCTTGGAAGTCA TGTTTACAC	Perfect Probe
IL-33	AAAGAAAGATAAG GTGTTACTGAGTTA	GCAACCAGAAGTC TTTTGTAGG	SYBR Green
NQO1	Sequences not available. Assay ID HS00168547_m1		Perfect Probe
TSLP	AATCCAGAGCCTAA CCTTCAATC	GTAGCATTTATCTG AGTTTCCGAATA	SYBR Green

Table 2.6. Primers used in qPCR reactions.

All primer sequences run from the 5'-end to the 3'-end of the primer sequence.

System	Step	Temp	Time	
Perfect Probe	Denaturation	95 °C	10 min	
	Denaturation	95 °C	15 s	Repeat cycle x50
	Annealing	50 °C	30 s	
	READ			
	Elongation	72 °C	15 s	
SYBR Green	Denaturation	95 °C	10 min	
	Denaturation	95 °C	15 s	Repeat cycle x50
	Annealing and Elongation	60 °C	60 s	
	READ			
	Melt Curve Denature	95 °C	3 min	
	Melt Curve Start	60 °C	1 min	
	Melt Curve	60 °C – 95 °C, 0.5 °C increments, read after each	5 s each	

Table 2.7. Thermal cycling conditions for qPCR.

2.19 Electron Microscopy

2.19.1 Fixing of cells for transmission electron microscopy (TEM)

After incubation and removal of supernatants, PBEC ALI cultures on Transwells were washed twice with PBS, applied to the apical and basal compartments of each well. After aspiration of the final wash of PBS, a fixative of 3% glutaraldehyde and 4% paraformaldehyde in 0. 1M PIPES buffer at pH 7.2 was applied, 300 µl to the apical compartment and 500 µl to the basolateral compartment. This was left at room temperature for 30 min, before wells were stored at 4 °C for up to 14 days.

2.19.2 Embedding cells for TEM

All steps were applied to both the apical and basal compartments of each Transwell, ensuring that the volume applied for each solution was in excess of that required to cover the Transwell from either side. Between all steps, solutions were aspirated from both compartments of each well. All steps were performed at room temperature unless stated otherwise.

The fixative in which the well was stored at 4 °C was aspirated. Two washes of rinse buffer (0.1M PIPES, pH 7.2) for 5 min each were followed by treatment with a post fixative solution of 1% osmium tetroxide in 0.1 M PIPES buffer at pH 7.2 for 1 h, followed by a rinse with distilled water. Cells were then treated with a 2% aqueous solution of uranyl acetate for 20 min, followed by four dehydration steps of 10 min each in, successively, 30%, 50%, 70%, and 95% ethanol. Dehydration was completed by two treatments of 20 min each in absolute ethanol.

Transwell membranes were then excised from wells using a scalpel, being regularly moistened with absolute ethanol, and immediately placed into individual specimen jars containing absolute ethanol. The absolute ethanol was aspirated and immediately replaced with approximately 1 ml acetonitrile per jar, and left for 10 min. This was then replaced with a 50:50 mixture of acetonitrile and Spurr resin, and left overnight at room temperature.

After overnight treatment, the acetonitrile/Spurr resin solution was aspirated and replaced with approximately 1 ml pure Spurr resin per specimen jar, and allowed to sit for 6 h. Membranes were removed from the resin, cut in half, and each half put into a separate, labelled, Spurr resin-filled capsule, oriented so that the face of the Transwell was parallel to one side of the capsule. The capsules were then placed in an oven at 70 °C for 24 h to allow for resin polymerisation to occur.

Following polymerisation, capsules containing resin blocks were stored at room temperature.

Ultrathin sections of approximately 60 nm thickness were cut using an ultramicrotome, and stained with Reynold's stain (lead citrate solution as previously described (417)) for 3 min prior to viewing on a Hitachi H7000 transmission electron microscope. Energy dispersive x-ray spectroscopy was performed on an FEI Techai12 EDAX transmission electron microscope.

2.20 Challenge of Cells with *Alternaria* Extract

24 h prior to challenge, cells were serum-starved as for experiments with particulate matter. Lyophilised *Alternaria alternata* and *Cladosporium herbarum* extracts were dissolved into supplement-free medium to make a stock of 10 mg/ml and stored at -20 °C until required. Aliquots were thawed and diluted as required, and added apically in varying concentrations. To assess the heat-lability of fungal activity, aliquots of the dissolved allergen extracts were heat-treated at 65 ºC for 30 min. To determine protease types present, 30 min prior to stimulation, prepared *Alternaria* extract was incubated at 37 °C with the protease inhibitors AEBSF (500 μM with *Alternaria*), E-64 (100 μM), or Pepstatin A (1 μg/ml), or cells were pre-treated with the p38 MAPK inhibitor SB203580 (50 μM applied apically, kept on the cells for the whole challenge period, reduced to 25 μM by addition of fungal challenge solution) for 30 min. For 16HBE challenge, fungal extracts were applied apically at concentrations of 50 μg/ml and 100 μg/ml in a final volume of 200 μl and TER measured at 1 h and 24 h post-challenge. For ALI challenge, 50 μl fungal extracts were added to the apical compartment at 25, 100, or 400 μg/ml to retain the air-liquid interface as much as possible. TER was measured immediately prior to the addition of extracts using chopstick electrodes connected to a Millicell ERS-2 epithelial volt-ohm meter, and thereafter at 3 h and 24 h. For TER measurements, 100 μl of $HBSS^-$ was added to the apical compartment, and this was removed immediately afterwards and discarded or combined with the harvested supernatant. At 24 h, apical and basal supernatants were harvested, with apical supernatants being centrifuged at 400 x *g* for 7 min to remove cell debris. Supernatants were then stored at -20 °C until required.

2.21 ELISA following *Alternaria* Challenge

ELISA was performed as described above, using kits to assay supernatant concentrations of IL-8, TNFα, TSLP, IL-18, and IL-33. In addition, a custom-developed ELISA kit to measure TSLP, developed by Novartis Plc, was also used (Table 2.2).

2.22 Fluorimetric Protease Assay

In order to determine the protease activity of *Alternaria* extract in a cell-free system, a commercially available protease fluorescent detection kit was used. This kit is an elegant yet straightforward way of measuring protease assay of a sample, and the use of inhibitors of specific protease activity can be built into the assay in order to quantify contributions of various types of proteases. The assay was performed according to the supplied instruction. Briefly, 10 μl of fungal extract (in this case 500 μg/ml of *Alternaria* or *Cladosporium* extract) was mixed with 20 μl of the supplied incubation buffer and 20 μl of substrate, a FITC-labelled casein solution. Protease activity digests the casein into smaller peptide fragments. After 24 h incubation at 37 °C, 150 μl 0.6 M trichloroacetic acid was added to each sample. This acid precipitates only the undigested casein, while the smaller, digested fluorescent peptide fragments remain in solution. Each sample was then centrifuged at 10,000 x *g* for 10 min to pellet the non-lysed protein. 10 μl of the each supernatant was added to 1ml assay buffer, and fluorescence read with λ_{exc}=485 nm and λ_{emi}=530 nm, with supernatants assayed in duplicate, using a Labsystems Fluoroscan FL fluorimeter. A standard curve for dilutions of trypsin (supplied with the kit) allowed protease activity to be quantified as having activity equivalent to a known concentration of trypsin. The lower limit of detection of this assay was protease activity equivalent to 25 ng/ml trypsin.

In order to determine the relative activities of serine, cysteine, and aspartate proteases in the *Alternaria* extract, aliquots of *Alternaria* extract were incubated with either AEBSF (2.5 mM when incubated with *Alternaria*), E-64 (500 μM), or Pepstatin A (5

μg/ml) at 37 °C for 30 min prior to assay. Although these inhibitor concentrations were, in absolute terms, higher than used with cells, they were the same as used in the cellular experiments on a stoichiometric basis relative to *Alternaria* concentration. Protease activity when *Alternaria* was treated with each inhibitor was then compared to the activity of uninhibited *Alternaria* for AEBSF and E-64, and to *Alternaria* treated with Pepstatin A diluent (10% glacial acetic acid in methanol) for Pepstatin A.

2.23 The Effects of *Alternaria* after Pre-Treatment of ALI Cultures with Ultrafine Underground Railway PM

To study whether pre-exposure to ultrafine underground railway PM could modify the responses of PBEC ALI cultures to *Alternaria* extract, ALI cultures were serum-starved as detailed above for 24 h. Basolateral medium was refreshed, and cultures were exposed apically to ultrafine underground railway PM at a concentration of 5.6 μg/cm^2 (25 μg/ml). Controls were also run, incubated apically with PBS-supplemented BEBM. After 24 h, supernatants were removed, the apical compartment was washed once with HBSS$^-$, basolateral starvation medium was again refreshed, and incubations with either BEBM (as control), 400 μg/ml *Alternaria* extract, or 400 μg/ml heat-treated *Alternaria* extract were performed as per the immediately preceding experiments. TER was measured prior to starvation, and prior to adding ultrafine PM to verify that a tight barrier had been formed (TER reading >1000 Ω). Readings for experimental analysis were taken immediately prior to *Alternaria* challenge (0 h), and at 3 h and 24 h thereafter. After 24 h, apical and basolateral supernatants were removed, centrifuged at 16,000 x *g* for 10 min at 4 °C, and the supernatants stored at -80 °C until required. Cells were washed once with HBSS, lysed with 200 μl Trizol per well, and lysates stored at –80 °C prior to RNA extraction and reverse transcription to cDNA.

ELISA was performed to determine apical and basolateral release of IL-8, and qPCR was performed to measure expression of HO-1 and IL-33 mRNA.

2.24 Statistical Analysis

All data analysis and graph drawing was performed using GraphPad Prism software. To determine whether data were normally distributed, and thus whether parametric or non-parametric statistical tests should be used, the Shapiro-Wilk statistic was examined, with a p-value of <0.05 indicating that the distribution deviated significantly from normally distributed data, and therefore that non-parametric tests should be performed. Conversely, if $p>0.05$, parametric tests were used.

For all tests where treatments were applied to different sets of cells from the same donor, repeated measure/before-and-after/paired analyses were used. Furthermore, for analysis of transition metal variations between size fractions of underground railway PM, the same protocol was used as sets of different size fractions were obtained on each different sampling day.

For comparison between several groups with normally distributed data, one-way repeated measures ANOVA was used, with Bonferroni correction to detect pairwise differences if the initial ANOVA found significant inter-group differences. For non-normally distributed data, a one-way repeated measures ANOVA on ranks (Friedman test) was used, with Tukey's correction applied for pairwise analysis. For analyses involving only two groups, a paired t-test was used to determine significance in the case of normally distributed data, while a Wilcoxon signed rank test was used in the case of non-normally distributed data.

For all statistical analyses, significance was considered to be reached if $p<0.05$.

3 Physicochemical Characterisation of Particulate Matter

3.1 Introduction

The source materials and processes involved in the generation of particulate matter play a major role in determining the physicochemical properties of the particles and, by extension, their biological activity and potential toxicity. However, the complex and varied chemistry of certain source materials, and the fact that this can be modified by equally complex processes involved in particle generation, such as combustion of fossil fuels involved in DEP and ROFA production, renders delineation of the importance of each of the separate constituents of these particles difficult and prone to variation, as evidenced by contradictory findings between many research groups. Particulate composition may also vary depending on season and climate (54). Furthermore, some particulate components, especially VOCs and polyaromatic hydrocarbons, are susceptible to change between collection and physicochemical/toxicological analysis (267).

Underground railway systems are widely used mass transit systems in many major cities, some carrying several million passengers per day (418). High mass concentrations of respirable PM with a mean aerodynamic diameter up to 10 μm (PM_{10}; coarse), 2.5 μm ($PM_{2.5}$; fine) or 0.1μm ($PM_{0.1}$; ultrafine) have been observed in several underground railway systems (67, 80, 81). In many cases, concentrations far exceed WHO recommended limits for 24 h average particle exposure of 50 and 25 $\mu g/m^3$ for PM_{10} and $PM_{2.5}$ respectively, presenting a potential risk for regular

passengers and employees, although these limits only apply to outside environments (61). Notably, $PM_{0.1}$ levels are currently unregulated. Importantly, exposure to PM has been noted to be greater for underground railway journeys than for equivalent journeys made by a variety of overground modes of transport (69), and time spent in underground railways has been suggested to be a better predictor of metal exposure than duration of exposure to traffic-derived metal pollutants (205).

There is evidence to suggest that underground railway PM has high concentrations of Fe and other transition metals compared to ambient PM (64, 66, 206). Transition metals are of interest as potential airborne toxicants because of their ability to generate the ROS superoxide ($^{\bullet}O_2^-$), hydrogen peroxide (H_2O_2) and, by the Fenton reaction, hydroxyl radical ($^{\bullet}OH$) *via* successive single-electron reductions of molecular oxygen (245). It is thought that many of the toxic effects of transition metals arise from oxidative stress due to ROS generation. Defined as an excess of oxidative species that outweighs the antioxidant capacity of a system, oxidative stress can result in oxidation and functional modification of biomolecules such as lipids, proteins, and nucleic acids and can result in inflammation and tissue injury (196). However, transition metals, and also a variety of other metals and metalloids such as lead and arsenic, can exert toxic effects *via* mechanisms other than direct generation of ROS; hence, study of concentrations of non-transition metals in airborne PM is also warranted.

The composition of metal-rich PM from a wide variety of sources has previously been studied, including PM from steel mills, smelting plants, and welding fume (189, 191, 192). However, underground PM studies generally focus on coarse and fine fractions, without parallel analysis of ultrafine PM composition (419). Although individual ultrafine particles have a lower surface area than fine or coarse particles (0.03 *vs.* 19.6 and 314 μm^2, respectively, for particles of 0.1, 2.5, and 10 μm diameter, assuming perfect sphericity), ultrafine PM is often present in a much greater number concentration than coarse or fine PM, and thus their contribution to overall PM surface area has the potential to be very important, possibly being a key determinant of toxicity (37). Furthermore, coarse and fine particles tend to accumulate in the airways by impaction and are rapidly cleared by the mucociliary escalator, whereas ultrafine particles predominantly settle by diffusion in the alveoli, from where clearance is much

slower (20). Ultrafine particles, unlike fine particles, are also able to translocate from the airway lumen to the pulmonary interstitium and potentially the systemic circulation, being detected in the liver, heart, kidneys, and brain (228, 420).

Because there is evidence that underground PM is an important potential toxicant, the aim of this study was to determine the concentration of transition and non-transition metals in respirable, size-fractionated PM collected at an underground railway station and to compare this to PM collected from other process-specific sources, namely a woodstove, a roadwear generator, a road tunnel, and diesel exhaust.

The work presented within this chapter has been published in the journal Environmental Science & Technology (421).

3.2 Results

3.2.1 Particulate Chemical Analysis by ICP-MS

PM was collected between 0830 and 1730 hours on three individual sampling days (all working weekdays in July 2010) at the underground railway station, yielding a mean±SEM underground railway PM_{10} mass concentration of 282±8 μg/m^3, with coarse $PM_{10\text{-}2.5}$ comprising 169±6 μg/m^3, fine $PM_{2.5}$ 75.3±5.9 μg/m^3, and ultrafine $PM_{0.18}$ 37.7±4.5 μg/m^3 (Figure 3.1).

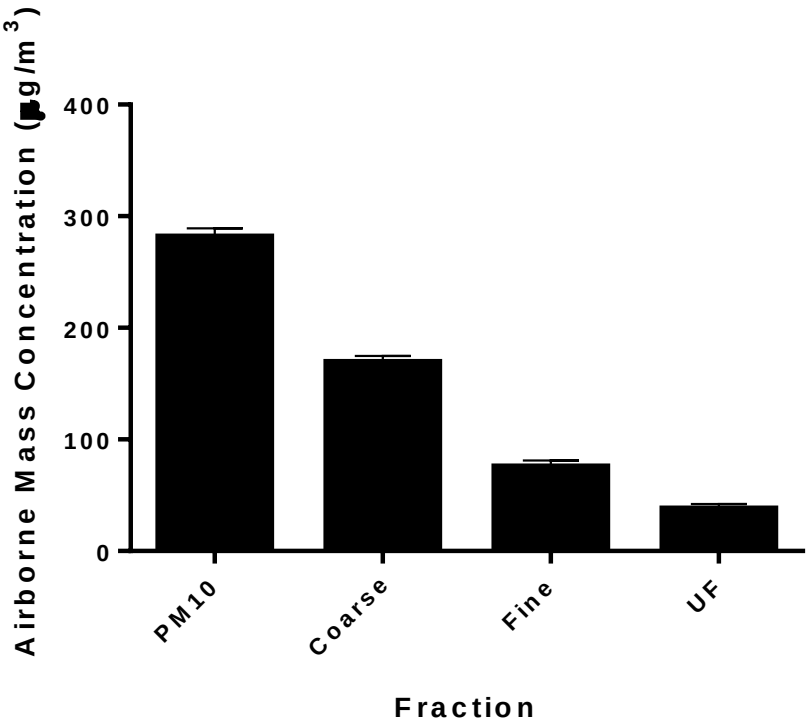

Figure 3.1. Airborne mass concentration of underground railway PM.

Underground railway PM (coarse $PM_{10\text{-}2.5}$, fine $PM_{2.5}$, and ultrafine $PM_{0.18}$) was collected on three separate sampling days. Bars represent mean±SEM airborne mass concentration of each fraction; n=3.

Chemical analysis by ICP-MS was carried out on underground railway PM as well as PM from the other three sources and, as an expected transition metal-poor source, DEP. For woodstove, roadwear, and underground railway PM sampling, individual daily samples were analysed separately. Road tunnel PM and DEP were analysed in the coarse fraction only, as well-characterised references for comparison. In general, underground railway PM was the most transition metal-rich PM, with Fe the most abundant element, comprising 407±43, 404±70, and 484±82 mg/g for coarse, fine, and ultrafine fractions respectively. Thus, Fe comprises greater than 40% of the total mass of the PM (Figure 3.2). Conversely, while all other PM samples contained detectable levels of Fe, only coarse and ultrafine roadwear PM (21.5±0.1 and 18.1±3.5 mg/g) and coarse road tunnel PM (27.7 mg/g) contained Fe levels greater than 1% of the total mass of the PM. Cu was also elevated in underground railway PM compared to PM from other sites, although the Cu concentration (21.9±2.5 mg/g C, 20.7±3.9 mg/g F, and 25.6±4.3 mg/g UF) was lower than that of Fe (Figure 3.3). As with Fe, these Cu levels were considerably higher than those seen in any other sampling locations, across all fractions analysed. Other transition metals that were present at high concentration in underground railway PM included Mn, Cr, and Zn, which are commonly added to steel to alter the properties of the finished material (Figure 3.3), and also Zr, Mo, and Sn. In addition, levels of V, Cr, Ni, Nb, and Hf were higher in underground PM than other sources, although they were found at lower absolute concentrations. Additionally, Ca was high in underground PM, particularly in the ultrafine fraction (54±31 mg/g), as was Ba, found in train braking systems (Figure 3.3) and also Mg, Ca, Zn, and Sb, with relatively high levels of Ga and As also noted (for all elements, see Figure 3.4). Statistical analysis was performed to determine whether there was any significant difference in the concentration of any element assayed across each of the size fractions. Only B showed any pairwise difference, the ultrafine fraction being high *vs.* coarse ($p<0.05$) and fine ($p<0.01$) fractions.

Woodstove PM showed a marked enrichment for K (Figure 3.3), while levels of B and Zn were similar to underground railway PM and in excess of levels in other PM types. Furthermore, Rb (144±3.2 μg/g F, 192±1.8 μg/g UF), Cd (40.4±7.1 μg/g F, 58.0±5.4 μg/g UF), and Pb (185±43 μg/g F, 266±37 μg/g UF) were also relatively high in

woodstove PM compared to other PM sources, although they were low in terms of absolute concentration.

Roadwear PM possessed especially high concentrations of Al, with the three fractions showing concentrations of 71.0±31, 27.3±1.8, and 53.9±7.2 mg/g respectively. These concentrations were second only to underground PM Fe concentrations in terms of the most prevalent metals found at any site. Roadwear PM also contained notably high levels of Ti and to a lesser extent Sr, whereas levels of Sc, La, and Hg were found to be greater than other PM types, albeit at trace levels. Pd was also higher in road tunnel PM, although only at a concentration of 0.129 μg/g, representing 0.0000129% of the total mass of this PM. Indeed, Pd was generally the least abundant of all metals tested.

Coarse road tunnel PM showed relatively high levels of Li, B, and Na. Road tunnel PM also contained elevated levels of Pb relative to other PM samples at 516 μg/g. DEP was also analysed, as a source of PM expected to be low in transition metals. As anticipated, the majority of elements analysed were present in lower concentrations in DEP compared to PM from the other sources tested, and many were not detected at all. There were, however, some differences between DEP samples, especially the high concentrations of zinc and cerium found in diesel sample 1, from a diesel exhaust generator pipe, relative to the other diesel and other PM samples. The potential causes of this are discussed later. Due to their general paucity, the levels of transition metals in DEP are not included in the graphs in Figure 3.4, but are instead shown in Table 3.1.

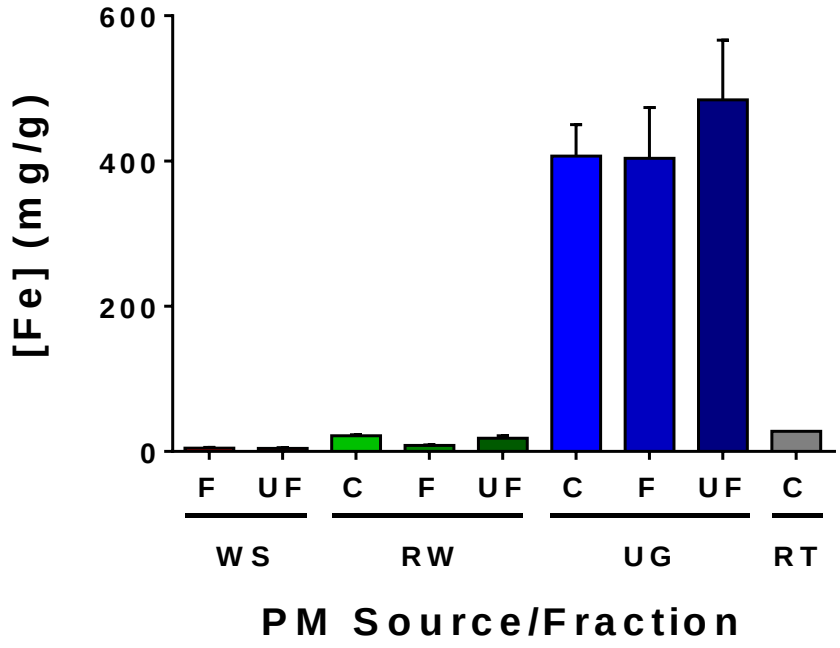

Figure 3.2. The concentration of Fe in PM from various sources.

Coarse (C), fine (F) and ultrafine (UF) PM was collected from a woodstove (WS; n=2), roadwear generator (RW; n=2), underground railway station (UG; n=3) and a road tunnel (RT; n=1). After acid digestion, PM elemental composition was analysed by ICP-MS. Bars represent mean±SEM Fe levels.

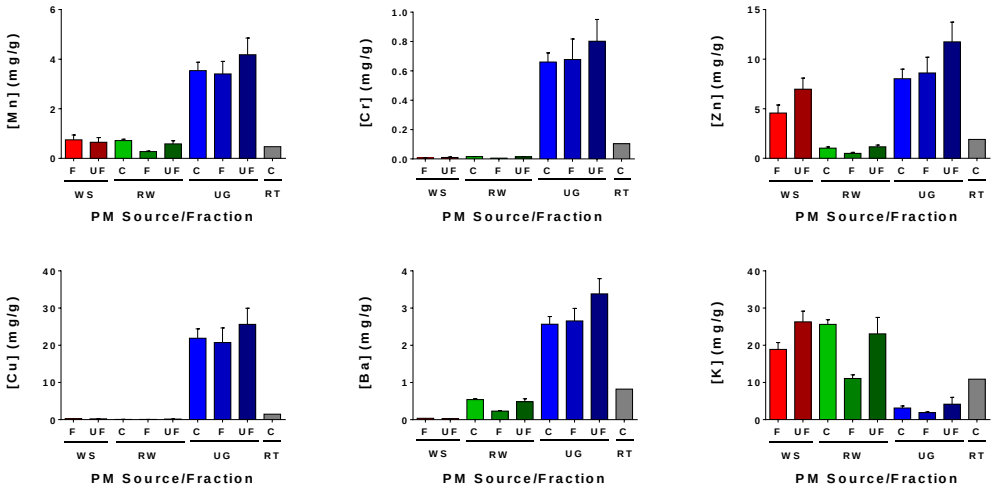

Figure 3.3. The concentration of Mn, Cr, Zn, Cu, Ba, and K in PM from various sources.

PM was collected and analysed as for Figure 3.2. Bars represent mean±SEM elemental concentrations.

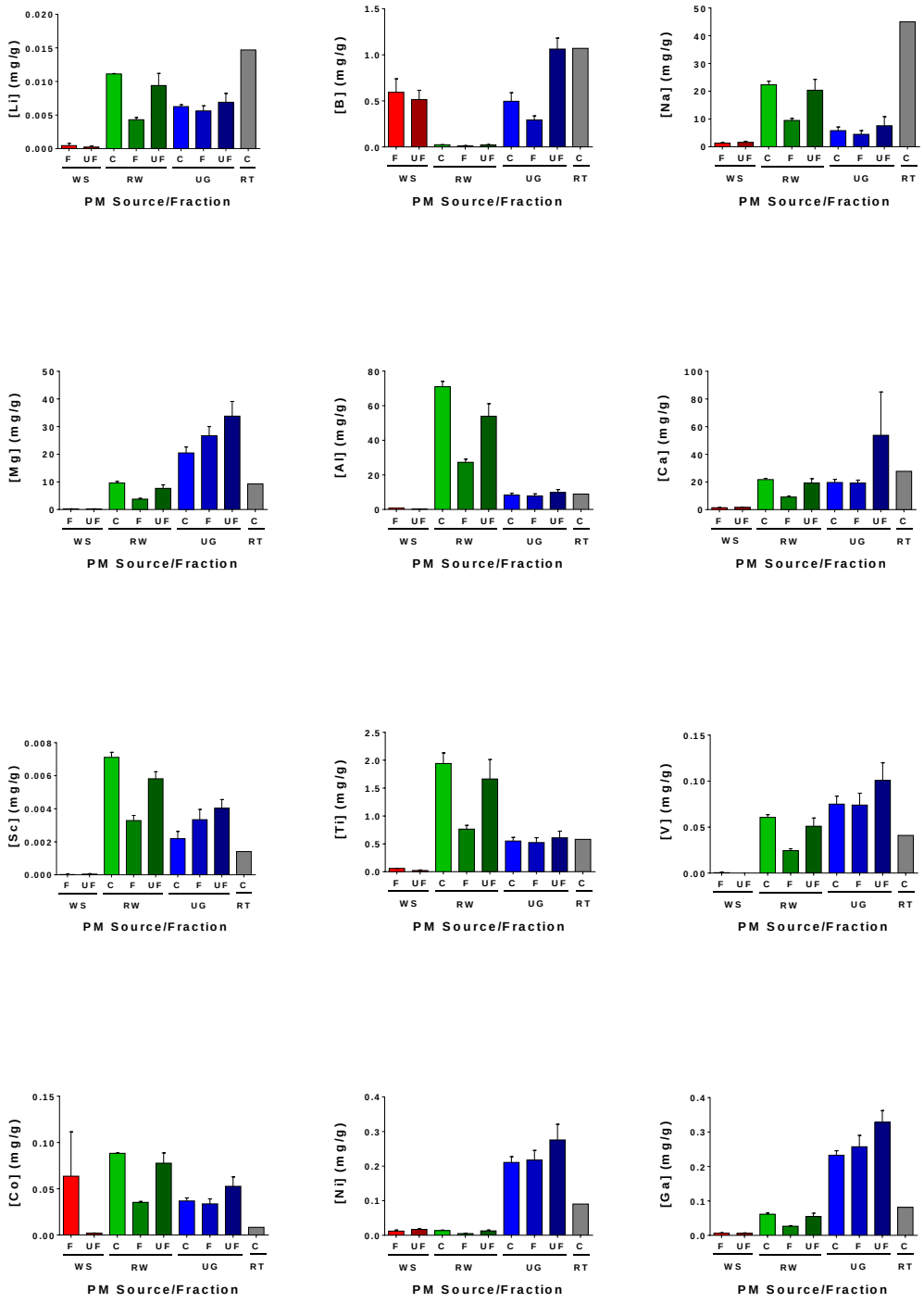

Figure 3.4. The concentrations of elements in PM from various sources.

PM was collected and elemental content analysed as for Figure 3.2. Bars represent mean±SEM elemental concentrations.

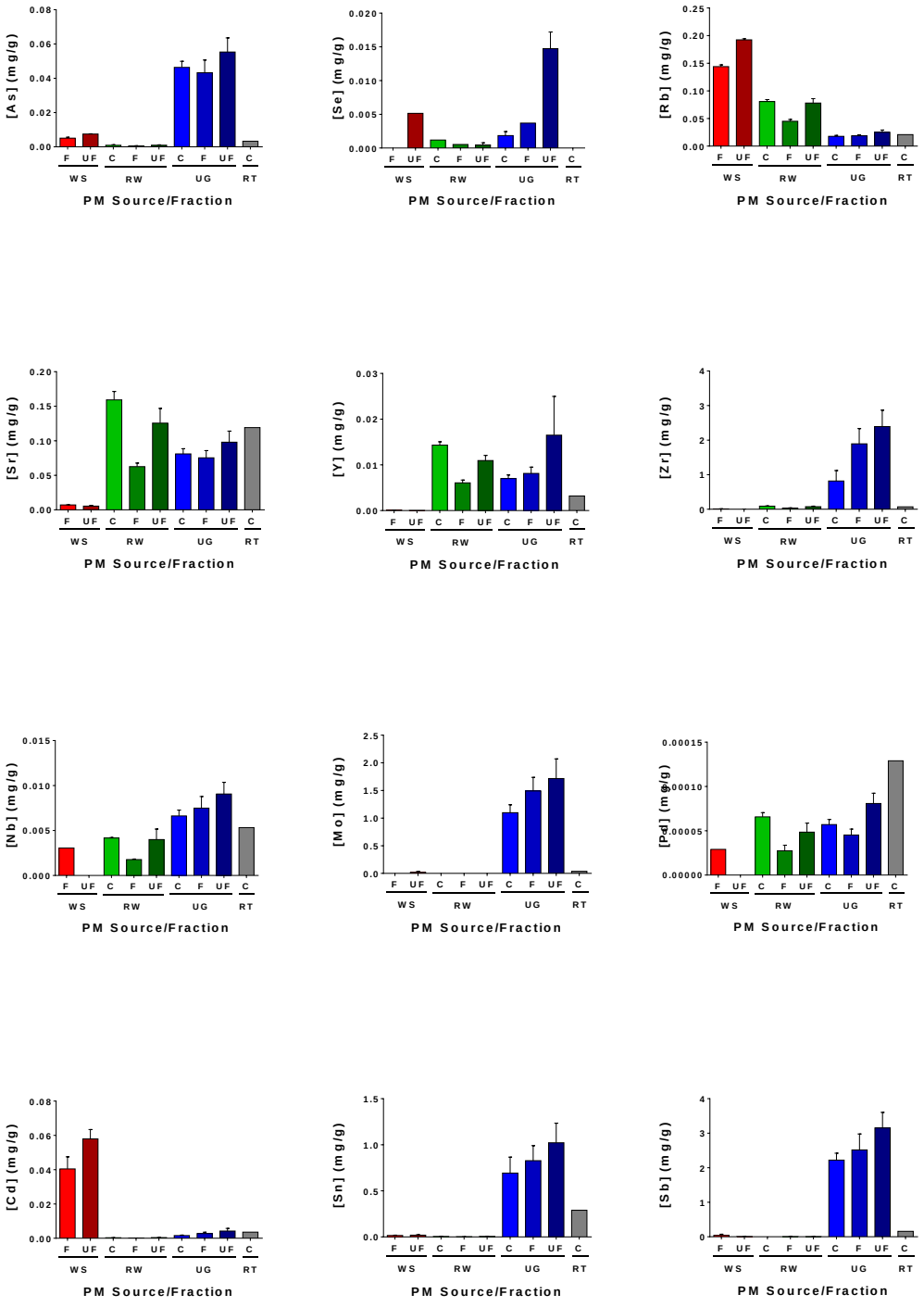

Figure 3.4 continued.

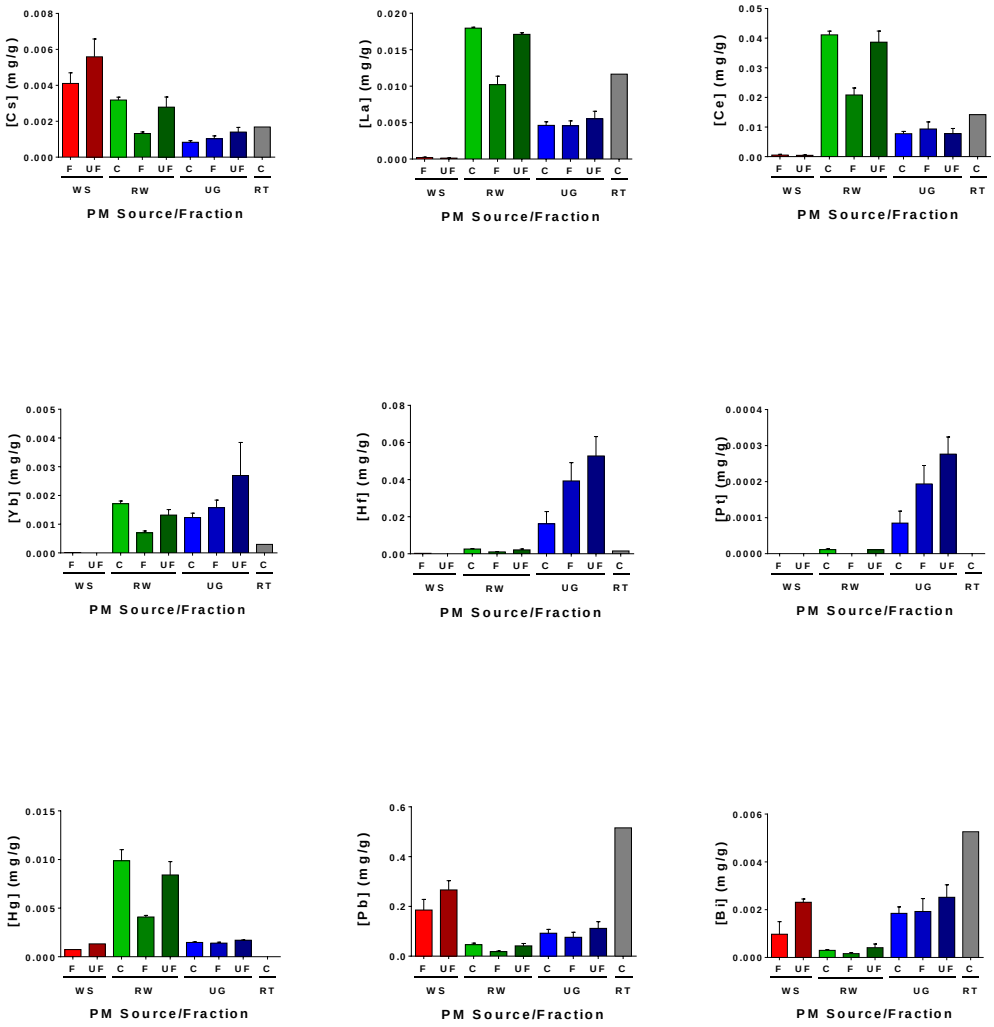

Figure 3.4 continued.

Element	*DEP1 (µg/g)*	*DEP2 (µg/g)*	*DEP3 (µg/g)*	*DEP4 (µg/g)*
Li	0.3	0.4	0.3	0.09
B	ND	12.6	ND	ND
Na	246	1777	2090	238
Mg	157	1072	83.6	544
Al	520	194	25.6	674
K	66.3	7377	404	90.9
Ca	4532	7052	842	1616
Sc	0.04	0.1	ND	0.2
Ti	12.6	8.8	1.9	136
V	0.4	0.7	ND	2.6
Cr	126	16.9	2.8	3.9
Mn	49.1	44.0	2.6	28.8
Fe	3160	220	9.4	795
Co	1.0	0.8	0.4	0.7
Ni	68.6	10.3	5.3	9.5
Cu	13.3	30.7	6.6	8.4
Zn	75827†	226	382	2458
Ga	0.6	0.3	0.1	0.6
As	0.2	ND	0.2	0.1
Se	ND	ND	ND	ND
Rb	0.2	4.8	0.6	0.3
Sr	2.0	5.7	1.9	6.7
Y	0.04	0.5	ND	0.3
Zr	0.2	0.7	0.06	2.5
Nb	ND	ND	ND	0.6
Mo	13.6	ND	ND	ND
Pd	ND	ND	ND	ND
Cd	0.2	0.2	0.8	0.02
Sn	2.4	0.8	0.2	ND
Sb	0.8	0.07	0.3	0.06
Cs	0.008	0.02	0.006	0.007

Element	*DEP1 (µg/g)*	*DEP2 (µg/g)*	*DEP3 (µg/g)*	*DEP4 (µg/g)*
Ba	2.8	3.1	0.9	5.3
La	0.05	0.06	0.005	0.5
Ce	124	1.1	0.03	0.9
Yb	0.007	0.07	ND	0.03
Hf	ND	0.002	ND	0.05
Pt	0.02	ND	ND	ND
Au	ND	ND	ND	ND
Hg	ND	ND	ND	ND
Pb	32.5	2.3	1.8	5.9
Bi	0.5	0.03	0.007	0.005

Table 3.1. Concentrations of elements in diesel exhaust particulate matter from four different sources.

DEP1 was collected from the outflow pipe of a diesel exhaust generator using CeO as an additive; DEP2 was collected from the roof of an inhalation chamber used for DEP exposure studies; DEP3 was collected from a diesel exhaust filter set; DEP4 was collected from a diesel-powered generator. † - Zn in DEP1 potentially elevated by contamination from galvanized exhaust pipe. ND – not detected above lower limit of detection.

The data were further analysed to test for correlations between Fe and other elements across the underground railway PM samples, testing with Spearman's rank correlation coefficient. Sr was the element most strongly correlated with Fe ($r=1.00$; $p<0.0001$). However, this may be of limited importance due to the low overall concentration of Sr. generally below 100 µg/g. Indeed, 32 of the 40 elements showed concentrations significantly correlated with those of Fe ($p<0.05$). The strongest correlations among the abundant metals were observed for Mn, Ni, and Cu, while V was also strongly correlated with Fe (Figure 3.5). Although no negative correlations with Fe were found, the crustal elements Na ($r=0.517$) and K ($r=0.433$) along with B ($r=0.467$) showed the weakest correlation with Fe.

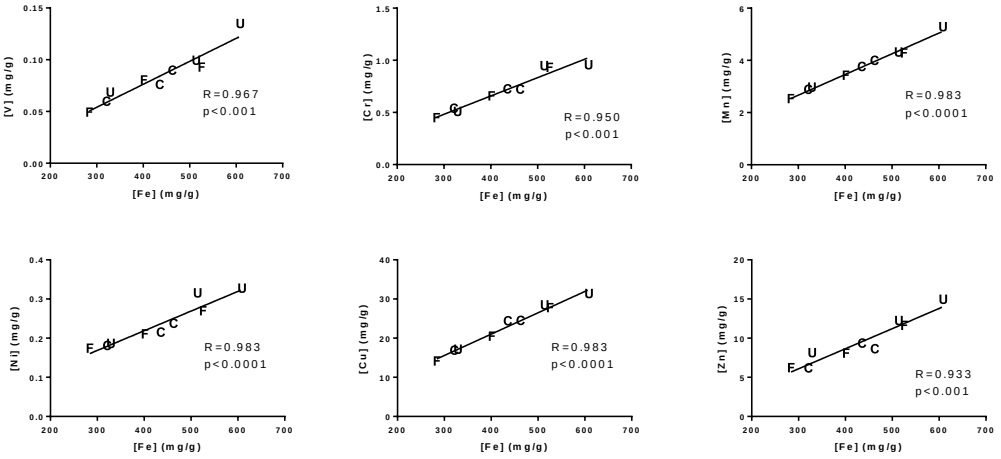

Figure 3.5. Correlations between Fe and other elements in underground railway PM. Coarse (C), fine (F), and ultrafine (U) underground railway PM (n=3 for each) were analysed for elemental composition by ICP-MS. Each point represents a single PM sample (C = coarse, F = fine, U = ultrafine). Analysis by Spearman's rank correlation coefficient.

3.2.2 Particulate Anion Analysis

Particulate anion concentration was assessed by sonicating PM suspensions for 1 h, followed by centrifugation and retention of the supernatant. Ion chromatography analysis showed that road tunnel PM possessed the highest concentrations SO_4^{2-}, Cl^-, and NO_3^- (Figure 3.6). Roadwear PM generally showed the lowest SO_4^{2-}, Cl^-, and NO_3^- concentrations of any of the PM tested, suggesting that these anions are derived from fuel combustion rather than road and mechanical sources in the road tunnel PM. When the concentrations of each species were compared between the three size fractions of underground PM, coarse and fine fractions showed similar levels of the three anions, but ultrafine underground railway PM showed enrichments of SO_4^{2-}, Cl^-, and NO_3^-, and for SO_4^{2-} this difference was of statistical significance versus coarse and fine fractions. Each anion showed only weak positive correlation with Fe concentration (r=0.583, 0.483 and 0.367 for SO_4^{2-}, Cl^-, and NO_3^-, respectively).

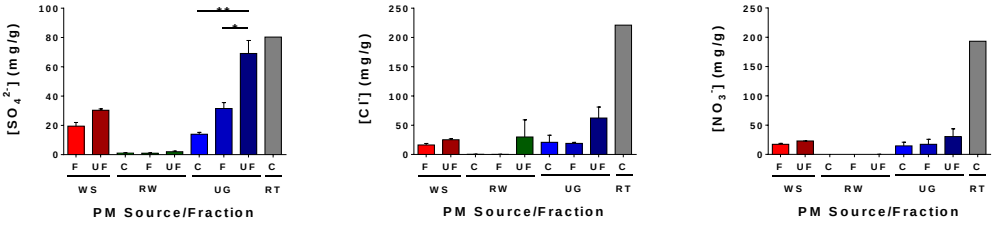

Figure 3.6. Anion concentrations in PM samples from various sources.

PM samples were collected as for Figure 3.2. Samples were sonicated and centrifuged, and the supernatant analysed by ion chromatography. Bars represent mean±SEM concentrations of SO_4^{2-} (left), Cl^- (centre), and NO_3^- (right).

3.2.3 PM Lipopolysaccharide Concentration

Underground railway PM LPS concentration was assayed by Limulus amoebocyte lysate assay. Only one of the three daily samples of underground railway PM was used in this analysis, that being the same sample set used for subsequent experiments in Chapter 4. The assay was performed as per the kit instructions, and each size fraction was analysed in duplicate, with a mean taken to give a final LPS concentration. The greatest concentration of LPS was found in the coarse fraction, at 8.5 EU/mg, with 6.7 EU/mg in the ultrafine fraction and 5.6 EU/mg in the fine fraction. Spiking of a sample of UF PM with 0.25 EU/ml LPS resulted in almost complete detection of this added LPS, suggesting that the interference of PM with the LAL assay is minimal.

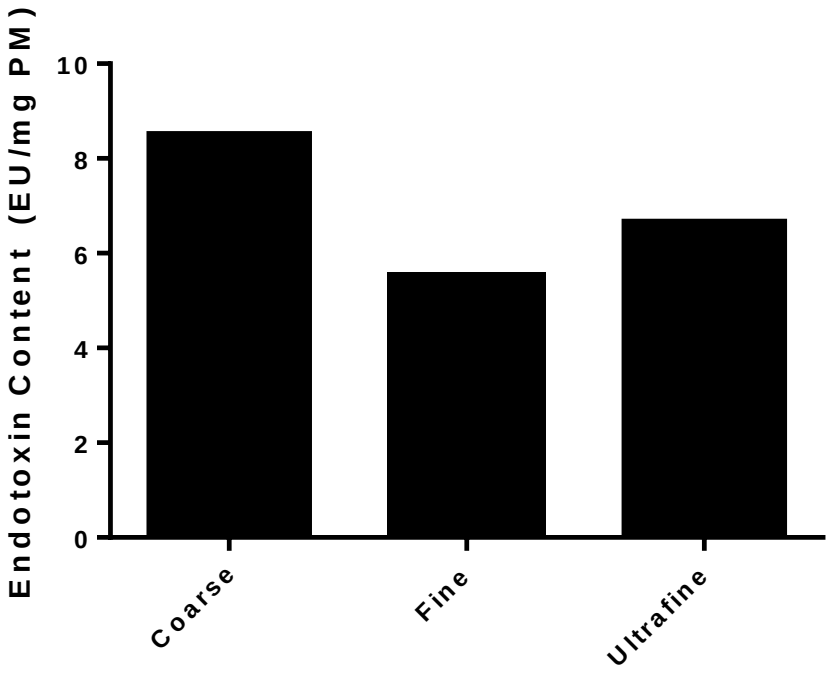

Figure 3.7. Lipopolysaccharide content of underground railway PM.

LPS concentration in underground railway PM from a single sampling day, thenceforth to be used for *in vitro* experiments, was assayed using a colorimetric Limulus amoebocyte assay. Bars represent mean of duplicate readings.

3.2.4 Overall PM Composition

The total mass concentrations of analysed transition metals, metals, and anions were calculated in order to determine their relative proportion in each size fraction of each PM sample (Figure 3.8). Although the analysis was not exhaustive since some transition metals (e.g. Ta, Ir) and metals (e.g. Fr, Ra) were not analysed, these omitted elements were expected to be present in only trace amounts, and thus their omission is not expected to markedly alter the outcome of such a calculation. It is clear that underground PM of all size fractions was the most transition metal-rich (442, 444, and 532 mg/g for coarse, fine, and ultrafine fractions respectively). Indeed, the next most transition metal-rich PM sample was coarse road tunnel PM, containing only 32 mg/g transition metals. Conversely, there was a lesser degree of variation in non-transition metals, particularly if the metal-poor woodstove PM was excluded. The total concentration of anions SO_4^{2-}, Cl^-, and NO_3^- was much greater in road tunnel coarse

PM (495 mg/g) than in any other PM sample, with ultrafine underground railway PM being the second-most anion rich (162 mg/g). There was also a substantial proportion of some of the PM samples, especially those from woodstove and roadwear, but also to a lesser extent coarse and fine underground railway PM and coarse road tunnel PM, which remained unidentified. O was not analysed by ICP-MS, but x-ray dispersive spectroscopy (XDS) measurements performed on underground railway PM suggested that oxygen accounted for 29-43% by mass of these PM samples, which is well in excess of that accounted for by SO_4^{2-} and NO_3^- (data not shown). C was also not analysed, and is likely to make up a significant proportion of the unidentified fraction, particularly for woodstove and road tunnel PM samples.

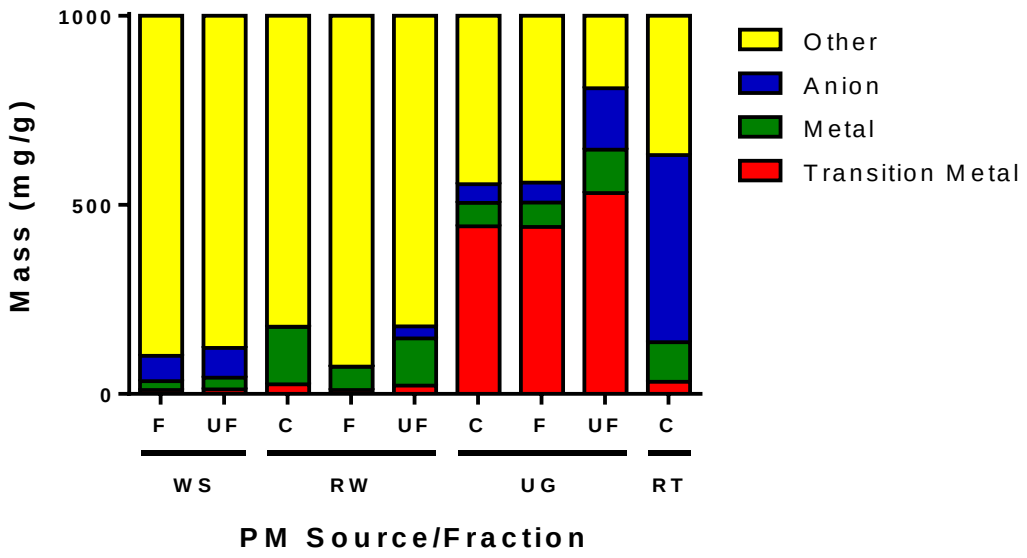

Figure 3.8. The chemical composition of PM from various sources by category.
Coarse (C), fine (F) and ultrafine (UF) PM was collected from a woodstove (WS; n=2), roadwear generator (RW; n=2), underground railway station (UG; n=3) and a road tunnel (RT; n=1). After acid digestion, PM elemental composition was analysed by ICP-MS. Bars show contribution of transition metals, metals, anions, and "other" unidentified constituents to each PM sample.

3.2.5 Particulate Morphology Analysis

A scanning electron microscope was used to examine at high resolution the morphology of underground railway particles, and in particular to try to discern any differences in particle morphology between size fractions (Figure 3.9).

Examination of the coarse fraction of underground railway PM revealed that, in terms of particle numbers, most particles were well below the 10 μm size used as a cutpoint for this fraction, with a smallest dimension of 2-3 μm or less. However, there was a clear population of particles with at least one dimension closer to the 10 μm cutpoint. The smaller particles were of non-uniform granular morphology, whereas the larger particles had a flake-like appearance with a relatively smooth face and jagged edges (Figure 3.9). When examined at a greater magnification, the flat surfaces of these larger, flake-like particles were often marked by ridges or indentations. Examination of the fine fraction of underground railway PM revealed a similar set of small particles, again with a largest diameter of approximately 2 μm. Significantly, there was an almost complete lack of the flake-like structures compared to the coarse fraction. The ultrafine fraction of underground railway PM was composed of particles with a non-uniform granular shape. All fractions contained some particles of a larger size than should theoretically have been permitted by the cutpoint of the virtual impactor. These larger particles were commonly composed of 1-2 μm particles agglomerated to form a single mass, suggesting agglomeration post-collection. Indeed, agglomerates were observed in all fractions, particularly the coarse and fine fractions (Figure 3.9). These were often clearly composed of particles in the 1-2 μm size range, apparently attached to each other to form a larger entity which was, in some cases, far larger than would be permitted to pass through the relevant virtual impactor.

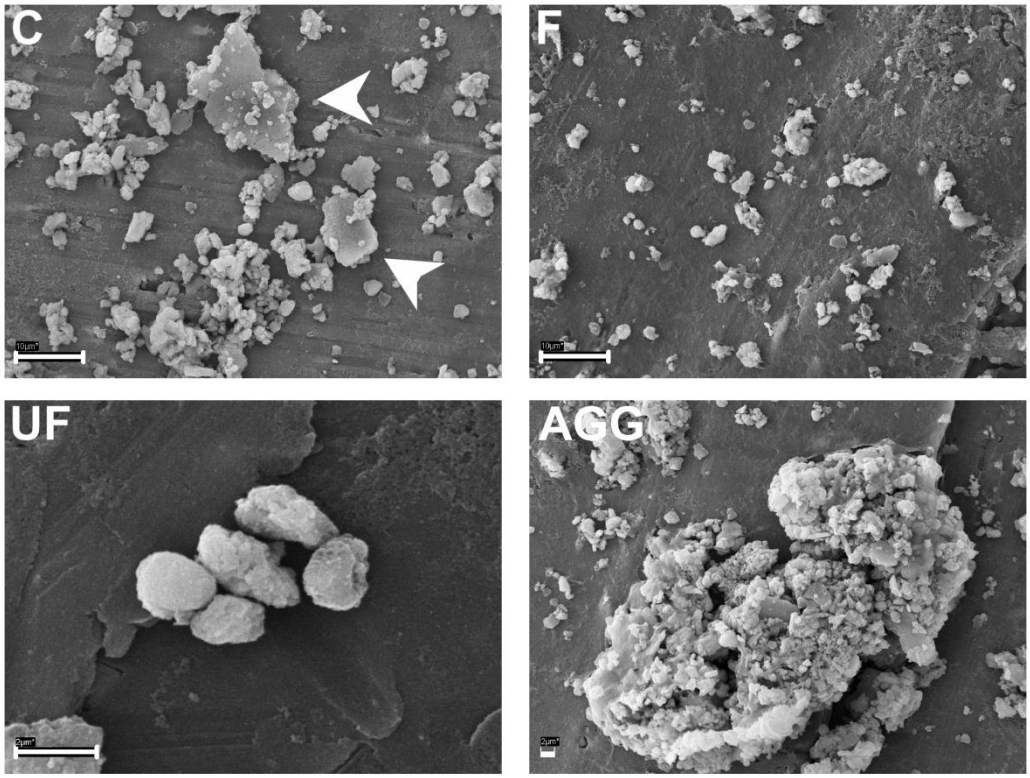

Figure 3.9. Scanning electron micrographs of underground railway PM.

Coarse PM (C; top left) comprised flake-like PM (arrowheads) characteristic of this fraction, and granular PM. Fine (F; top right) and ultrafine (UF; bottom right) fractions were generally granular. Large agglomerates were seen, especially in the coarse and fine fractions (AGG; example bottom right). All micrographs x5,000, except bottom left x30,000, scale bars 10 μm except bottom right 2 μm.

3.3 Discussion

This study examined the levels of transition and non-transition metals and selected metalloids in size-fractionated underground railway PM, with woodstove, roadwear, road tunnel, and diesel exhaust PM used as comparators. ICP-MS analyses of a large range of metals, especially in the rarely studied ultrafine fraction, provides new information on the chemistry of underground airborne PM. The underground railway station on which this study focused forms part of an international mainline railway. This is important because (1) the studied railway draws power from an overhead catenary, as opposed to an electrified rail, and (2) trains running on this line are larger than would generally be found on urban underground railway networks. The effects of increased load on rail wear have been detailed previously (422).

Elemental analysis of PM composition uncovered some interesting and remarkable findings. First, underground railway PM of all size fractions was considerably more metal-rich than PM from all other sources analysed. Furthermore, diesel exhaust PM was generally metal-poor compared to PM from other sources. Examination of levels of each individual analyte element suggested that the concentrations of many metals were several fold higher in underground railway PM than in other PM but that, in absolute terms, Fe was the most elevated element although it was by no means the only element whose levels were notably higher. Furthermore, certain other elements were found at greater concentrations in PM from other locations, such as Al and Ti in roadwear PM, and Cd in woodstove PM, while road tunnel PM contained considerably elevated levels of Na and Pb.

Analyses of urban particulate matter frequently show trace levels of transition metals, such as Fe, Sn, Co, V, Zn, and Cu, generally in the coarse and fine size fractions of PM. However, comparison between such urban PM studies and PM of the type used in this study is potentially misleading, because the samples used in this study are all from environments characterised by certain activities which could reasonably be expected to contribute significantly to the suspended PM.

The present study showed that underground railway PM contained a notably high concentration of iron. This observation is in agreement with other studies, which have found high iron content in underground railway PM (e.g. 40%-59% in Stockholm underground railway PM_{10} (64, 204), 61% and 41.8% from Paris RER and Metro PM_{10} respectively (80)). This metal-rich nature of underground railway PM is in clear contrast with samples from road traffic-predominant areas, which tend to be rich in elemental carbon (67).

Unlike the majority of studies into underground PM, the present study also analysed the elemental composition of ultrafine PM ($PM_{0.18}$), which is rarely studied. In urban environments, ultrafine PM is generally observed to be metal-poor (36, 121, 255), and mainly composed of elemental C along with the products of secondary reactions between gaseous pollutants which condense to form PM (36, 87, 307). In terms of their chemistry, these secondary ultrafine particles are thought to be of very little toxicological significance (423). However. some processes involving high temperatures and resultant vaporisation or combustion of substrate material have the potential to generate metal-rich PM (239, 424). Indeed, most metals analysed in this study were found in higher concentrations in the ultrafine fraction compared to the coarse and fine fractions, although the differences were not statistically significant for any metal. Furthermore, the present study may underestimate the relatively metal-rich nature of the ultrafine fraction compared to the fine fraction as the VACES equipment includes some ultrafine PM in the $PM_{2.5}$ fraction (113). The majority of particles in underground railway PM samples are thought to be derived from interaction between wheels, rails, and brakes (67), generating particles that consist mainly of Fe but also contain among others Mn, Cr, V, Zn, and As (425). Although abrasive forces between wheels, rails, and brakes can clearly generate coarse and fine PM due to shearing, there is evidence to suggest that ultrafine PM can be generated *via* the high temperatures of friction at interfaces between these components, with subsequent vaporisation of the substrate (422, 424). There is also likely to be a contribution from arcing of the electrical current from the third rail or overhead catenary to the collector shoe/pantograph on the train through which electrical current is drawn (70, 76). Crucially, however, unlike most urban underground railway systems, which draw electric current through a third rail running parallel to the other rails, the railway in the

present study is powered by an overhead catenary, with the current drawn through a pantograph. This may explain the levels of Cu found in underground railway PM, which are relatively high compared to other underground systems. Contact wires which run above the railway line are generally composed of Cu, alloyed with 0.1-0.5% Ag, Sn, Mg, or Cd, such as those supplied by Liljedahl Bare Wire (Helsingborg, Sweden and Mannheim, Germany) or Lamifil (Hemiksem, Belgium), used on systems such as the French high-speed Thalys network, and also on the Eurostar network (426, 427). The precise composition of these wires depends on the speed reached by trains drawing current. Similarly, Cu or Cu-Pb-Sn alloys form the contact material of the pantograph, although in this case it is generally as a component of a metallised carbon contact strip (428, 429). However, it should be noted that the underground railway station, as well as accommodating commuter trains servicing the local metropolitan area, is also used as a stop on intercity networks, connecting the station to Paris, Berlin and, in the future, Brussels. Therefore, while the exact composition of the contact wire at the underground railway station is not known, it is likely to be similar to these examples. This can be contrasted with the third-rail system of power, where although similar materials are used on the current-collecting component (in this case a third-rail "shoe"), the third rail itself is an Al-stainless steel composite, with a thin layer of stainless steel rolled over an extruded rail of aluminium, to provide high conduction and low wear to the collector shoe (430). As such, underground railways powered by overhead catenary may be expected to show increased airborne Cu and decreased Fe compared to those powered by electrified third-rail. By using the previously stated underground airborne PM mass concentrations for each size fraction described above, in conjunction with the concentration of Mn in each fraction, the mean±SEM airborne Mn concentration over the three sampling days is calculated as 1010±93 ng/m^3, well in excess of the WHO recommended limit of 150 ng/m^3 annual average (431). This level still exceeds the limit after allowing for working a 35 h exposure period per week, with zero Mn exposure outside of working hours. Because Mn overexposure in welders and miners has been linked to symptoms resembling those of Parkinsonism (432), further research is needed into the potential effects of chronic exposure to underground railway dust.

Perhaps the most comparable situation in terms of ultrafine metals is that of welding where, in a similar process to that seen on the underground, arcing of an electrical current is able to vaporise metal, resulting in formation of ultrafine metal PM (192, 193). Metal fume fever is a well-documented condition, and shows that transition metals in the ultrafine fraction of PM are able to exert quite serious effects after acute exposure (258). As discussed in Chapter 1, coarse PM is thought to exert its effects through its chemistry, whereas ultrafine PM effects are thought to be due to its large surface area and penetrative ability. Clearly, metal-rich ultrafine PM has the potential to exert effects through both mechanisms, and therefore further study of metal-rich ultrafine PM is required.

As the antithesis of an element found to be relatively enriched in underground railway PM, K was particularly high in woodstove PM. Wood combustion is a significant contributor to airborne K (49, 305, 433), so it is unsurprising that K was found at high levels in wood burner emissions. Interestingly, woodstove PM displayed levels of Cd which, although in absolute terms were not as high as those seen with many of the other elements, were markedly greater than in other PM. Cd is a characteristic waste product of many industrial processes such as metal mining and smelting, accumulates in the environment, and is toxic to several organs (434). While it is beyond the scope of this research to identify a reason for the enrichment of Cd in the woodstove PM samples, one potential source is a large waste incineration plant in the vicinity of the area from which the wood for burning was obtained. Waste incineration plants have been shown to release Cd and other heavy metals as part of the incineration process (435, 436), and so it could reasonably be suggested that such a facility may be the source of the elevated Cd in the woodstove PM. Indeed, Pb was also enriched in woodstove PM compared to all other PM samples with the exception of road tunnel PM. It is well documented that the alkali metals Rb and Cs (which was also elevated in woodstove PM compared to other PM, although only at trace levels) act as analogues for K, also an alkali metal, in plant cation uptake, explaining their accumulation in plant material (437).

Both roadwear PM and road tunnel PM showed slightly increased levels of Ba compared to woodstove PM, although these were well below those seen in

underground railway PM. Ba is also found in the brake shoes of trains; hence, brake wear is a possible source of the high Ba concentration in underground railway PM and this may be an indicator of brake wear (438), although Cu, another potential marker of brake wear, was found to constitute only 0.15% of road tunnel PM mass, and was almost absent from roadwear PM, although this may reflect low brake usage in these situations. Both roadwear and road tunnel PM also have high concentrations of Na, while roadwear PM was relatively rich in Al, K, Ti, and Sr, and road tunnel PM in B and Pb. These differences may reflect generation: roadwear PM is from an artificial roadwear generator designed to simulate PM generation from the action of studded tyres on the road, while road tunnel PM is from an operational road tunnel. Ti and K are both found in brake pads (439), while road dust contains aluminosilicates (440). Elevated Na levels in road tunnel PM likely derive from the nearby (approximately 30 km away) North Sea coast or from the use of road salt. The elevated concentration of Pb in road tunnel PM is noteworthy in that lead is not currently used in Dutch petrol, where it was previously used as an anti-knocking agent to prevent auto-ignition of fuel. However, Pb, as well as Sr, has been detected in road dust samples in other studies (433, 439), and additional toxic anthropogenic metals, unlike the more commonly found crustal metals, have been found in especially high levels in the fine fraction of road dust (441). The levels of lead in road tunnel PM probably reflects the greater volatility of Pb compared to other anthropogenically enriched toxic metals (441).

Diesel exhaust particulates generally contained either very low or undetectable levels of metals. Notable exceptions to this were in diesel sample 1, which contained high concentrations of Zn and Ce, and in diesel sample 2, which showed relatively high K levels. The level of cerium in diesel 1 is due to the presence of CeO_2 nanoparticles as a catalyst to reduce soot emissions. The presence of Zn cannot easily be explained, but may be due to contamination from galvanised components of the diesel exhaust generator, either during diesel combustion or during particle collection. Finally, the presence of relatively high levels of K in diesel 2 may be due to residue from biodiesel combustion – biodiesel manufacture involves the use of KOH as an esterification agent.

A limitation of the analysis here is that it does not inform about the precise nature of the particulate chemistry – only the elemental concentration. While this information is important, a more detailed assessment of the biochemical impacts of these elevated metals would require data concerning their oxidation states. For example, differentiation between iron in the ferrous Fe(II) or ferric Fe(III) oxidation states is important in evaluating the potential for participation in Fenton reactions and radical formation, due to the ability of Fe^{2+} to act as a reductant, with Fe^{3+} usually acting as an oxidant. This subsequently influences interactions with biomolecules. Furthermore, it does not identify the precise nature of the compound in which an element is found, and this can impact significantly on metal toxicity. For example, environmental iron is often found in insoluble oxide form (184, 310), whereas metal chlorides are generally soluble, and therefore often used when the effects of elements are to be studied individually (303). Indeed, more than one form of iron oxide has been observed in airborne PM, with urban PM iron being mainly in the form of the ferric oxide haematite (Fe_2O_3), while the predominant species of underground railway PM iron has been reported for different underground systems as being magnetite (Fe_3O_4, a complex of haematite and ferrous oxide wustite (FeO)) or metallic Fe, with minor haematite levels (204, 252). While it is possible to separate ions prior to ICP-MS analysis by use of ion chromatography in series with the mass spectrometer, these facilities were unavailable. Improved identification of particular compounds would be attained by use of x-ray diffraction (XRD) as has previously been used by other groups to distinguish between iron oxide species (204) and barium sulphate species in railway brake shoes (438), amongst others. However, XRD is only able to show relative proportions of different moieties within a sample, and gives no information about absolute concentrations of elements between samples. Therefore, while XRD may be useful for more in-depth analysis of samples, it would be of little use as a potential replacement for ICP-MS in studies such as this. Furthermore, this study only considered the predominant isotope of each element for study. Since ions are detected on the basis of their mass/charge ratio, only one isotope of each element was able to be detected. However, there is no evidence that this could adversely affect the data presented here.

Analysis of metal concentrations in all PM samples showed a large degree of correlation between different elements. In particular, Fe, which is one of the best characterised of these elements in terms of respiratory toxicity, was positively correlated with 32 of the elements assayed, including several of the most abundant transition metals, such as V, Cr, Mn, Co, Ni, Cu, and Zn. It is likely that these correlations are due partly to elements coming from the same source, such as Fe being alloyed with other elements to modify the properties of steel, but also partly due to the level of mechanical activity contributing to the PM load.

Ion chromatography analyses showed that road tunnel PM contained the highest concentrations of SO_4^{2-}, Cl^-, and NO_3^-. This finding is unsurprising, since much of the PM from a road tunnel is likely to be derived from fuel combustion, and be most representative of urban PM that is known to contain large concentrations of these anions (34, 78, 181, 433). There is also likely to be a contribution from aged PM originating from outside the tunnel, which has accumulated these anions during transport to the sampling site. The lack of these anions in roadwear PM compared to other particles analysed accords with their predominance in environments where combustion is taking place, which also explains the levels seen in woodstove PM. However, it may be noteworthy that, of all the PM sources, with the exception of road tunnel, underground railway PM showed the greatest concentration of anions. Weak correlations of SO_4^{2-}, Cl^-, and NO_3^- with Fe concentration indicates that they are unlikely to be derived from mechanical wear. One source may be motor vehicles in the vicinity of the station. The airport at which the underground railway station is located is, by passenger number, one of the busiest airports in the world, and there is a considerable level of motor vehicle usage in the vicinity of the airport. In particular, the railway station lies beneath and adjacent to a complex of car parks, and also below the main drop off/pick-up point of the passenger terminal. Thus, it is likely that PM from car exhaust is drawn into the station by the "piston action" of train movement, although the extent of this input is a matter of debate (72, 73, 442). Indeed, there may also be contribution from road traffic emissions as two motorways pass close to the airport terminal building (within 1km and 2km respectively). A second explanation is that diesel-powered goods trains pass through the station at night. Although no such trains passed through the station during sampling periods, particles

deposited by diesel locomotives could be re-entrained by trains passing during the day or by cleaning vehicles that are in regular use. Finally, the contribution of aircraft particulate emissions cannot be ruled out (443), although the distance between the railway station and the runways of the airport means that this may be of limited significance.

As this study focused on metals in PM, there remains a proportion of the mass of underground railway PM that was not identified in this study (446, 441, and 192 mg/g for coarse, fine, and ultrafine fractions respectively). Although Si is theoretically detectable by ICP-MS, the use of hydrofluoric acid (HF) precludes this. HF was used in order to digest the elemental carbon component of PM, but with the disadvantage the HF reacts with silicates to form the volatile compound silicon tetrafluoride. As such, the potential for loss of silicon during the digestion process renders silicon quantification impossible after the acid digestion procedure used. However, Si has been found in underground PM by other groups and has been ascribed to either brake blocks or the dumping of sand to improve wheel traction under braking (67, 81). However, this may vary between underground systems, with a paucity of Si contained in London Underground PM (77). Furthermore, oxygen as found in metal oxides was not measured – only oxygen in SO_4^{2-} and NO_3^- were quantified. Because underground railway PM contains substantial levels of iron oxide, it is likely that oxygen makes up a significant proportion of the unidentified PM mass (319). Finally, carbon, either elemental or organic, was not assayed. A wide range of organic compounds have been found in underground railway PM (419), and while these may be derived from diesel train passage, it has also been noted that PM in areas located immediately below ground level, as with the station in this study, may be more influenced by above-ground sources than would be the case for deeper environments (444). This is particularly pertinent in the present study as the underground station lies directly beneath a large multi-storey car park. Indeed, underground railway PM is likely to contain toxicants such as polyaromatic hydrocarbons and redox active quinones (207), although the source of these is harder to verify. They are likely to be derived from above-ground traffic sources, and their concentrations may vary depending on the underground system (e.g. ventilation controls), above-ground urban pollution levels, and weather conditions.

This study also examined the morphology of underground railway PM because morphology can often serve as an indicator of the source of the particulates or at least the processes involved in their creation (67). In terms of particle numbers, most particles in all size fractions had a granular appearance, with rough, uneven faces. No fibrous structures were observed. However, coarse PM contained a considerable number of particles of a flake-like, angular appearance, characteristic of generation by abrasion and shearing. Such flakes may have considerably lower aerodynamic diameters than geometric diameters, resulting in an increased likelihood of evading the particle-trapping features of the upper airways and subsequent deposition in the respiratory tract. Similar morphology has previously been observed in underground railway PM from other systems (67, 81, 204). This angular morphology can be contrasted with the flocculated and wispy appearance of soot (41). Very few flake-like particles were observed in the fine fraction, while none were seen in the ultrafine PM. The relevance of these flake-like particles is not fully understood. Whether particulate angularity affects uptake by cells or particle-particle interactions is not known. However the angular nature of these particles may allow them to impinge upon the structure of the cell, possibly posing a risk to cell membrane integrity and embedding themselves into the cell (204).

Particle agglomerates were seen in all fractions, smaller structures comprising fewer than ten individual particles, while larger structures were also observed, well in excess of the respective VACES cutpoint, suggesting that the agglomerate had formed after collection. It was also observed that some particles, particularly in the ultrafine ($PM_{0.18}$) fraction were clearly larger than the stated cutpoint, although this may be reconciled by understanding of the virtual impactor and the collection process. When the particles are drawn into the virtual impactor, they are separated into the minor airflow for collection, or the major airflow for rejection, based upon their aerodynamic diameter. Aerodynamic diameter relates to aerodynamic behaviour equivalent to a sphere of unit-density of a set diameter (445). Therefore, aerodynamic diameter is a function of particle shape, size, and density. As such, a particle may have an aerodynamic diameter lower than that suggested by consideration of only its largest dimension (222), particularly for fibrous structures such as asbestos or carbon

nanotubes. Furthermore, the stated VACES cutpoint is not an absolute value but a 50% elimination value, meaning that, although 50% of particles lower than the cutpoint of 0.18 μm are eliminated, some larger particles, including up to 5% of those above 0.5 μm, may remain (113). There also exists the possibility for smaller particles to enter larger cutpoint fractions by adhering to larger particles (425).

3.4 Conclusion

This aim of this research was to characterise some of the physicochemical properties of particulate matter from various sources. The results show that underground railway PM contains a high concentration of Fe, correlated with levels of other transition metals, notably Mn, Ni, Cu, and V, which are significantly elevated compared to PM from woodstove, roadwear generator, and road tunnel. Crucially, ultrafine underground railway PM was at least as rich in metals as coarse and fine underground railway PM, which may have important implications for potential hazards to health posed by underground PM, and warrants further study of the hitherto neglected ultrafine fraction in particular.

4 *In Vitro* Activity of Underground Particulate Matter

4.1 Introduction

It has long been known that air pollution can exert harmful, and even potentially fatal effects, with the Meuse Valley pollution incident of 1930 and the London smog of 1952 being amongst the first scientifically studied air pollution events (26, 28). However, such studies tended to examine the outcomes of such air pollution, with less emphasis on the causative agents within the pollution. In 1993, a seminal study looking at air pollution and health effects in six US cities found that coarse and fine PM was linked to mortality from lung cancer and cardiopulmonary disease (42), while other studies have looked at the epidemiology of health effects due to pollution from more specific sources (57, 388). However, it is only relatively recently that investigations have moved beyond epidemiological studies of the effects of air pollution, and into the laboratory, to attempt to understand the precise nature of the toxicants involved, and the mechanisms by which they exert their deleterious effects.

Special interest is focused on the differences in toxicity between samples from different areas. Attempts are then made to link these differences in toxicity to fundamental characteristics of the PM – size fraction and surface chemistry, for example (36, 213). These characteristics are in turn determined by the processes involved in PM generation, and thus studies of locations and characterisation of certain PM properties which are typical of that particular site or environment are driving understanding of the hazard posed by air pollution in a variety of situations.

Such toxicity can be measured *in vivo* or *in vitro*. *In vitro* techniques generally involve examining cell death or inflammatory mediator release, while *in vivo* techniques can examine protein or cellular markers of these in BALF, and also look at airway damage through influx of plasma protein into the airway lumen. They are also able to examine lung function, the latter being more often seen in humans compared to laboratory animals, although this is not exclusively so.

Interest has focused on particular components of airborne particulates, such as transition metals, polyaromatic hydrocarbons and VOCs, and allergens. In terms of uptake and localisation within cells, coarse and fine PM have generally been seen to be sequestered within lipid-bound vesicles, while ultrafine PM may pose a greater risk due to its greater surface area and its potential to enter mitochondria (255).

Transition metals are of key importance in particulate toxicity due to their ability to catalyse generation of ROS (196, 245). Although this reaction involves a series of oxidation and reduction reactions between oxygen-containing species, it can be simplified as a series of successive one-electron reductions, with molecular oxygen (O_2) as the species participating in the initial reduction:

$$O_2 \rightarrow {}^{\bullet}O_2^- \rightarrow H_2O_2 \rightarrow {}^{\bullet}OH$$

In this series, each reaction involves a one-electron reduction of, successively, molecular oxygen, superoxide, and hydrogen peroxide, with the final product, the hydroxyl radical, being formed in the Fenton reaction (188, 245, 253). While superoxide and hydrogen peroxide are able to exert toxic effects, it is the hydroxyl radical which is particularly toxic in light of its ability to react with most biomolecules with a rate constant so rapid that reactions are generally limited only by rate of diffusion (188). The electrons for these reactions come from transition metals, which have a characteristic ability to exist stably in different oxidation states, and thus can act as electron donors for such reactions.

ROS are able to react with a range of biological molecules such as DNA, proteins, lipids, and antioxidants, and also with nitric oxide to form reactive nitrogen species, possibly perturbing nitric oxide signalling (188, 398). As a means of protection against ROS attack, cells are able to upregulate production of antioxidant molecules and enzymes such as glutathione peroxidase, HO-1, and superoxide dismutase (SOD), although asthmatics may be defective in their antioxidant responses (254, 400, 408). If increased antioxidants are unable to ameliorate the presence of ROS, an inflammatory response may be seen. Finally, if ROS attack continues, cell death may occur (271, 272).

Airborne particles found in underground railways have been seen to possess markedly raised levels of transition metals, and have also been shown to be more toxic than particles from other sources by certain measures of toxicity (299, 319). Furthermore, research has shown that the treatment of metal-rich particulates with metal chelators is able to attenuate the toxicity of such particles (80). Therefore, it appears that transition metals within airborne PM can exert toxic effects. However, *in vivo* studies of the effects have proven inconclusive, with reports suggesting increased levels of the procoagulant factors PAI-1 and fibrinogen in the blood of underground train drivers, and elevated hs-CRP in the blood of platform workers, suggestive of increased systemic inflammation (89). Other studies have suggested effects on T cells, and differences in these effects between healthy and mildly asthmatic volunteers possibly indicating a greater susceptibility to underground railway PM-induced inflammation in asthmatic airways (64, 446). However, deleterious effects on lung function (84), and incidence of myocardial infarction (90) and lung cancer (92) have not been found.

The aim of the research contained within this chapter was to examine the effects of coarse, fine, and ultrafine PM collected from the underground railway station on cultured bronchial epithelial cells using measures of pro-inflammatory mediator release, cell death, ROS generation, perturbation of epithelial barrier function, and induction of gene expression. The hypothesis being tested was that underground railway PM would be able to elicit a pro-inflammatory and antioxidant response in a size-dependent manner, by virtue of its iron content. The results suggest that, at subcytotoxic concentrations, all three size fractions are able to elicit modest pro-

inflammatory changes, generate ROS in a manner dependent on their size and iron content, and induce changes in gene expression.

4.2 Results

4.2.1 Initial Determination of Dose-Response Relationship for IL-8 Release with Underground Railway PM in PBEC Monolayers

In order to characterise basic dose-response relationships between PBECs and underground railway PM, PBECs were seeded in 24-well plates at 20,000 cells per well and cultured as monolayers until 80-90% confluent before being challenged with underground railway PM in suspension for 24 h. Underground railway PM concentrations expressed as mass per cell culture surface area were 1.1 μg/cm^2, 2.2 μg/cm^2, 5.6 μg/cm^2, and 11.1 μg/cm^2, corresponding to 5 μg/ml, 10 μg/ml, 25 μg/ml, and 50 μg/ml respectively (dose metric conversions in Table 2.1 in Methods section). The maximum PM concentration used was limited by the concentrations of PM in the stock suspensions supplied, as concentration of suspensions by evaporation was avoided to minimise modification of PM prior to application to cells, and to avoid bacterial growth which has been observed previously in the process of concentrating PM suspensions by evaporation (447) . Because PM was used as a suspension in water, controls were performed with varying concentrations of PBS to account for potential changes in osmolarity. After 24 h, supernatants were removed and stored for ELISA analysis, and untreated control cell lysates kept for LDH assay, all at -80 °C

Measurement of release of the neutrophil chemoattractant cytokine IL-8 into monolayer supernatants of PBEC monolayers grown from healthy donor cells showed a general increase in IL-8 concentration (Figure 4.1). However, the highest concentration of coarse PM, 11.1 μg/cm^2, did not elicit a statistically significant increase in IL-8 release (median 225% of control, IQR 188-245%). Conversely, 11.1 μg/cm^2 of the fine fraction elicited a significant increase in IL-8 release (234% of control, IQR 185-383%, $p<0.05$), while the 11.1 μg/cm^2 of the ultrafine fraction induced a supernatant IL-8 concentration 315% of the control (IQR 280-1302%, $p<0.01$). None of the underground railway PM fractions induced significant IL-8 release from these cultures below the highest concentration of 11.1 μg/cm^2. However,

it was notable that 10 ng/ml TNFα resulted in a median IL-8 release 1453% of control (IQR 739-1848%), suggesting that the concentrations of underground railway PM used were unable to elicit a response anywhere near the maximum possible. Incubation of the highest concentration of ultrafine PM (50 μg/ml) with IL-8 standard at 250 pg/ml, followed by centrifugation as per the experimental protocol, gave an IL-8 reading of 231 pg/ml, compared to a reading of 249 pg/ml of the standard as prepared. This 7 % decrease in detected IL-8 indicated that PM did not markedly influence the detection and measurement of IL-8.

The same experiment was then performed with PBEC monolayers grown from severely asthmatic donor cells, to investigate whether asthma status affected IL-8 release (Figure 4.1). As with the response in healthy donor PBEC monolayers, there was a general trend for increasing IL-8 concentration in supernatants as underground railway PM concentration was increased. In this case, only the highest concentration of the fine fraction was able to elicit a significant response, giving a median IL-8 concentration 241% of the control concentration (IQR 189-845%). As with the healthy donor PBECs, even the maximum concentration of coarse underground railway PM was unable to elicit significant IL-8 release at a median 208% of control release (IQR 140-533%). However, while 11.1 $\mu g/cm^2$ of the ultrafine fraction elicited a significant increase in IL-8 release from healthy donor PBEC monolayers, there was no such significance seen in severely asthmatic donor cultures, reaching a median 196% of control concentrations (IQR 188-394%). Interestingly, 10 ng/ml TNFα elicited a median response of 775% of control IL-8 concentration (IQR 519-1780%). This not only shows that, as for the healthy donor PBEC experiments, none of the PM concentrations elicited a near-maximal release of IL-8 but also that the maximal response of severely asthmatics may be lower than that of healthy cells (1453% in healthy donor cultures, 775% in severely asthmatic donor cultures). Furthermore, in terms of absolute IL-8 release (i.e. not control corrected), there was a bell-shaped concentration-response relationship, with decreased release of IL-8 with 11.1 $\mu g/cm^2$ PM of all size fractions compared to 5.6 $\mu g/cm^2$. However, this was seen in the corresponding controls to an even greater extent, suggesting that it was not an effect of the particulate matter itself.

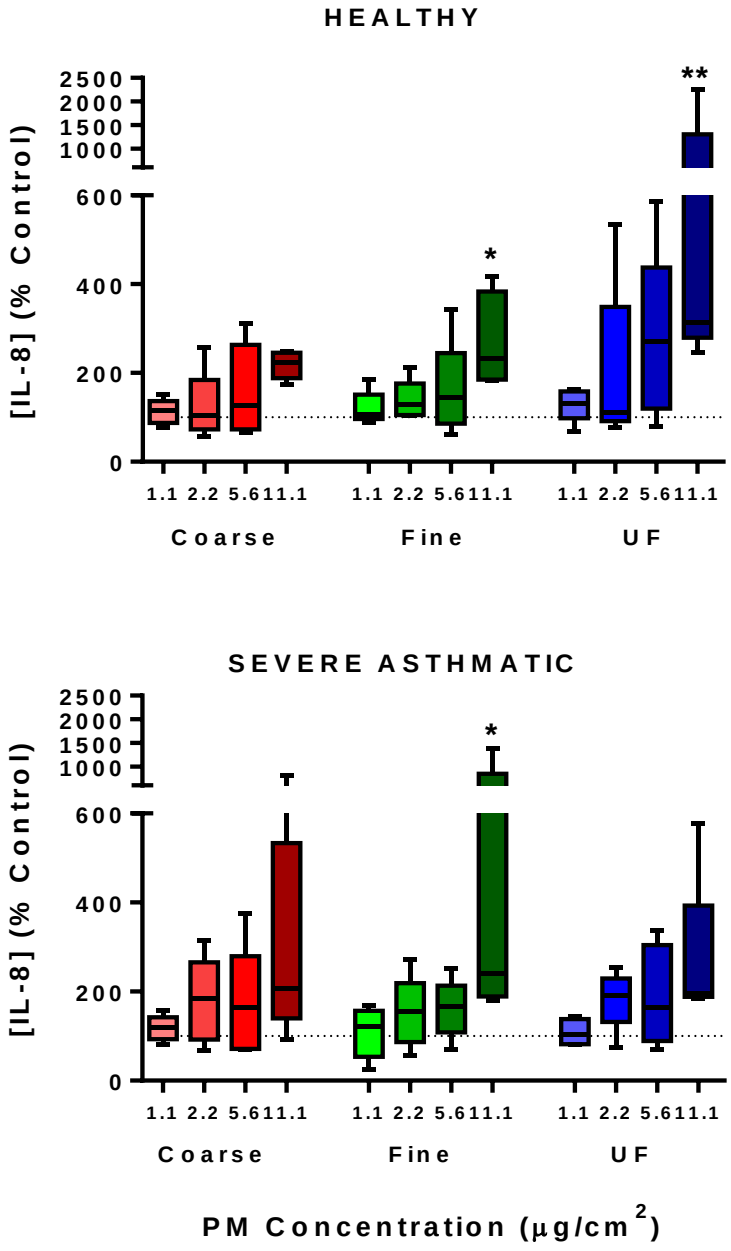

Figure 4.1. The effect of underground railway PM on IL-8 release from healthy and severely asthmatic donor PBEC monolayers.

Epithelial cell monolayers grown from cells of healthy (top) or severely asthmatic (bottom) donors were exposed to varying concentrations of coarse, fine, or ultrafine underground railway PM for 24 h. Supernatant IL-8 concentration was analysed by ELISA, with supernatants assayed in duplicate. IL-8 release is expressed as percentage of IL-8 release from cells incubated in control medium for 24 h. Results presented as median with 25th and 75th percentile, whiskers represent 10th and 90th percentiles. Analysis by Friedman test with Tukey's correction for pairwise analysis, * - $p<0.05$ *vs.* control, ** - $p<0.01$ *vs.* control. n = 5 healthy donors, 5 severely asthmatic donors.

4.2.2 Measurement of Underground Railway PM-Induced Cytotoxicity

Having observed a decrease in absolute IL-8 release with the highest concentration of underground railway PM, and also for the corresponding PBS control, cytotoxicity was considered as a potential cause of this drop. Since an overarching aim of this work was to study the effects of underground railway PM beyond merely a cytotoxic concentration effect, future experiments were to be performed using concentrations of underground railway PM below those which would cause significant and frank cytotoxicity. As such, LDH assays were performed on supernatants from these experiments. LDH is a constitutively present cytosolic enzyme which is released from cells if permeability of the cell membrane increases. Since permeabilisation of the cell membrane is a marker of cytotoxicity and cell death, supernatant LDH concentrations can be measured as a means of determining the level of cytotoxicity exerted by a certain treatment. Lysis of a particle-free, PBS-free medium treated culture with 1% Triton X-100 can be used as a means of determining total cellular LDH content, against which LDH release from test cultures can be compared. The percentage cytotoxicity induced by a particular treatment was determined as the percentage of LDH activity in supernatant compared to the LDH activity of the lysate. The relevant control percentage cytotoxicity was then subtracted to give a corrected cytotoxity induced by PM.

Treatment of healthy donor PBEC monolayer cultures did not induce significant release of LDH for any PM fraction/concentration combination (Figure 4.2). A similar outcome was noted in severely asthmatic donor PBEC cultures. Clearly, there was no significant increase in cytotoxicity with underground railway PM.

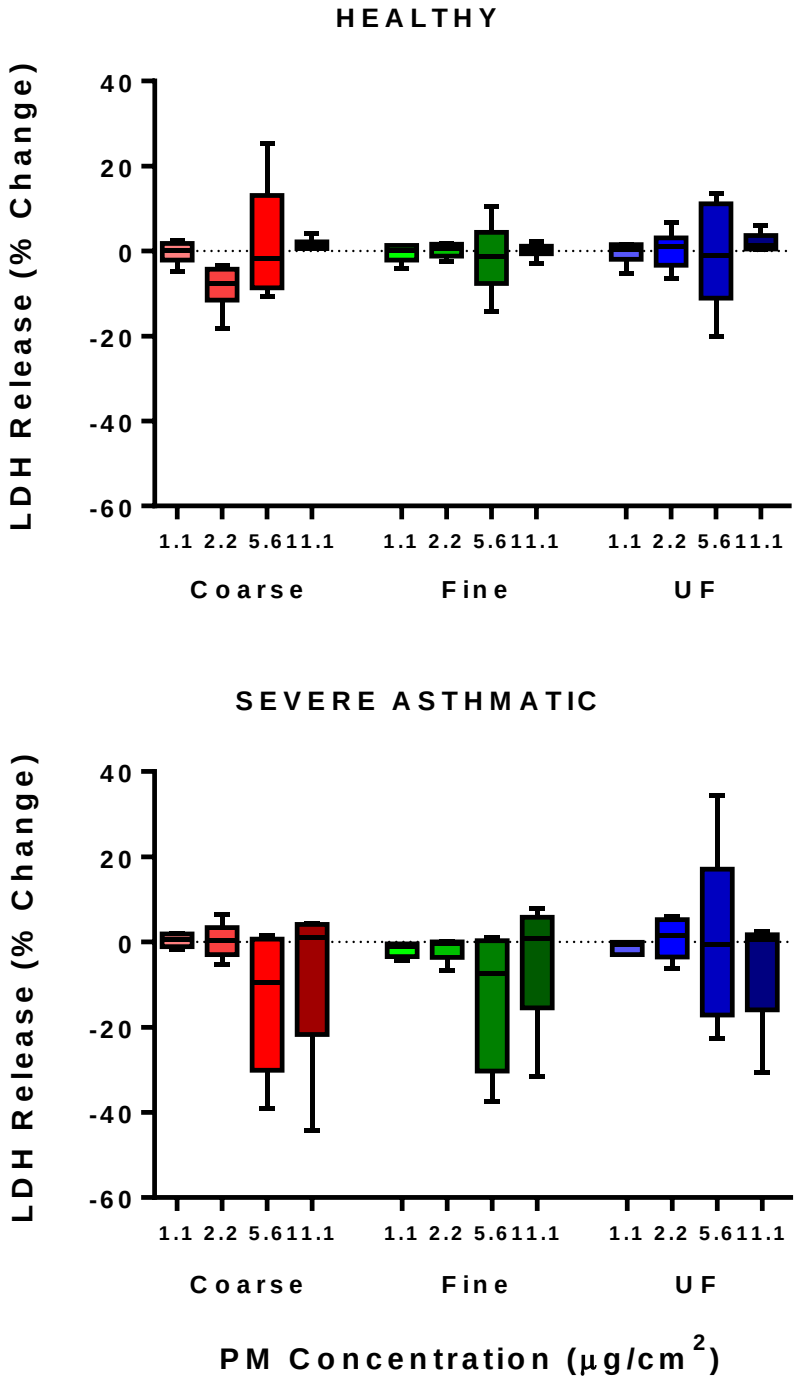

Figure 4.2. The effect of underground railway PM on LDH release from PBEC monolayers. Healthy (top) and severely asthmatic (bottom) donor PBEC monolayers were treated as for Figure 4.1. LDH release as a result of 24 h challenge was measured and calculated as a percentage change from control values compared to total cellular LDH. Results presented as median with 25th and 75th percentile, whiskers represent 10th and 90th percentiles, n = 6 healthy donors, 5 severely asthmatic donors.

Despite its continued widespread use, there has been some doubt cast upon the reliability of the LDH assay to determine cytotoxicity induced by particulates. Therefore, cultures were also examined by light microscope to verify that there was no marked cell death (Figure 4.3). While sometimes displaying patches of cell death, cultures generally appeared in good condition after 24 h treatment. Importantly, there appeared to be no obvious difference in cell morphology and detachment levels between cultures treated with underground railway PM and cultures treated with the corresponding PBS-supplemented controls.

The combination of negative LDH assay results and visual examination of cultures therefore suggests that underground railway PM, at concentrations up to 11.1 $\mu g/cm^2$, is unable to cause significant cell death. However, the bell-shaped dose-response curve of absolute IL-8 release suggested that 2.2 $\mu g/cm^2$ or 5.6 $\mu g/cm^2$, although not inducing significant IL-8 release, may be the optimum for further study of the effects of underground railway PM, since the drop in IL-8 release between 5.6 $\mu g/cm^2$ and 11.1 $\mu g/cm^2$ could not be explained by the occurrence of increased cell death.

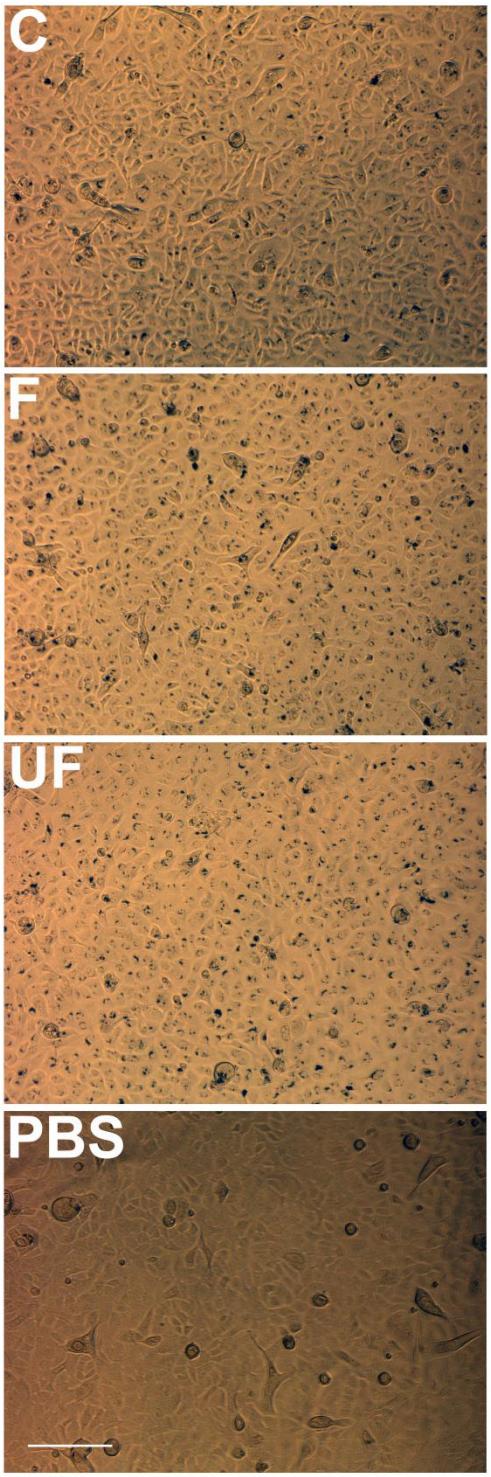

Figure 4.3. Healthy PBEC monolayers after 24 h treatment with underground railway PM. Coarse, fine, or ultrafine underground railway PM was applied to PBEC monolayer cultures as a suspension for 24 h. Images show 11.1 µg/cm^2 cultures. LDH assay suggested no significant cytotoxic effect, and examination of cells under a light microscope supported this observation. All images taken at x10 magnification, scale bar represents 200 µm.

4.2.3 Characterisation of Reactive Oxygen Species Generation by Underground Railway PM

Increased IL-8 release has been suggested to be as a result of ROS generation by PM. Since underground railway PM is extremely rich in transition metals, predominantly iron, and such elements are known to be able to catalyse generation of ROS *via* electron donation, examination of the ROS-generating capacity of underground railway PM was warranted. The dye DCF was used as a measure of ROS, being undetectable in its reduced form, but fluorescing at an emission wavelength of 530 nm (excitation wavelength 485 nm) when oxidised. This dye was loaded into cells for 30 min, following which cells were washed and exposed to underground railway PM, with DCF fluorescence being monitored over time.

Initially, DCF fluorescence was measured over time after challenge of healthy donor PBEC monolayers with 0.6 $\mu g/cm^2$, 3.1 $\mu g/cm^2$, 6.3 $\mu g/cm^2$, and 12.5 $\mu g/cm^2$ of coarse, fine, or ultrafine underground railway PM, along with respective PBS-supplemented controls. Fluorescence was then calculated as the fold change compared to the fluorescence of the respective control.

The lowest concentration of PM, 0.6 $\mu g/cm^2$, resulted in a progressive increase in fluorescence *vs.* control over the entire 24 h duration of monitoring, reaching 1.5±0.1, 2.0±0.2, and 2.3±0.2 times the level of fluorescence seen in control wells for coarse, fine, and ultrafine fractions respectively (Figure 4.4 and Figure 4.5). However, for the three higher concentrations of PM, no such progressive increase was observed. For 3.1 $\mu g/cm^2$ PM, fluorescence peaked *vs.* control at 3 h after the start of the experiment, 4.1±0.5, 5.7±0.4, and 6.1±0.3 times control fluorescence, before steadily decreasing. For 6.3 $\mu g/cm^2$, peak fluorescence was reached even sooner, at 2 h, with peak fluorescence *vs.* control of 6.4±0.5, 9.1±0.5, and 9.8±0.8 times control levels for the three respective fractions. A similar outcome was observed with 12.5 $\mu g/cm^2$, with peak fluorescence *vs.* control at 2h with 8.0±1.0, 10.0±0.3, and 12.4±1.0 for the three respective fractions.

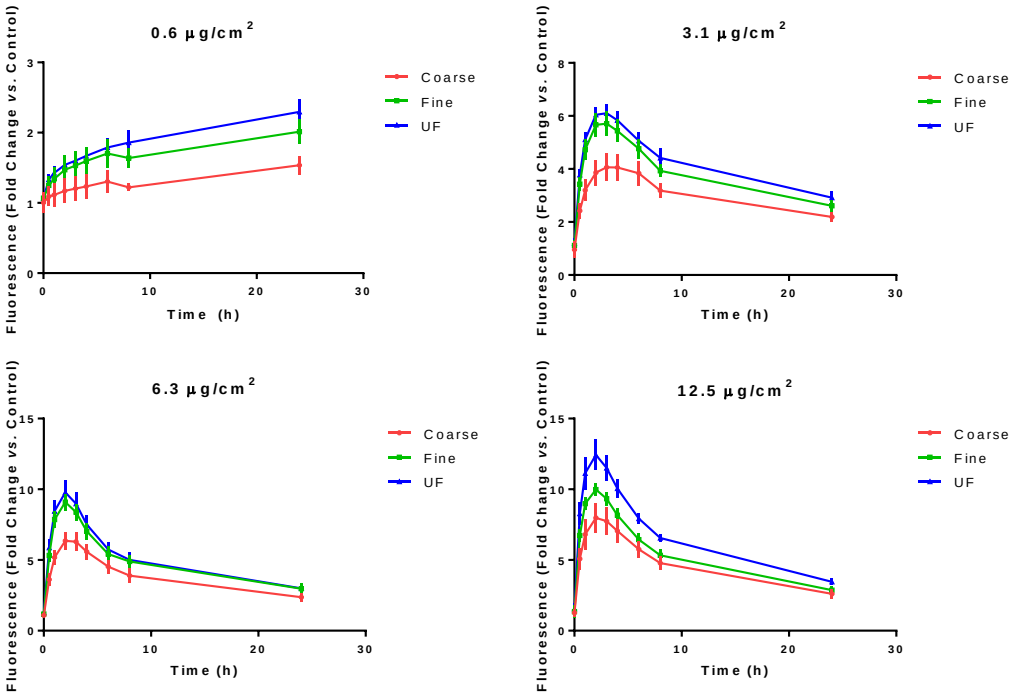

Figure 4.4. Changes in DCF fluorescence over time with underground railway PM. Healthy donor PBEC monolayers were loaded with DCF-DA, and incubated with underground railway PM. DCF fluorescence was measured over time for 24 h. Data expressed as mean fluorescence intensity of two replicate wells for each exposure divided by mean fluorescence intensity of cells exposed to PBS-supplemented culture medium as controls. Background fluorescence was negligible. Points represent mean fold change, error bars represent SEM, n = 4-5 healthy donors.

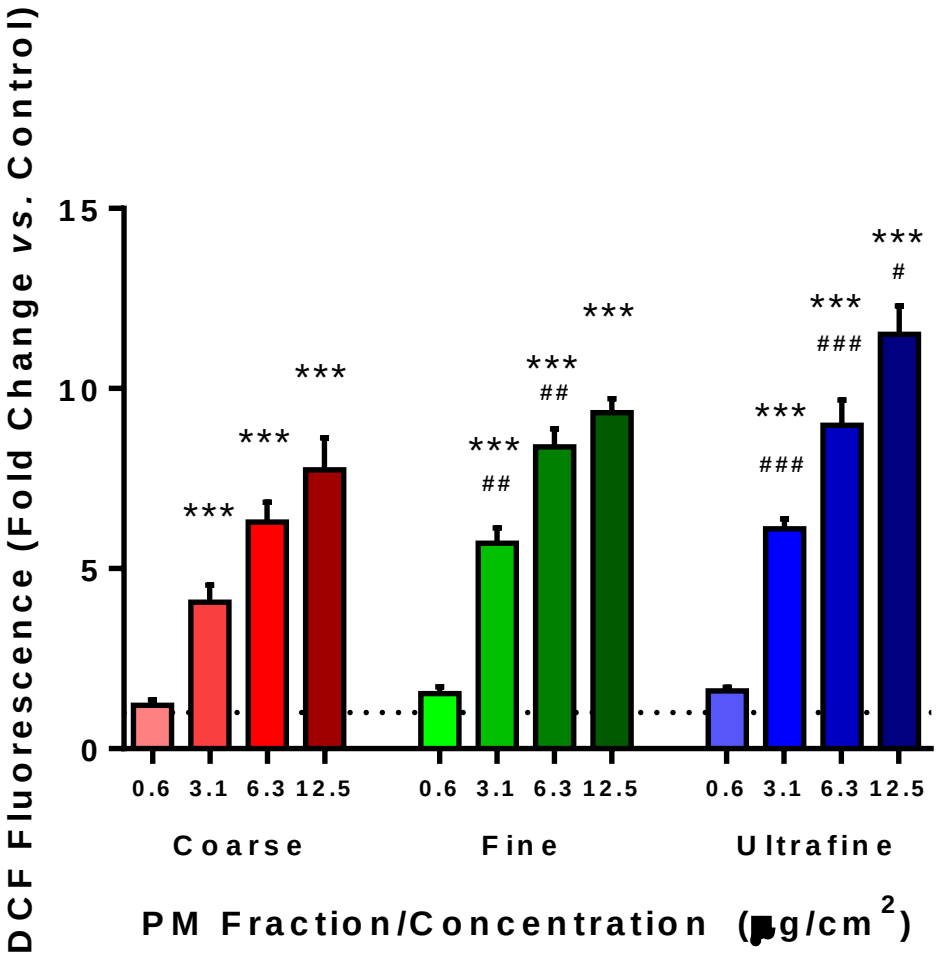

Figure 4.5. Changes in DCF fluorescence after 3 h with underground railway PM.

Data as for Figure 4.4, with only 3 h timepoint illustrated. Analysis by one-way repeated measures ANOVA with Bonferroni correction for pairwise analysis. *** - P<0.001 *vs.* control. # - p<0.05, ## - p<0.01, ### - p<0.001 *vs.* respective concentration of coarse PM, n = 5 healthy donors.

After 24 h, it was noticed upon removal of the supernatant and measurement of fluorescence of supernatant and $HBSS^-$-washed cells separately that the vast majority (usually >99%) of the fluorescence was located in the supernatant, with extremely low levels of fluorescence in the washed cells. Furthermore, this was also noted if the reaction was terminated after 4 h. It therefore appears that DCF is leaking out of the cells following the start of the experiment. The implications of this are discussed later.

Despite the fact that two of the PM concentrations showed a greatest fluorescence relative to control at 2 h, the 3 h timepoint with a concentration of 3.1 $\mu g/cm^2$ was

selected for further investigation for four reasons. First, the preparation of the plate took approximately 10 minutes from addition of the first sample to addition of the last sample. Therefore, at 2 h, cells in the final wells to which challenge was added had been exposed for almost 10% less time than those exposed first, with this percentage difference being less for a reading 3 h post-challenge. Second, addition of hydrogen peroxide after 24 h of exposure to PM failed to elicit an increase in fluorescence, suggesting that by 24 h, all DCF had been oxidised (data not shown). It was likely that the apparent drop in fluorescence relative to control after the early peak was due to a decrease in reduced DCF available for oxidation, and therefore DCF may act as a limiting step in detecting ROS generation by PM at later timepoints. Third, there was generally little difference between the 2 h and 3 h readings even for those concentrations which peaked at 2 h. Finally, further investigation was to involve attempts to modify PM oxidative activity with additional reagents. It was thought that if any modifying effects were to be seen with these reagents, they were likely to require lower concentrations if used with a lesser concentration of PM; this was advantageous because there would be less likelihood of off-target effects than at higher concentrations of DFX and NAC. Indeed, at 3 h, 3.1 $\mu g/cm^2$ underground railway PM produced an obvious marked and significant increase in DCF fluorescence, albeit one which was not as great as seen with the higher concentrations of PM.

Examination of the relative DCF fluorescence *vs.* control elicited by all concentrations of underground railway PM after 3 h incubation (Figure 4.5) shows that, at all but the lowest PM concentration used, coarse, fine, and ultrafine fractions all induced significant increases in fluorescence compared to control. Furthermore, at the two intermediate concentrations, both fine and ultrafine fractions induced a significantly greater increase in fluorescence than did the coarse fraction ($p<0.01$ for F *vs.* C, $p<0.001$ for UF *vs.* C). At the highest concentration of 12.5 $\mu g/cm^2$ however, only the ultrafine fraction was significantly more efficacious in inducing fluorescence than the coarse fraction ($p<0.035$).

In light of the apparently greater potential of the ultrafine fraction to generate ROS compared to fine and coarse fractions, and its metal-rich nature, further work was carried out to investigate ROS generation by this fraction, using 3.1 $\mu g/cm^2$ at a 3 h

timepoint, as explained previously. This work focused on the use of two reagents – DFX and N-acetylcysteine (NAC). These experiments were performed using monolayers of the bronchial epithelial cell line 16HBE, due to the requirement for a large number of cells for repeat experiments. Considering the previous observation that when experiments were performed with PBEC monolayers, the great majority of DCF fluorescence was in the supernatant and not the cells themselves and that this was noted even at early time points in the experiments, it was thought likely that the reduced, non-fluorescent form of DCF was leaking out of the cells after loading, and subsequently being oxidised by ROS generated by underground railway PM, and therefore the cells were acting as a leaking pool of DCF.

DFX is a bacterial siderophore, chelating free iron and also binding to solid phase iron, rendering it unable to undergo change in oxidation state (448). Therefore, since redox inactivation should prevent iron acting as an electron donor in ROS generation, DFX can be used to determine the extent to which ROS generation is mediated by iron. 3.1 $\mu g/cm^2$ PM was prepared in suspension as for previous experiments, except with the addition of DFX to varying concentrations. DCF fluorescence was measured after 3 h incubation (Figure 4.6). The lowest concentrations of DFX had no noticeable ability to inhibit ROS generation by ultrafine PM, and in fact induced a slight increase in ROS generation. However, a DFX concentration of 1.6 μM inhibited ultrafine PM-induced ROS generation by a mean (±SEM) 66.2±4.1%. At DFX concentrations above 1.6 μM, there was a further increase in inhibition of fluorescence, albeit to a lesser degree, with maximal inhibition seen with 40 μM DFX, inhibiting fluorescence by a mean of 82.9±1.4%.

NAC is a cysteine derivative which, by virtue of its thiol group, is able to act as an antioxidant and free radical scavenger. Therefore, NAC was added to ultrafine underground railway PM suspensions immediately prior to exposure of cells, to determine whether oxidation of DCF was mediated *via* ROS intermediates, or by a direct interaction between DCF and PM. As with DFX, the lowest concentrations of NAC caused an increase in DCF fluorescence, although the effect was more pronounced with NAC than with DCF. 40 μM NAC increased DCF fluorescence by a mean of 73.1±14.6%. However, increasing the NAC concentration to 1 mM

inhibited DCF fluorescence by 60.4±3.5%, and 25 mM NAC resulted in a mean inhibition of 77.6±4.1%.

These results therefore suggest that the majority of oxidation of DCF by ultrafine underground railway PM is iron-mediated and occurs *via* free radical intermediates, and not by direct interaction of DCF with ultrafine PM.

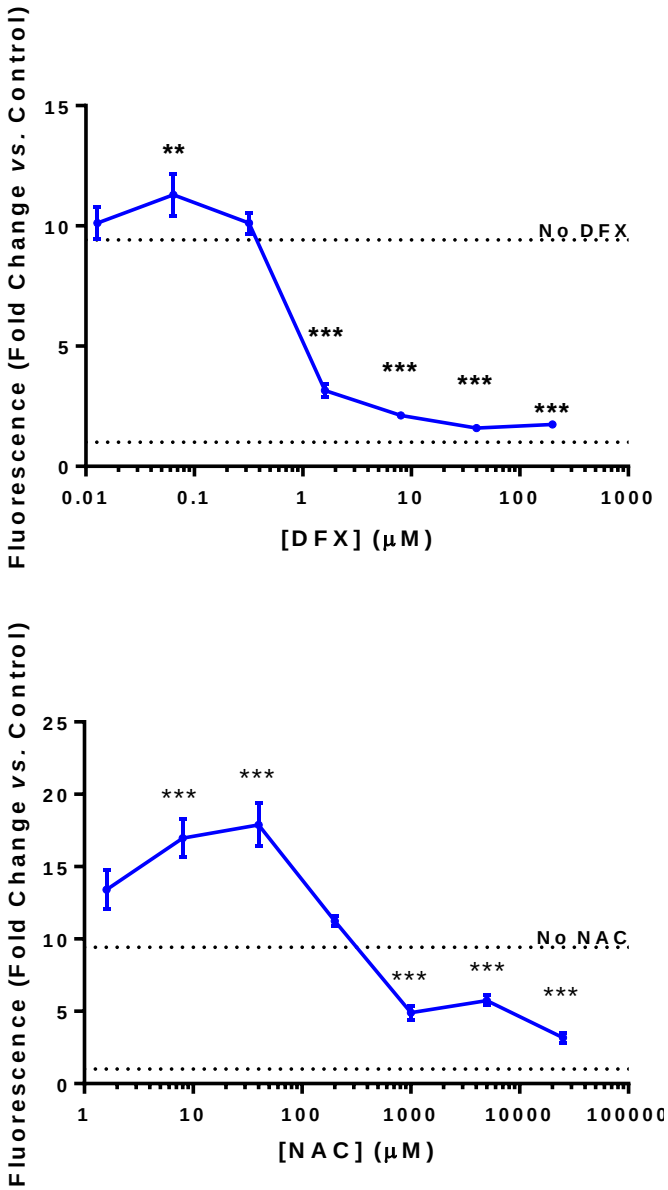

Figure 4.6. Modulation of ROS generation by desferrioxamine and N-acetylcysteine.

The effect of increasing desferrioxamine (DFX; top) and N-acetylcysteine (NAC; bottom) on DCF fluorescence induced by ultrafine underground railway PM was studied by challenging 16HBE monolayers with 3.1 µg/cm^2 ultrafine PM mixed with varying concentrations of either DFX or NAC. DCF fluorescence was measured after 3 h incubation. Data were calculated as mean fluorescence intensity of two replicate wells for each exposure divided by mean fluorescence intensity of cells exposed to PBS-supplemented culture medium with the corresponding concentration of DFX or NAC as controls. Analysis by pairwise repeated-measures t-test, ** - $p<0.01$, *** - $p<0.001$ *vs.* DFX/NAC-free culture, n = 3 for DFX experiments, n = 4 for NAC experiments.

4.2.4 The IL-8 Response of ALI Cultures to Underground Railway PM

Having characterised basic responses to underground railway PM of PBEC monolayers in terms of IL-8 release, LDH release, and ROS generation, further work was aimed at assessing responses in ALI cultures of PBECs. PBECs cultured at an air-liquid interface over 21 days in the presence of retinoic acid as a driver of differentiation are different to monolayers cultured from the same cells in a number of ways. First, ALI cultures, in having both apical and basolateral compartments with the potential for differences between them express apicobasal polarity, with the apical and basolateral sides of cells being different, for example in terms of their membrane proteins and mediator release. Furthermore, the application of toxicants or drugs to a single surface allows for a more physiologically representative assessment of the actions of xenobiotics. Second, ALI cultures exhibit cellular differentiation, with the development of cilia on the apical surfaces of populations of cells, and the formation of goblet cells. As a result of the presence of goblet cells, the surface of ALI cultures is coated with mucus, which may be an important modifier of cellular responses by influencing the access of stimuli to the underlying epithelial cells. Initial experiments were conducted with monolayers for reasons of cost, so that a reasonable concentration range could be established. However, more detailed investigations warranted the more physiologically accurate representation afforded by ALI cultures.

As a direct comparison of the responses of PBEC ALI cultures to PBEC monolayers, ALI cultures were exposed to 2.2, 5.6, or 11.1 $\mu g/cm^2$ coarse, fine, or ultrafine underground railway PM for 24 h, after which time apical and basolateral supernatants were harvested and processed exactly as for the monolayer experiments. Basolateral IL-8 release was assayed by ELISA. In contrast to the previous results with submerged PBEC monolayers, challenge of ALI cultures did not result in a significantly altered concentration of IL-8 in the basolateral compartment in either healthy or severe asthmatic donor cultures (Figure 4.7). In the course of performing these experiments it was observed that, unlike for PBEC monolayers unprotected by a mucous layer, where after removal of the supernatant and washing with $HBSS^-$ there

still remained a visible quantity of PM apparently either stuck to, embedded in, or located within the cells, the same procedure in ALI cultures left no PM remnants visible under light microscope. Furthermore, immediately prior to removal of the supernatants, PM in ALI cultures appeared to be suspended and exhibited some movement as the microscope stage was moved. Conversely, much of the PM in monolayer cultures did not move, lending further support to the notion of it being attached to the cells in some way. The observations are supported by the formation of small greyish pellets in the apical supernatants after post-harvest centrifugation (16,000 x *g*, 10 min, 4 °C), which was generally not observed when the same experiments were performed with PBEC monolayers.

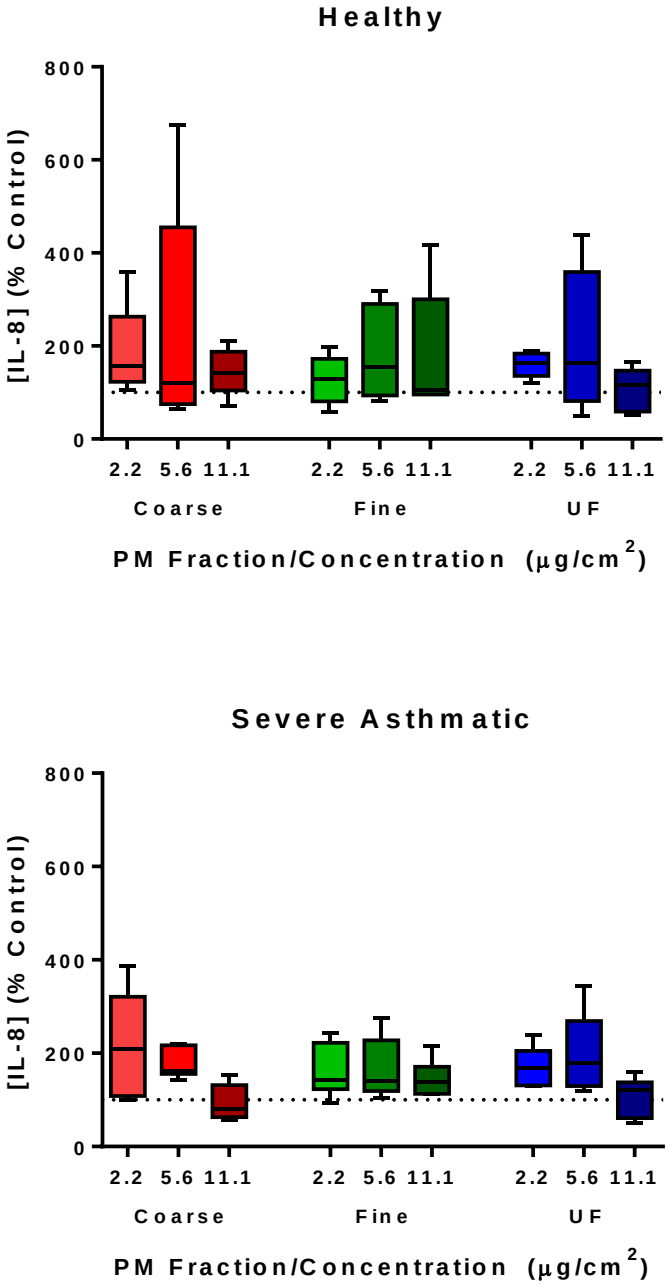

Figure 4.7. The effect of underground railway PM on basolateral IL-8 release from healthy and severely asthmatic donor PBEC ALI cultures.

Cells were treated exposed to underground railway PM for 24 h before medium was harvested. IL-8 was assayed by ELISA. Results presented as median with 25th and 75th percentile, whiskers represent 10th and 90th percentiles, n = 5 healthy donors, 5-6 severely asthmatic donors.

4.2.5 Changes in Epithelial Barrier Permeability in the Presence of Underground PM

As well as being intricately involved in the mounting of inflammatory responses after PM inhalation, the airway epithelium also acts as a physical barrier to prevent ingression of inhaled toxicants. If this barrier is compromised, access of pollutants, allergens, bacteria and viruses to the subepithelial tissue may be facilitated, with potentially damaging consequences. In the case of underground railway PM, any impairment in the ability of the epithelium to provide a physicochemical barrier may result in ingression of PM or PM constituents to the subepithelial tissue. Therefore, the effect of underground railway PM on epithelial paracellular permeability in PBEC ALI cultures was measured using the macromolecule dextran, tagged with the fluorophore FITC. 4 kDa dextran was used, with increased passage of dextran to the basolateral compartment indicating increased epithelial permeability, and thus an increased likelihood of transgression of ultrafine PM and soluble PM components through the epithelium. To determine whether these responses were dependent on PM concentration or size fraction, three concentrations of each PM were used – 2.2 $\mu g/cm^2$, 5.6 $\mu g/cm^2$, 11.1 $\mu g/cm^2$, with incubations performed over a 24 h incubation period as for previously described experiments. PBEC ALI cultures were exposed to underground railway PM for 24 h, followed by aspiration of PM solutions and application of FITC-dextran solution. Following further 24 h incubation, basolateral FITC fluorescence was measured and FITC-dextran concentration was determined from a standard curve. Basolateral FITC-dextran concentration as a result of a particular concentration of underground railway PM was then corrected by subtracting the basolateral FITC-dextran concentration seen as a result of exposure to the corresponding PBS-supplemented medium control. Thus, a positive value indicated in increase in permeability compared to control, while a negative value indicated a decrease in permeability.

For ALI cultures of PBECs from healthy donors, there was no significant change in epithelial permeability induced by any concentration of any of the three fractions (Figure 4.8). Coarse PM showed a tendency to slightly decrease epithelial permeability

with increasing concentration, from a median increase over control of 35 μg/ml basolateral FITC-dextran (IQR -16-113 μg/ml) with 2.2 μg/cm^2, to a median of -21 μg/ml (IQR -60.1-22 μg/ml) with 11.1 μg/cm^2. Fine PM showed an inverse bell-shaped dose-response effect, with 5.6 μg/cm^2 eliciting a control-corrected basolateral concentration of -13.7 μg/cm^2 (IQR -88-86 μg/ml), with the lowest and highest concentrations of fine PM having little effect on permeability. Conversely, ultrafine PM also produced a bell-shaped dose-response curve for epithelial permeability, but unlike fine PM, the peak response here was towards an increase in permeability with 23.3 μg/ml FITC-dextran (IQR -47-118 μg/ml). Therefore, although some changes in permeability were noted, these were not statistically significant. Furthermore, in terms of raw levels of FITC-dextran detected in the basolateral compartment, the greatest median level of FITC-dextran in the basolateral compartment, 174 μg/ml (IQR 69-269 μg/ml) after 2.2 μg/cm^2 coarse PM, was considerably less than the median 504 μg/ml (IQR 448-524 μg/ml) detected in the basolateral compartment after the same procedure was performed on a well which had not been seeded with cells, representing free diffusion (not shown on graph). Comparing this to the perturbation of FITC-dextran passage over the concentration range used, it is clear that underground railway PM had little effect on epithelial permeability to 4 kDa FITC-dextran.

When ALI cultures of PBECs from severely asthmatic donors were tested, a similar outcome was observed, suggesting that there was no obvious impairment of epithelial barrier function by underground railway PM in severely asthmatic donor cell ALI cultures.

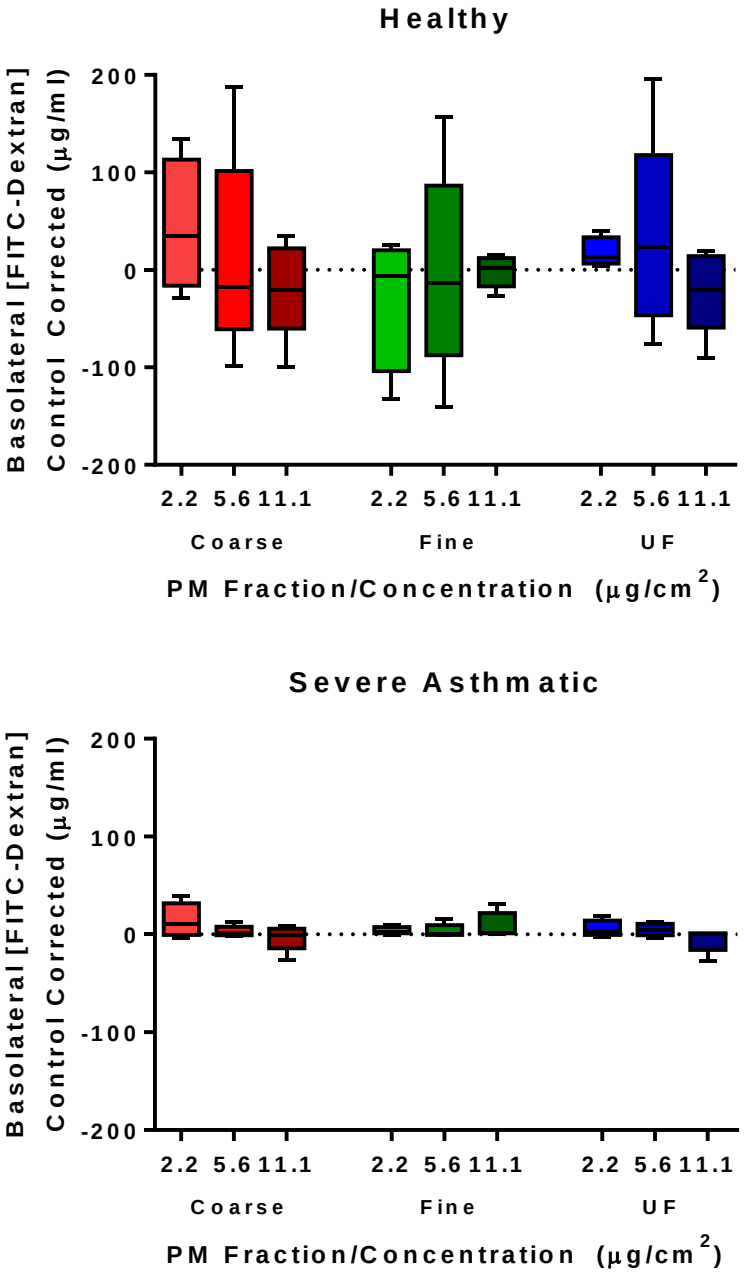

Figure 4.8. The effect of underground railway PM on epithelial barrier function.

ALI cultures were exposed to underground railway PM for 24 h, following which cells were washed once before 100 µl 2 mg/ml FITC-dextran solution was applied apically. Basolateral FITC-dextran was measured after 24 h, determined by FITC fluorescence intensity using a standard curve. Results presented as median with 25th and 75th percentile, whiskers represent 10th and 90th percentiles, n = 5 healthy donors, 4 severely asthmatic donors.

4.2.6 Cellular Antioxidant Responses to Ultrafine PM

Having determined that ultrafine underground railway PM is able to generate ROS in an iron-dependent manner, but that only a modest cytokine response to any fraction is seen after 24 h incubation, experiments were performed to determine whether PBECs mount an antioxidant defence after challenge with ultrafine PM. Since previous work had suggested that maximal responses in terms of uncorrected IL-8 release were seen at approximately 5.6 $\mu g/cm^2$, this concentration was selected for stimulation of cells. Ultrafine PM suspension, or PBS-supplemented culture medium, was applied to the apical surface of ALI cultures from healthy donors and incubated for either 2, 4, 6, 8, 24, or 48 h, at which time cells were lysed with Trizol. RNA was extracted, reverse transcribed to cDNA, and gene expression was measured using qPCR.

Expression levels of two antioxidant genes were quantified – HO-1 and NQO1 (Figure 4.9). HO-1 expression rose steadily to a peak at 24 h, a significant mean fold increase of 7.2±1.5 over control levels ($p<0.05$). By 48 h, levels had begun to fall, although still remained elevated compared to control. For NQO1, a biphasic response was seen, albeit much less pronounced than the response by HO-1. NQO1 levels rose to an initial peak at 6 h, 1.6±0.3 times greater than control levels. After a slight drop at 8 h, levels peaked at 24 h, 2.3±0.4 times control levels, before falling at 48 h, as was seen for HO-1. Although HO-1 was considerably more responsive to ultrafine underground railway PM than was NQO1, increasing to an extent more than three times greater than that seen for NQO1 at 24 h, expression of both antioxidants nonetheless reached a peak after 24 h of exposure, and decreased thereafter.

Gene expression of IL-8 was also analysed, and showed a profile of induction over time similar to HO-1, with a peak at 24 h of 4.0±2.4 fold over control, which had fallen to 1.7±0.4 fold over control by 48 h.

As a comparator, gene expression of the Th2 cytokines TSLP and IL-33 were investigated. TSLP is released by epithelial cells and potently activates dendritic cells to release a battery of cytokines which then act on $CD4^+$ T-cells to switch them to a

Th2 phenotype (449). TSLP is of interest in development of an allergic phenotype, and also because dendritic cells have been seen to play a role in particulate uptake (450). IL-33 is a novel cytokine whose release may be triggered by the action of the alarmin ATP on the $P2Y_2$ receptor, and which is linked to development of a Th2 phenotype (451, 452). Both TSLP and IL-33 exhibited similar profiles of induction over time, peaking at 6h, where there was an increase in TSLP of 2.5±1.2 fold over control, and in IL-33 of 2.1±0.8 fold over control. However, there was a notable degree of inter-donor variability, and neither of these increases reached statistical significance.

The aim of these initial experiments was to gain an idea of the time course of gene induction when healthy donor PBECs were cultured at ALI and exposed to 5.6 $\mu g/cm^2$ ultrafine underground PM. The results, although generally not repeated enough times to achieve statistical significance, suggest that the genes examined peak at either 24 h (HO-1, IL-8), 6 h (TSLP, IL-33), or show a biphasic response, with peaks at both 6 h and 24 h (NQO1). Since HO-1 showed the greatest induction of the genes tested, HO-1 was chosen for further examination. Furthermore, since this increase in HO-1 expression was most apparent after 24 h exposure, further experiments were conducted over exposure periods of 24 h, matching the time course of experiments for determination of release of IL-8 and LDH, and effects on epithelial barrier permeability.

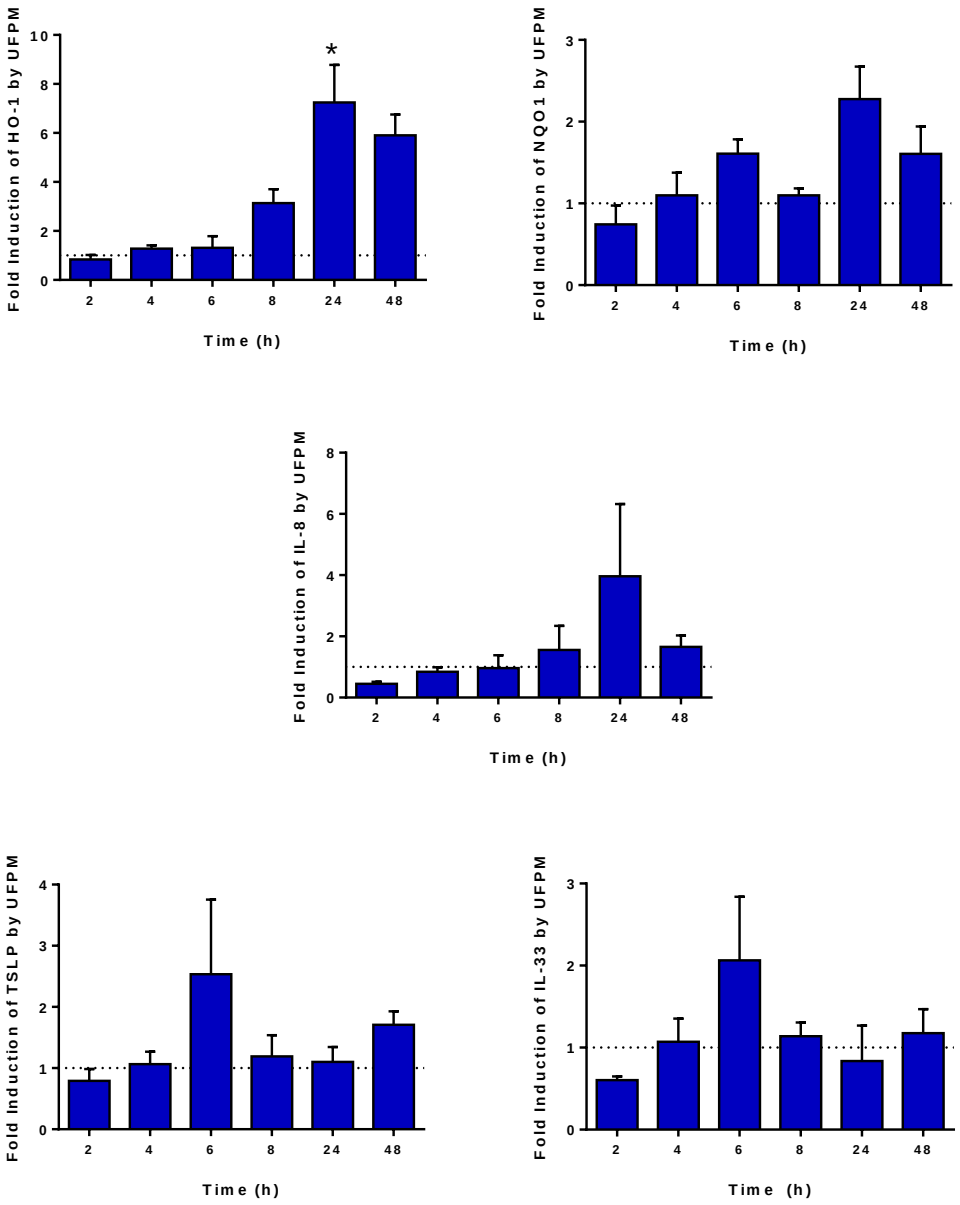

Figure 4.9. Changes in antioxidant and inflammatory cytokine gene expression with time after challenge with ultrafine underground railway PM.

Healthy donor PBEC ALI cultures were challenged with 5.6 µg/cm^2 ultrafine underground railway PM. At various time points, cells were lysed and gene expression determined by RT-qPCR. Data calculated by the ΔΔCt method, normalising first to housekeeping gene (UBC/GAPDH) expression, and then to expression of control (PM-free) wells for each timepoint. Data presented as mean±SEM. Analysis by one-way repeated measures ANOVA with Bonferroni correction for pairwise analysis, * - $p<0.05$ *vs.* UF PM-free control at respective timepoint, n = 3 healthy donors.

Previous experiments showed that the ROS generating activity of ultrafine underground PM could be abrogated by either the iron chelator and redox inactivator DFX or the free radical scavenger NAC. Therefore, cells were challenged with 5.6 μg/cm^2 ultrafine PM in the presence of either DFX or NAC. Initially, the previous DCF experiments were used as a guide to the concentrations of DFX and NAC which may be required. Concentrations of 2 μM and 20 μM DFX and 0.2 mM and 2 mM NAC were chosen, since these ten-fold different concentrations resulted in close to zero inhibition or maximal inhibition respectively of ultrafine underground PM-induced DCF fluorescence. However, these concentrations of DFX and NAC proved insufficient to have any inhibitory effect on the induction of HO-1 expression by ultrafine PM, and indeed the lower of the two concentrations of DFX and NAC both resulted in increased HO-1 expression, similar to the increased DCF fluorescence in the presence of NAC and DFX at the lower end of the concentration range (data not shown). Therefore, increased concentrations, roughly matching those used in the literature were adopted, specifically 200 μM DFX and 20 mM NAC. Fold change in HO-1 was determined relative to cells in the absence of UF PM, with DFX or NAC to correspond to the UF PM-challenged cells.

Exposure of healthy donor PBEC ALI cultures to 5.6 μg/cm^2 ultrafine underground railway PM resulted in a median 8.6-fold increase in HO-1 expression (IQR 5.7-17). DFX 200 μM significantly inhibited this effect, with ultrafine PM only eliciting a median 2.0-fold induction of HO-1 (IQR 1.9-2.3, $p<0.01$ *vs.* DFX-free UF PM). Similarly, NAC moderately ameliorated HO-1 induction by ultrafine underground PM to 5.1-fold (IQR 4.2-6.1), although this did not reach significance (Figure 4.10). These data suggest that the increase in HO-1 elicited by ultrafine underground PM is predominantly due to the iron content of the PM. Interestingly, a 10-fold increase in DFX concentration did not further inhibit HO-1 induction, suggesting that there is an approximate 2-fold induction in HO-1 which is not due to the iron content of the ultrafine PM, similar to the 1.7-fold increase in DCF fluorescence induced by UF PM which could not be inhibited by DFX (Figure 4.6) Although the higher concentration of NAC decreased the induction of HO-1 by underground PM, the lack of significance means that the induction of HO-1 cannot be definitely attributed to the presence of ROS.

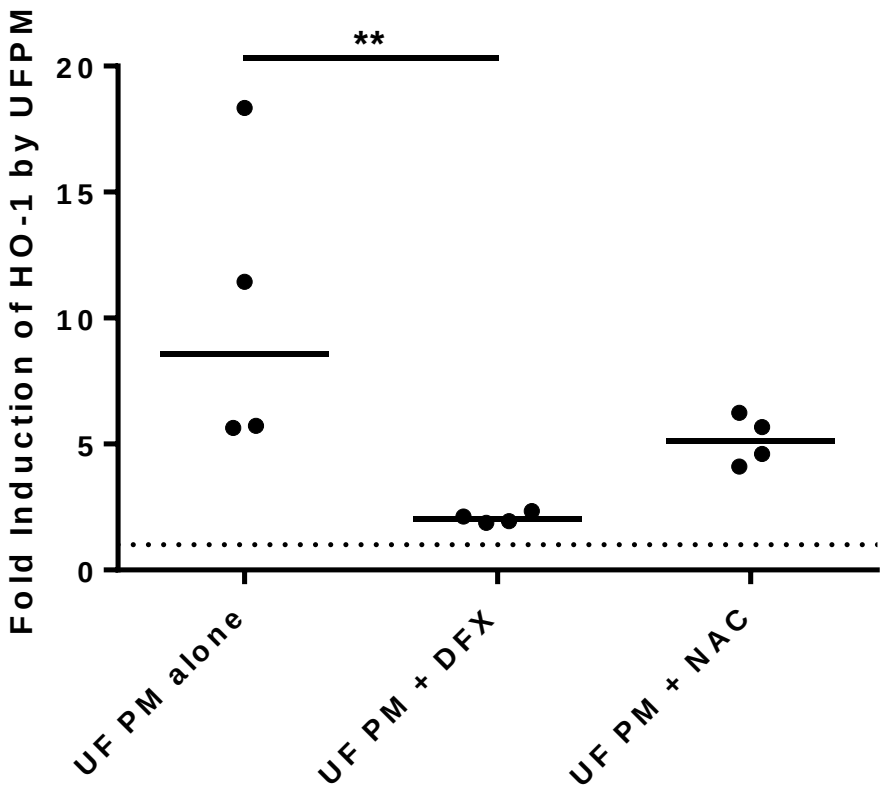

Figure 4.10. The effect of an iron chelator (DFX) and a free radical scavenger (NAC) on HO-1 induction by ultrafine underground PM.

Healthy ALI cultures were incubated for 24 h with 5.6 μg/cm^2 ultrafine underground PM, after which time RNA was harvested. HO-1 expression was determined by RT-qPCR in duplicate and normalised to PM-free incubations (with DFX, NAC, or neither) by the ΔΔCt method. Individual data points are shown, line represents median value. Analysis by Friedman test with Tukey's correction for pairwise analysis, ** - $p<0.01$, n = 4 healthy donors.

4.2.7 Uptake of Underground Railway PM by ALI Cultured PBECs

The results outlined thus far suggest that underground railway PM is able to elicit modest increases in inflammatory cytokine release in submerged monolayer cultures lacking a mucous layer, and that despite protection from such a mucous layer, ALI cultures of differentiated epithelial cells are in some way accessed by ultrafine underground railway PM, responding with upregulation of antioxidant expression, although epithelial barrier function appears unperturbed. These effects prompt the question as to whether PM is excluded from the inside of cells, and exerts effects extracellularly, or whether PM is able to enter cells, with the potential for intracellular sites of action. Therefore, PBECs cultured at ALI were exposed to underground PM of each size fraction, at concentrations of 3 and 12 $\mu g/cm^2$ for 24 h. Cultures were then fixed, embedded in resin, and sectioned for TEM. At least five sections from each of two distinct sites within the embedded culture were examined.

TEM suggested that underground railway PM is indeed able to enter epithelial cells. The aim of this work was not to attempt to quantify PM uptake, which would have required examination of a large number of sections from multiple donors. Given the time needed to find PM within cells of each section observed, much time would have been required for such a study. Nonetheless, intracellular PM was observed for each of the three size fractions used. PM was observed in various intracellular compartments, including free within the cytosol, in membrane-bound vesicles, and in structures which resembled mitochondria, particularly in their double-membraned structure (Figure 4.11), although no PM was observed within the nucleus. However, the scale of PM uptake appeared to be low, with cells generally containing no more than a maximum of five separate particulates/particulate aggregates. Furthermore, the majority of cells did not appear to contain intracellular PM. Finally, those cells in which intracellular PM could be seen were not noticeably morphologically different than those with no observable intracellular PM.

In order to confirm that the observed intracellular PM was, in fact, underground railway PM, and not an artefact arising from contamination of cells with, for example,

airborne dust during fixing, embedding, or sectioning of the cells for TEM, PM-like structures were analysed for elemental composition by energy-dispersive x-ray analysis (EDAX). Analysis was performed on four particles, three of which showed a peak consistent with the presence of iron, while one did not (Figure 4.12). The predominant metal peaks were representative of osmium and uranium, from contrast agents used prior to the sample embedding stage, and lead from the lead citrate stain used after the sections were cut. Although the analysis was performed on point and area sections, rather than the whole field of view, copper was also detected, probably from the grid on which the samples were mounted, despite the fact that the area of analysis was not in the same field of view as any section of the grid. None of these peaks overlapped with the area on the spectrum where iron would be observed if it were present. Spot analysis of a part of the section outside of the cells showed a reduced, although not absent, signal for these elements. These findings therefore validate the observation that metal-rich particles are able to enter PBECs cultured at the air-liquid interface. Although it cannot be proved conclusively that the particles within the cells were from the applied underground railway PM, their iron-rich nature makes it highly unlikely that they are artefactual.

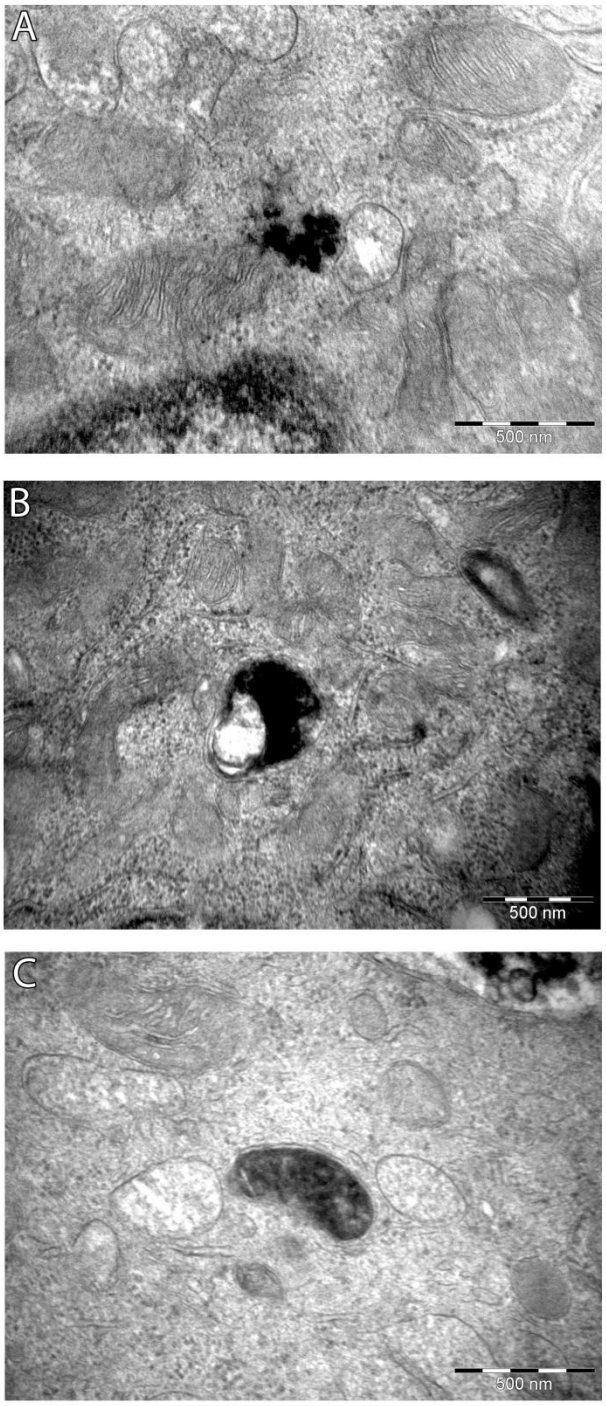

Figure 4.11. Intracellular localisation of underground railway PM in PBEC ALI cultures after 24 h incubation.

Healthy donor ALI cultures were incubated with underground railway PM for 24 h, after which time they were washed, fixed, and embedded for transmission electron microscopy. At least eight ultrafine sections were viewed for each of two areas per culture, with areas at least 100 µm apart. PM can be seen free in the cytosol in proximity to a mitochondrion (A), within a membrane-bound vesicle (B), and within a mitochondrion itself (C). No PM was observed within cell nuclei.

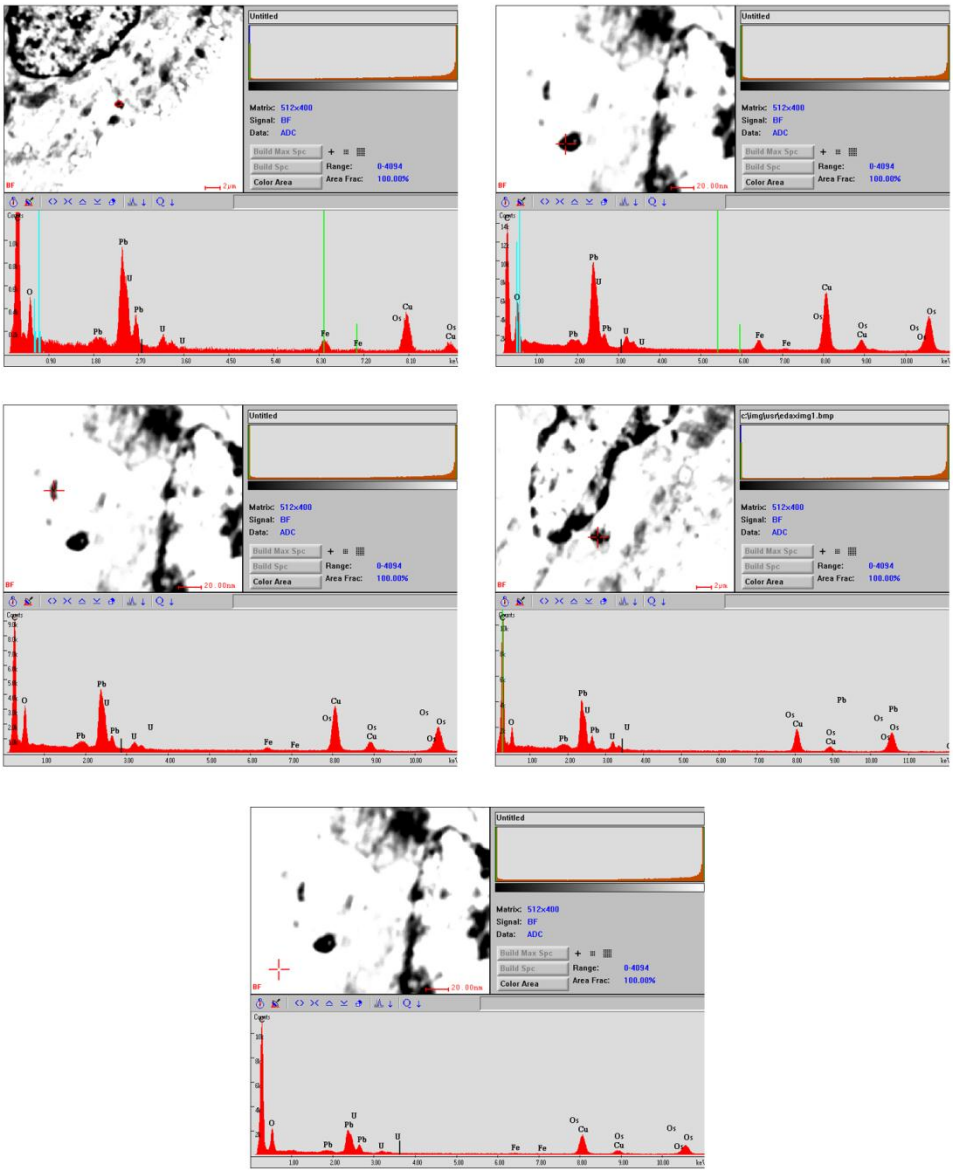

Figure 4.12. X-ray analysis of intracellular PM.

The sections were prepared for viewing as for Figure 4.11. Intracellular PM-like structures were located using TEM, after which time imaging was switched to scanning TEM, as shown in the upper left panel of each image above. Energy dispersive x-ray analysis was performed on four individual particle-like structures. Three of these (top left, top right, middle left) showed emission peaks characteristic of iron, strongly suggesting that these were particulates applied at the beginning of the incubation period, and not artefactual. One particulate (middle right) did not show an emission peak for iron. As a negative control, a spot of the resin section outside the cell and not covering a particulate was analysed (bottom centre).

4.3 Discussion

There is a considerable body of evidence which suggests that airborne particulate matter is both toxic to epithelial cells of the respiratory system, and inflammogenic even at sub-cytotoxic concentrations. The majority of such studies are carried out using urban or ambient particulate matter, either collected by the researchers or by use of a standard such as NIST1648, an urban particulate matter standard reference as supplied by the National Institute of Standards and Technology in the United States (298, 300, 453). However, other environments, particularly those associated with a specific activity such as woodburning or oil combustion can have considerably different profiles, both in terms of the resulting airborne concentration of particulate matter, and also the chemical composition of the particulate matter (122, 319, 454). Since both concentration and chemistry are thought to influence the toxicity of airborne particulates, studies of particles from sources beyond urban PM are required to understand the potential risks. The particles used in this study, from a mainline underground railway station, have been characterised in terms of their metal content and morphology (Chapter 3), and it was hypothesised that the high metal content, and particularly the high iron content, of the particles would confer upon them the ability to exert damaging effects on bronchial epithelial cells, the cells which form the deposition site for much of the inhaled PM.

Initial experiments used monolayers to characterise cellular responses to four concentrations of coarse, fine, and ultrafine underground railway PM. Although monolayers are a poor approximation of the cellular configuration of the airway epithelium, since they contain only one cell type, do not permit the expression of apicobasal polarity, and do not differentiate into ciliated epithelial cells and mucus-secreting goblet cells, they are an acceptable alternative in the case of basic dose-response characterisation, particularly where results will be used to inform smaller concentration sets for further experiments on other culture systems which may be more expensive in terms of labour or equipment costs. The underground railway particulate matter used in this study was supplied as a suspension in water at varying concentrations for each size fraction, the lowest being the ultrafine PM at a

concentration of 119 μg/ml, and therefore initial experiments were carried out using a high concentration of 50 μg/ml, to allow for upward extension of the concentration range if merited by initial results. There has been much debate about the correct way to measure the applied concentration of PM, the so-called "dose metric", in terms of how to measure the quantity of PM, either by mass, surface area, PM number, or other more derivative metrics such as oxidative stress. Mass is by far the easiest to measure, and although surface adsorption methods such the Brunauer-Emmett-Teller (BET) method of measuring the adsorption of nitrogen to the surface of a sample of particulates can be used to determine PM surface area, this is difficult in cases where there is a limited availability of particles, and therefore is perhaps more suited to commercially available engineered metal nanoparticles (215, 455). Particle number is somewhat difficult to measure and is not generally used in dose metrics. In addition, there is little agreement between studies about whether the applied concentration, when expressed in the mass form, should be calculated per volume of culture medium or per area of cells. Although the solubility of the underground railway particles used here has not been studied, other studies have reported that iron, which accounts for over 40% of the mass of each fraction, is found in the form of relatively water-insoluble oxides (66, 204, 252, 419, 438, 456). Therefore, since dissolution of the particles is expected to be low, and mass is the only viable method of measuring PM load in the current study, concentrations are expressed as micrograms per square centimetre of cell culture area (μg/cm^2). As PM was supplied as a suspension in water, required concentrations were also calculated as micrograms per millilitre (μg/ml) – conversion between these metrics is shown in Table 2.1.

Altered release of IL-8 is one of the most commonly measured effects of PM in bronchial epithelial cell cultures, with IL-8 functioning as a neutrophil chemoattractant and activator (457-460), and appears to be important in epithelial wound repair (461-463). Here, a linear relationship was observed between PM concentration and IL-8 release. Interestingly, in the present work, there was little difference in IL-8 response between cultures from healthy donors and those from severe asthmatics. Asthmatic airways have been seen to have lower levels of antioxidants, which may be important in defending against the potential toxic effects of airborne PM. However, it appears that there is no work on assessing whether these differences are reproduced in cell

culture models as used here. Furthermore, it is possible that mechanisms other than those involving oxidants are involved in inducing IL-8 release, in which case any potential defect in antioxidant defences in asthmatic donor cells may be of little relevance. Importantly, the extent to which IL-8 release could be induced by any of the fractions of underground railway PM at the tested concentrations was markedly lower than was induced by 10 ng/ml TNFα, suggesting that the cells are not mounting a maximal response to underground railway PM in terms of IL-8 release. Although PM concentrations of up to 22.2 $\mu g/cm^2$ (100 μg/ml) were feasible, 11.1 $\mu g/cm^2$ was not exceeded due to the bell-shaped dose response relationship seen at the concentrations initially employed. Subsequent work suggested than gene expression of IL-8 in response to underground railway PM is greatest after 24 h. Therefore, it may be that 24 h was not sufficient to observe the greatest IL-8 effect, and therefore further incubations of up to a week could be performed to examine an expanded time-course of IL-8 release.

Cell death is often observed at the upper concentrations of PM used in published work. There are a number of ways of quantifying cell death, including cell counts with Trypan blue exclusion dye to discount dead cells, tetrazolium dyes such as MTT, XTT, and WST-1, which change colour when reduced, indicating the metabolic activity of the cells in the culture tested, and the LDH assay, which involves measurement release of the cytosolic enzyme LDH, which increases with cell membrane integrity decreases. The present study measured concentrations of LDH in culture supernatants, with no change in LDH concentration as a percentage of total cellular LDH, as a measure of percentage cell death. However, the LDH assay, although arguably the most commonly used of these assays, has drawbacks. Whereas the other assays involve incubation with PM followed by, for example, incubation with the tetrazolium dye after the PM exposure period, the LDH assay measures an analyte which may have accumulated in the supernatant over the entire 24 h incubation. Since LDH is susceptible to degradation over time, it is conceivable that the cytotoxicity of PM which causes an initial rapid release in LDH may be underestimated if the LDH is degraded prior to collection. There have also been doubts raised concerning the interaction of particles with the assay. It is possible that PM could deactivate LDH, rendering it undetectable by the assay used here either by inactivating or binding the

enzyme (464). PM-bound LDH would then be removed from the supernatant by the centrifugation step and not detected. However, the tetrazolium dye-based methods of measuring cytotoxicity do not measure cell death *per se*, but rather mitochondrial metabolic activity, and the continued widespread use of the LDH assay suggests that these drawbacks are insufficient to stop its use. Indeed, since inspection of cultures under a light microscope after 24 h incubation also suggested that cell death was minimal, it appears unlikely that the LDH assay was under-reporting the genuine level of cell death. This provided reassurance for any further work using this concentration range of ultrafine PM, since the aim of the study was to examine effects on cells which were not due to overt cell death – that is, effects towards the lower and middle sections of the hierarchy of PM effects suggested by Nel and co-workers (271).

Although the increases in IL-8 release were statistically significant, their biological significance is more debateable in light of the much greater release of IL-8 which could be induced by TNFα. Therefore, since ROS are considered to be a major intermediate by which airborne PM exerts its effects, ROS generation was measured using the dye DCF. These experiments indicated that underground railway PM generates ROS in a concentration-dependent manner, dependent upon the iron content of the PM. DCF is loaded as DCF-DA, the reduced form of the dye with two acetate groups attached to the central carbon ring. These acetate groups render the dye lipophilic, allowing it to enter the cell, whereupon the acetate groups are cleaved by cytosolic esterases, the dye becomes hydrophilic, and is "locked" within the cell (465, 466). In the present research, it was noted that even after 3 h incubation with underground railway PM, the great majority of the detectable fluorescence was within the supernatant, and not the cells themselves. This indicates that either the reduced form of the dye is somehow exiting the cell and becoming oxidised to its fluorescent form within the supernatant, or that it is being oxidised within the cell and subsequently leaking into the supernatant. Indeed, this propensity of DCF to leak from the cell has been noted previously (467, 468), may be dependent on cell type (465), and is potentially related to the cleavage, or lack thereof, of the acetyl groups, as result of either differential esterase activity or differential partitioning of DCF-DA inside the cell (469). There are alternative forms of the dye available which may offer improved intracellular retention, such as carboxy-DCF-DA, whose carboxyl groups endow the molecule with additional

negative charges to increase lipophobicity, and chloromethyl DCF-DA and succinimidyl ester DCF-DA, which covalently bind intracellular thiol and amine groups respectively. However, trials with these alternative forms were unsuccessful at preventing apparent leakage of DCF (data not shown). Furthermore, the LDH assay data and microscopic evaluation of cultures did not indicate any significant cell lysis, suggesting that leaking of DCF following cell death is unlikely. Therefore, these results do not allow conclusions to be drawn about whether underground railway PM induces intracellular ROS generation. However, it is clear that the PM can generate ROS, which may be still be toxic if generated extracellularly, since ROS are known to be able to attack cell membrane lipids, and indeed the products of such reactions may be used as a measure of PM toxicity. For instance, malondialdehyde and TBARS are products of membrane lipid peroxidation which can be detected as a result of ROS attack *in vitro* (174, 270) while malondialdehyde may also have applications for determining oxidative stress *in vivo* when measured in lung fluid or exhaled breath condensate (318). Furthermore, some studies incubate DCF-DA with PM in a cell-free compartment, with prior use of sodium hydroxide or medium supplemented with serum containing acetylases, to cleave the acetate groups since DCF is more readily oxidised once the acetate groups are removed (466, 470). These studies are thus only powered to examine generation of ROS in a cell-free solution. In spite of the apparent leakage of DCF from cells in the present study, there remains the possibility of amelioration of ROS generation by antioxidants secreted from the cells, and therefore the method used in the present research provides a more realistic account of the potential for ROS generation *in vivo* than do experiments conducted in the absence of cells.

Another caveat for the use of DCF is its specificity. DCF is usually described as being a reagent for the detection of ROS. Furthermore, since superoxide and hydrogen peroxide do not react directly with DCF (471), it is generally considered that DCF fluorescence is due to the presence of the hydroxyl radical. However, there is good evidence to suggest that DCF is capable of reacting with species other than these, such as reactive nitrogen species and carbonate anion radicals, while the second electron reduction may proceed with molecular oxygen, forming fluorescent DCF and superoxide (see review by Kalyanaraman *et al* (472)). Furthermore, cytochrome c,

which may be released from mitochondria, is able to reduce DCF to its fluorescent form (473, 474), while free ferrous iron may be mobilised by lysosomal membrane permeabilisation as part of apoptosis or necrosis, favouring the reduction of DCF (475). Similar observations have been made regarding haem (476), while it has also been suggested that DCF may itself participate in the generation of reactive oxygen species (477). Therefore, although DCF fluorescence is able to indicate the presence of oxidative stress in a system, it may also reflect increased concentrations of one or more of these species.

The aforementioned limitations notwithstanding, the results of the experiments with DCF yielded three important findings. First, on an equal mass concentration basis, underground railway PM generated ROS to a greater extent as particle size decreased. The PM surface area/volume ratio is an important determinant of PM reactivity since, unless a particle is soluble, only the surface of the particle is able to interact with the surrounding milieu – the part of the particle hidden within is not accessible to the surrounding environment. There is a dramatic increase in the percentage of a particle's constituent atoms which are located on the surface as particle size decreases (212). However, while surface area can influence ROS generation in particles where chemical composition is constant across size fractions, it does not necessarily follow that ultrafine PM must be more potent in generating ROS than coarse PM, since surface chemistry is also important. For example, transition metals are often found in greater abundance in coarse PM than ultrafine PM, which may be composed of the products of secondary reactions between gases around a carbon core. However, a novel finding from Chapter 3, that in size fractionated underground railway PM the ultrafine fraction is at least as rich in iron and other transition metals as the coarse and fine fractions, suggests that ultrafine underground railway PM may be the most potent ROS generator of the three fractions. This was supported by DCF fluorescence levels after 3 h incubation, whereby UF > F (not significant), and UF > C (significant), with further size effects with F > C (significant).

Further work on the ultrafine fraction using the iron (Fe^{3+}) chelator DFX showed that this ROS generation is mediated *via* the iron content of the ultrafine PM, while the decrease in fluorescence in the presence of NAC indicates that DCF was oxidised *via*

ROS intermediates, and not merely by direct interaction with the ultrafine PM. The implications of having a metal-rich ultrafine PM capable of significant ROS generation are discussed later.

There is an important caveat in the interpretation of these results, in that they show elicitation of IL-8 release and DCF fluorescence on the basis of particle mass concentration as applied to cell cultures. However, in terms of relating these results to the underground railway environment, it is important to remember that the three size fractions are not present in equal mass concentrations in the air. The mean concentrations of coarse, fine, and ultrafine fractions of PM over the three sampling days was 169 $\mu g/m^3$, 75 $\mu g/m^3$, and 38 $\mu g/m^3$ respectively, which may be expressed as a ratio of approximately 4.5 : 2 : 1. This means that, for a given outcome *in vitro*, a given mass concentration of ultrafine PM would have to have 4.5 times the effect of coarse PM in order to indicate that airborne ultrafine PM may be more toxic than coarse PM. Taking the mean DCF fluorescence induced by 6.3 $\mu g/cm^2$ PM (Figure 4.5), it can be seen that although ultrafine PM has a greater effect than coarse PM, it does not approach 4.5 times the effect of coarse PM (fluorescence *vs.* control of 6.3, 8.4, and 9.0 for coarse, fine, and ultrafine PM respectively). Similarly, 11.1 $\mu g/cm^2$ of the three fractions increased median IL-8 release by 225%, 234%, and 315% respectively. This emphasises that, per unit volume of air as found in the underground station, coarse PM possesses the greatest ability to induce IL-8 release and ROS generation. However, a further level of complexity is added when it is considered that airway deposition is not the same across the three size fractions. Coarse particles are more likely to be trapped by the particle-trapping mechanisms of the upper airways, while ultrafine particles are able to penetrate more deeply into the terminal airways, alveoli, and possibly translocate into the circulation. Furthermore, they have the ability to enter cells, where their long-term consequences are completely uninvestigated, but their presence in a number of organelles suggests the potential for long-term toxicity. Therefore, when attempting to measure the potential toxic effects of each size fraction, an ideal approach would also take into account the deposition sites of such particles, as well as their likely retention times and potential for translocation into cells and the circulation, all of which are likely to result in a relative increase in toxicity as particle size decreases.

Since data now showed that, in spite of having only moderate effects on IL-8 release and no clear effects on cell death, the underground railway PM was capable of inducing ROS generation in a size- and iron-dependent manner, ALI cultures of PBECs were used for further experiments. As previously noted, these cultures provide a more realistic model of the airway epithelium since they express apicobasal polarity and facilitate differentiation of the seeded cells to form ciliated epithelial cells and mucus-secreting goblet cells. Although the cultures are differentiated for 21 days at air-liquid interface, with culture medium in the basolateral compartment, but the apical surface of the culture exposed to air, PM exposures were performed with PM in suspension, and therefore the air-liquid interface was not present over the period of exposure. ALI cultures of PBECs from healthy donors were exposed to underground railway PM at the same concentrations (by $\mu g/cm^2$ and $\mu g/ml$) as were the monolayers. After 24 h incubation, basolateral medium was harvested and IL-8 was measured by ELISA. Interestingly, whereas there was a moderate but significant concentration-dependent increase in IL-8 release *vs.* control seen in the PBEC monolayer experiments, no such increase was seen with ALI cultures. All concentrations of coarse, fine, and ultrafine PM produced slight increases in IL-8 release, but there was no clear trend with concentration, and significance was not reached for any PM concentration with any of the three size fractions of PM. When the same experiments were performed with ALI cultures of PBECs from severely asthmatic donors, there was again no statistically significant change in IL-8 release, and again no clear trend.

The most likely explanation for this apparent lack of effect compared to that seen in the monolayer cultures may lie in the mucus secreted by the goblet cells which have differentiated from the seeded cells over the 21 day ALI culture period. Centrifugation of the apical supernatant after incubation produced a clear, albeit small, grey pellet on the side of the eppendorf tube, seemingly particulate matter, which was not seen when supernatants from the monolayer incubations was centrifuged. Furthermore, after removal of the supernatant, very little PM remained, and this was removed with a single wash of $HBSS^-$. Conversely, after removal of the monolayer supernatants and an identical wash step, there still remained a clear presence of PM, either within, partially embedded inside, or adhered to the surface of the cells. These

observations, although somewhat rudimentary and arbitrary, suggest that the mucus is protecting the cells from at least the insoluble component of the underground railway particulate matter. However, subsequent electron microscopy studies suggested that some PM is still able to penetrate the mucous layer within the 24 h incubation period.

Another explanation for the lack of observed pro-inflammatory effect of underground railway PM is that the increase in pro-inflammatory cytokines is not necessarily global, with different PM and PM constituents being able to elicit increases in different cytokines (232, 310).

In addition to having no significant effect on IL-8 release, underground railway PM was also seen to have no effect on epithelial barrier permeability as measured by passage of 4 kDa FITC-labelled dextran. Passage of dextran from the apical to the basal compartment is a measure of the macromolecular permeability of the epithelium to macromolecules smaller than 4 kDa and particles smaller than the hydrodynamic radius of the FITC-dextran – in this case, 4 kDa FITC-dextran has a hydrodynamic diameter of 2.8 nm. Conversely, TER measures ionic flux across the epithelium, and therefore degraded epithelial function may be observed by TER without a concomitant effect on dextran passage. In this case, FITC-dextran was chosen as a more relevant measure to indicate the potential for particle transgression, although TER measurements also indicated little perturbation in terms of ionic flux (not shown). Indeed, TER has been suggested to be an indicator of viability after exposure to nanoparticles (478), and therefore this lack of effect on TER correlates well with the lack of effect of underground railway PM on LDH activity in monolayers.

Since most *in vitro* studies of the effect of PM on airway epithelium are conducted using monolayers, permeability studies such as this are rarely performed. An *in vivo* study of the effect of urban PM on mouse gut epithelium found increased 4 kDa FITC-dextran in the blood after application by gavage following 48 h particulate dosing, and this increased permeability was replicated by decreased TER readings in Caco-2 cells grown on cell culture inserts (479). Studies using TER are more common, although the effect of PM on epithelial barrier function is nonetheless rarely investigated, but produce conflicting results. Bayram and colleagues showed that

normal human bronchial epithelial cells increased TER in response to DEP in a concentration-dependent manner (480). Conversely, Lehmann and co-workers found that 125 μg/ml DEP reduced 16HBE monoculture TER accompanied by deranged tight junction occludin distribution when the epithelial cells were in monocultures (177). Other studies have indicated that zinc oxide and copper oxide nanoparticles both exert deleterious effects on transepithelial resistance in rat alveolar epithelial cell cultures and Calu-3 cells respectively (258, 478). In addition, studies examining the effects of tracheobronchial instillation of PM or inhalation of aerosolised PM in rats have observed increased levels of protein in BALF, suggesting increased epithelial permeability, for instance when humans have been exposed to coarse PM collected in the vicinity of a steel mill (481), or when rats have been exposed to underground railway, traffic-related, or oil fly ash PM (80, 203, 305), although the time-points at which these observations were made varies between studies. The present study, however, found no such effect. One possible explanation for this is the presence of mucus, as detailed above. It is also possible that epithelial permeability is modified by the presence of other cells or factors secreted by other cells with may be present in the airways *in vivo* but which are not present in epithelial cells in monoculture *in vitro*. For instance, the aforementioned study by Lehmann and co-workers which found a decrease in 16HBE monoculture TER in the presence of DEP found that there was no such decrease in a triple cell co-culture of 16HBE, macrophages, and dendritic cells (177). Indeed, although macrophages and dendritic cells fulfil roles as phagocytic and antigen presenting cells, there is also evidence that they can express tight junctional proteins and participate in the formation of a tight epithelial barrier (450, 482). Conversely, macrophages have been observed to secrete TNFα in response to urban PM_{10} (285, 483), which may be at least partly due to the presence of LPS on the PM (118, 122). TNFα has been demonstrated by other groups to cause impairment of epithelial barrier function in the intestine (484, 485) although a search of the literature suggests that the effect of TNFα on airway epithelial permeability has not been studied.

Although there appeared to be no pro-inflammatory or cytotoxic effects of underground PM, their ability to generate ROS suggested that it would be rational to examine effects towards the lower end of Nel's hierarchy by examining effects on

antioxidant gene expression. Only ultrafine underground railway PM was examined since the metal content of this fraction was the most novel finding of the research performed thus far. A concentration of 5.6 $\mu g/cm^2$ was chosen since this was the concentration which produced maximal uncorrected IL-8 release, whereas using a higher concentration may have mirrored the apparently reduced response as seen for IL-8 release. A lower concentration was not used since DCF experiments suggested increased ROS generation across the entire PM concentration range. In order to determine the optimum time-point at which to examine antioxidant gene expression levels, ALI cultures were exposed to PM for 2-48 h.

Two antioxidant genes, HO-1 and NQO1, were examined, both of which have been seen to be upregulated by particulate matter in the literature. HO-1 in particular was markedly upregulated, while NQO1 was upregulated to a lesser extent. The time course of induction of the two genes was also different, with NQO1 gene induction showing a smaller peak at 6 h, whereas HO-1 induction followed a monophasic time course. Furthermore, IL-8 followed a similar time course to HO-1, albeit with a lesser maximal induction, whereas the Th2 cytokine genes TSLP and IL-33 both peaked after 6 h. Very few studies have examined the effect of PM on TSLP. Exposure of primary human bronchial epithelial cell monolayers to a concentration of DEP (3 $\mu g/cm^2$) similar that of ultrafine underground railway PM used in the RNA work in the present study resulted in an increase in TSLP mRNA of 11- and 15-fold at 4 h and 18 h incubation respectively, along with increased release of TSLP, and these effects were reduced in the presence of NAC (486). Through this process, DEP can induce Th2 polarisation of dendritic cells (486, 487). This has subsequently been suggested to involve the aryl hydrocarbon receptor, perhaps explaining a lack of effect in underground PM, which has a lower aromatic hydrocarbon content than DEP and ambient PM, which elicited similar effects (488). However, this does not appear to be the only pathway by which PM can induce TSLP (488). Data on IL-33, which may function as an alarmin, are scarce. Intratracheal instillation of multi-walled carbon nanotubes in mouse lung result in an increased release of IL-33 (489) and upregulated expression of IL-33 mRNA (490), which may then result in development of airways hyperresponsiveness (491). However, there is a paucity of studies of IL-33 responses to more frequently encountered PM, and these reports are inconclusive, for example

the lack of change in BEAS-2B cell IL-33 mRNA in response to DEP after 4 h incubation (492).

Since responses in antioxidant genes were of principle interest, and since induction of HO-1 was notably higher than NQO1, HO-1 was selected for further study whereby the effects of DFX and NAC in the underground railway PM were studied. The iron chelator DFX greatly reduced the ability of ultrafine underground railway PM to elicit expression of HO-1, while NAC more moderately, non-significantly, reduced HO-1 expression induced by ultrafine underground railway PM. Similarly, HO-1 mRNA has been seen to be increased in RAW 264.7 macrophages in response to ambient ultrafine PM and amine-coated polystyrene nanoparticles, and this effect was inhibited by NAC (234). Furthermore, ZnO nanoparticles have been seen to increase HO-1 mRNA and protein levels in RAW 274.7 and BEAS-2B cells (493) although, interestingly, Fe_2O_3 nanoparticles induced only a moderate increase in HO-1 mRNA in RAW 264.7 cells and no increase in A549 alveolar epithelial cells (494). However, this surprising result is suggested to derive from differences in the Nrf2 system, whereby A549 cells lack the Nrf2 anchor Keap1, meaning that in these cells Nrf2 is constitutively active and thus there is a lesser potential for further activation. This suggestion is supported by generally reduced perturbation of the expression of Nrf2-controlled genes in the study (494). DEP and organic extracts thereof can also induce expression of HO-1 and NQO1, while HO-1 expression in rats was not affected by inhalation of carbon nanoparticles (266, 316). Knockout of Nrf2 in mice diminished the effects of DEP on HO-1, further indicating a key role for Nrf2 in regulating oxidant-induced antioxidant expression, although other work has shown that knockout of Keap1 in Clara cells leads to increased expression of NQO1 but not HO-1 (274, 275). These observations suggest that, although Nrf2 may act as a master regulator of antioxidant expression, the process is likely to be further controlled by other co-activators or repressors (274). Thus, further work examining altered levels of Nrf2 and Keap1 in response to underground railway PM, and also nuclear translocation of Nrf2, would shed light on the processes controlling the response to such PM.

Interestingly, the ultrafine PM was able to elicit a moderate increase in HO-1 expression even in the presence of DFX, and this increase was of a similar magnitude

to the increase seen when the optimal concentration of DFX was used in the previously discussed DCF assay. In both instances, an approximately two-fold greater response was observed even in the presence of DFX. This is potentially due to the fact that DFX is able to chelate ferric iron (Fe^{3+}), while showing no detectable affinity for ferrous iron (Fe^{2+}) (448). The consequence of this is that although DFX may be able to inhibit the reduction of Fe(III) to Fe(II) as occurs in the Haber-Weiss reaction series in redox cycling of iron, which is itself a source of ROS, it may be unable to prevent the successive series of reductions of molecular oxygen to hydroxyl radical, including the Fenton reaction, as catalysed by ferrous iron (207, 402). As such, DFX may inhibit the progression of:

$$Fe^{3+} + H_2O_2 \rightarrow Fe^{2+} + {}^{\bullet}O_2^{-} + 2H^{+}$$

$$Fe^{3+} + {}^{\bullet}O_2^{-} \rightarrow Fe^{2+} + O_2$$

$$Fe^{2+} + H_2O_2 + H^{+} \rightarrow Fe^{3+} + H_2O + HO^{\bullet}$$

but with ostensibly no effect on:

$$Fe^{2+} + O_2 \rightarrow Fe^{3+} + {}^{\bullet}O_2^{-}$$

$$Fe^{2+} + {}^{\bullet}O_2^{-} + 2H^{+} \rightarrow Fe^{3+} + H_2O_2$$

$$Fe^{2+} + H_2O_2 + H^{+} \rightarrow Fe^{3+} + H_2O + HO^{\bullet}$$

DFX may be able to shield particulate iron from the surrounding milieu, but no redox inactivation of Fe^{2+} is likely to occur. Such an effect has been observed experimentally, where the antioxidant depleting ability of various types of PM was ameliorated to a greater extent by diethlyene triamine pentaacetic acid (DTPA, which chelates both ferrous and ferric iron) than by DFX, although this may also be attributable to other transition metals which can be chelated by DTPA (172). Indeed, in addition to reduction by reaction with hydrogen peroxide as per Haber-Weiss cycling, ferric iron may also be reduced to ferrous iron by antioxidants, as are present

in the respiratory tract, and as has been demonstrated experimentally by increased formation of dihydrobenzoic acids from oxidation of salicylic acid after addition of various antioxidants to ferric iron and also cuprous copper (495). It has been suggested that there is a "crossover", whereby low concentrations of antioxidants may be detrimental because although they are less effective at reducing transition metals to an oxidation state in which they are primed to partake in Fenton chemistry, they are also less able to terminate radical generation reactions. For example, *in vivo* administration of 500 mg ascorbate per day led to an increase in lymphocyte 8-oxoadenine levels, a marker of oxidative damage to DNA, although levels of 8-oxoguanine were unaffected (496). However, the physiological effects of ascorbate are a matter of debate, and may depend on experimental design (497).

Another possible reason for the residual effect of ultrafine PM after DFX addition is that there is a component of ROS generation by the ultrafine underground railway PM which is not caused by the iron within the PM, or that there is a constituent of the particles which is able to induce ROS generation by the cell without itself being a generator of ROS. One potential constituent is LPS, which induces increased HO-1 gene expression in rat lung epithelial cells, as well as in RAW 264.7 macrophages (498). This could be further investigated by pre-treating PM with the antibiotic polymyxin B, to chelate LPS, reducing its activity (119). However, in the present study, levels of LPS in the ultrafine fraction were low (6.65 EU/mg), which compares well with other studies of underground PM LPS levels (Chapter 3), and thus it is unlikely that the LPS is responsible for the increased levels of HO-1 in these experiments. Indeed, the aforementioned work found marked increases in HO-1 expression only with LPS concentrations of at least 100 ng/ml (498). Conversely, using the LPS concentration of ultrafine underground railway PM from Chapter 3, and working on the basis that 1 EU = 0.1 ng LPS (499, 500) indicates that concentrations in the work presented here were approximately 16.6 pg/ml, almost four orders of magnitude lower. Furthermore, epithelial cells lack CD14 which is required for binding of LPS in order to activate TLR4 – unless cells either possess CD14 or there is soluble CD14 in the medium, such as from serum, LPS generally has little effect on epithelial cells (117). Alternatively, it is possible that in both cases the concentration of DFX required to maximally inhibit ROS generation was not used – in the experiments using DCF to measure ROS

generation, successive DFX concentrations were five-fold different from each other, and therefore greater inhibition may have been achieved by exploring the concentration-inhibition curve further.

Therefore, while PBECs grown at ALI did not respond to underground railway PM of any fraction in terms of IL-8 release or altered barrier permeability, an increase was seen in antioxidant gene expression induced by the ultrafine fraction of underground railway PM, and this increase was principally as a result of the iron content PM. This may indicate that the antioxidant defence mounted by the epithelial cells against the PM is, in the ALI cultures, sufficient to diminish the oxidative stress to a level below that at which pro-inflammatory effects would be seen. Alternatively, as suggested previously, it may be that inflammatory cytokines other than IL-8 show an increase after exposure of cells to PM. Indeed, it may be that the presence of mucus shifts the oxidative stress to a lower level than would be seen in the monolayers. Therefore, to better understand the interaction of underground railway PM with the ALI cultures of PBECs, healthy donor ALIs were incubated for 24 h in the presence of coarse, fine, or ultrafine PM, and subsequently fixed, embedded, and sectioned for viewing by TEM. The results here compare well with those seen in other studies, whereby PM was able to enter the cell and was found free in the cytosol, within lipid-bound vesicles and also in mitochondria. Importantly, there was no nuclear PM noted. Several studies have examined cellular uptake of particles, most often nanoparticles, although attempts to study uptake have yielded inconsistent results. A study of the uptake of carbon black and titanium dioxide nanoparticles by MRC5 fibroblasts and 16HBE epithelial cells showed that uptake is not necessarily PM concentration-dependent, and that uptake does not appear to be linked to cytotoxicity (223). Uptake of nanoparticles by Calu-3 and 16HBE epithelial cells was seen to be less than in A549 alveolar epithelial cells and LK004 fibroblasts (224), but a comparison of the uptake of titanium dioxide nanoparticles between A549 cells and NHBE cells found no difference after 2 h and 24 h incubation, although differences in uptake between different nanoparticle types were seen, and suggested to be related to the stability of nanoparticle agglomerates, with nanoparticles forming more stable agglomerates being less readily taken up (501). Furthermore, A549 cells have been seen to take up lead sulphate nanoparticles more readily than calcium sulphate or zinc sulphate nanoparticles, although the latter

resulted in the apparent presence of zincosomes in the cytoplasm (502). In the present study, PM was found free in the cytosol and in cytoplasmic membrane-bound vesicles, with one instance of PM within mitochondria noted, but all PM-containing cells appeared intact. Exposure of 16HBE cells to a similar concentration of DEP resulted in the presence of cytoplasmic phagosomes with a similar lack of overt damage in DEP-containing cells (308), while other studies have noted that intracellular PM is generally found in vesicles or free within the cytosol in 16HBE and A549 cells, and almost never in the nucleus (223, 298, 502, 503). However, there are isolated reports of PM being seen within mitochondria and the nucleus, such as copper oxide nanoparticles in A549 cells (504). It seems that much higher concentrations of PM, such as 100 $\mu g/cm^2$, are required to cause cell destruction by particle overload (503). The first step in particle uptake seems to be adsorption of the particle or particle agglomerate to the cell surface, causing morphological changes to the cell (298).

The mechanisms potentially involved in particle uptake have been reviewed thoroughly elsewhere (505). However, the major candidate mechanisms appear to be active (i.e. not diffusion) *via* phagocytosis/endocytosis or macropinocytosis (503, 504). Additionally, it has been suggested that vesicle-enveloped particles might be able to be excreted apically, at least in air-liquid interface cultures of NHBE cells repeatedly exposed to fine ambient PM (506). Once inside the cell, particles may induce oxidative stress and inflammation, both of which have been correlated with levels of particle uptake (214). Furthermore, particles of around 39 nm diameter or less (including protein corona) appear to have the potential to enter the nucleus *via* the nuclear pore complex, although this was not observed in the present study, nor in much of the published literature, perhaps due to the time taken for such a process to occur, or perhaps due to intrinsic properties of the particles making this unlikely (507). These smallest particles have also been observed as being able to enter the mitochondria in RAW 264.7 macrophages and BEAS-2B cells, causing mitochondrial damage and destruction which was not caused by coarse or fine PM from the same sources, sequestration of which was limited to cytoplasmic vacuoles (255). Mitochondrial damage by ultrafine particles and their constituents is generally focused on the electron transport chain, and may result in reduced mitochondrial membrane potential and increased ROS generation due to uncoupling of the electron transport chain (257). In

fact, mitochondrial damage and increased ROS may itself be a consequence of particulate-mediated ROS generation (508), since iron-rich underground railway PM_{10} from Stockholm was found to induce mitochondrial depolarisation to a lesser extent than DEP, but to a greater extent than roadwear or street PM_{10} (509). Another study found that copper (II) oxide nanoparticles caused greater mitochondrial membrane depolarisation than did micrometer particles of the same composition, which were nonetheless more damaging than haematite or magnetite nanoparticles (218). More in-depth investigation into the effects of ultrafine ambient PM on mitochondrial activity has suggested that increased mitochondrial calcium levels are seen alongside mitochondrial swelling and a rapid depolarisation of the mitochondrion. The resultant toxicity could be ameliorated with NAC, but this may be *via* effects on mitochondrial ROS, since NAC also reduced toxicity induced by cationic amide-coated polystyrene nanoparticles. Interestingly, this cationic surface coating endowed the polystyrene NPs, which were able to penetrate into mitochondria, with greater toxicity than the mitochondrial-impermeant carboxylated polystyrene nanoparticles, indicating a role for surface charge in effects on mitochondria (234). Such effects may not only apply to PM-exposed cells, but persist in the progeny of the exposed cell (256).

Particles may also cross the epithelial barrier by transcytosis, which may be more common for ultrafine and nanoparticles than coarse or fine PM (41, 212). However, in the present study, no particles were observed in the intercellular space, and nor were there any particles trapped between the basal side of the cells and the Transwell membrane, suggesting that there was negligible movement of particles in this manner. Since particle retention is considered to be more of a problem than the low level of particle translocation *via* the transcellular pathway (223), the effects of intracellular accumulation of underground railway PM, and particularly the metal-rich ultrafine fraction, require more work.

Validation that the particles observed intracellularly in such studies are not merely artefacts of contamination during the dehydration/embedding process, or from contamination of the section prior to viewing, is an important step sometimes missing from work in the literature, perhaps due to the lack of suitable equipment. Here, EDAX was used to assess the iron content of PM-like structures, confirming that of a

small sample of PM analysed, most contained iron, therefore suggesting that they were unlikely to be the result of contamination. However, although iron was the most predominant element in the underground railway PM used here, it nonetheless only accounted for 40.7%, 40.4% and 48.4% by mass of coarse, fine, and ultrafine fractions respectively. It is likely that a significant proportion of the underground railway PM is carbon based, and indeed a small number of particles observed within the cell had the appearance of carbon PM which has been noted previously (41, 510). However, the processing of resin-embedded sections involved the use of three contrast stains: uranyl acetate, osmium tetroxide and, prior to viewing, lead citrate. As such, EDAX of all sections showed peaks representing uranium, osmium, and lead, as well as copper, a major constituent of the grids upon which sections are mounted for viewing. These peaks can obscure peaks for other elements, especially if such elements are present in relatively small amounts, and therefore show smaller peaks. The contrast agents listed were used to produce good quality images of the ultrastructure of the cells, since the main aim of the TEM work was to identify whether any PM was able to enter the cells and, if so, where it was located in the ultrastructure of the cells. The omission of contrast agents at the electron microscopy processing stage would improve chemical speciation of the PM, but at the cost of reduced image quality, and therefore no such sections were produced.

4.4 Conclusion

In summary, these results indicate that coarse, fine, and ultrafine fractions of underground railway PM are able to induce a modest pro-inflammatory response from both primary bronchial epithelial cells, which may be ameliorated in the presence of mucus. Generation of ROS by underground railway PM is size-dependent, and is due mainly to the presence of iron in the particles. Although the epithelial barrier is not weakened by underground railway PM, it appears that the presence of the PM is detected by the cells since there is marked upregulation of antioxidant genes and also genes involved in the inflammatory response and Th2-type responses. The antioxidant response also seems to be due to the presence of iron within the PM. Furthermore, in spite of protection conferred by the mucous layer, PM is able to enter the epithelial cells and is found not only sequestered in membrane-bound vesicles but also free in the cytosol and in mitochondria.

Given the unusual iron rich nature of the ultrafine fraction, and its potency in generating ROS, further work is required to determine whether the ultrafine fraction in particular of underground railway PM has the potential to damage health.

5 The Effect of *Alternaria* on Bronchial Epithelial Cells

5.1 Introduction

Asthma is a chronic inflammatory airways disease characterised physiologically by airway hyperresponsiveness to innocuous stimuli, and pathologically by Th2 inflammation and structural remodelling of the airways. The majority of asthma is associated with atopy, where an IgE response to specific aeroallergens has developed. The airway epithelium which forms a physical barrier and an interface with the immune system *via* expression of adhesion molecules and secretion of a myriad cytokines, chemokines, and inflammatory mediators (3, 9, 511), is the first tissue encountered by such inhaled allergens. However, recent evidence has suggested that the asthmatic bronchial epithelium is structurally perturbed, resulting in impairment of barrier function (512).

Allergens from fungi including species of *Alternaria*, *Cladosporium*, and *Aspergillus* present a major risk factor for the development of asthma, with evidence supporting a link between sensitisation to fungi and prevalence or severity of asthma (130, 155), and also between spore prevalence and asthma (346, 513). Further reports have found links between sensitivity to the ubiquitous *Alternaria* species of fungi, particularly *Alternaria alternata*, and asthma (156, 158, 345, 346, 514). Unlike with pollens, exposure to fungi can occur year-round, and may occur both outdoors and indoors (156, 158). Interestingly, fungi including *Alternaria* and *Cladosporium* species have been found in the air of underground railway stations in London (515), Milan (516), St Petersburg (517),

and Cairo (518), and their levels have been found be greater in such stations than in the outside air (515). The airway epithelium is the first tissue encountered by such inhaled allergens. Pathogenic fungi secrete a range of proteases (138), and have been implicated in epithelial cell detachment and cytokine production (519). Proteases of the serine class have been particularly associated with asthma (520). *In vitro* studies have shown that serine proteases from *Aspergillus fumigatus* and *Alternaria alternata* induce production of IL-8 and IL-6 *via* NF-κB and NF-IL-6, as well as causing epithelial cell detachment (135, 136, 147). This action is reported to occur *via* activation of PAR-2 (143, 149), a receptor activated by proteolytic cleavage of a tethered-ligand, which has been observed to be upregulated in the bronchial epithelium of asthmatic subjects (521), and can be replicated by use of a synthetic PAR-2 activating peptide (148). Similar effects have been seen with the HDM serine and cysteine protease allergens Der p 1 and Der p 3 (149, 522), and also serine proteases from German cockroach extract (140). *Alternaria*-induced PAR-2 cleavage has also been suggested to be responsible for TSLP release from epithelial cells, and the activity of proteases as adjuvants in allergic sensitisation (142, 159, 523).

Aside from their activity towards PARs, proteases can also perturb the epithelial barrier by directly cleaving tight junction proteins, facilitating permeation of allergens and pathogens to the underlying tissue. Der p 1 can degrade occludin and trigger ZO-1 breakdown, resulting in tight junction disassembly and increased paracellular permeability (15, 151). Similar effects have also been seen with HDM serine proteases, although only at levels above those required to induce cytokine release, suggesting that inflammatory response is seen before TJ degradation occurs (152). The *Penicillium* allergen Pen ch 13, a serine protease, has been reported to cleave occludin (524), and effects on occludin, ZO-1, and claudin-1 have been noted with serine and cysteine proteases in pollen from a variety of sources (150).

Previous studies have focused on the use of epithelial cell lines which are not covered by a cytoprotective mucous layer that protects the airways *in vivo*, which may explain their susceptibility to the proteolytic effects of allergen-derived proteases. The additional observation that there is impaired epithelial barrier function in asthma (512) prompted investigation into the effect of *Alternaria* on epithelial barrier function, and

study of whether there is a differential response to *Alternaria* extract between fully differentiated cultures of primary human bronchial epithelial cells (PBECs) from healthy donors and those from asthmatic donors. As *Alternaria* has been observed to be both pro-inflammatory (147) and to induce development of a Th2-type response (451, 525), vectorial secretion of IL-8, TNFα, TSLP, IL-18 and IL-33 was also analysed.

The hypotheses to be tested within these experiments were:

1. *Alternaria* extract is able to induce inflammatory cytokine release and impair epithelial barrier function in polarised 16HBE cells.

2. This effect is due to protease activity within the extract.

3. Air-liquid interface cultures of primary bronchial epithelial cells from severely asthmatic donors are more susceptible to the effects of *Alternaria* extract than those cells from healthy donors.

4. Priming healthy primary bronchial epithelial cells with ultrafine underground railway particulate matter before exposure to *Alternaria* extract will make cultures more susceptible to the effects of *Alternaria*.

Therefore, the aims of this work were to study the effect of *Alternaria* extract on polarised 16HBE cells to confirm its effects on cytokine production and epithelial barrier disruption, and to extend this by studying mode of action. Further work was aimed at studying the interaction of asthma status and exposure to ultrafine underground railway PM on responses in primary bronchial epithelial cell ALI cultures.

The work presented within this Chapter, with the exception of that examining the interaction between ultrafine underground railway PM and *Alternaria*, has been published in the journal PLOS ONE (526).

5.2 Results – The Effects of *Alternaria* on 16HBE Cells

5.2.1 The Effect of *Alternaria* on the Release of Pro-Inflammatory Cytokines by 16HBE Cells

Since *Alternaria* extract is a complex biological substance, initial experiments aimed to characterise its effects on 16HBE cells and compare these to published data. Polarised 16HBE cells were challenged with *Alternaria* extract, and inflammatory mediator release after 24 h was measured by ELISA. *Alternaria* induced a concentration-dependent increase in apical IL-8 release (Figure 5.1), with 100 μg/ml *Alternaria* extract (Alt100) stimulating a release of 5900±1100 pg/ml, compared to 2300±340 pg/ml for control ($p<0.001$). IL-8 release in the presence of Alt100 was also significantly higher than that stimulated by 100 μg/ml heat-treated *Alternaria* extract (Alt100HT) ($p<0.001$), and 100 μg/ml *Cladosporium* extract (Clad100) ($p<0.001$). While Alt100 induced a significant increase in basolateral IL-8 release of 6300±700 pg/ml compared to control of 4500±590 pg/ml ($p<0.001$), this was less marked than apical release. Clad100 did not increase basolateral IL-8 release above baseline, and heat treatment of the *Alternaria* extract reduced the capacity of *Alternaria* to elicit IL-8 release, to 1700±300 pg/ml apically ($p<0.001$ *vs.* Alt100), whereas there was no significant effect on basolateral IL-8 secretion.

Analysis of TNFα release after *Alternaria* challenge revealed similar results to IL-8 analysis (Figure 5.2). *Alternaria* induced a concentration-dependent increase in TNFα release into the apical compartment, from 850±90 pg/ml in control to 1800±140 pg/ml after challenge with Alt100 ($p<0.001$), an increase of similar magnitude to that seen for IL-8. Again, this increase was abolished by prior heat-treatment of the *Alternaria* ($p<0.001$), and was significantly higher than induced by Clad100 (950±130 pg/ml; $p<0.001$). Basolaterally, Alt100 resulted in increased TNFα release, of a lesser magnitude than apically (960±40 pg/ml *vs.* 730±70 pg/ml for control; $p<0.01$). As with IL-8, the reduction in TNFα release seen when *Alternaria* was heat-treated did not

reach significance in the basolateral compartment, perhaps due to the lesser degree of *Alternaria*-stimulated release of TNFα into this compartment in general.

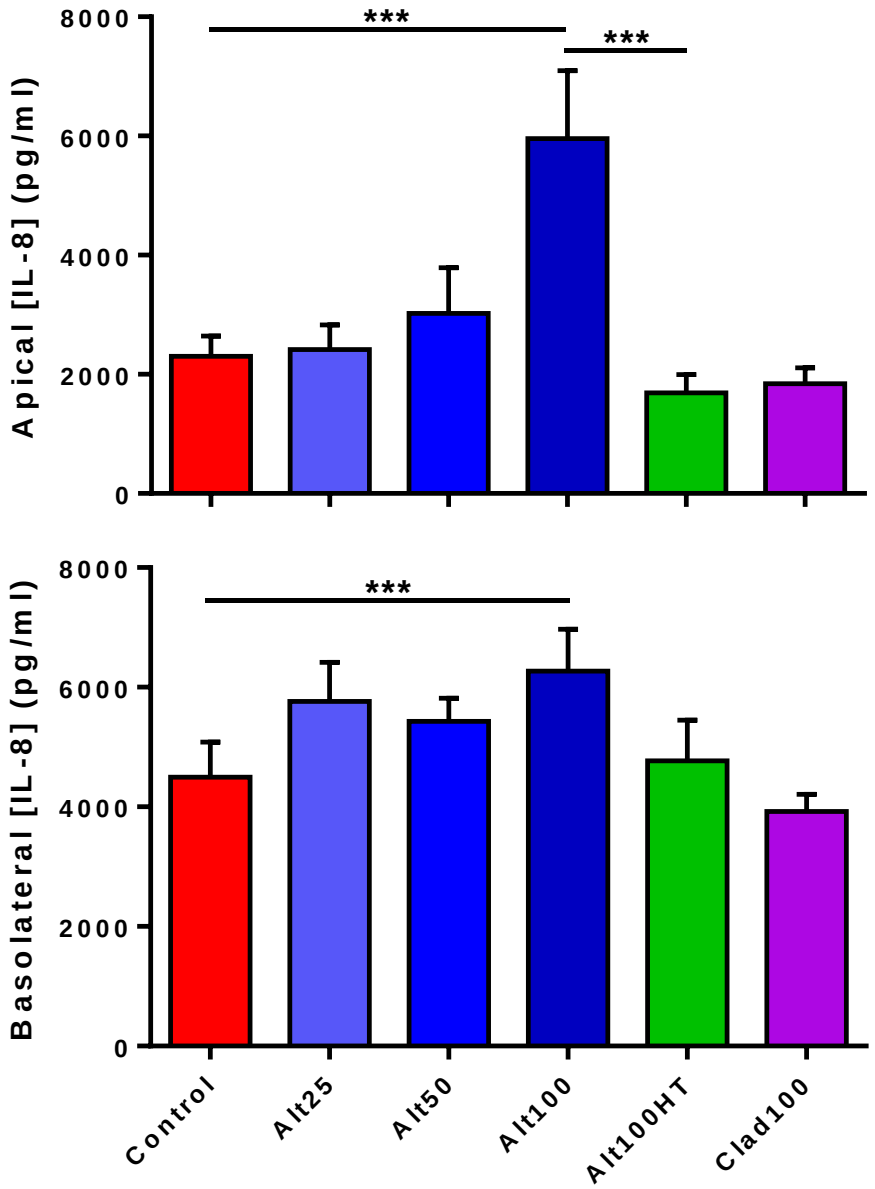

Figure 5.1. The effect of *Alternaria* extract on IL-8 release from polarised 16HBE cells. Polarised 16HBE cells on Transwells were challenged apically with varying concentrations of *Alternaria* (Alt) or *Cladosporium* (Clad) fungal extracts, or heat-treated *Alternaria* extract (HT). Apical and basolateral supernatants were harvested 24 h post-challenge. IL-8 concentration was determined by ELISA. Analysis by one way repeated measures ANOVA with Bonferroni correction for pairwise analysis. Bars represent mean±SEM; *** - P<0.001; n=4-9

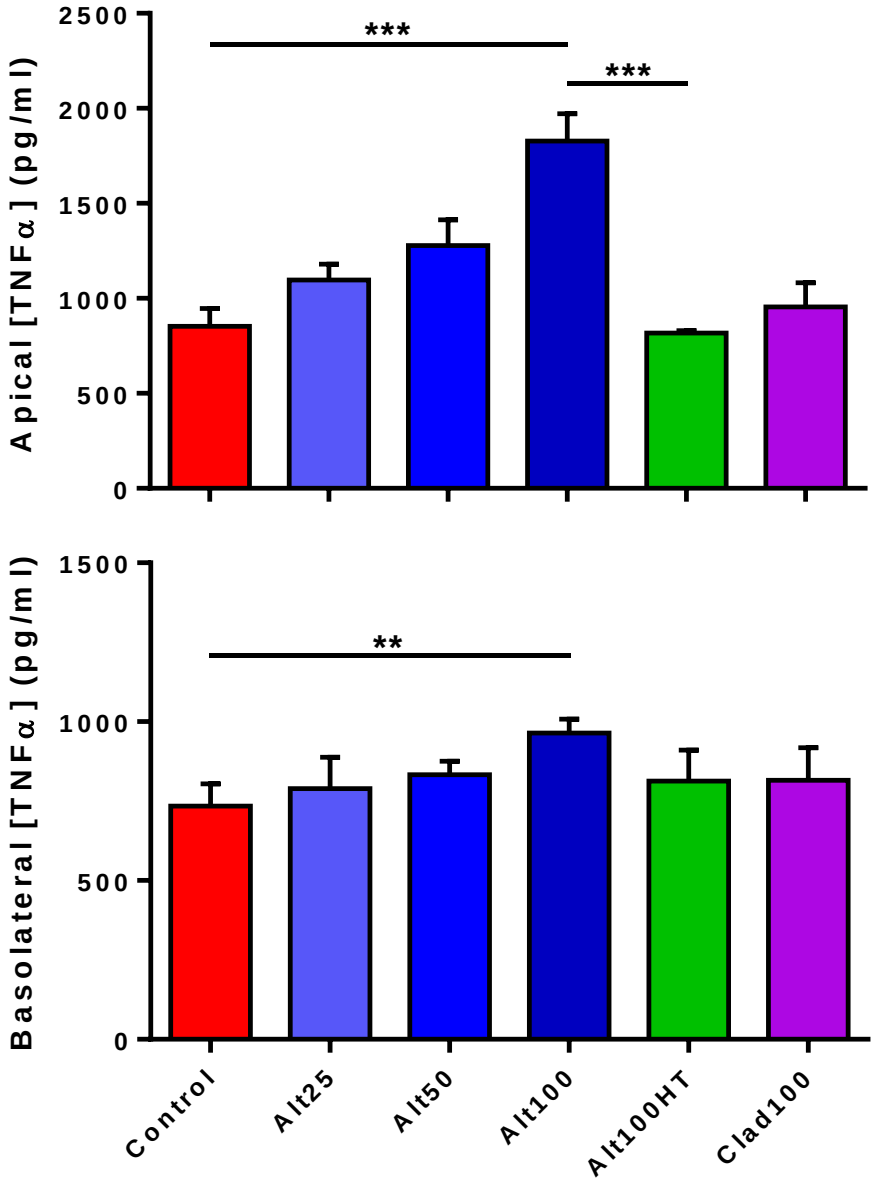

Figure 5.2. The effect of *Alternaria* on TNFα release from polarised 16HBE cells.

Polarised 16HBE cells on Transwells were challenged apically with *Alternaria* (Alt) or *Cladosporium* (Clad) fungal extracts as for Figure 5.1. Apical and basolateral supernatants were harvested 24 h post-challenge. TNFα concentration was determined by ELISA. Analysis as for Figure 5.2. Bars represent mean±SEM; ** - $p<0.01$, *** - $p<0.001$; n=3-9.

5.2.2 The Effect of *Alternaria* on 16HBE TER

Having observed the effects of *Alternaria* on the induction of cytokine release, the effect of *Alternaria* on epithelial permeability was investigated by measuring changes in TER, indicative of alterations in ionic permeability of the epithelium. A significant concentration-dependent decrease in TER was observed 1 h after challenge, with drops of 51±8% and 74±4% for 50 μg/ml (Alt50) and 100 μg/ml (Alt100) respectively (Figure 5.3). With Alt50, the drop in TER began to reseal almost immediately, particularly from 3 h onwards, reaching control levels by 6 h (Figure 5.3). After challenge with Alt100, the TER remained significantly lower than control even 24 h post-challenge (Figure 5.3). As found with cytokine release, Alt100HT showed no significant effect on TER at any time point. Similarly, Clad100 did not affect TER. This concentration-dependent, heat-labile increase in epithelial permeability was confirmed by studies with FITC-labelled 4 kDa dextran, suggesting that *Alternaria* affects both ionic and macromolecular permeability; however the extent to which passage of the 4 kDa macromolecule was facilitated by exposure of the epithelium to *Alternaria* was small compared to the effect of the calcium chelator EGTA (50 μM) (Figure 5.4). None of the challenges induced significant LDH release compared with control cultures (data not shown).

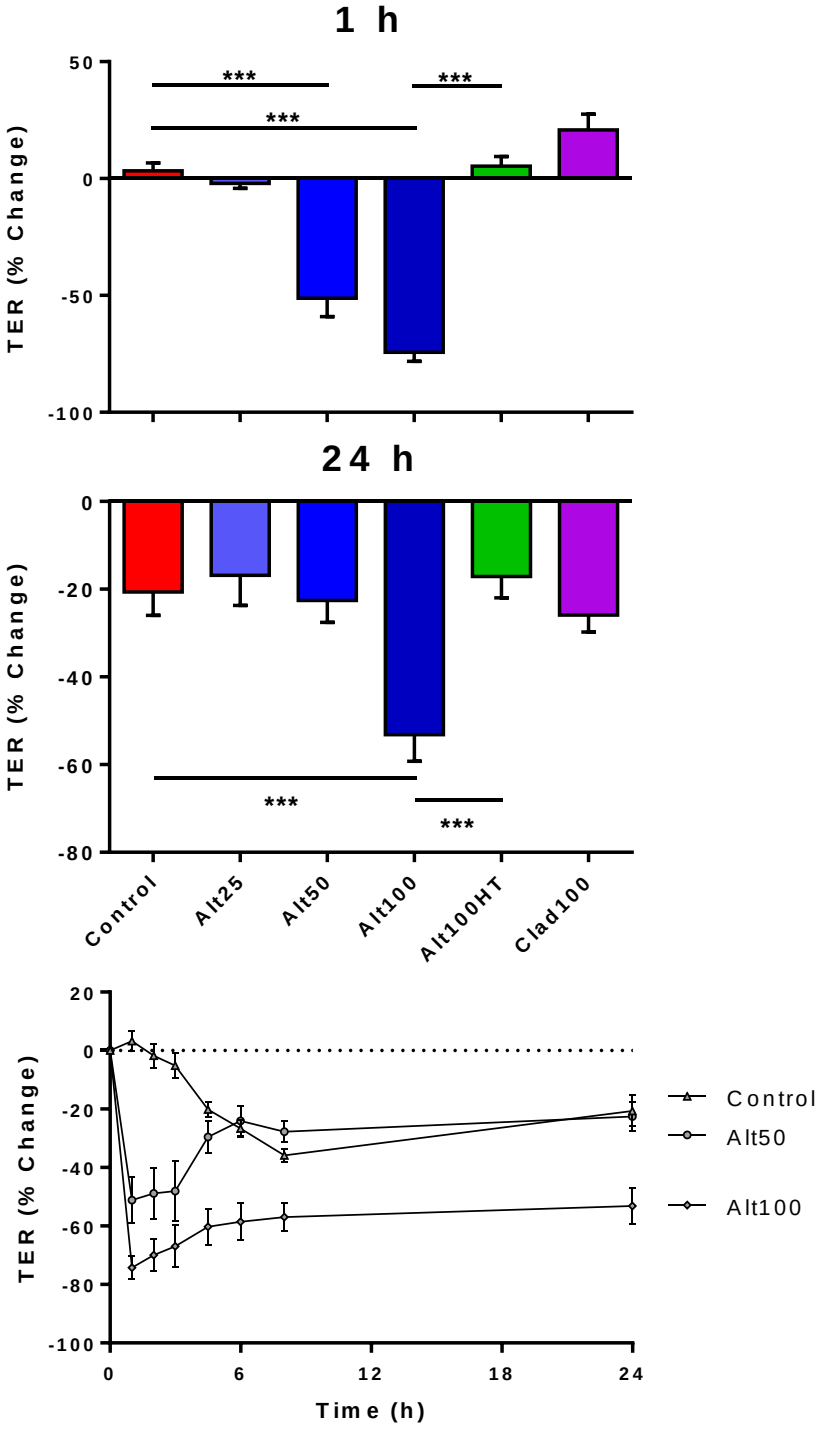

Figure 5.3. The effect of *Alternaria* on TER in polarised 16HBE cells.

Polarised 16HBE cells on Transwells were challenged apically with varying concentrations of *Alternaria* (Alt) or *Cladosporium* (Clad) fungal extracts, or heat-treated *Alternaria* extract (HT). TER was measured before challenge and at regular intervals thereafter. Analysis as for Figure 5.1. Bars and points represent mean±SEM; *** - P<0.001; n=4-15

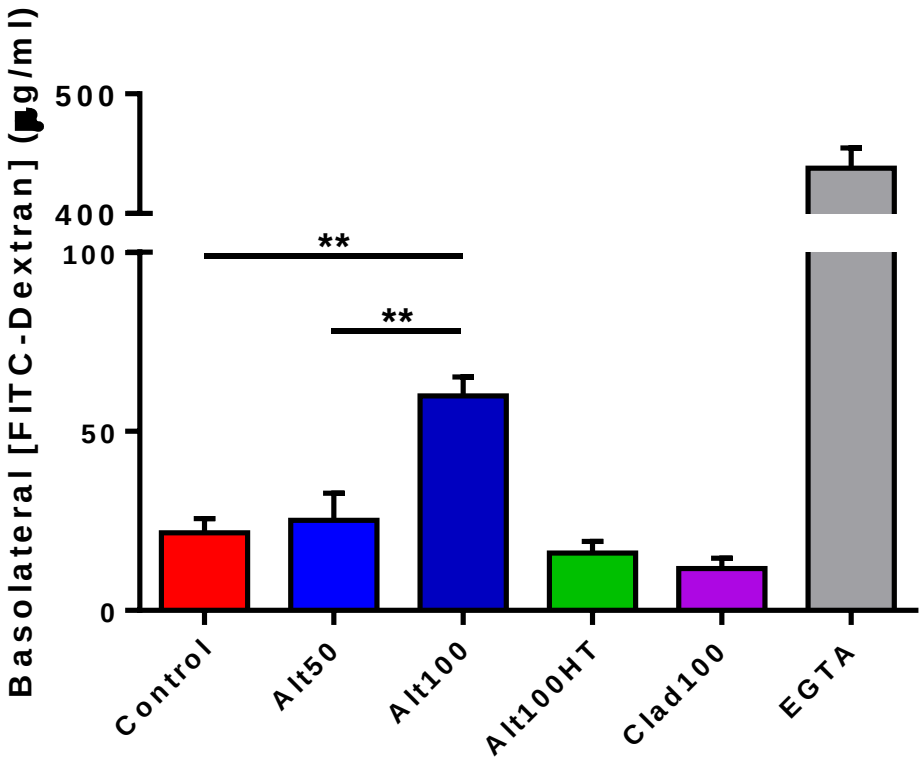

Figure 5.4. The effect of *Alternaria* extract on epithelial macromolecular permeability. Polarised 16HBE cells on Transwell inserts were challenged with *Alternaria* or *Cladosporium* extracts or 50 μM EGTA 1 h before addition of 2 mg/ml 4 kDa FITC-dextran. After 24 h challenge, basolateral FITC-dextran concentration was determined fluorimetrically against a standard curve. Analysis as for Figure 5.1. Bars represent mean±SEM; ** - $p<0.01$; n=4.

5.2.3 Protease Activity of *Alternaria* Extract

To determine the type(s) of protease activity in *Alternaria* extract, a fluorescent protease assay was performed in the presence of a variety of protease inhibitors (Figure 5.5). The serine protease inhibitor AEBSF reduced the protease activity of *Alternaria* extract to 32±6% of the uninhibited *Alternaria* ($p<0.001$). Pepstatin A had only a small effect on the protease activity of *Alternaria*, reducing it to 79±8% (p=non-significant) of that seen when *Alternaria* was incubated with the same concentration of Pepstatin A diluent (10% glacial acetic acid in methanol). The cysteine protease inhibitor E-64 had no effect on *Alternaria* protease activity, with E-64-treated *Alternaria* having 107±10% of the activity of untreated *Alternaria*. Heat-treatment of the

Alternaria extract reduced protease activity to below the detection limit of the assay. No inhibitor possessed intrinsic proteolytic activity.

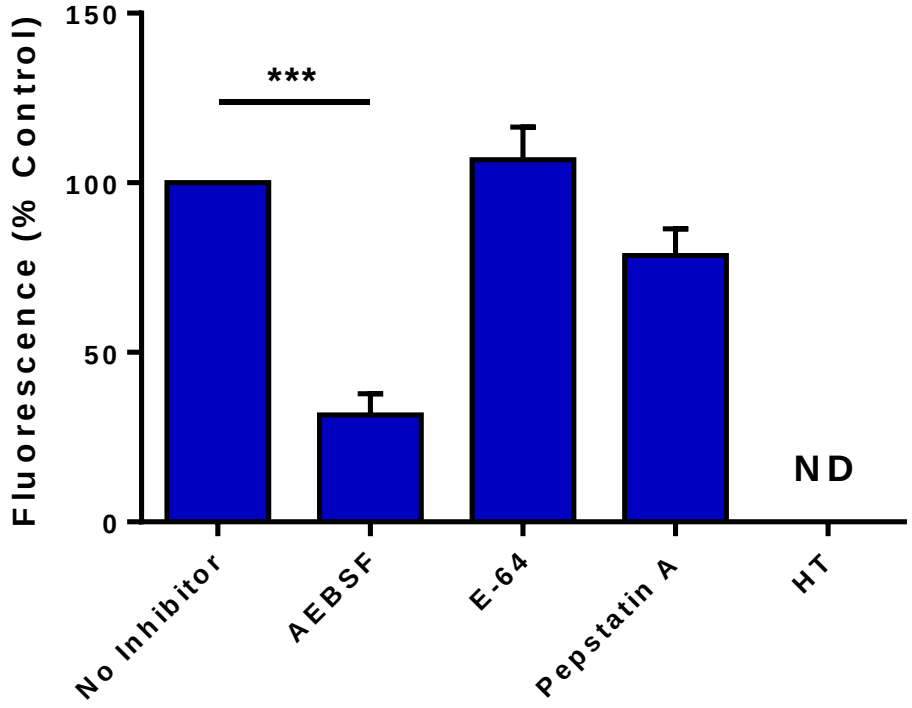

Figure 5.5. Protease activity of *Alternaria* extract.

FITC-labelled casein was incubated with *Alternaria* extract (500 µg/ml) alone or in the presence of either AEBSF (2.5 mM), E-64 (500 µM), Pepstatin A (5 µg/ml) or heat-treated. Soluble fluorescence was measured after 24 h, relative to a trypsin standard. Protease activity of 100 µg/ml *Alternaria* was equivalent to 6.7±2.5 µg/ml trypsin; for comparison, *Cladosporium* protease activity was equivalent to 3.3±0.0 µg/ml trypsin. Analysis as for Figure 5.1. Bars represent mean fluorescence relative to inhibitor-free control±SEM; *** - $p<0.001$; n=4 separate experiments, assayed in duplicate.

5.2.4 The Effect of Protease Inhibitors on Pro-Inflammatory Cytokine Release Elicited by *Alternaria*

To examine whether proteases contributed to the effect of *Alternaria* on epithelial cell cytokine release, Alt100 was pre-incubated with protease inhibitors prior to challenge of the epithelial cultures; control cultures were tested in the presence of inhibitor alone. Inhibition of cytokine release was calculated by subtracting the cytokine release

in the presence of inhibitor alone from the cytokine release in the presence of *Alternaria* and inhibitor together, and dividing this value by the cytokine release in the presence of *Alternaria* alone, after similar subtraction of the *Alternaria*- and inhibitor-free cytokine concentration. This value was then expressed as a percentage. Apical release of IL-8 in response to Alt100 was not significantly affected by any of the protease inhibitors; in contrast both AEBSF and Pepstatin A significantly reduced basolateral IL-8 release, to -3±54% and 4±17% of uninhibited levels ($p<0.05$ for both) (Figure 5.6). In addition, the effect of a p38 MAPK inhibitor was investigated, as this has previously been shown to inhibit pollen-induced apical IL-8 release, without affecting transcription (527). This inhibitor, SB203580, significantly reduced apical IL-8 release to 34±10% of the uninhibited level without affecting basolateral release (Figure 5.6).

Apical release of TNFα elicited by Alt100 was not significantly affected by any of the inhibitors tested, although the degree of inhibition was greatest with E-64 and SB203580, at 57±14% and 54±27% of uninhibited release respectively. While basolateral release was also not significantly affected by any of the inhibitors, both AEBSF and Pepstatin A tended towards significant inhibition at 10±77% and 28±12% of uninhibited release respectively, as had been seen previously for IL-8 release (Figure 5.7). The large error for the AEBSF-treated *Alternaria*-induced basolateral TNFα release is due to one outlier. If this outlier is removed, the mean value becomes higher, at 86%.

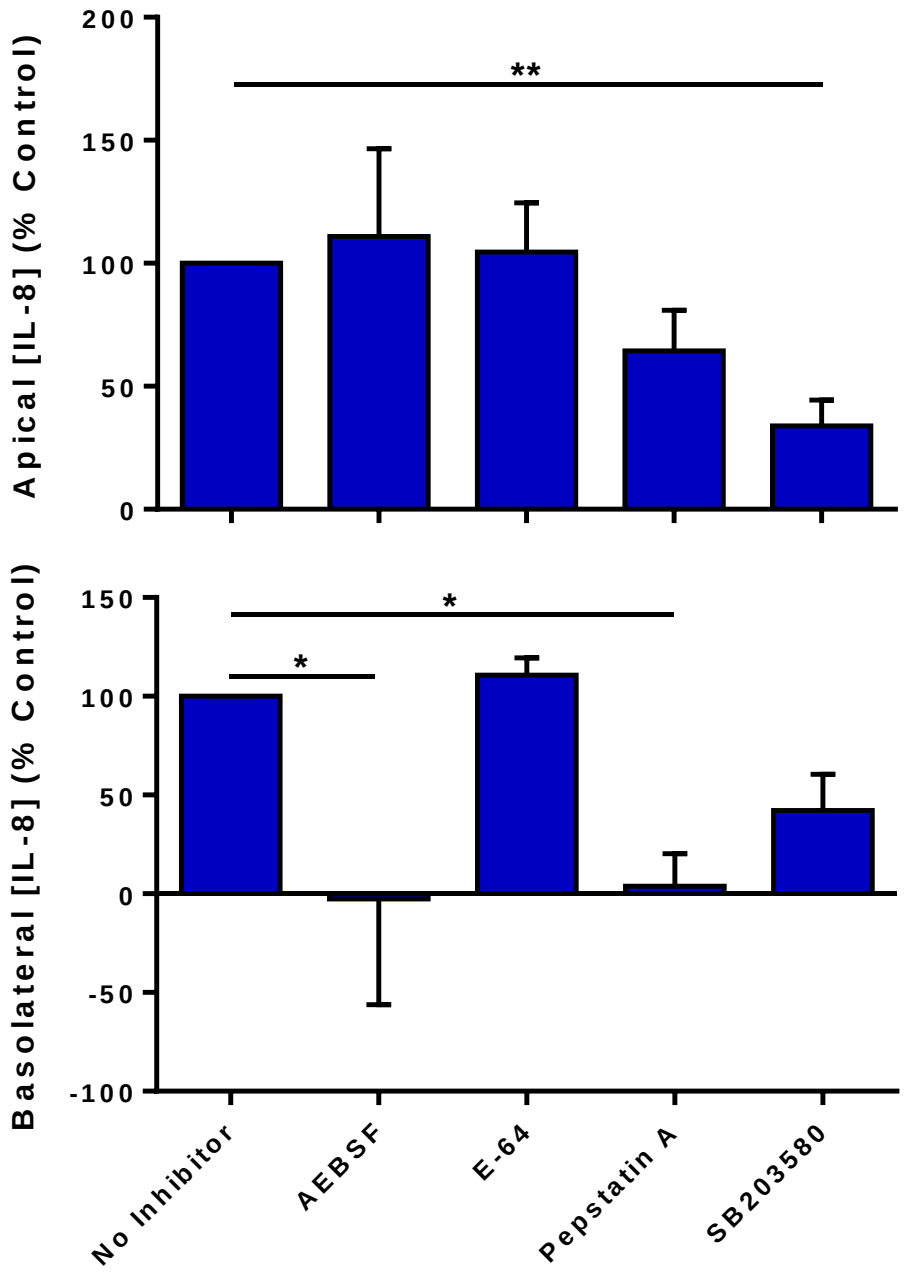

Figure 5.6. Inhibition of *Alternaria*-induced IL-8 release by protease and p38 MAPK inhibitors. The effect of *Alternaria* extract (100 µg/ml) on 16HBE cells was tested alone or in the presence of AEBSF (250 µM), E-64 (50 µM), Pepstatin A (0.5 µg/ml) or SB203580 (25 µM). IL-8 release 24 h post-challenge was calculated as "Release (% control) = ((Alt_{INHIB} – No Alt_{INHIB}) / ($Alt_{NO\ INHIB}$ – No $Alt_{NO\ INHIB}$) x 100", to correct for any effect of the inhibitors on baseline IL-8 release without *Alternaria*. Analysis as for Figure 5.1. Bars represent mean±SEM; * - $p<0.05$, ** - $p<0.01$; n=3-8.

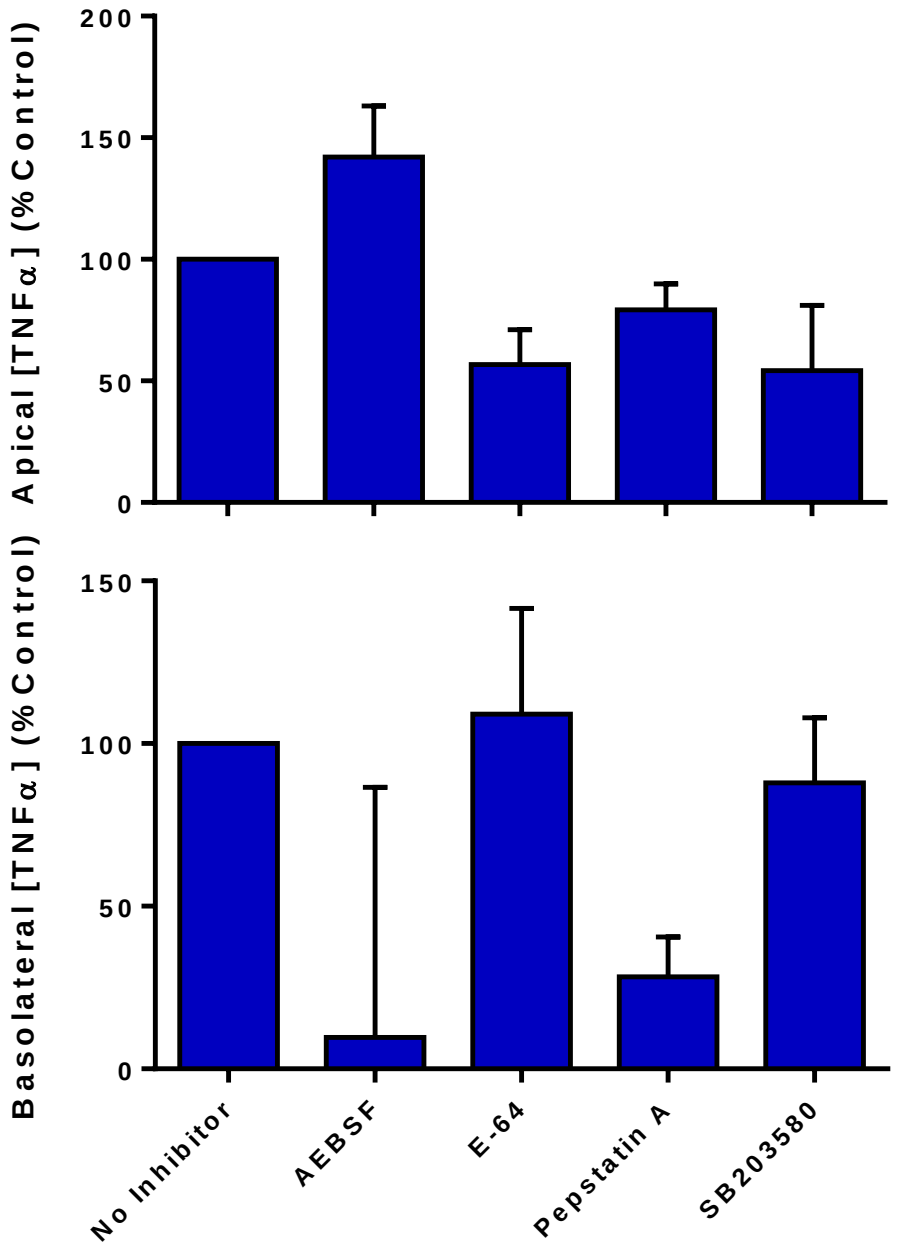

Figure 5.7. Inhibition of *Alternaria*-induced TNFα release by protease and p38 MAPK inhibitors. The effect of *Alternaria* extract (100 µg/ml) on 16HBE cells was tested alone or in the presence of AEBSF (250 µM), E-64 (50 µM), Pepstatin A (0.5 µg/ml) or SB203580 (25 µM). TNFα release 24 h post-challenge was calculated as "Release (% control) = ((Alt_{INHIB} – No Alt_{INHIB}) / ($Alt_{NO\ INHIB}$ – No $Alt_{NO\ INHIB}$) x 100", to correct for any effect of the inhibitors on baseline IL-8 release without *Alternaria*. Analysis as for Figure 5.1. Bars represent mean±SEM; * - $p<0.05$, ** - $p<0.01$; n=3-8.

5.2.5 The Effect of Protease Inhibitors on the Permeabilising Activity of *Alternaria*

To explore further the effect of protease inhibition, TER changes were investigated using Alt100 pre-treated with the same inhibitors (Figure 5.8) At 1 h post-challenge, a 72±9% drop in TER with *Alternaria* was ameliorated to a 55±4% drop in the presence of E-64 ($p<0.01$). AEBSF and Pepstatin A did not significantly inhibit the ability of *Alternaria* to induce a drop in TER after 1 h exposure. At 24 h post-challenge, while inter-treatment differences approached significance, the significance threshold was not crossed. However, there was a notable attenuation of the effect of *Alternaria* on TER from 21±8% drop in TER with *Alternaria* alone to 3±3% with AEBSF and 7±5% with Pepstatin A.

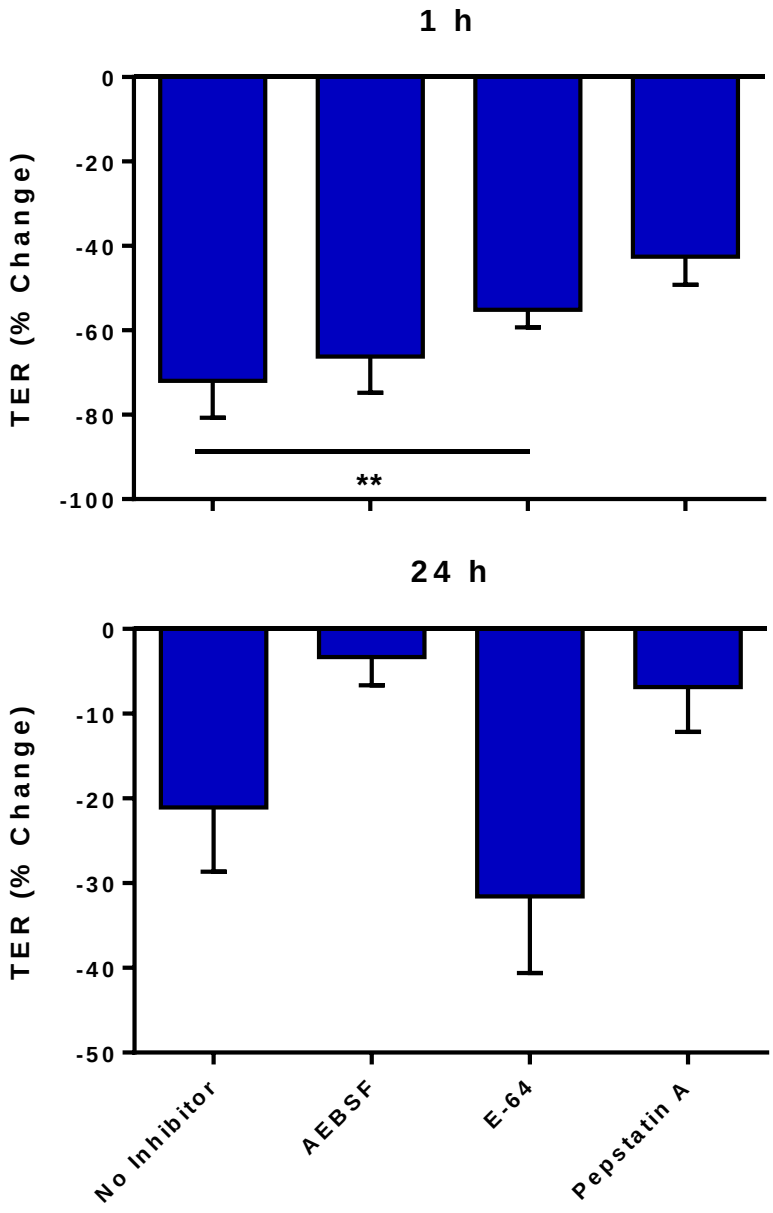

Figure 5.8. Inhibition of *Alternaria*-induced epithelial leakiness by protease inhibitors.
The effect of *Alternaria* extract (100 µg/ml) on 16HBE cells was tested alone or in the presence of AEBSF (250 µM), E-64 (50 µM), or Pepstatin A (0.5 µg/ml). TER was measured at 1 h and 24 h post-challenge, calculated as percentage change from pre-challenge, and corrected for any effect of the inhibitor alone by subtracting the percentage change in TER in the absence of *Alternaria* from the percentage change in TER in the presence of *Alternaria*, with each respective inhibitor or inhibitor-free condition. Analysis as for Figure 5.1. Bars represent mean±SEM; ** - $p<0.01$; n=3-6.

5.3 Results – The Effects of *Alternaria* on PBEC ALI Cultures

5.3.1 The Effect of *Alternaria* on Pro-Inflammatory Cytokine Release in PBEC ALI Cultures

Having observed the significant inflammogenic and barrier-modulating properties of *Alternaria* using the 16HBE cell line, experiments were performed using primary bronchial epithelial cells grown and differentiated at an air-liquid interface (ALI), since this is a more accurate representation of the airway epithelium. Preliminary studies showed that higher concentrations of *Alternaria* were required to elicit responses in ALI cultures compared to 16HBE, and therefore concentrations of 25, 100, and 400 μg/ml were used, along with 400 μg/ml heat-treated *Alternaria* (Alt400HT) and *Cladosporium* (Clad400).

In ALI cultures from healthy donors, the highest dose of *Alternaria* (Alt400) significantly induced an approximate doubling of IL-8 release apically versus heat-treated *Alternaria*, at 3400 pg/ml (IQR 1700-7600 pg/ml) compared to 1500 pg/ml (IQR 1100-2400 pg/ml) respectively (Figure 5.9). *Alternaria* also tended to cause a concentration-dependent increase in the basolateral release of IL-8, significant for Alt400 with IL-8 levels eight-fold higher than control (5200 pg/ml (IQR 3700-7700 pg/ml) *vs.* 650 pg/ml (IQR 520-1700 pg/ml). *Cladosporium* extract had no significant effect on IL-8 release. Thus, in a reversal of what was seen in 16HBE cells, basolateral IL-8 release appeared to be more responsive to *Alternaria* than was apical IL-8 release (Figure 5.10), with all donors showing increased basolateral IL-8, although the degree of inter-donor variability makes it difficult to draw robust conclusions regarding this directionality. When the same experiments were performed in ALI cultures of severely asthmatic donor PBECs, none of the challenges elicited a significant increase in release of IL-8 into either compartment (Figure 5.9). TNFα levels were generally below the lower detection limit of the high-sensitivity ELISA kit (0.5 pg/ml).

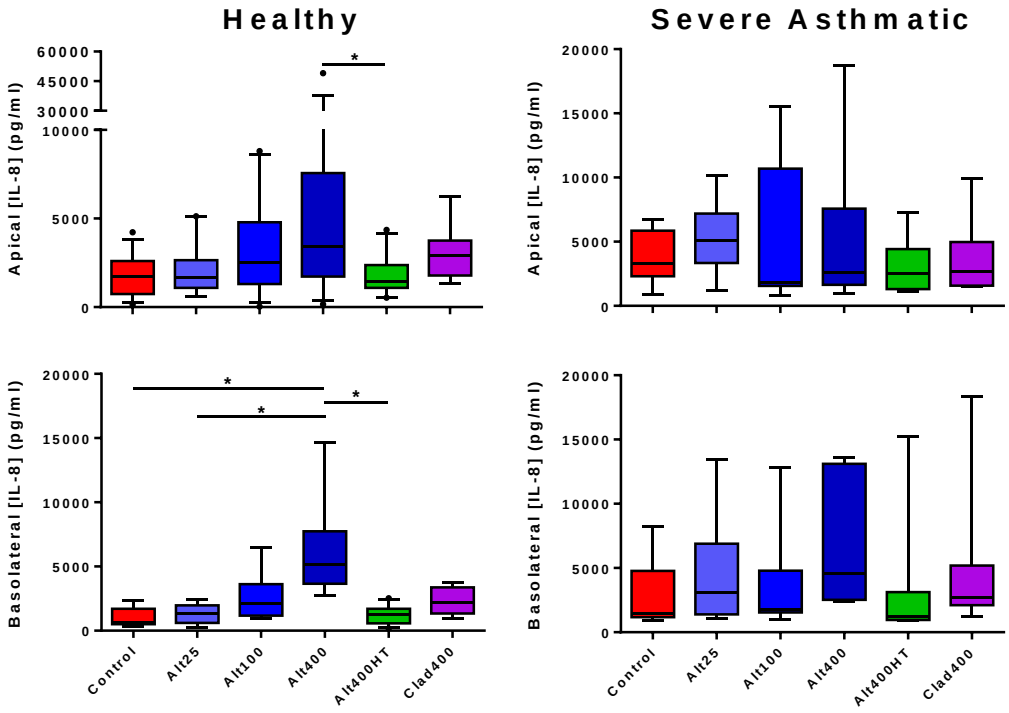

Figure 5.9. Differences in *Alternaria*-induced IL-8 release between healthy and severely asthmatic donor ALI cultures.

ALI cultures from healthy (n=8-12) or severely asthmatic (n=6-7) donors were differentiated at air-liquid interface, prior to challenge with *Alternaria* (Alt) or *Cladosporium* (Clad) fungal extracts. IL-8 release 24 h post-challenge was determined by ELISA. Box shows median and 25th/75th percentiles, whiskers show 10th/90th percentiles. Analysis by Friedman test with Tukey's correction for pairwise analysis; * - $p<0.05$.

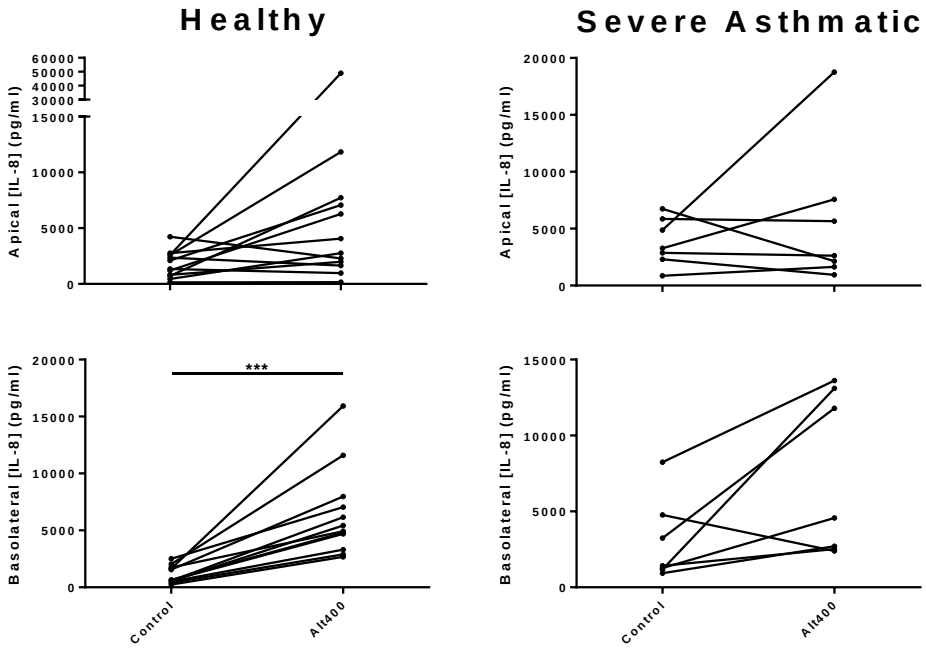

Figure 5.10. The differing effects of *Alternaria* on apical and basolateral IL-8 release in ALI cultures.

ALI cultures were treated as for Figure 5.1. IL-8 release 24 h post-challenge was determined by ELISA. Lines represent difference in individual donor cultures between control and Alt400-stimulated IL-8 release. Analysis by Wilcoxon Matched Pair test; *** - $p<0.001$.

Given the previous association of *Alternaria* with development of a Th2 phenotype (451, 525, 528), further analysis was performed to determine the release of IL-18, IL-33, and TSLP by ALI cultures after exposure to *Alternaria*. Using commercially available ELISA kits, these cytokines were undetectable (see Table 2.2 for lower limits of detection) in either apical or basolateral supernatants across all groups. However, using an "in-house" TSLP ELISA developed by Novartis Plc., basolateral TSLP was detectable but there was no significant difference in TSLP secretion comparing untreated or *Alternaria*-stimulated ALI cultures from either healthy or severely asthmatic donors (Figure 5.11) . No apical secretion of TSLP was detectable.

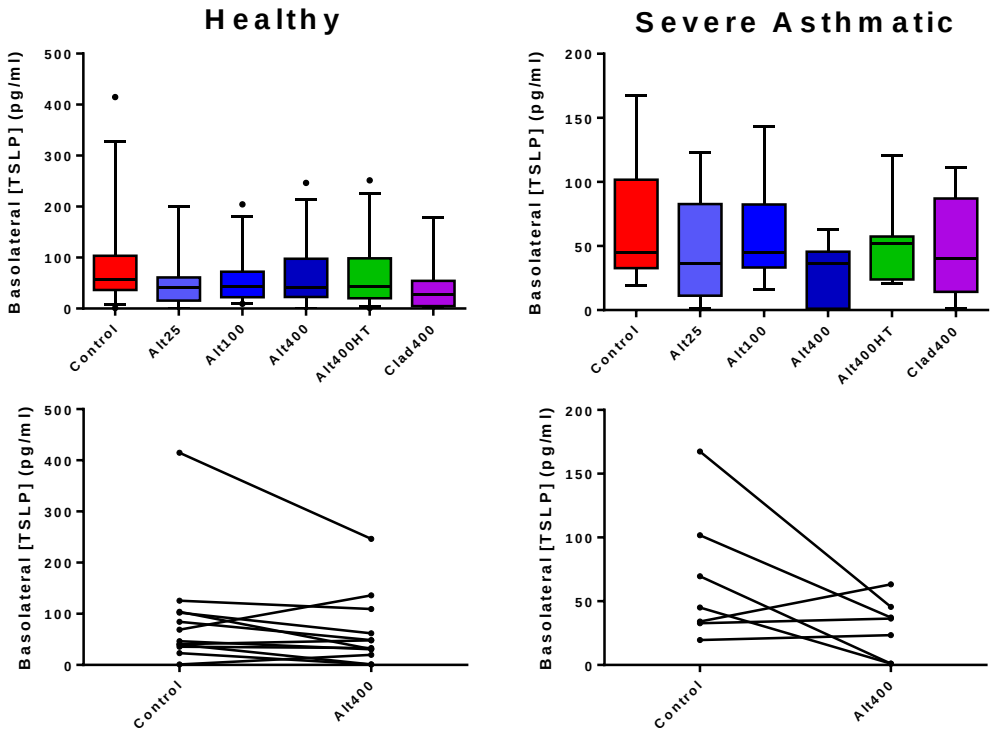

Figure 5.11. Differences in *Alternaria*-induced TSLP release between healthy and severely asthmatic donor ALI cultures.

ALI cultures were treated as for Figure 5.9. TSLP 24 h post-challenge was determined by ELISA. Top: Box shows median and 25th/75th percentiles, whiskers show 10th/90th percentiles. Bottom: Lines represent difference in individual donor cultures between control and Alt400-stimulated TSLP release.

5.3.2 The Effect of *Alternaria* on ALI Culture Transepithelial Electrical Resistance

In ALI cultures from healthy donors, *Alternaria* had a significant effect on TER after 3 h (Figure 5.12). By 24 h, TERs in the healthy donor ALIs were all increased to 8-14% of their baseline levels, with no difference between challenges. In contrast, cultures derived from severely asthmatic donors responded to *Alternaria* challenge with a rapid dose-dependent decrease in TER of 24±7% at 3 h ($p<0.01$ *vs.* control) compared to control (8±4%) and heat-treated *Alternaria* (5±6%, $p<0.05$ *vs.* Alt400HT). By 24 h post-challenge, no difference existed between treatments. These results suggest that,

unlike ALI cultures from healthy donors, asthmatic donor ALI cultures are susceptible to a rapid loss of epithelial barrier function after exposure to *Alternaria*. The heat lability of this effect suggests that it is protease-mediated.

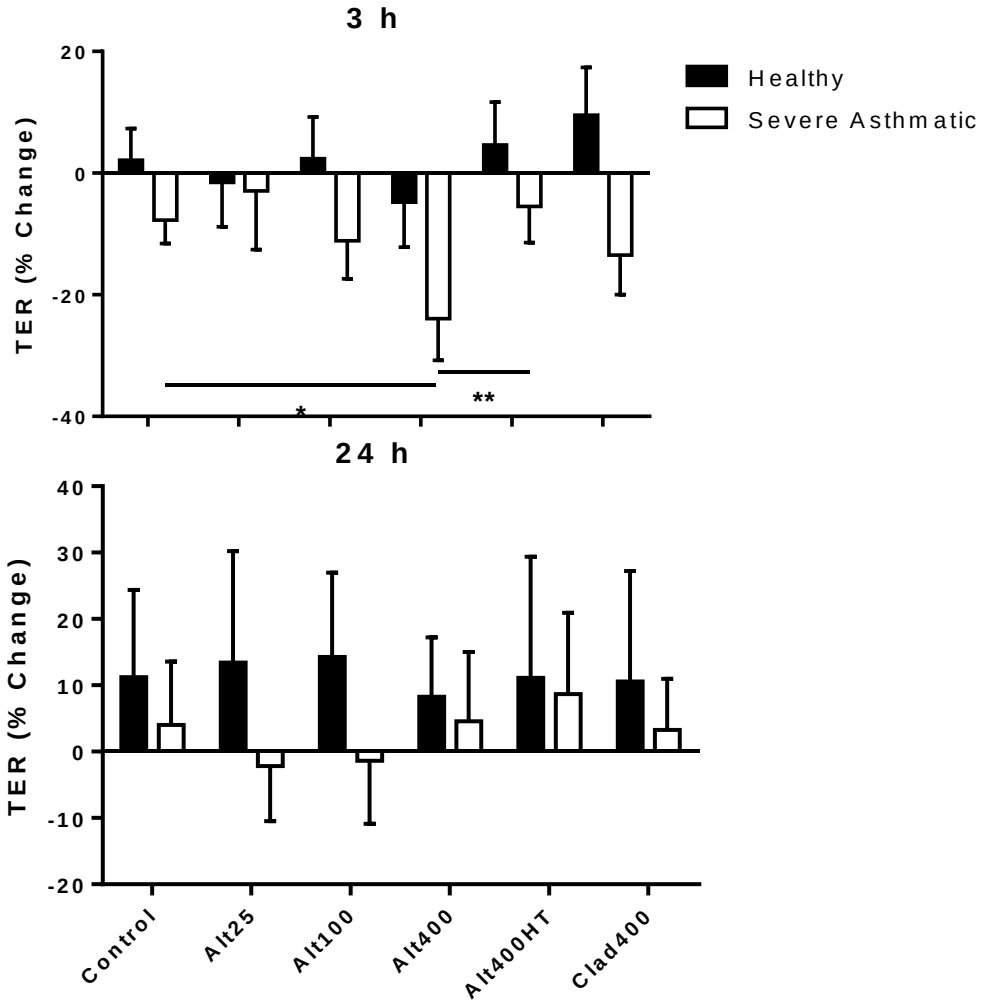

Figure 5.12. Differences in *Alternaria*-induced epithelial leakiness between healthy and severely asthmatic donor ALI cultures.

Healthy (n=7-9) and severely asthmatic (n=6-7) donor ALI cultures were treated as for Figure 5.9. TER was measured pre-challenge and at 4 h and 24 h post-challenge. Results are expressed as percentage change in TER relative to pre-challenge readings and are shown as mean±SEM. Analysis as for Figure 5.1. * - $p<0.05$, ** - $p<0.01$.

5.4 Results – The Effects of Pre-Treatment with Underground Railway PM on Responses to *Alternaria*

5.4.1 The Effect of Pre-Treatment with Underground Railway PM on *Alternaria*-Induced IL-8 Release

Previous results have shown that ultrafine underground railway particulate matter is rich in transition metals, especially iron, allowing it to generate ROS and induce oxidative stress (Chapter 4). The results within the present chapter suggest that *Alternaria* extract can induce pro-inflammatory changes in ALI cultures of PBECs from healthy donors. Since *Alternaria* fungus has been found in several underground railway systems, the effect of the two in combination was studied by pre-treating healthy donor ALI cultures with either 5.6 μg/cm^2 ultrafine underground railway PM or a PBS-supplemented control for 24 h, removing this, and then challenging with either BEBM, 400 μg/ml *Alternaria* extract, or 400 μg/ml heat-treated *Alternaria* extract.

As seen in previous experiments, *Alternaria* extract induced a marked increase in IL-8 release (Figure 5.13). Apically, release increased from 2200 pg/ml (IQR 1000-5400 pg/ml) with BEBM to 5400 pg/ml (IQR 5000-9600 pg/ml) with Alt400 in cells not primed with ultrafine underground railway PM, and from 2600 pg/ml (IQR 2500-6100 pg/ml) to 5900 pg/ml (IQR 3700-10000 pg/ml) in cells subjected to the ultrafine PM pre-treatment. Importantly, for cells treated with either BEBM or Alt400, there was very little difference in response between those pre-treated with ultrafine PM and those not. As expected, apical release of IL-8 after exposure to Alt400HT was similar to control levels in cells not pre-treated with ultrafine PM. In pre-treated cells, there was an IL-8 concentration intermediate between control and Alt400-treated cultures, although this was due to one sample only – the other two sets of cells showed little difference.

As with previous results, the basolateral release of IL-8 was more responsive to *Alternaria* than was the apical release. In cells not pre-treated with ultrafine PM, IL-8 rose from 1100 pg/ml (IQR 670-2600 pg/ml) to 7200 pg/ml (IQR 5400-10000 pg/ml) while in those cells pre-treated with ultrafine PM, the rise was from 1300 pg/ml (620-2800 pg/ml) in control cells to 7700 pg/ml (IQR 5300-9000 pg/ml) in those challenged with Alt400. As for apical release, there was little effect of pre-treatment with ultrafine underground railway PM and, as expected, heat-treated *Alternaria* had little effect over control regardless of PM pre-treatment.

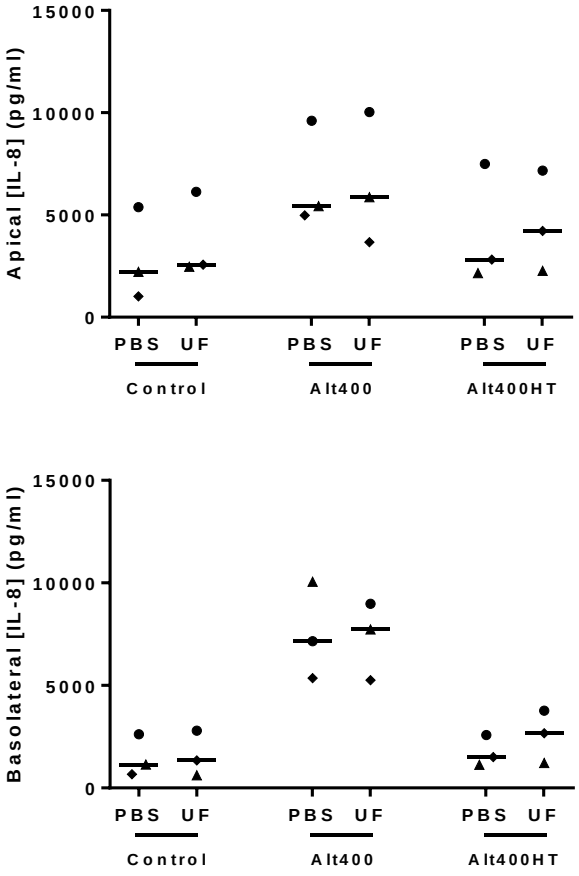

Figure 5.13. The effect of ultrafine PM on IL-8 release with *Alternaria*.

ALI cultures from healthy donors were pre-treated with either 5.6 µg/cm^2 ultrafine underground railway PM or PBS-supplemented BEBM as control. After 24 h, apical medium was removed, basolateral medium replaced, and cells were challenged with *Alternaria* as for Figure 5.9. Points represent IL-8 concentrations for each donor, with different symbols representing different donors. Line represents median IL-8 release. n=3.

5.4.2 The Effect of Pre-Treatment with Underground Railway PM on *Alternaria*-Induced TER Changes

Previous experiments showed that there was no effect of *Alternaria* on epithelial barrier permeability if cultures were grown from cells donated by healthy individuals. At 3 h after *Alternaria* was applied, the TER change for each *Alternaria* treatment was not significantly different between cells which had been pre-treated with ultrafine underground railway PM and those which had not (Figure 5.14). Although *Alternaria* appeared better able to elicit a drop in TER in cells not pre-exposed to ultrafine PM compared to those which where, this is likely due to the small sample size used here (n=3), since previous experiments here indicated a lack of effect on TER in healthy donor cultures. After 24 h exposure, all TER values were raised, and there was no clear difference between TERs with either *Alternaria* treatment type or ultrafine PM pre-exposure.

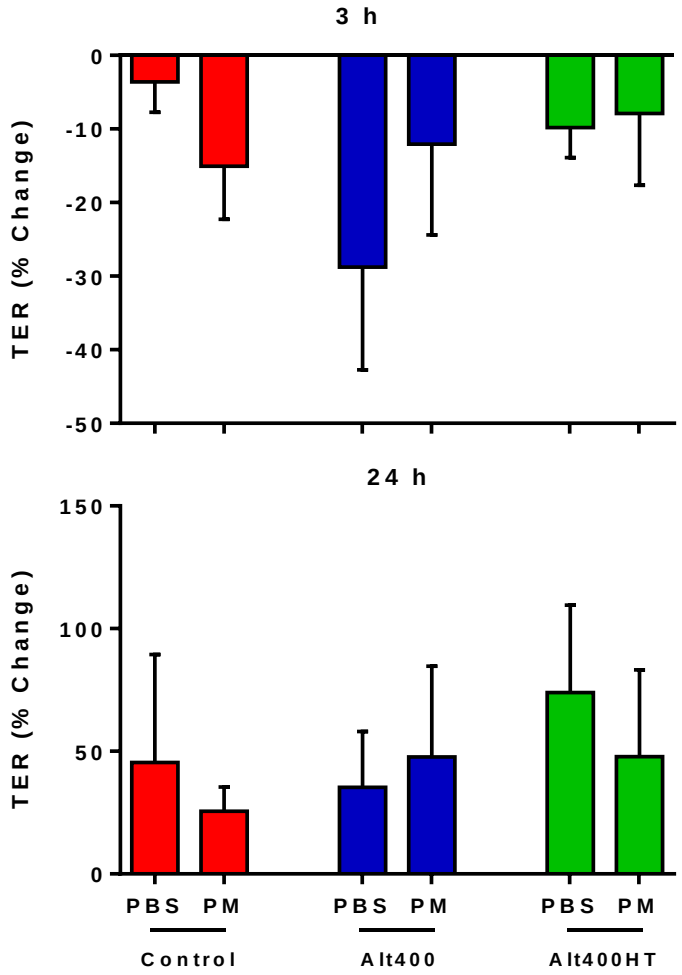

Figure 5.14. The effect of ultrafine PM on *Alternaria*-induced epithelial leakiness.

Cultures were treated as for Figure 5.13. TER was measured at 3 h and 24 h post-challenge. Results are expressed as percentage change in TER relative to pre-*Alternaria* challenge readings, shown as mean±SEM. n=3 .

5.4.3 The Effect of Underground Railway PM on *Alternaria*-Induced Changes at the mRNA Level

In order to further examine the potential interaction between ultrafine underground railway PM and *Alternaria*, cells treated as above were washed and lysed after 24 h *Alternaria* challenge. After RNA extraction and cDNA synthesis, qPCR was performed to determine gene expression levels of HO-1 and IL-33. Interestingly,

although there was no effect of pre-treatment with ultrafine underground railway PM in cells subsequently exposed to Alt400, nor in those cells incubated with BEBM, in cells exposed to Alt400HT, there was a greater increase in both HO-1 and IL-33 gene expression for those cultures which had previously been treated with ultrafine PM compared to those which had not (1.3±0-fold and 1.4±0-fold respectively *vs.* cells not pre-treated with ultrafine PM (both $p<0.05$; Figure 5.15)).

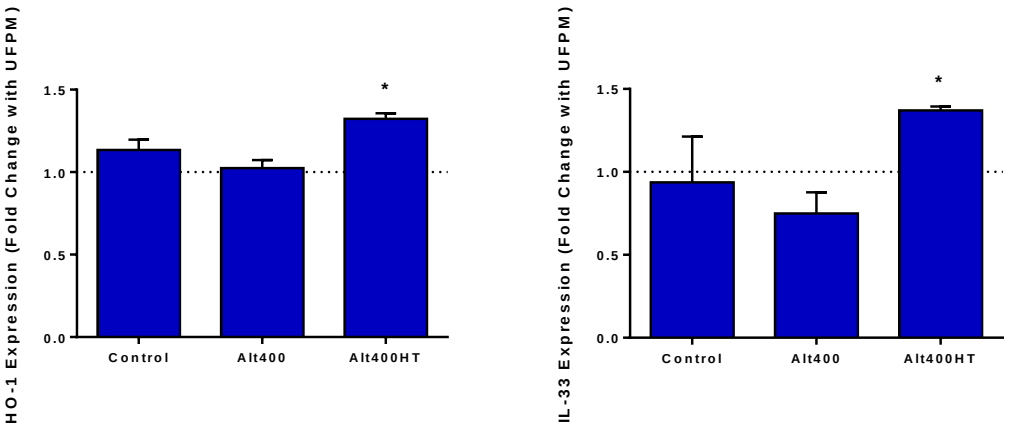

Figure 5.15. The effect of ultrafine PM on *Alternaria*-induced changes in HO-1 and IL-33 gene expression.

Cultures were treated as for Figure 5.13. Cells were lysed after 24 h challenge with *Alternaria*. Bars represent mean±SEM fold increase in gene expression in cells pre-treated with ultrafine underground railway PM *vs.* no PM pre-treatment, calculated by the ΔΔCt method. * - $p<0.05$ *vs.* no change. n=3 .

5.5 Discussion

This study investigated the potential of *Alternaria* proteases to perturb airway epithelial barrier function using cultures that are fully differentiated and covered by a layer of cytoprotective mucus as occurs *in vivo*, and to determine whether these responses are different in cultures from severely asthmatic donors. The main findings were that ALI cultures from severely asthmatic donors exhibited a more variable IL-8 response to *Alternaria* extract relative to those from healthy donors, while only cultures from severely asthmatic donors were susceptible to the barrier-weakening effects of *Alternaria*. Furthermore, while previous studies with cell lines have suggested that exposure to *Alternaria* extracts leads to production of cytokines that promote a Th2 response, it was not possible to detect any epithelial release of IL-33 or IL-18 (451, 528), while basolateral TSLP secretion did not change in response to *Alternaria*.

5.5.1 Effects and Mechanism of Action of *Alternaria* on 16HBE Cells

Induction of inflammation has previously been shown to increase upon challenge with fungal serine proteases from *Aspergillus fumigatus* (136) and *Alternaria* extract (146, 529) *via* an NF-κB-dependent mechanism (135). However, such studies did not take into account apicobasal polarisation, and were thus unable to study the apicobasal directionality of cytokine release, which is important in the context of the role of establishing a chemotactic gradient for IL-8 to act as a neutrophil chemoattractant (458, 459, 530, 531). The results of this study suggest that *Alternaria* extract increases release of IL-8 and TNFα both apically and basally but that, in 16HBE cells, the predominant direction of increased IL-8 is towards the apical compartment. However, it cannot be stated unequivocally that this increased apical IL-8 is due purely to increased apical release, as the effect could alternatively be ascribed to increased diffusion of IL-8 from the basal side to the apical side. However, in contrast to IL-8, the baseline TNFα concentration was predominantly apical. This apical bias became more pronounced with *Alternaria*, suggesting vectorial release. Since TNFα is larger

than IL-8 (17kDa(532) compared to 8kDa(457)) it is possible that IL-8 is predominantly induced basolaterally, but that the *Alternaria*-damaged epithelium facilitated basolateral-to-apical diffusion, with the larger size of TNFα precluding its apical-to-basolateral diffusion. Experiments with FITC-dextran show that there is increased permeability of the *Alternaria*-challenged epithelium to molecules of at least 4 kDa in size, but further work with dextrans of varying size would be needed to confirm the precise size-selectivity of any leakage. The results of this study also emphasise the importance of cell differentiation since *Alternaria*-induced release of IL-8 and TNFα was, unless the aforementioned transepithelial diffusion constituted the major determinant of IL-8 concentration, predominantly apical for 16HBE cells, whereas for differentiated ALI cultures the greatest fold stimulation was observed for the basolateral compartment (median 2.9-fold *vs.* 7.1-fold basolateral in healthy donor cultures). Also of note is the observation that TSLP is released exclusively into the basolateral compartment, highlighting the importance of epithelial polarisation for vectorial cytokine secretion. This may be significant in terms of establishing appropriate concentration gradients for chemoattractants that direct cells to the luminal or subepithelial compartments.

Inflammatory cytokine release was markedly affected by the inhibitors in *Alternaria*-free medium, particularly AEBSF, which markedly increased release of IL-8 and TNFα, and E-64 and SB203580, which both reduced TNFα secretion. However, given the role of TNFα in stimulating IL-8 release *via* NF-κB (457, 458, 533) it must be considered that this could also have interfered with IL-8 release as well. Indeed, given the importance of proteases in cell function, it is to be expected that such effects may occur, and thus care must be taken when interpreting results of protease-modulation. Furthermore, it is possible that the increase in cytokine release due to inhibitors may reduce the extent to which the cell can be further stimulated by *Alternaria*, thus falsely suggesting protease inhibition. Bearing this caveat in mind, results here suggest that *Alternaria*-induced IL-8 release into the basolateral compartment was markedly inhibited by AEBSF and Pepstatin A, suggesting a protease-mediated effect. Conversely, protease inhibition failed to affect apical IL-8 release, which was instead sensitive to inhibition of p38 MAPK, which is thought to play a role in stabilising IL-8 mRNA (534). On the other hand, apart from inhibition of basolateral release of

TNFα by Pepstatin A which approached significance, none of the inhibitors used affected TNFα release into either compartment. Although it has been well established that some growth factors are selectively sorted to the basolateral surface *via* information that usually resides in the cytoplasmic tail of the cargo (535), this does not explain how trafficking of a protein such as IL-8 is differentially regulated towards the apical or basolateral domains. Although this question has not been explored in detail, it has recently been shown that trafficking of IL-8 in ALI cultures challenged with grass pollen extract is post-transcriptionally regulated with apical release being selectively regulated by p38 MAPK (527), as observed in the present study using *Alternaria*. While the PAR-2 agonist trypsin, as well as a PAR-2 activating peptide, have been shown to activate p38 MAPK expression weakly (536), it seems unlikely that PAR-2 activation lies upstream of p38 MAPK activation in mediating *Alternaria*-induced apical IL-8 release as this response was insensitive to protease inhibitors.

NF-κB was not investigated in the present study, but it has been shown that PAR-2 activation results in activation of NF-κB (537), while the increased secretion of IL-8 in response to proteases from *Aspergillus fumigatus*, but not the baseline, unstimulated release of these cytokines, is mediated in part by NF-κB (135). Therefore, ERK1/2 and NF-κB would be transcription factors of interest to study in order to further delineate the mechanisms by which *Alternaria* extract induces release of IL-8.

Although HDM serine and cysteine proteases have been reported to increase epithelial permeability (151, 152), there is a paucity of work on the effect of fungal extracts on epithelial permeability, particularly using *Alternaria*. The present study suggests that heat-labile activities in *Alternaria* extract significantly and rapidly weakens the epithelial barrier, initially due to cysteine protease activity, and also *via* a p38 MAPK-mediated mechanism. However, both E-64 and SB203580 exhibited non-specific barrier-weakening effects at the 1 h time point, and this may be a factor in the apparent reduction of activity of *Alternaria* in this respect. At 24 h a lesser degree of non-specific barrier-weakening activity was displayed by the inhibitors, and serine and aspartate protease inhibition appeared to show a trend for inhibition of the reduction in TER caused by *Alternaria*.

Numerous studies of HDM proteases have been published suggesting that serine and possibly cysteine protease activity is able to rapidly degrade tight junction structure in MDCK and 16HBE cells, but that repair can be completed within 24 h, in agreement with our findings on TER (150, 152). In partial agreement with these studies, present attempts to characterise *Alternaria* protease activity in barrier degradation suggested that cysteine protease was responsible for the early barrier-weakening effects of *Alternaria via* p38 MAPK, although non-specific effects of the inhibitors in decreasing TER were apparent.

Fungal proteases fulfil a number of functions, particularly the external digestions of macronutrients, but are also intrinsic to the pathogenesis of diseases arising from fungal exposure (538). Taken together, these results suggest that the effects of *Alternaria* at the epithelium are predominantly due to serine and, to a lesser extent, aspartate protease activity, with the involvement of proteases in general being supported by a lack of activity of heat-treated *Alternaria* extract. This is in agreement with the results of a cell-free fluorescence-based protease assay presented in the current report, indicating that the majority of protease activity in *Alternaria* extract is of the serine protease type, while there is also a detectable, albeit non-significant, level of aspartate protease activity, but no detectable cysteine protease activity. Recent reports have suggested a role for serine and aspartate proteases in the cellular effects of *Alternaria* but this appears to be the first work which suggests that both classes of protease exert significant effects.

Recent *in vivo* experiments by Boitano and co-workers have suggested that the active component of *Alternaria* in the induction of inflammatory response is serine, and not aspartate, protease-dependent, and this was also demonstrated using a fluorescence assay kit of the same type used in the present study (529), although this has not been confirmed *in vivo* (539). In contrast, Matsuwaki and colleagues have suggested recently that the action of *Alternaria* in inducing cytokine release from epithelial cells, and inducing eosinophil degranulation, is sensitive to aspartate protease inhibition, but not to serine or cysteine protease inhibition (144, 145, 540). The presence of PAR-2 receptors in both epithelial cells and eosinophils probably absolves cell-type differences as being the cause of the differences in this instance. In the present

studies, serine proteases were the dominant activity in the protease assays, although inhibition of either serine or aspartate protease activity had a potent suppressive effect on IL-8 release. This discrepancy may be explained by the relative sensitivity of the fluorescence assay for serine and aspartate proteases or alternatively it is possible that the effect of Pepstatin A on IL-8 release may be due in part to the inhibition of endogenous proteases. For example, it has been reported that challenge of epithelial cells with *Aspergillus fumigatus* triggers the release of lysosomal enzymes including the aspartate protease, cathepsin D (541), which may affect subsequent cytokine responses. The use of inhibitors to study proteases and their effects is made more difficult by the differing IC_{50} values for each inhibitor. Although these values are available for archetypal targets such as trypsin and renin, there is variability between IC_{50} values across proteases within a target class such that, for example, a single serine protease inhibitor may have different IC_{50} values for inhibition of various serine proteases (542, 543). Therefore, since the identity of the protease(s) in Alternaria is unknown, it is impossible to test inhibitors on the basis of identical inhibitory ability. However, it is documented that the proteases used in the present study are class specific (542-544), and therefore the effects of AEBSF, E-64, and Pepstatin A can be attributed to inhibition of serine, cysteine, and aspartate proteases respectively, and not to non-specific inhibitory effects . Furthermore, the effects on baseline responses of cells in the present study suggests that increased concentrations would be unsuitable for use, while similarity to concentrations stated in the literature indicates that this is unlikely to be a significant source of error. Indeed, the great majority of protease activity in the fluorescence protease assay was accounted for by serine and aspartate protease inhibition.

In addition to proteases, other constituents of *Alternaria* extract such as β-glucans and chitin (cell wall components) have been noted to exert immunomodulatory effects (545-547). However, the lack of residual effect after heat-treatment of *Alternaria* in the present study suggests that the effect of β-glucans was negligible in our studies, although the effect of other unidentified components, either proteinaceous or small molecules, which may be affected by heat treatment, cannot be excluded.

There is also a possibility that variation between studies may be the result of differences in the preparation of the *Alternaria* extract used. The *Alternaria* extracts used in the present study were produced by Greer Laboratories Inc. and grown under Current Good Manufacturing Practice (cGMP) regulations, whereby seed cultures are maintained and controlled to help assure lot-to-lot consistency, and to assure the identity and purity of each lot. Fungi are grown in medium in which secretions are collected, and this culture medium is then extracted and lyophilised (548). The controlled conditions of this process suggest that there is little potential for inter-batch variability in content. Since the great majority of published studies also use *Alternaria* extract from Greer, it is likely that the *Alternaria* extract used in the present study is not significantly different to that which is used in other studies, and is unlikely to underlie any differences in the findings from various studies.

It is unlikely differential inhibitory effects were due to insufficient or excess inhibitor concentrations, as such concentrations were seen to have inhibitory effects in the current fluorescence assay, and these concentrations were generally within the limits of those used in other studies for AEBSF (137, 150), E-64 (142, 146, 149, 150, 522), and Pepstatin A (529). Additionally, while all concentrations were within respective manufacturers' recommendations, increasing further these concentrations may increase the inherent effects of the inhibitors on cells, and thus is not a viable option.

5.5.2 Interaction of *Alternaria* with Asthma Status in ALI Cultures

The study was then extended to examine primary bronchial epithelial cells in ALI cultures, as a more accurate model of human airway exposure. ALI cultures from non-asthmatic donors exhibited increased IL-8 release in response to *Alternaria*, while responses of cultures from asthmatic donors exhibited a trend of being blunted and not statistically significant, although considerable inter-individual variability was observed.

ALI cultures from healthy donors were resistant to the increase in epithelial permeability seen when ALI cultures from severely asthmatic donors were challenged

with *Alternaria*. This appears to be the first study which has examined differential responses to *Alternaria* between healthy and asthmatic donor ALI cultures. The implications are potentially significant: if the permeability of the bronchial epithelium in asthma is significantly increased by *Alternaria*, passage of inhaled allergens to the subepithelial tissue may be facilitated, and epithelial homeostasis disrupted. Since ALI cultures from asthmatic donors also displayed a lack of response to *Alternaria* in terms of IL-8 secretion, the ability to upregulate recruitment of neutrophils and clearance of allergens and toxicants in response to *Alternaria* may be affected. This impaired response of the epithelial cells from asthmatic donors to *Alternaria* is unlikely to be due to a carry-over of corticosteroids used for asthma control therapy, as it has previously been shown that similar ALI cultures respond to pollen extract with a significant increase in IL-8 release irrespective of whether they were derived from healthy or severely asthmatic donors (527).

Using commercially available ELISA kits, it was not possible to detect any release of IL-18, IL-33 or TSLP by ALI cultures. IL-33 release has been shown to be increased by *Alternaria* in murine BAL fluid and in normal human bronchial epithelial cells (NHBE) (451), however in the latter case the epithelial cell cultures were undifferentiated. It is of note that in the present work, a four-fold higher concentration was required to elicit IL-8 responses in differentiated ALI cultures compared 16HBE cells, which may be due to the presence of mucus-secreting goblet cells in in the ALI cultures, and either subsequent inactivation of proteases by components of the mucus or the action of the mucus in forming a physical barrier. This supports findings from the previous chapter, where the induction of IL-8 release by underground railway PM was reduced in mucus-covered ALI cultures compared to PBEC monolayers without such a mucous layer. In contrast, others have failed to detect IL-33 or TSLP secretion from either NHBEs challenged with *Alternaria* (528) or mouse lung epithelial cells challenged with *Aspergillus fumigatus* (547). It was also not possible to detect IL-18, despite a recent report of a marked rapid release of IL-18 after *Alternaria* challenge of NHBE cells (528). However, control experiments performed in the same laboratory as the present work and assayed at the same time showed detectable IL-18 and TSLP production in response to rhinovirus challenge (data not shown), suggesting that the lack of any observable effect with *Alternaria* was

not due to defective epithelial synthesis or release of these mediators. Although there was an initial failure to detect TSLP with a commercial ELISA (from R&D Systems), use of an alternative "in-house" ELISA (developed by Novartis Plc.) enabled detection and quantification of basolateral TSLP release, however no apical secretion was evident. It is postulated that this difference in detection is due to differences in antibody recognition of recombinant and native TSLP, making the commercial ELISA kit much less sensitive for detection of the naturally produced protein. Having observed such a large difference in sensitivity for detection of TSLP, it is conceivable that the ELISAs employed for the measurement of IL-33 and IL-18 may be similarly compromised.

TSLP is secreted by epithelial cells and potently activates human dendritic cells to release a battery of cytokines which results in Th2-skewing of naïve CD4+ T cells (449). *Alternaria* has been shown to increase TSLP expression and release from airway epithelial cells *in vitro via* PAR-2 activation (142). However, even with the increased confidence in the "in-house" ELISA system, we found no significant change in TSLP release in response to *Alternaria*. One likely explanation is the use of fully differentiated ALI cultures in the present work, as opposed to undifferentiated monolayers in the previous studies, emphasising the importance of using models that closely mimic the *in vivo* state. While there is strong evidence to suggest that *Alternaria* exposure can induce Th2-type responses *in vivo*, and that TSLP release from structural cells can act as a potent mediator for Th2 skewing (16), it is possible that epithelial cells require the presence of other cell types of multiple stimuli for *Alternaria* to have such an effect. For example, IL-4 and double-stranded RNA potently synergise to stimulate TSLP release from bronchial epithelial cells *in vitro* (549).

5.5.3 Interaction of *Alternaria* with Ultrafine Particulate Matter

A literature search revealed little by way of previous work examining a potential interaction between particulate air pollution and the effects of airborne fungus. A 2004 study which found a potential synergistic relationship between aeroallergen levels and ozone levels on asthma hospitalisations (348), and a further study by the same

group in 2012, showed that the risk of asthma hospitalisation with increasing concentration of deuteromyocytes (a group of fungal species including *Alternaria*) was heightened by increased PM_{10} levels (550). There is also evidence that the grass pollen allergen Lol p 1 can bind to diesel exhaust particles, suggesting that inhaled particles may be able to act as a delivery vehicle for allergens into the lungs, and possibly into cells (551).

Previous results in this chapter have shown that *Alternaria* can induce inflammatory cytokine release and asthma-dependent TER decreases as a result of heat-labile activity which could be inhibited by protease inhibitors. Pre-treatment of ALI cultures with ultrafine underground railway PM had no effect on the subsequent ability of *Alternaria* to elicit IL-8 release or a change in TER. However, when expression of the antioxidant gene HO-1 and the Th2-type cytokine and alarmin IL-33 were examined, heat-treated *Alternaria* extract induced a greater increase in the genes when cells were primed with ultrafine PM compared to cells not subject to PM pre-exposure. Crucially, this pre-exposure made no difference in cells exposed to fresh *Alternaria* or controls incubated in BEBM. This suggests that there is a component(s) of *Alternaria* which is not heat-labile, and which can exert certain effects on cells primed with ultrafine underground railway PM. It is unclear as to why fresh *Alternaria* extract, which must also contain such components, does not exert similar effects. It is possible that there are heat-labile components of *Alternaria* which reduce HO-1 and IL-33 responses in PM-primed cells compared to non-primed cells, and so the effect in of heat treatment unmasks the effects of the heat-stable components. Indeed, IL-33 expression induced by *Alternaria* tended to be lower in cells pre-primed with ultrafine PM although this did not reach significance – repeat experiments would allow more rigorous statistical analysis of this effect to be performed. It is also possible that ultrafine PM pre-treatment activates certain defence mechanisms in the cultures which can ameliorate the effects of heat-labile components of *Alternaria* extract, but are less able to affect heat-stable components. To this end, it would be useful to determine cellular production of antiproteases after exposure to ultrafine PM. Additionally, identification of the heat-stable component of *Alternaria* extract may be aided by treatment of the *Alternaria* extract with β-glucanase or chitinase enzymes, since these are two components of fungal cell walls which have previously been reported to exert

effects upon cells (see Chapter 1). This work could also give rise to similar experiments with ultrafine underground railway PM and *Alternaria* extract being applied to cells simultaneously, or with the cells being pre-treated with *Alternaria* for either 3 h, when maximal response on TER was seen, or for 24 h, by which time IL-8 has accumulated. Simultaneous incubation may provide a better idea of the risks of co-exposure as might occur in an underground railway, and might also facilitate the uptake of components of the fungal extract when adhered to particles, as has been suggested in the literature (551) although such an experimental protocol may also make it more difficult to identify precisely the causative agent of any observed changes.

This work only investigated one possible exposure scenario – that of exposure to underground dust priming cells for subsequent exposure to *Alternaria*. There are, however, other possible exposures which were not investigated. For example, since *Alternaria* is found in underground stations, it could be argued that simultaneous challenge with ultrafine underground railway PM and *Alternaria* extract may better represent the actual exposure scenario. Conversely, since Alternaria was seen to have maximal impact on TER after 3 h exposure, it may be equally rational to treat cells with Alternaria for 3 h, and then to replace the Alternaria extract with underground railway PM, to simulate a potential "worst case" scenario. The protocol used in the present work was designed on the basis of reports in the literature indicating that ambient PM levels may aggravate the subsequent response to airborne *Alternaria*, resulting in increased hospital admissions (550). Nonetheless, investigations of the other possible scenarios would be equally valid and may shed more light on the mechanism of interaction.

This preliminary identification of a potential role for heat-stable components of *Alternaria* extract in interacting with ultrafine underground railway PM exposure suggests that, in addition to the reported effects of fungal proteases on inflammation and allergy induction, there may also be a role for non-proteolytic components in the development of a Th2 phenotype. These components are relatively understudied in the literature, perhaps on account of their inability to elicit a response in the frequently-measured cytokine IL-8. Further work should be performed to determine

whether other Th2 cytokines may be affected by an interaction between PM pre-treatment and heat-stable components of *Alternaria*. Furthermore, since asthma is a disease which can exhibit decreased lung antioxidant status and a Th2 phenotype, these experiments should be repeated in severely asthmatic donor cultures to determine the effects of heat-stable components of *Alternaria* on expression of IL-33 and other Th2 cytokines.

5.6 Conclusion

This study demonstrates that *Alternaria* extract is able to significantly induce release of inflammatory cytokines and to increase the permeability of a polarised airway epithelial cell line. These effects were attributed to a heat-labile component of the *Alternaria*, identified as being serine and possibly aspartate protease mediated. Crucially, this study is the first to demonstrate that fully differentiated epithelial cultures from severely asthmatic donors appear to have a blunted IL-8 response to high levels of *Alternaria*, while at the same time being more susceptible to the barrier-weakening effect of *Alternaria*, than those from healthy donors. Furthermore, heat-stable components of *Alternaria* may interact with ultrafine underground railway PM to exert additional deleterious effects which merit further investigation.

6 Final Discussion and Future Work

6.1.1 Novel findings

The work which constitutes this thesis contributes to the field of respiratory toxicology, and in particular furthers knowledge of the effects of underground railway particulate matter, in a number of ways. The finding that ultrafine underground railway PM is just as rich in metals as coarse and fine PM, with over 40% by mass of the particles being iron (Chapter 3) raises several important issues. Ultrafine PM is generally thought to pose a risk on account of its surface area which acts as a good predictor of toxicity (493) while chemically, although ultrafine PM can contain transition metals and redox-generating organic molecules, it is often composed of the anionic products of secondary reactions, which are thought not to be toxic (483). This finding suggests that underground railway ultrafine PM may exert effects as a result of **both** its surface area and chemistry. Second, the use of ALI cultures of primary bronchial epithelial cells is not usual in particulate toxicology, with cell lines being more commonly used than primary cells, and monolayers more common than polarised or air-liquid interface cultures. The use of primary cells allows the disease status of the donor to be taken into account, and provides a more accurate representation of the cells in the human airways *in vivo*. Culture of these cells at ALI in the presence of retinoic acid allows them to differentiate, forming ciliated columnar epithelial cells and goblet cells. This was illustrated by the significant (albeit moderate) effect of fine and ultrafine underground railway PM on IL-8 release in undifferentiated monolayers from both healthy and severely asthmatic donors, but not in ALI cultures from donors of either disease state (Chapter 4). This finding has implications for other studies in which PM is applied to monolayers, since it is possible that such models overestimate the effects of PM on mucus-coated airway epithelium as is found *in vivo*.

Interestingly, despite the presence of mucus, particles of all size fractions were able to enter epithelial cells cultured at ALI (Chapter 4). Therefore, although the mucus may ameliorate the pro-inflammatory effects of PM, it is unable to completely prevent the ingression of PM. PM was found to enter a variety of compartments of cells, including vesicles bound by membranes which may sequester and render the particles relatively harmless, but also free within the cytosol and within mitochondria, which may lead to further ROS production by derangement of the electron transport chain and thus uncoupling, with potentially increased superoxide production.

Despite the protection which may be afforded by the presence of a mucous layer, there was still a notable iron-dependent increase in antioxidant enzyme gene expression induced by ultrafine underground railway PM, which underlines the importance of taking into account more than one outcome when determining the effects of particles on cell culture, since there was much less of a response to underground railway PM when IL-8 release was measured.

There has been little work on the interactions of air pollution with other challenges to the airways at the cellular level, with such studies generally taking an epidemiological approach. The present work shows that ultrafine underground railway particles may also influence the cellular response to *Alternaria* (Chapter 5), although the component of *Alternaria* whose effects appear to be exacerbated by the prior presence of underground railway PM appears to be different to that responsible for the increased barrier permeability and IL-8 release also elicited by *Alternaria* alone. The increased oxidative stress (indicated by HO-1) and potential skew towards a Th2 response (IL-33) are both markers of asthma, so it is possible that the combination of PM and *Alternaria* may increase the risk of asthmatic responses after combined exposure to both underground railway PM and *Alternaria*.

6.1.2 The Effect of Asthma on Cellular Responses to PM

The present work did not find any significant differences in response to underground railway PM between asthmatic and non-asthmatic donor cell cultures. This may be regarded as surprising since it was demonstrated using DCF that the PM used was a potent generator of reactive oxygen species, and one feature of asthma is a decreased ability to produce antioxidants and an increased level of oxidative stress in the airways, with greater susceptibility to these effects in epithelial cell cultures from asthmatic donors (400, 403) . However, epidemiological studies and analyses of lung fluid are not the same as cell culture models as used in the present work. Although ALI cultures of asthmatic donor bronchial epithelial cells have been shown to be more susceptible to smoke-induced oxidative stress than those from non-asthmatic donors (512), it is possible that not all features of the asthmatic phenotype are recapitulated *in vitro,* and this further underlines the need to look at multiple outcomes. Even when oxidative stress is considered, different modes of generation of oxidative stress may show varying outcomes when disease state is considered as a modifier, and hence oxidative stress induced by the application of hydrogen peroxide may produce disease-modified responses not seen when the oxidative stress is generated by particulate matter. For instance, the increased mucus secretion seen as part of the asthmatic phenotype may be able to interfere with certain processes which are important in particle-mediated toxicity, such as the movement of particles towards cells and subsequent uptake (7), while such defences may be inadequate against soluble stressors. However, even when mucus-free monolayer cultures of PBECs were used, there was no difference in IL-8 release or cell death between those from healthy donors and those from severely asthmatic donors. This finding lends further weight to the investigation of other outcomes, especially in order to establish disease state-dependent responses. In particular, due to constraints of time and resources, there was no examination of the antioxidant response to underground railway PM in severe asthmatic donor ALI cultures. Indeed, in terms of characterising the recapitulation of *in vivo* characteristics in primary cell cultures, a first step would be to perform qPCR and possibly western blotting to determine mRNA and protein expression levels of antioxidants and antioxidant enzymes such as HO-1 and GSH (and associated synthesis and recycling enzymes) at baseline. Following this, experiments could be

performed exactly as those in the present work to determine the time course of antioxidant responses to ultrafine underground railway PM, examining whether there is any difference in either the magnitude or the speed of the response which may indicate an increased susceptibility to the effects of the PM. Furthermore, if such a difference existed, particle co-application with antioxidants as was performed with NAC in the present work may shed light on whether differing responses are the sole result of a defective antioxidant defence mechanism, or whether there are other differences which cannot be ascribed to compromised defence mechanisms.

6.1.3 Cell Culture Models

The current work was performed on cell cultures grown from primary bronchial epithelial cells, cultured either as monolayers or at air-liquid interface. As previously described, the ALI culture model offers an increased complexity and physiological accuracy of the culture, by way of differentiation of the epithelium to form ciliated cells and mucus-secreting goblet cells. Nonetheless, such a model can still only be regarded as a monoculture, and as such is unable to take into account responses of other cell types which would normally be found in the airways, and the complex network of interactions between them. There is considerable evidence that the responses of epithelial cells to particulate matter is modified by the presence of other cell types. For example, it has been observed that DEP can cause increased epithelial leakiness in 16HBE cell monocultures, but not when the 16HBE cells are co-cultured with dendritic cells and macrophages (177). Furthermore, macrophages release a battery of cytokines upon exposure to PM (80, 299, 552-554), which may themselves have an effect on epithelial cells.

Animal models are sometimes used to test particle toxicity, either by instilling a particulate suspension in the tracheobronchial region of the airways, or by exposing the animal (usually rat or mouse) to an aerosolised particle suspension. However, the former method does not necessarily represent inhalation any better than a submerged cell culture model, while the latter is poorly representative of particle deposition in human airways since rodents are obligate nose breathers, and therefore deposition

patterns are poorly representative of deposition in humans (230). Finally, animal models poorly recapitulate asthma, and so are poorly suited for research into the differences in response to particles between healthy and asthmatic airways (555). As such, for studies of particle-airway interactions, carefully designed *in vitro* models can be equally as useful, if not more so, as *in vivo* models.

There are two ways to increase the complexity of the cultures used in the present work. The simplest, but less ideal, method would be to perform conditioned media experiments whereby, for example, macrophages would be incubated with PM, and after a set time the medium would be harvested, centrifuged to remove cells and free particles, and then applied to epithelial cell cultures to determine the epithelial response to factors secreted by macrophages following PM challenge. Such experiments could equally be performed by exposing epithelial cells as the first step, and then applying the conditioned media to cultures of fibroblasts, to examine how epithelial responses to particulate matter may influence fibroblast function. However, conditioned media experiments are not without their shortcomings. The conditioned medium is only a "snapshot" of the responses of the initially-exposed cells at the time the medium was harvested. Different responses may develop over different time periods, and therefore early responses and late responses are unlikely to be represented accurately in medium harvested at a specific timepoint. Second, the procedure does not allow for the interplay between cells where reciprocal interactions occur, as it only allows for unidirectional modelling of responses. For example, if the cell exposed to the conditioned medium were to release a factor in response to a cytokine released by the initially-exposed cells, in a way which would set up a positive or negative feedback loop between the two cell types *in vivo*, this would not be captured by *in vitro* conditioned medium experiments. Third, although conditioned media experiments allow for cell-cell interactions *via* soluble factors, they do not allow for interactions between cells where mediated by membrane bound, cell surface molecules such as cluster of differentiation molecules. The "gold standards" for *in vitro* models are co-culture or explanted tissue models, which do not suffer from these limitations, although they can be more difficult to generate on account of the differing culture requirements of each constituent cell type. Since macrophages are the principle phagocytic cell type in the lower airways, and there is already evidence that particle

phagocytosis can have indirect effects on epithelial cells, epithelial cell-macrophage co-cultures would allow a more in-depth study of the effects of underground railway PM. However, the model could be further extended to incorporate fibroblasts to determine whether PM may elicit profibrotic responses in subepithelial tissue, endothelial cells in conjunction with alveolar epithelial cells instead of columnar epithelium to study the effects of PM on the alveolar capillary bed, or dendritic cells to determine how particle uptake and sampling is performed.

There is also a further consideration for cell cultures models of PM deposition. The protocols in the present work consistently used PM suspensions diluted to the requisite concentration in culture medium with no added serum or protein. However, the absence of these may not accurately reproduce *in vivo* conditions, and this is particularly true for monolayers which do not have the advantage of a particle-free basolateral compartment into which these medium components can be added. The presence of protein or serum in the a particle suspension can markedly alter the cellular response to the particles, because the protein coat which forms around the particle – the corona – is the part of the particle "seen" by the cell. As such, not only does the surface of the particle become masked by the protein corona, but responses to the particle can depend on the proteins themselves, which may differ depending on the particle surface. A protein corona has been reported to reduce particle uptake by reducing nanoparticle adhesion to the cell membrane in the initial step of uptake after particles were exposed to serum (556, 557), although it has also been suggested that a protein corona can act as a dispersant, reducing agglomerate size and thus increasing the potential uptake of particles (558), and subsequent toxicity (559). Work with silica nanoparticles has also shown that nanoparticles pre-incubated in complete medium were coated with proteins indicative of immune processing (immunoglobulin, complement, apolipoprotein) while nanoparticles presented to the cells in serum-free conditions became coated with cell membrane and cytoskeletal proteins, suggestive of damage to the structure of the cell (556). However, different coronae may modify particle-cell interactions in different ways, and the precise nature of the corona may depend on the size and composition of the particle itself (557), with the nanoparticle-corona dissociation constant decreasing, indicating a stronger attachment, as particle size decreases (560). Therefore, there is an obvious need for the particle suspension

medium to be taken into account when interpreting results and, ideally, moves towards establishing certain standardisations for PM exposure experiments which will reduce the potential for confounding factors such as corona formation. Indeed, the situation becomes even more complex when it is considered that the corona composition may change as the particle moves between different compartments in the body, which may produce differences in particle uptake for the same particle in different body compartments (561, 562). Moreover, the corona may evolve over time even when the particle is kept in a single suspension, with the protein corona initially being formed of those proteins which are the most mobile and abundant within the milieu, but being replaced over time by proteins with a greater affinity for the nanoparticle – the Vroman effect (563, 564). Therefore, it is not even sufficient to take into account solely the composition of a particle suspension, because particles in suspensions of identical composition may have different coronae, and thus different interactions with cells, if the time spent by the particles in suspension differs.

A further complexity, and a clear source of difference between monolayers and ALI cultures of PBECs, is the presence of a mucous layer, and therefore the need to consider particle-mucus interactions which occur before the particles have even reached the cells. The retardation of movement of particles through the glycoprotein mesh of mucus is not purely size dependent, but also depends on electrostatic and hydrophobic interactions, which in turn depend on the particle surface (565-567). Furthermore, as well as the action of mucus on particles, particles may modify mucus by increasing the size of the pores formed by the constituent mucins (568). As such, the use of mucus-producing cells, as in the present study, represents a great improvement over mucus-free monolayers for the study of particle effects, albeit a costly and labour-intensive one.

6.1.4 Delivery of Particles to the Cell Surface

The experiments in the present study were performed using primary bronchial epithelial cells cultured in two different ways – monolayer cultures with the cells adhered directly to the tissue culture plastic and submerged under a volume of cell

culture medium, and ALI cultures with the cells adhered to a porous membrane which is suspended over, but in contact with, medium within the basolateral compartment of the well. In monolayer cultures, the particles must be applied in culture medium as a suspension, since there is no way to separate the application of particles from the application of medium. However, when cells are cultured at an air-liquid interface, it is only necessary for medium to be present in the basolateral compartment. In the aforementioned ALI experiments, PM was applied apically as a suspension exactly as for the monolayers. One advantage of this approach is that it allows for comparison of the effects of PM between monolayers and ALI cultures both in terms of PM concentration by volume and PM concentration by cell culture surface area, because conversion between the two is approximately the same for both culture types. Furthermore, the use of the same medium (BEBM with no added protein) for suspension of particles in both monolayer and ALI experiments means that there is less likely to be a difference in particle agglomeration between the two culture types. Therefore, the protocols for exposure of cells to PM as both monolayers and ALI cultures as in the present work are suited to comparing responses between the two. Indeed, similar exposure protocols are found in the great majority of the literature. However, the application of PM as a suspension has little resemblance to *in vivo* exposure, where particles are carried in the inhaled air and deposited, by means dependent on their size, on the mucous or surfactant layer coating the apical surface of the epithelial cells. Efforts are being made to improve methods of applying particles to cell culture surfaces, with the aim of better approximating the *in vivo* exposure situation. In such systems, PM in suspension is sonicated and aerosolised, and subsequently deposited onto the surface of cells, thus maintaining the air-liquid interface. Alternatively, exhaust gases may be directly channelled to exposure chambers without being collected as a suspension or on filters (569), and metal nanoparticles may be generated by flame spray pyrolysis for direct deposition onto cells (570, 571). Current forms of such apparatus, such as the air-liquid interface cell exposure system (ALICE), use vibrational sonication to reduce shearing of particles, and cloud settling rather than air jets to reduce stress to cells (572), or air flow at a speed low enough not to cause significant loss of cell viability (573). However, although it seems that particle distribution over the cells is generally uniform (573), such systems are also extremely wasteful, since there is a uniform coverage of PM

aerosol settling over the entire bottom surface of the exposure chamber (572). Therefore, even if the chamber were only as large as a 6 x 4 well plate, and all wells contained Transwell membranes, only 8 cm^2 of the deposition surface would be cells, of a total area of 110.5 cm^2 (plate dimensions 13 cm x 8.5 cm). Greater value is added to such systems by the use of static charging equipment, to give each particulate an electrical charge (574), as used in the Electrostatic Aerosol *in Vitro* Exposure System (EAVES) (575). Charged plates underneath each well can then be used to attract particles to land on the cell culture surface, reducing particle wastage through deposition on the surface of the incubation chamber and the plastic culture apparatus. However, such equipment is still in the process of design and validation, although initial results suggest that toxicity may be seen at lower PM concentrations when examined by EAVES deposition compared to exposure in submerged cultures (576). Furthermore, differences in the effects of flame-generated zinc oxide particles applied as a suspension and as a submerged culture have been suggested to be a result of the presence of gases in addition to particles in the direct aerosol exposure, although this is only relevant if PM is applied to cells directly rather than being collected as a suspension prior to aerosolisation (571). One limitation of much of the current aerosol deposition apparatus is that aerosolisation of PM samples may require considerable amounts of PM, and therefore this is likely to be unsuitable when sampling campaigns are conducted over limited periods, and where portions of the collected PM are required for other procedures such as chemical analysis. There are further drawbacks, such as the difficulty in delivering a precisely metred dose to the cells, and while this has been measured by examining TEM grids exposed in parallel (569), or by using a quartz crystal microbalance (572), it is nonetheless difficult to apply PM in an exact predetermined quantity, and also difficult to apply different concentrations of PM to different cultures on the same plate within a small timeframe. Nonetheless, these promising new techniques offer the opportunity to recreate more accurately *in vivo* exposures in *in vitro* experiments. Although the required apparatus is currently not commercially available, and is only suitable for the most rudimentary of particle exposure studies, as these techniques become more refined and commercially available they may replace traditional submerged exposures in air-liquid interface culture experiments.

6.1.5 Extension of the Culture Model to Study Non-Bronchial Effects

The present work studied the effects of underground railway PM using two different cell culture systems and examining various endpoints, such as cell death, cytokine release, and antioxidant enzyme expression. However, the conducting airways are only part of the airway epithelium which is exposed to inhaled particulate matter. The present work shows that underground railway particulate matter is just as rich in transition metals, principally iron, as the coarse and fine fractions, and more potent at generating ROS. While coarse particles generally deposit in the upper airways, and fine particles in the upper and lower airways, ultrafine particles are uniquely able to deposit in the terminal bronchioles and alveoli, and therefore consideration needs to be given to the effect of deposition of such particulate matter on cells other than the mucus-covered ciliated columnar epithelium of the bronchi. This is important for a number of reasons. First, unlike the bronchial epithelium, the alveolar epithelium is neither ciliated nor mucus covered. There is a thin layer of surfactant secreted by alveolar type 2 (ATII) cells, which contains surfactant lipids and proteins and allows the air sacs to remain patent by virtue of its ability to lower the surface tension of the alveolar fluid. However, alveolar surfactant is unlikely to provide the protection against particles which is afforded by the bronchial mucus. Therefore, it may be expected that alveolar epithelial cells, and particularly the alveolar type 1 (ATI) cells which constitute the majority of the alveolar surface area, may be at greater risk of the effects of particles deposited there compared to cells in the upper airways. There is also evidence that suggests that, even in monocultures where protective mucus and surfactant are missing, different cell types (both primary and immortalised lines) exhibit markedly different responses to the same particulate matter (501). There also arises the question of particle uptake and epithelial permeability. The present work suggested that the bronchial epithelial barrier remains intact after deposition of underground railway PM at the concentrations used, but this may not be the case with the alveolar epithelium which is not as impermeable in the first place. In addition, if particles were to leave the airway lumen, the epithelial layer itself is thicker in the upper and lower airways than the alveoli, there is an underlying *lamina reticularis* which is absent in the alveoli and, distally from the lumen, there is a layer of fibroblasts. Even if particles were able

to penetrate the epithelial barrier, their progression away from the airways would likely be slow, and perhaps only increased in speed with uptake and translocation by macrophages or dendritic cells. Conversely, the alveoli contain only a single layer of squamous ATI cells lying above vascular endothelium. Particles passing through the alveolar epithelium, either *via* the paracellular pathway between cells or, perhaps more importantly, *via* the transcellular route involving uptake at the apical surface and release at the basolateral surface (577), would have access to the endothelial cells of the alveolar capillaries, and also the alveolar capillary blood supply. Therefore, there is a greater risk of particles entering the systemic circulation after deposition in the alveoli compared to deposition in the bronchi and bronchioles. Furthermore, although alveolar macrophages are able to phagocytose such material, there is evidence that this process is inefficient for particles below a certain size or whose aspect ratio is such that alveolar deposition is possible but complete phagocytosis is impossible (222, 577). As such, much consideration needs to be given to (a) the effect of metal-rich ultrafine underground railway PM on the alveolar epithelium, and also (b) the potential consequences of translocation of such PM to the systemic circulation. The first of these would be accomplished by the culture of alveolar type I cells on Transwell membranes. This would allow for study of the cytotoxicity, inflammogenicity, and antioxidant-inducing effects of ultrafine PM to be studied (coarse and fine PM are not deposited within the alveoli). Furthermore, changes in permeability of the alveolar epithelium could be investigated as in the present study, using FITC-dextran, although this could be extended to include different sizes of dextran other than the 4 kDa moiety used here. However, it would also be pertinent to study the potential translocation of particulate matter itself, rather than a marker of increased permeability such as dextran, by performing ICP-MS on the basolateral medium. Such a study would require careful selection of the element(s) to be used to trace particle movement, since the sensitivity of ICP-MS renders data susceptible to contamination, especially if such experiments are not performed in designated "clean" laboratories. However, such a technique has recently been used *in vivo* to measure translocation of PM from rat lung, by measuring levels of the lanthanide europium after it was used as a dopant to coat gadolinium oxide nanoparticles. In this way, the stability of the nanoparticle labelling could be determined by measuring the europium/gadolinium ratio, while europium levels themselves were a measure of the level of nanoparticle

accumulation in a particular organ (578). This could be contrasted with, for example, iron, whereby any inflammogenic properties of particles may be expected to increase blood flow to the affected tissue, and thus induce increased concentrations of iron from non-particulate sources (i.e. haemoglobin).

An extension to this system would potentially facilitate the *in vitro* study of the potential effects of inhaled ultrafine particulate matter on tissues and organs distinct from the lung. For example, as detailed below, although there is clear evidence that particulate air pollution can lead to rising cardiovascular morbidity and mortality (42, 43, 46, 47, 260, 579), the mechanisms by which this occurs are poorly understood. C-reactive protein, a marker of systemic inflammation, has been seen to be raised during air pollution episodes (580), and IL-6 has been suggested to enter systemic circulation after production in mouse lung (581), providing evidence for an indirect inflammatory mechanism, whereby lung inflammation results in the release of inflammatory cytokines into the systemic circulation. PM has also been seen to reduce heart rate variability, indicating decreased autonomic control of the heart (579, 582). PM and/or associated oxidative stress has been linked to formation of atherosclerotic lesions in mice (583), development of electrical irregularity and cardiac arrhythmia as a result of calcium calmodulin kinase II activation in rats and isolated rat hearts (584), and fibrotic heart remodelling in mice (585). Furthermore, cultured cardiac myocytes exposed directly to PM show transcriptomic changes indicative of injury (586). There is also evidence of potentially pathological structural damage to vascular endothelium as a result of PM-induced oxidative stress (587). In order to study the potential for such effects, alveolar epithelial cells would be cultured on a Transwell membrane, preferably with a layer of vascular endothelial cells on the underside of the Transwell membrane to approximate the alveolar vascular endothelial wall. A separate cell culture would be created, containing cells of interest representing the target organ, for example cardiac myocytes. The two wells would then be connected by a microfluidic system in order to allow real-time transport to the second culture of basolaterally released factors from the alveolar/endothelial cell co-culture and also any translocated particulate matter. Techniques used in the present work – cytotoxicity assays, ELISA to study cytokine release, and qPCR – could all be used to study the response in the target tissue culture, but further techniques could also be used to determine organ-

specific effects. For example, if the study aimed to determine the effect of inhaled PM on cardiac tissue, the electrical activity of the culture could be measured, and indeed a recent publication outlined a microfluidic system which incorporated an electrode array to allow measurement of electrical activity in the nematode worm (588). Similarly, if the target organ of interest was the liver, enzymes whose levels may indicate liver damage could be analysed, such as aspartate transaminase and alanine aminotransferase. The treatment of particulate matter with metal chelating agents or antioxidants and free radical scavengers as in the present work may then provide important clues as to how organs other than the lungs may be affected by the inhalation of airborne particulate matter.

6.1.6 Experimental Findings Informing Regulation

As more data regarding the effects of particulate matter at the epidemiological, whole organism, and cellular level becomes available, there will be a greater basis on which to suggest limits for exposure to ultrafine particulate matter, both outdoor, ambient levels, and also occupational exposure limits, potentially including dust-specific limits. Indeed, further work may also refine the existing limits, since there is evidence that exposure to PM may have deleterious health effects at exposure levels well below the current recommendations, leading to resetting of the no observed adverse effect level (NOAEL) (44, 61, 589). Furthermore, current limits do not take account of differences in inter-individual exposures or inter-individual responses. Current limits make no allowances for the impact of physical exertion or disease-related alterations in airway geometry which may increase PM deposition in the airways. Nor do they allow for potential interactions between PM and other pollutants, allergens (590), infection (591, 592), asthma, heart disease and other diseases which affect PM target organs other than the lungs, genetic factors (593), stress (594), smoking status, or socioeconomic status (326).

It is also of interest to determine the amount of particulate matter which may enter the airways. Rudimentary attempts at such a calculation have been made in the literature (125, 595). As a worked example here, inhalation of 500 ml air per breath at a rate of

12 breaths per minute equates to inhalation of 2.9 m^3 air in an 8 h working shift. If this air contains a PM_{10} concentration of 282 $\mu g/m^3$ as in the present study, approximately 820 μg PM_{10} will be inhaled in this period. Assuming an average lung area of 70 m^2 suggests an average deposition of 11.7 pg/cm^2 in the lungs which is a far lower concentration than used in the present study, or indeed almost all studies within the literature. The actual figure for mass of PM deposited may be even lower since not all PM which is inhaled will be deposited. Conversely, deposition throughout the airways and lungs is not uniform, with "hot spots" for deposition particularly located at airway bifurcations and wherever flow is turbulent (596, 597), such as the carinal ridges (598). Furthermore, other factors can increase PM inhalation and deposition, including exercise, oral rather than nasal breathing, airway geometry, and proximity to the source of PM (599). Additionally, it has been suggested that airway constrictions as found in asthma and COPD may increase particle deposition by up to one order of magnitude compared to healthy airways (600). Indeed, "hot spots" at airway bifurcations in individuals whose breathing rate and type favour PM ingression to the tracheobronchial region may receive 3,000-25,000 times the concentration of PM suggested by average deposition calculations as above (599). As such, one reason for increased responses of asthmatics at an *in vivo* or epidemiological level may not purely be an increased response to particles on the basis of equal concentrations, but an increased exposure. Clearly, further work on this area, which is currently confined predominantly to *in silico* models, albeit of ever-increasing complexity, may allow for more accurate modelling of the differences in deposition between airways of difference disease states, facilitating incorporation of such differences into experimental design for i*n vitro* testing. However, in light of the current lack of information regarding differential deposition levels, experiments which investigate the effects of PM at concentrations such as in the present work, and perhaps even higher, are certainly warranted to evaluate a "worst case scenario" of particle deposition.

There are two distinct ways to investigate the effects of PM from different environments specifically with a view to setting exposure limits. A reductionist approach examines PM constituents and may try to link them to disease at the epidemiological level, or to deleterious effects at the cellular level, the aim being to identify specific PM components which might pose a risk to health. By this method,

sometimes termed "pattern recognition" (601, 602), those components of PM which pose a particular risk can be investigated, and any methods for screening untested PM could look initially at whether levels of these constituents are high enough to warrant concern, in effect using certain components as markers of potential toxicity. However, this approach is unable to take into account interactions between particle constituents which may synergise or antagonise each other, and is often hindered by the high degree of correlation between concentrations of several particulate components. The other approach would be to consider PM from different environments (e.g. underground railway station, heavily trafficked road), taking a holistic approach to each, by first considering the concentration of PM required to elicit a certain response, and investigating the culpable constituents only as a secondary priority. However, this approach is problematic in that similar environments can contain PM of different profiles, and so the PM next to the side of one heavily trafficked road may differ from that collected at a different heavily trafficked road site, or one underground railway station may contain PM which is different in composition to another underground station in a different city, or even the same city (80). Therefore extrapolation of findings between sites is difficult.

One way in which such studies may be improved is by careful selection of the sites at which PM will be collected, so that sites with contrasting PM profiles can be analysed, giving a greater potential for identification of the toxic constituents of PM. One example of this is a study entitled "Risk of Airborne Particles, a Toxicological-Epidemiological hybrid Study" (RAPTES). This study aims to investigate the potential health effects of airborne PM at various sites by collecting and chemically analysing PM from various sources, linking this to oxidative and pro-inflammatory changes *in vitro*, and finally examining *in vivo* effects, both on the airways and cardiovascular system. The RAPTES project, which commenced in 2007, is led by Professors Bert Brunekreef, Flemming Cassee, and Raymond Pieters, and Dr Gerard Hoek, as a collaboration between the University of Utrecht and the Dutch National Institute for Public Health and the Environment (RIVM). The initial phase of the study involved sampling from eight locations hypothesised to have contrasting airborne PM profiles, including urban sites with varying traffic profiles, a farm, an underground railway station, a harbour, and a steelworks. Size-fractionated airborne PM at these sites was

quantified and analysed for chemical composition (454, 603), followed by analysis of particulate oxidative potential (by DTT assay) and ability to induce release of TNFα, IL-6, and MIP-2 by RAW 264.7 macrophages (447). From these results, the underground station, continuous and stop-go traffic sites, a farm, and urban background site were chosen for *in vivo* exposure work as the five sites with the most contrasting PM profiles, to reduce correlations between PM at different sites (604). At these sites, exhaled nitric oxide was especially associated with particle number concentration and iron content, while detrimental effects on FVC were associated with particle number concentration, NO_2 and NO_x immediately post-exposure, with associations for the latter two components still present the morning after exposure (604). This was followed by examination of the pro-inflammatory effects of site-specific PM *in vivo*, with the interesting observation that nasal lavage fluid, inflammatory mediators, and other markers of inflammation were associated with particulate organic carbon, endotoxin, and NO_2, but not the ability of PM to deplete ascorbate or GSH, suggesting mechanisms other than simple oxidative stress (605). More recently, publications from the RAPTES projects have examined the potential cardiovascular effects of airborne PM at the five selected sites, again noting a lack of effect of oxidative potential, but associations between blood markers of cardiovascular stress and particulate organic carbon, NO_3^-, and SO_4^{2-} (606), and similar results for thrombin generation observed *ex vivo* after blood sampling from exposed volunteers (607). This approach, taking account of PM characteristics and using this to refine site selection for subsequent *in vitro* and *in vivo* work, may yield new information regarding components of PM responsible for observed effects, especially since the selection of a number of contrasting study sites appears able to reduce inter-site correlations which may otherwise obfuscate the identity of the toxic components. It is also an example of how such studies can extend *in vivo* findings from airways as the site of PM deposition, to examining potential effects on the cardiovascular system, which has been epidemiologically connected to PM toxicity, but considerably less studied.

Studies such as RAPTES may shed more light on the constituents and mechanisms underlying particle toxicity. However, there remain problems with such studies when examining the chronic effects of exposure to particulate matter, since individuals may be exposed to more than one type of PM, for example underground railway

commuters who are likely to spend a large proportion of their time in polluted city environments. Moreover, the modelling of chronic responses in the laboratory is very difficult, since despite recent attempts to model repeated exposures, cell cultures are difficult to maintain for longer than a period of several weeks (506). There is evidence that repeated exposure to PM in mice produces different outcomes to single exposures, with the differences varying depending on what parameter is measured (608). To this end, there exists the potential for the use of RNA sequencing (RNAseq) to identify as-yet unexplored effects of particulate matter, both on the airways and other organs and tissues (609, 610). RNA microarray has already been used to examine cellular responses to particulate matter and smoking both in healthy and diseases individuals, and also *in vitro* (611-613). However, RNAseq is an improvement over RNA microarray in that the former is not complicated by the potential for cross-hybridisation (RNA binding to a probe which is not fully complementary) meaning that there is less "noise", and RNAseq is also able to give absolute numbers of gene transcripts, rather than expressing results merely in relative terms. Finally, RNAseq is better able to detect and quantify hitherto unrecognised splice variants. After data analysis, genes of interest which have been identified by RNAseq can be verified by standard RT-qPCR. Additionally, RNAseq data can be used to build maps of interconnected genes which response to particulate matter, and thus responses at the pathway level can be identified (614). This holistic approach to the effects of inhaled PM, examining changes to the functioning of the cell as a whole rather than just inflammatory or antioxidant pathways, is likely to shed new light on the toxic effects of particulate matter. Indeed, while this approach may not be as effective as the hypothetical study of the effects of particles on cell cultures over many years, RNAseq with subsequent pathway analysis may yield new information on the potential chronic effects of exposure to particulate matter. Furthermore, it may suggest which biomarkers (or more likely groups of biomarkers) would be suitable for measurement as biomarkers of exposure to, and the toxicity of, particulate matter. Although markers of processes which may be important in the effects of long-term exposure to PM can be measured, perhaps best by using techniques such as RNAseq as above, it is difficult to take into account PM accumulation and clearance and, as discussed above, the potential for translocation of PM to other sites in the body. Therefore, it is clear that such studies have to be informed by epidemiological findings. Yet again,

however, there are problems with relying on the epidemiological approach, since chronic effects may only become apparent after many years of exposure, by which time there may be many individuals who have been put at risk. Furthermore, while epidemiological studies may be able to determine trends within large populations, they may be less well-powered to unmask the dangers of PM exposure in certain subgroups, especially if these subgroups are defined by a marker whose interaction with air pollution is not yet known (for example, a genetic polymorphism which is hitherto unrecognised as causing predisposition to the effects of airborne PM).

6.1.7 Potential Measures to Reduce the Risk Posed by PM

Alongside experimental research, which takes time, there needs to be consideration of how to protect passengers and, perhaps more importantly, rail workers, from the potential effects of underground railway particulate matter. There are two aspects which require consideration here – how to reduce exposure and, accepting that exposure is likely to continue, how to lessen the potential effects of exposure.

The literature offers a paucity of suggestions as to how exposure to underground railway PM may be ameliorated. It has been suggested that trains running on pneumatic tyres generate less toxic PM than those running with steel wheels on steel rails (80), and that concrete ballast produces less dust than gravel ballast (although concrete ballast is also more expensive and produces more noise and vibration) (252). However, changing the wheel or ballast type in an entire underground system would be hugely expensive and likely to result in great disruption to services. Such methods are, therefore, unviable in all but the long-term or by phased replacement. There are other potential methods of reducing PM levels which do not involve alterations to existing features of the railway. One such option is the washing of tunnel walls to remove deposited PM, thereby preventing its re-entrainment by passing trains. However, it is uncertain how effective this would be (65, 72), and on large underground railway networks is likely to be impractical. Second, it has been suggested that, on account of the magnetic nature of underground railway PM as found in some studies (252, 456), giant electromagnets located on station platforms

could be used to collect PM, removing it from the air (252). However, this is likely to have implications for other magnetic objects which may be carried by passengers, and potentially electronic devices such as mobile phones and, disconcertingly, cardiac pacemakers. As such, this suggestion is unlikely ever to be put into practice. A final suggestion is the use of platform-edge doors (93, 252), which are more commonly used to prevent suicide attempts. There are certain caveats to this approach – it is likely to be expensive, the cost and practicality of fitting such equipment to old stations (as opposed to having the equipment in new stations) is likely to be high, the barrier would need to cover the entire height of the tunnel from platform to ceiling, and there would be no effect on reducing the exposure to PM of anyone on the train. However, for potentially reducing the levels of PM to which platform staff and commuters waiting for trains are exposed, this may be the best method. Alternatively, personal exposure monitors could be provided to workers as a more discreet way to monitor exposure of members of staff according to their activities undertaken at work (93). It is known that, in indoor environments, there is a discrepancy between background PM levels as measured by monitors or impactors such as in this study, and in personal levels of exposure, which can be attributed to the so-called "cloud effect" (615, 616). The exact cause and magnitude of this effect is not fully understood, but is thought to be a consequence of the resuspension of particulate matter by human movement (615). One study attempting to mathematically relate microenvironment background PM_{10} concentrations to personal exposures showed a good correlation between the two, but only when a personal cloud correction was taken into account (617). Therefore, such personal monitoring would provide more accurate information about the levels of PM to which underground railway workers are exposed. Personal monitoring may allow targeting of screening methods (see below) to those workers who are exposed to the highest concentrations of PM. However, personal monitoring would do nothing to actually ameliorate background or personal PM exposure, and may well be of little use since it is already well understood that underground railway systems contain markedly raised concentrations of airborne particulate matter. In this regard, such personal monitoring is perhaps a more useful tool for scientific research rather than the protection of employee health.

Instead of reducing the levels of PM in the air in underground railway stations, an alternative method to reduce particle inhalation would be to supply underground railway workers with dust masks. It has been shown that different jobs within an underground railway system result in differing PM exposure levels, with maintenance work, particularly track maintenance, bringing about especially high exposure levels (93). Therefore, certain workers could be provided with masks to reduce their inhalation of particulate matter. However, this is unlikely to be viable for customer-facing staff and train drivers, since the sight of platform staff wearing masks is likely to cause alarm to the travelling public, and probably a slew of alarmist stories in the tabloid press.

Therefore, it seems unlikely that any practical measures can be found to significantly reduce exposure to airborne particulate matter, at least in the short term. An alternative approach is to attempt to ameliorate any adverse health effects of particulate air pollution in underground railways. To do so would require a programme of occupational health screening to be initiated. This should take into account the health status of workers especially, but not limited to, the presence of asthma or COPD or symptoms thereof, cardiovascular disorders, and smoking status. At the very least, this should involve a questionnaire of the individual worker's symptoms (e.g. upper airway irritation, breathing difficulty at rest and varying levels of exertion) but should ideally involve lung function testing, since reduced lung function appears to be a consistent marker of the deleterious effect of particulate air pollution, and cardiovascular checks such as blood pressure.

Of course, one drastic option would be to avoid the further construction of underground railway systems altogether. However, it must be remembered that overground environments in cities are also somewhat polluted, and that journeys above ground (e.g. by bus or walking along a busy street) may take several times longer than the same journeys made by underground railway. Indeed, there is evidence that urban metro systems can reduce urban carbon monoxide levels, indicating decreased vehicular pollution (618). Therefore, while exposure to underground railway particulate matter may perturb the airways in the short-term on account of its high concentration of metal-rich particles, including a metal-rich ultrafine fraction, and

there may also be health effects with chronic exposure, it seems likely that further research to understand the effects of such exposure, and regular health monitoring of the most exposed groups, is the most sensible way forward, and perhaps the best of a series of less-than-ideal options (Figure 6.1).

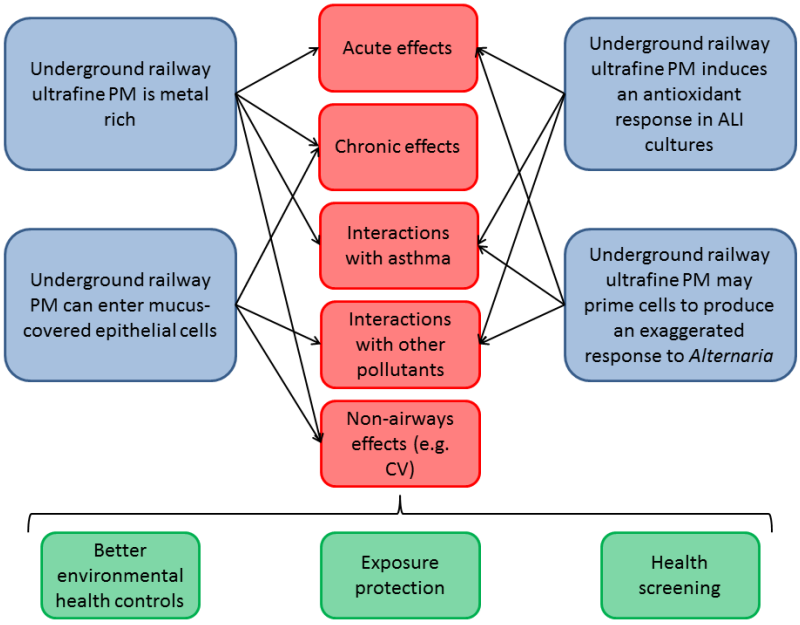

Figure 6.1. The novel findings presented in this thesis, and their potential implications. The four overriding novel findings of this thesis (blue) may have a range of implications which need to be considered in further work (red). Such work will better inform the measures which can be taken to lessen the potentially damaging effects of underground railway particulate matter (green).

6.2 Final Conclusion

The work detailed within this thesis has found that underground railway PM, notably the ultrafine fraction thereof, is rich in iron and other transition metals, allowing the particles to induce increased antioxidant gene expression in primary bronchial epithelial cell cultures, even those covered with a cytoprotective mucous layer. This mucous layer also fails to prevent the ingression of particles to a variety of intracellular compartments, with potential ramifications for chronic responses. Preliminary findings indicate that ultrafine underground railway PM may prime bronchial epithelial

cells to respond to the airborne fungus *Alternaria* with a greater expression of antioxidants and Th2 cytokines, both of which may be deranged in asthma. Further work is required to determine the chronic effects of underground railway particulate matter, whether there is an increased risk posed by the interaction of different types of airborne particulates, and whether there is a greater susceptibility to these effects in asthmatics.

7 References

1. International Commission on Radiological Protection. Task Group on Reference Man. 1975. *Report of the Task Group on Reference Man : a report*. Pergamon Press, Oxford ; New York.

2. Davies, J. A., and D. R. Garrod. 1997. Molecular aspects of the epithelial phenotype. *Bioessays* 19: 699-704.

3. Knight, D. A., and S. T. Holgate. 2003. The airway epithelium: structural and functional properties in health and disease. *Respirology* 8: 432-446.

4. Reynolds, S. D., and A. M. Malkinson. 2010. Clara cell: Progenitor for the bronchiolar epithelium. *Int J Biochem Cell B* 42: 1-4.

5. Crapo, J. D., B. E. Barry, P. Gehr, M. Bachofen, and E. R. Weibel. 1982. Cell Number and Cell Characteristics of the Normal Human Lung. *American Review of Respiratory Disease* 126: 332-337.

6. Swindle, E. J., J. E. Collins, and D. E. Davies. 2009. Breakdown in epithelial barrier function in patients with asthma: Identification of novel therapeutic approaches. *Journal of Allergy and Clinical Immunology* 124: 23-34.

7. Cone, R. A. 2009. Barrier properties of mucus. *Adv Drug Deliver Rev* 61: 75-85.

8. Williams, O. W., A. Sharafkhaneh, V. Kim, B. F. Dickey, and C. M. Evans. 2006. Airway mucus - From production to secretion. *American Journal of Respiratory Cell and Molecular Biology* 34: 527-536.

9. Bals, R., and P. S. Hiemstra. 2004. Innate immunity in the lung: how epithelial cells fight against respiratory pathogens. *Eur Respir J* 23: 327-333.

10. Knowles, M. R., and R. C. Boucher. 2002. Mucus clearance as a primary innate defense mechanism for mammalian airways. *Journal of Clinical Investigation* 109: 571-577.

11. Holgate, S. T. 2007. Epithelium dysfunction in asthma. *Journal of Allergy and Clinical Immunology* 120: 1233-1246.

12. Hardyman, M. A., E. Wilkinson, E. Martin, N. P. Jayasekera, C. Blume, E. J. Swindle, N. Gozzard, S. T. Holgate, P. H. Howarth, D. E. Davies, and J. E. Collins. 2013. TNF-alpha-mediated bronchial barrier disruption and regulation by src-family kinase activation. *J Allergy Clin Immunol* 132: 665-675 e668.

13. Capaldo, C. T., and A. Nusrat. 2009. Cytokine regulation of tight junctions. *Biochim Biophys Acta* 1788: 864-871.

14. Sajjan, U., Q. Wang, Y. Zhao, D. C. Gruenert, and M. B. Hershenson. 2008. Rhinovirus Disrupts the Barrier Function of Polarized Airway Epithelial Cells. *American Journal of Respiratory and Critical Care Medicine* 178: 1271-1281.

15. Wan, H., H. L. Winton, C. Soeller, E. R. Tovey, D. C. Gruenert, P. J. Thompson, G. A. Stewart, G. W. Taylor, D. R. Garrod, M. B. Cannell, and C. Robinson. 1999. Der p 1 facilitates transepithelial allergen delivery by disruption of tight junctions. *J Clin Invest* 104: 123-133.

16. Hammad, H., and B. N. Lambrecht. 2008. Dendritic cells and epithelial cells: linking innate and adaptive immunity in asthma. *Nature Reviews Immunology* 8: 193-204.

17. Tran, C. L., D. Buchanan, R. T. Cullen, A. Searl, A. D. Jones, and K. Donaldson. 2000. Inhalation of poorly soluble particles. II. Influence of particle surface area on inflammation and clearance. *Inhalation Toxicology* 12: 1113-1126.

18. Heyder, J., J. Gebhart, G. Rudolf, C. F. Schiller, and W. Stahlhofen. 1986. Deposition of Particles in the Human Respiratory-Tract in the Size Range 0.005-15 μm. *Journal of Aerosol Science* 17: 811-825.

19. U.S. EPA. 2009. Integrated Science Assessment for Particulate Matter (Final Report). United States Environmental Protection Agency, Washington, DC.

20. Lippmann, M., D. B. Yeates, and R. E. Albert. 1980. Deposition, retention, and clearance of inhaled particles. *British journal of industrial medicine* 37: 337-362.

21. Curentec. 2013. Salt Therapy. Curentec.

22. Lemanske, R. F., and W. W. Busse. 2010. Asthma: Clinical expression and molecular mechanisms. *Journal of Allergy and Clinical Immunology* 125: S95-S102.

23. Lambrecht, B. N., and H. Hammad. 2012. The airway epithelium in asthma. *Nat Med* 18: 684-692.

24. Holloway, J. W., I. A. Yang, and S. T. Holgate. 2010. Genetics of allergic disease. *Journal of Allergy and Clinical Immunology* 125: S81-S94.

25. Vestbo, J., S. S. Hurd, A. G. Agusti, P. W. Jones, C. Vogelmeier, A. Anzueto, P. J. Barnes, L. M. Fabbri, F. J. Martinez, M. Nishimura, R. A. Stockley, D. D. Sin, and R. Rodriguez-Roisin. 2013. Global Strategy for the Diagnosis, Management, and Prevention of Chronic Obstructive Pulmonary Disease. GOLD Executive Summary. *American Journal of Respiratory and Critical Care Medicine* 187: 347-365.

26. Firket, J. 1931. Sur les causes des accidents survenus dans la vallée de la Meuse, lors des brouillards de décembre 1930 : résultats de l'expertise judiciaire faite par MM Delahu, Schoofs, Mage, Batta, Bovy et Firket. *Bull Acad R Belg* 11: 683-734.

27. Nemery, B., P. H. M. Hoet, and A. Nemmar. 2001. The Meuse Valley fog of 1930: an air pollution disaster. *Lancet* 357: 704-708.

28. Logan, W. P. 1953. Mortality in the London fog incident, 1952. *Lancet* 1: 336-338.

29. Waller, R. E., and P. J. Lawther. 1955. Some observations on London fog. *British medical journal* 2: 1356-1358.

30. Waller, R. E., and P. J. Lawther. 1957. Further observations on London fog. *British medical journal* 2: 1473-1475.

31. Commins, B. T., and R. E. Waller. 1967. Observations from a ten-year-study of pollution at a site in the City of London. *Atmospheric Environment (1967)* 1: 49-68.

32. Seaton, A., W. Macnee, K. Donaldson, and D. Godden. 1995. Particulate Air-Pollution and Acute Health-Effects. *Lancet* 345: 176-178.

33. Valavanidis, A., K. Fiotakis, and T. Vlachogianni. 2008. Airborne Particulate Matter and Human Health: Toxicological Assessment and Importance of Size and Composition of Particles for Oxidative Damage and Carcinogenic Mechanisms. *Journal of Environmental Science and Health Part C-Environmental Carcinogenesis & Ecotoxicology Reviews* 26: 339-362.

34. Dockery, D. W., and C. A. Pope. 1994. Acute Respiratory Effects of Particulate Air-Pollution. *Annu Rev Publ Health* 15: 107-132.

35. Brunekreef, B., and S. T. Holgate. 2002. Air pollution and health. *Lancet* 360: 1233-1242.

36. Cho, S. H., H. Y. Tong, J. K. McGee, R. W. Baldauf, Q. T. Krantz, and M. I. Gilmour. 2009. Comparative Toxicity of Size-Fractionated Airborne

Particulate Matter Collected at Different Distances from an Urban Highway. *Environmental Health Perspectives* 117: 1682-1689.

37. Peters, A., H. E. Wichmann, T. Tuch, J. Heinrich, and J. Heyder. 1997. Respiratory effects are associated with the number of ultrafine particles. *American Journal of Respiratory and Critical Care Medicine* 155: 1376-1383.

38. Churg, A., and M. Brauer. 1997. Human lung parenchyma retains PM2.5. *American Journal of Respiratory and Critical Care Medicine* 155: 2109-2111.

39. Stanier, C. O., A. Y. Khlystov, and S. N. Pandis. 2004. Nucleation events during the Pittsburgh air quality study: Description and relation to key meteorological, gas phase, and aerosol parameters. *Aerosol Sci Tech* 38: 253-264.

40. Sioutas, C., R. J. Delfino, and M. Singh. 2005. Exposure assessment for atmospheric ultrafine particles (UFPs) and implications in epidemiologic research. *Environmental Health Perspectives* 113: 947-955.

41. BeruBe, K., D. Balharry, K. Sexton, L. Koshy, and T. Jones. 2007. Combustion-derived nanoparticles: Mechanisms of pulmonary toxicity. *Clin Exp Pharmacol P* 34: 1044-1050.

42. Dockery, D. W., C. A. Pope, X. P. Xu, J. D. Spengler, J. H. Ware, M. E. Fay, B. G. Ferris, and F. E. Speizer. 1993. An Association between Air-Pollution and Mortality in 6 United States Cities. *New England Journal of Medicine* 329: 1753-1759.

43. Pope, C. A., R. T. Burnett, M. J. Thun, E. E. Calle, D. Krewski, K. Ito, and G. D. Thurston. 2002. Lung cancer, cardiopulmonary mortality, and long-term exposure to fine particulate air pollution. *Journal of the American Medical Association* 287: 1132-1141.

44. Raaschou-Nielsen, O., Z. J. Andersen, R. Beelen, E. Samoli, M. Stafoggia, G. Weinmayr, B. Hoffmann, P. Fischer, M. J. Nieuwenhuijsen, B. Brunekreef, W.

W. Xun, K. Katsouyanni, K. Dimakopoulou, J. Sommar, B. Forsberg, L. Modig, A. Oudin, B. Oftedal, P. E. Schwarze, P. Nafstad, U. De Faire, N. L. Pedersen, C. G. Ostenson, L. Fratiglioni, J. Penell, M. Korek, G. Pershagen, K. T. Eriksen, M. Sorensen, A. Tjonneland, T. Ellermann, M. Eeftens, P. H. Peeters, K. Meliefste, M. Wang, B. Bueno-de-Mesquita, T. J. Key, K. de Hoogh, H. Concin, G. Nagel, A. Vilier, S. Grioni, V. Krogh, M. Y. Tsai, F. Ricceri, C. Sacerdote, C. Galassi, E. Migliore, A. Ranzi, G. Cesaroni, C. Badaloni, F. Forastiere, I. Tamayo, P. Amiano, M. Dorronsoro, A. Trichopoulou, C. Bamia, P. Vineis, and G. Hoek. 2013. Air pollution and lung cancer incidence in 17 European cohorts: prospective analyses from the European Study of Cohorts for Air Pollution Effects (ESCAPE). *The lancet oncology* 14: 813-822.

45. Mokdad, A. H., J. S. Marks, D. F. Stroup, and J. L. Gerberding. 2004. Actual causes of death in the United States, 2000. *Journal of the American Medical Association* 291: 1238-1245.

46. Shah, A. S., J. P. Langrish, H. Nair, D. A. McAllister, A. L. Hunter, K. Donaldson, D. E. Newby, and N. L. Mills. 2013. Global association of air pollution and heart failure: a systematic review and meta-analysis. *Lancet*.

47. Carey, I. M., R. W. Atkinson, A. J. Kent, T. van Staa, D. G. Cook, and H. R. Anderson. 2013. Mortality Associations with Long-Term Exposure to Outdoor Air Pollution in a National English Cohort. *American Journal of Respiratory and Critical Care Medicine* 187: 1226-1233.

48. Halonen, J. I., T. Lanki, T. Yli-Tuomi, M. Kulmala, P. Tiittanen, and J. Pekkanen. 2008. Urban air pollution, and asthma and COPD hospital emergency room visits. *Thorax* 63: 635-641.

49. Norris, G., S. N. YoungPong, J. Q. Koenig, T. V. Larson, L. Sheppard, and J. W. Stout. 1999. An association between fine particles and asthma emergency department visits for children in Seattle. *Environmental Health Perspectives* 107: 489-493.

50. Slaughter, J. C., E. Kim, L. Sheppard, J. H. Sullivan, T. V. Larson, and C. Claiborn. 2005. Association between particulate matter and emergency room visits, hospital admissions and mortality in Spokane, Washington. *J Expo Anal Environ Epidemiol* 15: 153-159.

51. Malig, B. J., S. Green, R. Basu, and R. Broadwin. 2013. Coarse Particles and Respiratory Emergency Department Visits in California. *Am J Epidemiol* 178: 58-69.

52. Gamble, J. F., and R. J. Lewis. 1996. Health and respirable particulate (PM(10)) air pollution: A causal or statistical association? *Environmental Health Perspectives* 104: 838-850.

53. Antonini, J. M., M. D. Taylor, S. S. Leonard, N. J. Lawryk, X. L. Shi, R. W. Clarke, and J. R. Roberts. 2004. Metal composition and solubility determine lung toxicity induced by residual oil fly ash collected from different sites within a power plant. *Molecular and Cellular Biochemistry* 255: 257-265.

54. Farina, F., G. Sancini, P. Mantecca, D. Gallinotti, M. Camatini, and P. Palestini. 2011. The acute toxic effects of particulate matter in mouse lung are related to size and season of collection. *Toxicology Letters* 202: 209-217.

55. Perrone, M. G., M. Gualtieri, V. Consonni, L. Ferrero, G. Sangiorgi, E. Longhin, D. Ballabio, E. Bolzacchini, and M. Camatini. 2013. Particle size, chemical composition, seasons of the year and urban, rural or remote site origins as determinants of biological effects of particulate matter on pulmonary cells. *Environ Pollut* 176: 215-227.

56. Sint, T., J. F. Donohue, and A. J. Ghio. 2008. Ambient air pollution particles and the acute exacerbation of chronic obstructive pulmonary disease. *Inhalation Toxicology* 20: 25-29.

57. Pope, C. A. 1989. Respiratory-Disease Associated with Community Air-Pollution and a Steel Mill, Utah Valley. *Am J Public Health* 79: 623-628.

58. Dye, J. A., J. R. Lehmann, J. K. McGee, D. W. Winsett, A. D. Ledbetter, J. I. Everitt, A. J. Ghio, and D. L. Costa. 2001. Acute pulmonary toxicity of particulate matter filter extracts in rats: Coherence with epidemiologic studies in Utah Valley residents. *Environmental Health Perspectives* 109: 395-403.

59. Dales, R., L. M. Kauri, S. Cakmak, M. Mahmud, S. A. Weichenthal, K. Van Ryswyk, P. Kumarathasan, E. Thomson, R. Vincent, G. Broad, and L. Liu. 2013. Acute changes in lung function associated with proximity to a steel plant: A randomized study. *Environ Int* 55: 15-19.

60. Lippmann, M., K. Ito, J. S. Hwang, P. Maciejczyk, and L. C. Chen. 2006. Cardiovascular effects of nickel in ambient air. *Environmental Health Perspectives* 114: 1662-1669.

61. World Health Organization. 2006. *Air quality guidelines : global update 2005 : particulate matter, ozone, nitrogen dioxide, and sulfur dioxide*. World Health Organization, Copenhagen, Denmark.

62. Health and Safety Executive. 2011. *EH40/2005 workplace exposure limits : containing the list of workplace exposure limits for use with the Control of Substances Hazardous to Health Regulations (as amended)*. HSE Books, Norwich.

63. Transport for London. 2013. Annual Report and Statement of Accounts 2012/13. TfL, London.

64. Klepczynska Nystrom, A., M. Svartengren, J. Grunewald, C. Pousette, I. Rodin, A. Lundin, C. M. Skold, A. Eklund, and B. M. Larsson. 2010. Health effects of a subway environment in healthy volunteers. *European Respiratory Journal* 36: 240-248.

65. Johansson, C., and P. A. Johansson. 2003. Particulate matter in the underground of Stockholm. *Atmospheric Environment* 37: 3-9.

66. Seaton, A., J. Cherrie, M. Dennekamp, K. Donaldson, J. F. Hurley, and C. L. Tran. 2005. The London Underground: dust and hazards to health. *Occup Environ Med* 62: 355-362.

67. Sitzmann, B., M. Kendall, J. Watt, and I. Williams. 1999. Characterisation of airborne particles in London by computer-controlled scanning electron microscopy. *Science of the Total Environment* 241: 63-73.

68. Murray, D. 2002. Passengers choke on the tube. *London Evening Standard*.

69. Adams, H. S., M. J. Nieuwenhuijsen, R. N. Colvile, M. A. S. McMullen, and P. Khandelwal. 2001. Fine particle (PM2.5) personal exposure levels in transport microenvironments, London, UK. *Science of the Total Environment* 279: 29-44.

70. Pfeifer, G. D., R. M. Harrison, and D. R. Lynam. 1999. Personal exposures to airborne metals in London taxi drivers and office workers in 1995 and 1996. *Science of the Total Environment* 235: 253-260.

71. Colvile, R. 2005. The London Underground: time for a thorough clean-up? *Occup Environ Med* 62: 354.

72. Branis, M. 2006. The contribution of ambient sources to particulate pollution in spaces and trains of the Prague underground transport system. *Atmospheric Environment* 40: 348-356.

73. Kang, S., H. Hwang, Y. Park, H. Kim, and C. U. Ro. 2008. Chemical Compositions of Subway Particles in Seoul, Korea Determined by a Quantitative Single Particle Analysis. *Environmental Science & Technology* 42: 9051-9057.

74. Fromme, H., A. Oddoy, M. Piloty, M. Krause, and T. Lahrz. 1998. Polycyclic aromatic hydrocarbons (PAH) and diesel engine emission (elemental carbon) inside a car and a subway train. *Science of the Total Environment* 217: 165-173.

75. Chan, L. Y., W. L. Lau, S. C. Zou, Z. X. Cao, and S. C. Lai. 2002. Exposure level of carbon monoxide and respirable suspended particulate in public transportation modes while commuting in urban, area of Guangzhou, China. *Atmospheric Environment* 36: 5831-5840.

76. Aarnio, P., T. Yli-Tuomi, A. Kousa, T. Makela, A. Hirsikko, K. Hameri, M. Raisanen, R. Hillamo, T. Koskentalo, and M. Jantunen. 2005. The concentrations and composition of and exposure to fine particles (PM2.5) in the Helsinki subway system. *Atmospheric Environment* 39: 5059-5066.

77. Hurley, J. F., J. Cherrie, K. Donaldson, A. Seaton, and C. L. Tran. 2003. Assessment of health effects of long-term occupational exposure to tunnel dust in the London Underground. Institute of Occupational Medicine, Edinburgh.

78. Gomez-Perales, J. E., R. N. Colvile, M. J. Nieuwenhuijsen, A. Fernandez-Bremauntz, V. J. Gutierrez-Avedoy, V. H. Paramo-Figueroa, S. Blanco-Jimenez, E. Bueno-Lopez, F. Mandujano, R. Bernabe-Cabanillas, and E. Ortiz-Segovia. 2004. Commuters' exposure to PM2.5, CO, and benzene in public transport in the metropolitan area of Mexico City. *Atmospheric Environment* 38: 1219-1229.

79. Chillrud, S. N., D. Epstein, J. M. Ross, S. N. Sax, D. Pederson, J. D. Spengler, and P. L. Kinney. 2004. Elevated airborne exposures of teenagers to manganese, chromium, and iron from steel dust and New York City's subway system. *Environmental Science & Technology* 38: 732-737.

80. Bachoual, R., J. Boczkowski, D. Goven, N. Amara, L. Tabet, D. On, V. Lecon-Malas, M. Aubier, and S. Lanone. 2007. Biological effects of particles from the Paris subway system. *Chemical Research in Toxicology* 20: 1426-1433.

81. Ripanucci, G., M. Grana, L. Vicentini, A. Magrini, and A. Bergamaschi. 2006. Dust in the underground railway tunnels of an Italian town. *Journal of Occupational and Environmental Hygiene* 3: 16-25.

82. Kim, K. Y., Y. S. Kim, Y. M. Roh, C. M. Lee, and C. N. Kim. 2008. Spatial distribution of particulate matter (PM10 and PM2.5) in Seoul Metropolitan Subway stations. *J Hazard Mater* 154: 440-443.

83. Park, D. U., and K. C. Ha. 2008. Characteristics of PM10, PM2.5, CO2 and CO monitored in interiors and platforms of subway train in Seoul, Korea. *Environ Int* 34: 629-634.

84. Bigert, C., M. Alderling, M. Svartengren, N. Plato, and P. Gustavsson. 2011. No short-term respiratory effects among particle-exposed employees in the Stockholm subway. *Scandinavian Journal of Work Environment & Health* 37: 129-135.

85. McNamara, M. L., C. W. Noonan, and T. J. Ward. 2011. Correction Factor for Continuous Monitoring of Wood Smoke Fine Particulate Matter. *Aerosol Air Qual Res* 11: 316-323.

86. Baccarelli, A., I. Martinelli, A. Zanobetti, P. Grillo, L. F. Hou, P. A. Bertazzi, P. M. Mannucci, and J. Schwartz. 2008. Exposure to particulate air pollution and risk of deep vein thrombosis. *Arch Intern Med* 168: 920-927.

87. Peters, A. 2011. Ambient Particulate Matter and the Risk for Cardiovascular Disease Introduction. *Prog Cardiovasc Dis* 53: 327-333.

88. Mills, N. L., K. Donaldson, P. W. Hadoke, N. A. Boon, W. MacNee, F. R. Cassee, T. Sandstrom, A. Blomberg, and D. E. Newby. 2009. Adverse cardiovascular effects of air pollution. *Nat Clin Pract Card* 6: 36-44.

89. Bigert, C., M. Alderling, M. Svartengren, N. Plato, U. de Faire, and P. Gustavsson. 2008. Blood markers of inflammation and coagulation and exposure to airborne particles in employees in the Stockholm underground. *Occupational and Environmental Medicine* 65: 655-658.

90. Bigert, C., K. Klerdal, N. Hammar, and P. Gustavsson. 2007. Myocardial infarction in Swedish subway drivers. *Scandinavian Journal of Work Environment & Health* 33: 267-271.

91. Budinger, G. R. S., J. L. McKell, D. Urich, N. Foiles, I. Weiss, S. E. Chiarella, A. Gonzalez, S. Soberanes, A. J. Ghio, R. Nigdelioglu, E. A. Mutlu, K. A. Radigan, D. Green, H. C. Kwaan, and G. M. Mutlu. 2011. Particulate Matter-Induced Lung Inflammation Increases Systemic Levels of PAI-1 and Activates Coagulation Through Distinct Mechanisms. *Plos One* 6: -.

92. Gustavsson, P., C. Bigert, and M. Pollan. 2008. Incidence of lung cancer among subway drivers in Stockholm. *American Journal of Industrial Medicine* 51: 545-547.

93. Grass, D. S., J. M. Ross, F. Family, J. Barbour, H. J. Simpson, D. Coulibaly, J. Hernandez, Y. D. Chen, V. Slavkovich, Y. L. Li, J. Graziano, R. M. Santella, P. Brandt-Rauf, and S. N. Chillrud. 2010. Airborne particulate metals in the New York City subway: A pilot study to assess the potential for health impacts. *Environ Res* 110: 1-11.

94. Pekkanen, J., E. J. Brunner, H. R. Anderson, P. Tiittanen, and R. W. Atkinson. 2000. Daily concentrations of air pollution and plasma fibrinogen in London. *Occupational and Environmental Medicine* 57: 818-822.

95. Nawrot, T. S., N. Kuenzli, J. Sunyer, T. M. Shi, T. Moreno, M. Viana, J. Heinrich, B. Forsberg, F. J. Kelly, M. Sughis, B. Nemery, and P. Borm. 2009. Oxidative properties of ambient PM2.5 and elemental composition: Heterogeneous associations in 19 European cities. *Atmospheric Environment* 43: 4595-4602.

96. Moller, W., K. Felten, K. Sommerer, G. Scheuch, G. Meyer, P. Meyer, K. Haussinger, and W. G. Kreyling. 2008. Deposition, retention, and translocation of ultrafine particles from the central airways and lung periphery. *American Journal of Respiratory and Critical Care Medicine* 177: 426-432.

97. Kim, C. S., and T. C. Kang. 1997. Comparative measurement of lung deposition of inhaled fine particles in normal subjects and patients with obstructive airway disease. *American Journal of Respiratory and Critical Care Medicine* 155: 899-905.

98. Brown, J. S., K. L. Zeman, and W. D. Bennett. 2002. Ultrafine particle deposition and clearance in the healthy and obstructed lung. *American Journal of Respiratory and Critical Care Medicine* 166: 1240-1247.

99. Arbex, M. A., G. M. D. Conceicao, S. P. Cendon, F. F. Arbex, A. C. Lopes, E. P. Moyses, S. L. Santiago, P. H. N. Saldiva, L. A. A. Pereira, and A. L. F. Braga. 2009. Urban air pollution and chronic obstructive pulmonary disease-related emergency department visits. *J Epidemiol Commun H* 63: 777-783.

100. Gong, H., W. S. Linn, K. W. Clark, K. R. Anderson, M. D. Geller, and C. Sioutas. 2005. Respiratory responses to exposures with fine particulates and nitrogen dioxide in the elderly with and without COPD. *Inhalation Toxicology* 17: 123-132.

101. May, K. R. 1945. The Cascade Impactor: An Instrument for Sampling Coarse Aerosols. *Journal of Scientific Instruments* 22: 187.

102. Hounam, R. F., and R. J. Sherwood. 1965. The cascade centripeter: a device for determining the concentration and size distribution of aerosols. *American Industrial Hygiene Association Journal* 26: 122-131.

103. John, W., D. N. Fritter, and W. Winklmayr. 1991. Resuspension Induced by Impacting Particles. *Journal of Aerosol Science* 22: 723-736.

104. Turner, J. R., and S. V. Hering. 1987. Greased and Oiled Substrates as Bounce-Free Impaction Surfaces. *Journal of Aerosol Science* 18: 215-224.

105. Lawson, D. R. 1980. Impaction Surface-Coatings Intercomparison and Measurements with Cascade Impactors. *Atmospheric Environment* 14: 195-199.

106. Chen, B. T., and H. C. Yeh. 1987. An Improved Virtual Impactor - Design and Performance. *Journal of Aerosol Science* 18: 203-214.

107. Loo, B. W., and C. P. Cork. 1988. Development of High-Efficiency Virtual Impactors. *Aerosol Sci Tech* 9: 167-176.

108. Sioutas, C., P. Koutrakis, and R. M. Burton. 1994. Development of a Low Cutpoint Slit Virtual Impactor for Sampling Ambient Fine Particles. *Journal of Aerosol Science* 25: 1321-1330.

109. Demokritou, P., I. G. Kavouras, S. T. Ferguson, and P. Koutrakis. 2002. Development of a high volume cascade impactor for toxicological and chemical characterization studies. *Aerosol Sci Tech* 36: 925-933.

110. McConnell, R., W. D. Wu, K. Berhane, F. F. Liu, G. Verma, D. Peden, D. Diaz-Sanchez, and S. Fruin. 2013. Inflammatory Cytokine Response to Ambient Particles Varies due to Field Collection Procedures. *American Journal of Respiratory Cell and Molecular Biology* 48: 497-502.

111. Daher, N., Z. Ning, A. K. Cho, M. Shafer, J. J. Schauer, and C. Sioutas. 2011. Comparison of the Chemical and Oxidative Characteristics of Particulate Matter (PM) Collected by Different Methods: Filters, Impactors, and BioSamplers. *Aerosol Sci Tech* 45: 1294-1304.

112. Kim, S., P. A. Jaques, M. C. Chang, T. Barone, C. Xiong, S. K. Friedlander, and C. Sioutas. 2001. Versatile aerosol concentration enrichment system (VACES) for simultaneous in vivo and in vitro evaluation of toxic effects of ultrafine, fine and coarse ambient particles - Part II: Field evaluation. *Journal of Aerosol Science* 32: 1299-1314.

113. Kim, S., P. A. Jaques, M. C. Chang, J. R. Froines, and C. Sioutas. 2001. Versatile aerosol concentration enrichment system (VACES) for simultaneous in vivo and in vitro evaluation of toxic effects of ultrafine, fine and coarse

ambient particles - Part I: Development and laboratory characterization. *Journal of Aerosol Science* 32: 1281-1297.

114. Degobbi, C., P. H. N. Saldiva, and C. Rogers. 2011. Endotoxin as modifier of particulate matter toxicity: a review of the literature. *Aerobiologia* 27: 97-105.

115. Thorne, P. S., K. Kulhankova, M. Yin, R. Cohn, S. J. Arbes, and D. C. Zeldin. 2005. Endotoxin exposure is a risk factor for asthma - The National Survey of Endotoxin in United States Housing. *American Journal of Respiratory and Critical Care Medicine* 172: 1371-1377.

116. Lu, Y. C., W. C. Yeh, and P. S. Ohashi. 2008. LPS/TLR4 signal transduction pathway. *Cytokine* 42: 145-151.

117. Pugin, J., C. C. Schurermaly, D. Leturcq, A. Moriarty, R. J. Ulevitch, and P. S. Tobias. 1993. Lipopolysaccharide Activation of Human Endothelial and Epithelial-Cells Is Mediated by Lipopolysaccharide-Binding Protein and Soluble Cd14. *P Natl Acad Sci USA* 90: 2744-2748.

118. Dong, W. M., J. Lewtas, and M. I. Luster. 1996. Role of endotoxin in tumor necrosis factor alpha expression from alveolar macrophages treated with urban air particles. *Exp Lung Res* 22: 577-592.

119. Morrison, D. C., and D. M. Jacobs. 1976. Binding of Polymyxin-B to Lipid-a Portion of Bacterial Lipopolysaccharides. *Immunochemistry* 13: 813-818.

120. Soukup, J. M., and S. Becker. 2001. Human alveolar macrophage responses to air pollution particulates are associated with insoluble components of coarse material, including particulate endotoxin. *Toxicology and Applied Pharmacology* 171: 20-26.

121. Alexis, N. E., J. C. Lay, K. Zeman, W. E. Bennett, D. B. Peden, J. M. Soukup, R. B. Devlin, and S. Becker. 2006. Biological material on inhaled coarse

fraction particulate matter activates airway phagocytes in vivo in healthy volunteers. *Journal of Allergy and Clinical Immunology* 117: 1396-1403.

122. Myatt, T. A., M. S. Vincent, L. Kobzik, L. P. Naeher, D. L. MacIntosh, and H. Suh. 2011. Markers of inflammation in alveolar cells exposed to fine particulate matter from prescribed fires and urban air. *Journal of occupational and environmental medicine / American College of Occupational and Environmental Medicine* 53: 1110-1114.

123. Imrich, A., Y. Y. Ning, H. Koziel, B. Coull, and L. Kobzik. 1999. Lipopolysaccharide priming amplifies lung macrophage tumor necrosis factor production in response to air particles. *Toxicology and Applied Pharmacology* 159: 117-124.

124. Gonzalez-Flecha, B. 2004. Oxidant mechanisms in response to ambient air particles. *Mol Aspects Med* 25: 169-182.

125. Jimenez, L. A., J. Thompson, D. A. Brown, I. Rahman, F. Antonicelli, R. Duffin, E. M. Drost, R. T. Hay, K. Donaldson, and W. MacNee. 2000. Activation of NF-kappa B by PM10 occurs via an iron-mediated mechanism in the absence of I kappa B degradation. *Toxicology and Applied Pharmacology* 166: 101-110.

126. Schulz, C., L. Farkas, K. Wolf, K. Kratzel, G. Eissner, and M. Pfeifer. 2002. Differences in LPS-induced activation of bronchial epithelial cells (BEAS-2B) and type II-like pneumocytes (A549). *Scand J Immunol* 56: 294-302.

127. Roos-Engstrand, E., A. Wallin, A. Bucht, J. Pourazar, T. Sandstrom, and A. Blomberg. 2005. Increased expression of p38 MAPK in human bronchial epithelium after lipopolysaccharide exposure. *European Respiratory Journal* 25: 797-803.

128. Shyamsundar, M., S. McKeown, C. Calfee, B. Thompson, C. O'Kane, D. Thickett, T. Craig, M. Matthay, J. S. Elborn, and D. McAuley. 2009. Clinical studies into the pathogenesis of acute lung injury. *Thorax* 64: A23-A27.

129. Thompson, P. J. 1998. Unique role of allergens and the epithelium in asthma. *Clinical and Experimental Allergy* 28: 110-116.

130. Denning, D. W., B. R. O'Driscoll, C. M. Hogaboam, P. Bowyer, and R. M. Niven. 2006. The link between fungi and severe asthma: a summary of the evidence. *Eur Respir J* 27: 615-626.

131. Nathan, A. T., E. A. Peterson, J. Chakir, and M. Wills-Karp. 2009. Innate immune responses of airway epithelium to house dust mite are mediated through beta-glucan-dependent pathways. *Journal of Allergy and Clinical Immunology* 123: 612-618.

132. Wan, G. H., C. S. Li, S. P. Guo, R. Rylander, and R. H. Lin. 1999. An airborne mold-derived product, beta-1,3-D-glucan, potentiates airway allergic responses. *Eur J Immunol* 29: 2491-2497.

133. Hammad, H., M. Chieppa, F. Perros, M. A. Willart, R. N. Germain, and B. N. Lambrecht. 2009. House dust mite allergen induces asthma via Toll-like receptor 4 triggering of airway structural cells. *Nat Med* 15: 410-416.

134. Trompette, A., S. Divanovic, A. Visintin, C. Blanchard, R. S. Hegde, R. Madan, P. S. Thorne, M. Wills-Karp, T. L. Gioannini, J. P. Weiss, and C. L. Karp. 2009. Allergenicity resulting from functional mimicry of a Toll-like receptor complex protein. *Nature* 457: 585-588.

135. Borger, P., G. H. Koeter, J. A. Timmerman, E. Vellenga, J. F. Tomee, and H. F. Kauffman. 1999. Proteases from Aspergillus fumigatus induce interleukin (IL)-6 and IL-8 production in airway epithelial cell lines by transcriptional mechanisms. *J Infect Dis* 180: 1267-1274.

136. Tomee, J. F., A. T. Wierenga, P. S. Hiemstra, and H. K. Kauffman. 1997. Proteases from Aspergillus fumigatus induce release of proinflammatory cytokines and cell detachment in airway epithelial cell lines. *J Infect Dis* 176: 300-303.

137. Chiu, L. L., D. W. Perng, C. H. Yu, S. N. Su, and L. P. Chow. 2007. Mold allergen, pen C 13, induces IL-8 expression in human airway epithelial cells by activating protease-activated receptor 1 and 2. *J Immunol* 178: 5237-5244.

138. Monod, M., S. Capoccia, B. Lechenne, C. Zaugg, M. Holdom, and O. Jousson. 2002. Secreted proteases from pathogenic fungi. *Int J Med Microbiol* 292: 405-419.

139. Winton, H. L., H. Wan, M. B. Cannell, D. C. Gruenert, P. J. Thompson, D. R. Garrod, G. A. Stewart, and C. Robinson. 1998. Cell lines of pulmonary and non-pulmonary origin as tools to study the effects of house dust mite proteinases on the regulation of epithelial permeability. *Clin Exp Allergy* 28: 1273-1285.

140. Bhat, R. K., K. Page, A. Tan, and M. B. Hershenson. 2003. German cockroach extract increases bronchial epithelial cell interleukin-8 expression. *Clin Exp Allergy* 33: 35-42.

141. Dery, O., C. U. Corvera, M. Steinhoff, and N. W. Bunnett. 1998. Proteinase-activated receptors: novel mechanisms of signaling by serine proteases. *Am J Physiol-Cell Ph* 274: C1429-C1452.

142. Kouzaki, H., S. M. O'Grady, C. B. Lawrence, and H. Kita. 2009. Proteases induce production of thymic stromal lymphopoietin by airway epithelial cells through protease-activated receptor-2. *J Immunol* 183: 1427-1434.

143. Adam, E., K. K. Hansen, O. Astudillo Fernandez, L. Coulon, F. Bex, X. Duhant, E. Jaumotte, M. D. Hollenberg, and A. Jacquet. 2006. The house dust mite allergen Der p 1, unlike Der p 3, stimulates the expression of interleukin-8

in human airway epithelial cells via a proteinase-activated receptor-2-independent mechanism. *J Biol Chem* 281: 6910-6923.

144. Matsuwaki, Y., K. Wada, T. A. White, L. M. Benson, M. C. Charlesworth, J. L. Checkel, Y. Inoue, K. Hotta, J. U. Ponikau, C. B. Lawrence, and H. Kita. 2009. Recognition of fungal protease activities induces cellular activation and eosinophil-derived neurotoxin release in human eosinophils. *J Immunol* 183: 6708-6716.

145. Matsuwaki, Y., T. White, K. Hotta, Y. Inoue, C. B. Lawrence, and H. Kita. 2007. Aspartate protease from Alternaria induced cytokine production, and calcium signaling in human airway epithelial cells through a protease-activated receptor-2 (PAR-2). *Journal of Allergy and Clinical Immunology* 119: S137.

146. Shin, S. H., Y. H. Lee, and C. H. Jeon. 2006. Protease-dependent activation of nasal polyp epithelial cells by airborne fungi leads to migration of eosinophils and neutrophils. *Acta Oto-Laryngologica* 126: 1286-1294.

147. Kauffman, H. F., J. F. C. Tomee, M. A. van de Riet, A. J. B. Timmerman, and P. Borger. 2000. Protease-dependent activation of epithelial cells by fungal allergens leads to morphologic changes and cytokine production. *Journal of Allergy and Clinical Immunology* 105: 1185-1193.

148. Asokananthan, N., P. T. Graham, J. Fink, D. A. Knight, A. J. Bakker, A. S. McWilliam, P. J. Thompson, and G. A. Stewart. 2002. Activation of protease-activated receptor (PAR)-1, PAR-2, and PAR-4 stimulates IL-6, IL-8, and prostaglandin E2 release from human respiratory epithelial cells. *J Immunol* 168: 3577-3585.

149. Asokananthan, N., P. T. Graham, D. J. Stewart, A. J. Bakker, K. A. Eidne, P. J. Thompson, and G. A. Stewart. 2002. House dust mite allergens induce proinflammatory cytokines from respiratory epithelial cells: the cysteine protease allergen, Der p 1, activates protease-activated receptor (PAR)-2 and inactivates PAR-1. *J Immunol* 169: 4572-4578.

150. Runswick, S., T. Mitchell, P. Davies, C. Robinson, and D. R. Garrod. 2007. Pollen proteolytic enzymes degrade tight junctions. *Respirology* 12: 834-842.

151. Wan, H., H. L. Winton, C. Soeller, D. C. Gruenert, P. J. Thompson, M. B. Cannell, G. A. Stewart, D. R. Garrod, and C. Robinson. 2000. Quantitative structural and biochemical analyses of tight junction dynamics following exposure of epithelial cells to house dust mite allergen Der p 1. *Clin Exp Allergy* 30: 685-698.

152. Wan, H., H. L. Winton, C. Soeller, G. W. Taylor, D. C. Gruenert, P. J. Thompson, M. B. Cannell, G. A. Stewart, D. R. Garrod, and C. Robinson. 2001. The transmembrane protein occludin of epithelial tight junctions is a functional target for serine peptidases from faecal pellets of Dermatophagoides pteronyssinus. *Clin Exp Allergy* 31: 279-294.

153. Coughlin, S. R. 2000. Thrombin signalling and protease-activated receptors. *Nature* 407: 258-264.

154. Noorbakhsh, F., N. Vergnolle, M. D. Hollenberg, and C. Power. 2003. Proteinase-activated receptors in the nervous system. *Nat Rev Neurosci* 4: 981-990.

155. Kauffman, H. F., and S. van der Heide. 2003. Exposure, sensitization, and mechanisms of fungus-induced asthma. *Curr Allergy Asthma Rep* 3: 430-437.

156. Neukirch, C., C. Henry, B. Leynaert, R. Liard, J. Bousquet, and F. Neukirch. 1999. Is sensitization to Alternaria alternata a risk factor for severe asthma? A population-based study. *J Allergy Clin Immunol* 103: 709-711.

157. Bush, R. K., and J. J. Prochnau. 2004. Alternaria-induced asthma. *J Allergy Clin Immunol* 113: 227-234.

158. Zureik, M., C. Neukirch, B. Leynaert, R. Liard, J. Bousquet, and F. Neukirch. 2002. Sensitisation to airborne moulds and severity of asthma: cross sectional study from European Community respiratory health survey. *BMJ* 325: 411-414.

159. Ebeling, C., T. Lam, J. R. Gordon, M. D. Hollenberg, and H. Vliagoftis. 2007. Proteinase-activated receptor-2 promotes allergic sensitization to an inhaled antigen through a TNF-mediated pathway. *J Immunol* 179: 2910-2917.

160. Flamant-Hulin, M., I. Annesi-Maesano, and D. Caillaud. 2013. Relationships between molds and asthma suggesting non-allergic mechanisms. A rural-urban comparison. *Pediatr Allergy Immu* 24: 345-351.

161. Matsuwaki, Y., K. Wada, H. Moriyama, and H. Kita. 2011. Human Eosinophil Innate Response to Alternaria Fungus through Protease-Activated Receptor-2. *Int Arch Allergy Imm* 155: 123-128.

162. Denis, O., S. van den Brule, J. Heymans, X. Havaux, C. Rochard, F. Huaux, and K. Huygen. 2007. Chronic intranasal administration of mould spores or extracts to unsensitized mice leads to lung allergic inflammation, hyper-reactivity and remodelling. *Immunology* 122: 268-278.

163. Diaz-Sanchez, D. 1997. The role of diesel exhaust particles and their associated polyaromatic hydrocarbons in the induction of allergic airway disease. *Allergy* 52: 52-56; discussion 57-58.

164. Harrison, R. M., J. X. Yin, D. Mark, J. Stedman, R. S. Appleby, J. Booker, and S. Moorcroft. 2001. Studies of the coarse particle (2.5-10 μm) component in UK urban atmospheres. *Atmospheric Environment* 35: 3667-3679.

165. Thorpe, A. J., R. M. Harrison, P. G. Boulter, and I. S. McCrae. 2007. Estimation of particle resuspension source strength on a major London Road. *Atmospheric Environment* 41: 8007-8020.

166. Thorpe, A., and R. M. Harrison. 2008. Sources and properties of non-exhaust particulate matter from road traffic: A review. *Science of the Total Environment* 400: 270-282.

167. Sagai, M., A. Furuyama, and T. Ichinose. 1996. Biological effects of diesel exhaust particles (DEP). III. Pathogenesis of asthma like symptoms in mice. *Free Radic Biol Med* 21: 199-209.

168. Ichinose, T., A. Furuyama, and M. Sagai. 1995. Biological effects of diesel exhaust particles (DEP). II. Acute toxicity of DEP introduced into lung by intratracheal instillation. *Toxicology* 99: 153-167.

169. Han, J. Y., K. Takeshita, and H. Utsumi. 2001. Noninvasive detection of hydroxyl radical generation in lung by diesel exhaust particles. *Free Radical Biology and Medicine* 30: 516-525.

170. Pourazar, J., I. S. Mudway, J. M. Samet, R. Helleday, A. Blomberg, S. J. Wilson, A. J. Frew, F. J. Kelly, and T. Sandstrom. 2005. Diesel exhaust activates redox-sensitive transcription factors and kinases in human airways. *American Journal of Physiology-Lung Cellular and Molecular Physiology* 289: L724-L730.

171. Sagai, M., H. Saito, T. Ichinose, M. Kodama, and Y. Mori. 1993. Biological Effects of Diesel Exhaust Particles. 1. In vitro Production of Superoxide and In vivo Toxicity in Mouse. *Free Radical Biology and Medicine* 14: 37-47.

172. Mudway, I. S., N. Stenfors, S. T. Duggan, H. Roxborough, H. Zielinski, S. L. Marklund, A. Blomberg, A. J. Frew, T. Sandstrom, and F. J. Kelly. 2004. An in vitro and in vivo investigation of the effects of diesel exhaust on human airway lining fluid antioxidants. *Archives of Biochemistry and Biophysics* 423: 200-212.

173. Behndig, A. F., I. S. Mudway, J. L. Brown, N. Stenfors, R. Helleday, S. T. Duggan, S. J. Wilson, C. Boman, F. R. Cassee, A. J. Frew, F. J. Kelly, T. Sandstrom, and A. Blomberg. 2006. Airway antioxidant and inflammatory

responses to diesel exhaust exposure in healthy humans. *European Respiratory Journal* 27: 359-365.

174. Park, S., H. Nan, N. H. Chung, J. D. Park, and Y. Lim. 2003. The role of iron in reactive oxygen species generation from diesel exhaust particles. *Free Radical Biology and Medicine* 35: S138-S138.

175. Billet, S., G. Garcon, Z. Dagher, A. Verdin, F. Ledoux, F. Cazier, D. Courcot, A. Aboukais, and P. Shirali. 2007. Ambient particulate matter (PM2.5): Physicochemical characterization and metabolic activation of the organic fraction in human lung epithelial cells (A549). *Environ Res* 105: 212-223.

176. Risom, L., P. Moller, and S. Loft. 2005. Oxidative stress-induced DNA damage by particulate air pollution. *Mutat Res-Fund Mol M* 592: 119-137.

177. Lehmann, A. D., F. Blank, O. Baum, P. Gehr, and B. M. Rothen-Rutishauser. 2009. Diesel exhaust particles modulate the tight junction protein occludin in lung cells in vitro. *Particle and Fibre Toxicology* 6: -.

178. McCreanor, J., P. Cullinan, M. J. Nieuwenhuijsen, J. Stewart-Evans, E. Malliarou, L. Jarup, R. Harrington, M. Svartengren, I. Han, P. Ohman-Strickland, K. F. Chung, and J. F. Zhang. 2007. Respiratory effects of exposure to diesel traffic in persons with asthma. *New England Journal of Medicine* 357: 2348-2358.

179. Behndig, A. F., N. Larsson, J. L. Brown, N. Stenfors, R. Helleday, S. T. Duggan, R. E. Dove, S. J. Wilson, T. Sandstrom, F. J. Kelly, I. S. Mudway, and A. Blomberg. 2011. Proinflammatory doses of diesel exhaust in healthy subjects fail to elicit equivalent or augmented airway inflammation in subjects with asthma. *Thorax* 66: 12-19.

180. Sydbom, A., A. Blomberg, S. Parnia, N. Stenfors, T. Sandstrom, and S. E. Dahlen. 2001. Health effects of diesel exhaust emissions. *European Respiratory Journal* 17: 733-746.

181. Barath, S., N. L. Mills, M. Lundback, H. Tornqvist, A. J. Lucking, J. P. Langrish, S. Soderberg, C. Boman, R. Westerholm, J. Londahl, K. Donaldson, I. S. Mudway, T. Sandstrom, D. E. Newby, and A. Blomberg. 2010. Impaired vascular function after exposure to diesel exhaust generated at urban transient running conditions. *Particle and Fibre Toxicology* 7: 19-29.

182. Mills, N. L., H. Tornqvist, M. C. Gonzalez, E. Vink, S. D. Robinson, S. Soderberg, N. A. Boon, K. Donaldson, T. Sandstrom, A. Blomberg, and D. E. Newby. 2007. Ischemic and thrombotic effects of dilute diesel-exhaust inhalation in men with coronary heart disease. *New England Journal of Medicine* 357: 1075-1082.

183. Mills, N. L., H. Tornqvist, S. D. Robinson, M. Gonzalez, K. Darnley, W. MacNee, N. A. Boon, K. Donaldson, A. Blomberg, T. Sandstrom, and D. E. Newby. 2005. Diesel exhaust inhalation causes vascular dysfunction and impaired endogenous fibrinolysis. *Circulation* 112: 3930-3936.

184. Pritchard, R. J., A. J. Ghio, J. R. Lehmann, D. W. Winsett, J. S. Tepper, P. Park, M. I. Gilmour, K. L. Dreher, and D. L. Costa. 1996. Oxidant generation and lung injury after particulate air pollutant exposure increase with the concentrations of associated metals. *Inhalation Toxicology* 8: 457-477.

185. Martin, L. D., T. M. Krunkosky, J. A. Dye, B. M. Fischer, N. F. Jiang, L. G. Rochelle, N. J. Akley, K. L. Dreher, and K. B. Adler. 1997. The role of reactive oxygen and nitrogen species in the response of airway epithelium to particulates. *Environmental Health Perspectives* 105: 1301-1307.

186. Pan, C. J., D. A. Schmitz, A. K. Cho, J. Froines, and J. M. Fukuto. 2004. Inherent redox properties of diesel exhaust particles: catalysis of the generation of reactive oxygen species by biological reductants. *Toxicol Sci* 81: 225-232.

187. Valavanidis, A., K. Fiotakis, E. Bakeas, and T. Vlahogianni. 2005. Electron paramagnetic resonance study of the generation of reactive oxygen species

catalysed by transition metals and quinoid redox cycling by inhalable ambient particulate matter. *Redox Report* 10: 37-51.

188. Bowler, R. P., and J. D. Crapo. 2002. Oxidative stress in allergic respiratory diseases. *Journal of Allergy and Clinical Immunology* 110: 349-356.

189. Hutchison, G. R., D. M. Brown, L. R. Hibbs, M. R. Heal, K. Donaldson, R. L. Maynard, M. Monaghan, A. Nicholl, and V. Stone. 2005. The effect of refurbishing a UK steel plant on PM10 metal composition and ability to induce inflammation. *Resp Res* 6: 43-58.

190. Kennedy, T., A. J. Ghio, W. Reed, J. Samet, J. Zagorski, J. Quay, J. Carter, L. Dailey, J. R. Hoidal, and R. B. Devlin. 1998. Copper-dependent inflammation and nuclear factor-kappa B activation by particulate air pollution. *American Journal of Respiratory Cell and Molecular Biology* 19: 366-378.

191. Schaumann, F., P. J. A. Borm, A. Herbrich, J. Knoch, M. Pitz, R. P. F. Schins, B. Luettig, J. M. Hohlfeld, J. Heinrich, and N. Krug. 2004. Metal-rich ambient particles (Particulate Matter(2.5)) cause airway inflammation in healthy subjects. *American Journal of Respiratory and Critical Care Medicine* 170: 898-903.

192. McNeilly, J. D., M. R. Heal, I. J. Beverland, A. Howe, M. D. Gibson, L. R. Hibbs, W. MacNee, and K. Donaldson. 2004. Soluble transition metals cause the pro-inflammatory effects of welding fumes in vitro. *Toxicology and Applied Pharmacology* 196: 95-107.

193. Zeidler-Erdely, P. C., L. A. Battelli, R. Salmen-Muniz, Z. Li, A. Erdely, M. L. Kashon, P. P. Simeonova, and J. M. Antonini. 2011. Lung Tumor Production and Tissue Metal Distribution After Exposure to Manual Metal ARC-Stainless Steel Welding Fume in A/J and C57BL/6J Mice. *J Toxicol Env Heal A* 74: 728-736.

194. Godri, K. J., D. C. Green, G. W. Fuller, M. Dall'Osto, D. C. Beddows, F. J. Kelly, R. M. Harrison, and I. S. Mudway. 2010. Particulate Oxidative Burden

Associated with Firework Activity. *Environmental Science & Technology* 44: 8295-8301.

195. Costa, D. L., and K. L. Dreher. 1997. Bioavailable transition metals in particulate matter mediate cardiopulmonary injury in healthy and compromised animal models. *Environmental Health Perspectives* 105: 1053-1060.

196. Kelly, F. J. 2003. Oxidative stress: Its role in air pollution and adverse health effects. *Occupational and Environmental Medicine* 60: 612-616.

197. Dreher, K. L., R. H. Jaskot, J. R. Lehmann, J. H. Richards, J. K. McGee, A. J. Ghio, and D. L. Costa. 1997. Soluble transition metals mediate residual oil fly ash induced acute lung injury. *J Toxicol Env Health* 50: 285-305.

198. Gavett, S. H., S. L. Madison, K. L. Dreher, D. W. Winsett, J. K. McGee, and D. L. Costa. 1997. Metal and sulfate composition of residual oil fly ash determines airway hyperreactivity and lung injury in rats. *Environ Res* 72: 162-172.

199. Pattanaik, S., F. E. Huggins, and G. P. Huffman. 2012. Chemical Speciation of Fe and Ni in Residual Oil Fly Ash Fine Particulate Matter Using X-ray Absorption Spectroscopy. *Environmental Science & Technology* 46: 12927-12935.

200. Quay, J. L., W. Reed, J. Samet, and R. B. Devlin. 1998. Air pollution particles induce IL-6 gene expression in human airway epithelial cells via NF-kappa B activation. *American Journal of Respiratory Cell and Molecular Biology* 19: 98-106.

201. Carter, J. D., A. J. Ghio, J. M. Samet, and R. B. Devlin. 1997. Cytokine production by human airway epithelial cells after exposure to an air pollution particle is metal-dependent. *Toxicology and Applied Pharmacology* 146: 180-188.

202. Dye, J. A., K. B. Adler, J. H. Richards, and K. L. Dreher. 1999. Role of soluble metals in oil fly ash-induced airway epithelial injury and cytokine gene

expression. *American Journal of Physiology-Lung Cellular and Molecular Physiology* 277: L498-L510.

203. Kodavanti, U. P., R. Hauser, D. C. Christiani, Z. H. Meng, J. McGee, A. Ledbetter, J. Richards, and D. L. Costa. 1998. Pulmonary responses to oil fly ash particles in the rat differ by virtue of their specific soluble metals. *Toxicological Sciences* 43: 204-212.

204. Karlsson, H. L., L. Nilsson, and L. Moller. 2005. Subway particles are more genotoxic than street particles and induce oxidative stress in cultured human lung cells. *Chemical Research in Toxicology* 18: 19-23.

205. Crump, K. S. 2000. Manganese exposures in Toronto during use of the gasoline additive, methylcyclopentadienyl manganese tricarbonyl. *Journal of Exposure Analysis and Environmental Epidemiology* 10: 227-239.

206. Chillrud, S. N., D. Grass, J. M. Ross, D. Coulibaly, V. Slavkovich, D. Epstein, S. N. Sax, D. Pederson, D. Johnson, J. D. Spengler, P. L. Kinney, H. J. Simpson, and P. Brandt-Rauf. 2005. Steel dust in the New York City subway system as a source of manganese, chromium, and iron exposures for transit workers. *Journal of Urban Health-Bulletin of the New York Academy of Medicine* 82: 33-42.

207. Ayres, J. G., P. Borm, F. R. Cassee, V. Castranova, K. Donaldson, A. Ghio, R. M. Harrison, R. Hider, F. Kelly, I. M. Kooter, F. Marano, R. L. Maynard, I. Mudway, A. Nel, C. Sioutas, S. Smith, A. Baeza-Squiban, A. Cho, S. Duggan, and J. Froines. 2008. Evaluating the toxicity of airborne particulate matter and nanoparticles by measuring oxidative stress potential - A workshop report and consensus statement. *Inhalation Toxicology* 20: 75-99.

208. Chen, X., and S. S. Mao. 2007. Titanium dioxide nanomaterials: Synthesis, properties, modifications, and applications. *Chem Rev* 107: 2891-2959.

209. Baughman, R. H., A. A. Zakhidov, and W. A. de Heer. 2002. Carbon nanotubes - the route toward applications. *Science* 297: 787-792.

210. Jiang, K. L., J. P. Wang, Q. Q. Li, L. A. Liu, C. H. Liu, and S. S. Fan. 2011. Superaligned Carbon Nanotube Arrays, Films, and Yarns: A Road to Applications. *Adv Mater* 23: 1154-1161.

211. Bera, D., L. Qian, T. K. Tseng, and P. H. Holloway. 2010. Quantum Dots and Their Multimodal Applications: A Review. *Materials* 3: 2260-2345.

212. Oberdorster, G., E. Oberdorster, and J. Oberdorster. 2005. Nanotoxicology: An emerging discipline evolving from studies of ultrafine particles. *Environmental Health Perspectives* 113: 823-839.

213. Duffin, R., C. L. Tran, A. Clouter, D. M. Brown, W. MacNee, V. Stone, and K. Donaldson. 2002. The Importance of Surface Area and Specific Reactivity in the Acute Pulmonary Inflammatory Response to Particles. *Ann Occup Hyg* 46: 242-245.

214. Hussain, S., S. Boland, A. Baeza-Squiban, R. Hamel, L. C. J. Thomassen, J. A. Martens, M. A. Billon-Galland, J. Fleury-Feith, F. Moisan, J. C. Pairon, and F. Marano. 2009. Oxidative stress and proinflammatory effects of carbon black and titanium dioxide nanoparticles: Role of particle surface area and internalized amount. *Toxicology* 260: 142-149.

215. Ho, M., K. Y. Wu, H. M. Chein, L. C. Chen, and T. J. Cheng. 2011. Pulmonary toxicity of inhaled nanoscale and fine zinc oxide particles: Mass and surface area as an exposure metric. *Inhalation Toxicology* 23: 947-956.

216. Duffin, R., L. Tran, D. Brown, V. Stone, and K. Donaldson. 2007. Proinflammogenic effects of low-toxicity and metal nanoparticles in vivo and in vitro: Highlighting the role of particle surface area and surface reactivity. *Inhalation Toxicology* 19: 849-856.

217. Horie, M., H. Fukui, S. Endoh, J. Maru, A. Miyauchi, M. Shichiri, K. Fujita, E. Niki, Y. Hagihara, Y. Yoshida, Y. Morimoto, and H. Iwahashi. 2012. Comparison of acute oxidative stress on rat lung induced by nano and fine-scale, soluble and insoluble metal oxide particles: NiO and TiO2. *Inhalation Toxicology* 24: 391-400.

218. Karlsson, H. L., J. Gustafsson, P. Cronholm, and L. Moller. 2009. Size-dependent toxicity of metal oxide particles-A comparison between nano- and micrometer size. *Toxicology Letters* 188: 112-118.

219. Oberdorster, G. 2001. Pulmonary effects of inhaled ultrafine particles. *Int Arch Occ Env Hea* 74: 1-8.

220. Geiser, M., M. Casaulta, B. Kupferschmid, H. Schulz, M. Semirriler-Behinke, and W. Kreyling. 2008. The role of macrophages in the clearance of inhaled ultrafine titanium dioxide particles. *American Journal of Respiratory Cell and Molecular Biology* 38: 371-376.

221. Poland, C. A., R. Duffin, I. Kinloch, A. Maynard, W. A. H. Wallace, A. Seaton, V. Stone, S. Brown, W. MacNee, and K. Donaldson. 2008. Carbon nanotubes introduced into the abdominal cavity of mice show asbestos-like pathogenicity in a pilot study. *Nat Nanotechnol* 3: 423-428.

222. Schinwald, A., F. A. Murphy, A. Jones, W. MacNee, and K. Donaldson. 2012. Graphene-Based Nanoplatelets: A New Risk to the Respiratory System as a Consequence of Their Unusual Aerodynamic Properties. *Acs Nano* 6: 736-746.

223. Belade, E., L. Armand, L. Martinon, L. Kheuang, J. Fleury-Feith, A. Baeza-Squiban, S. Lanone, M. A. Billon-Galland, J. C. Pairon, and J. Boczkowski. 2012. A comparative transmission electron microscopy study of titanium dioxide and carbon black nanoparticles uptake in human lung epithelial and fibroblast cell lines. *Toxicol in Vitro* 26: 57-66.

224. Schaudien, D., J. Knebel, and O. Creutzenberg. 2012. In vitro study revealed different size behavior of different nanoparticles. *J Nanopart Res* 14.

225. Teeguarden, J. G., P. M. Hinderliter, G. Orr, B. D. Thrall, and J. G. Pounds. 2007. Particokinetics in vitro: Dosimetry considerations for in vitro nanoparticle toxicity assessments. *Toxicological Sciences* 95: 300-312.

226. Gottstein, C., G. H. Wu, B. J. Wong, and J. A. Zasadzinski. 2013. Precise Quantification of Nanoparticle Internalization. *Acs Nano* 7: 4933-4945.

227. Muhlfeld, C., P. Gehr, and B. Rothen-Rutishauser. 2008. Translocation and cellular entering mechanisms of nanoparticles in the respiratory tract. *Swiss Med Wkly* 138: 387-391.

228. Nemmar, A., H. Vanbilloen, M. F. Hoylaerts, P. H. M. Hoet, A. Verbruggen, and B. Nemery. 2001. Passage of intratracheally instilled ultrafine particles from the lung into the systemic circulation in hamster. *American Journal of Respiratory and Critical Care Medicine* 164: 1665-1668.

229. Choi, H. S., Y. Ashitate, J. H. Lee, S. H. Kim, A. Matsui, N. Insin, M. G. Bawendi, M. Semmler-Behnke, J. V. Frangioni, and A. Tsuda. 2010. Rapid translocation of nanoparticles from the lung airspaces to the body. *Nat Biotechnol* 28: 1300-U1113.

230. Kreyling, W. G., M. Semmler-Behnke, S. Takenaka, and W. Moller. 2013. Differences in in the Biokinetics of Inhaled Nano- versus Micrometer-Sized Particles. *Accounts Chem Res* 46: 714-722.

231. Miyata, R., N. Bai, R. Vincent, D. D. Sin, and S. F. Van Eeden. 2013. Statins Reduce Ambient Particulate Matter-Induced Lung Inflammation by Promoting the Clearance of Particulate Matter < 10 μm From Lung Tissues. *Chest* 143: 452-460.

232. Cho, W. S., R. Duffin, C. A. Poland, S. E. M. Howie, W. MacNee, M. Bradley, I. L. Megson, and K. Donaldson. 2010. Metal Oxide Nanoparticles Induce Unique Inflammatory Footprints in the Lung: Important Implications for Nanoparticle Testing. *Environmental Health Perspectives* 118: 1699-1706.

233. Sohaebuddin, S. K., P. T. Thevenot, D. Baker, J. W. Eaton, and L. P. Tang. 2010. Nanomaterial cytotoxicity is composition, size, and cell type dependent. *Particle and Fibre Toxicology* 7.

234. Xia, T., M. Kovochich, J. Brant, M. Hotze, J. Sempf, T. Oberley, C. Sioutas, J. I. Yeh, M. R. Wiesner, and A. E. Nel. 2006. Comparison of the abilities of ambient and manufactured nanoparticles to induce cellular toxicity according to an oxidative stress paradigm. *Nano Lett* 6: 1794-1807.

235. Borm, P. J. A., F. Kelly, N. Kunzli, R. P. F. Schins, and K. Donaldson. 2007. Oxidant generation by particulate matter: from biologically effective dose to a promising, novel metric. *Occupational and Environmental Medicine* 64: 73-74.

236. Lu, S. L., R. Duffin, C. Poland, P. Daly, F. Murphy, E. Drost, W. MacNee, V. Stone, and K. Donaldson. 2009. Efficacy of Simple Short-Term in Vitro Assays for Predicting the Potential of Metal Oxide Nanoparticles to Cause Pulmonary Inflammation. *Environmental Health Perspectives* 117: 241-247.

237. Cho, W. S., R. Duffin, F. Thielbeer, M. Bradley, I. L. Megson, W. MacNee, C. A. Poland, C. L. Tran, and K. Donaldson. 2012. Zeta Potential and Solubility to Toxic Ions as Mechanisms of Lung Inflammation Caused by Metal/Metal Oxide Nanoparticles. *Toxicological Sciences* 126: 469-477.

238. Zhang, H. Y., Z. X. Ji, T. Xia, H. Meng, C. Low-Kam, R. Liu, S. Pokhrel, S. J. Lin, X. Wang, Y. P. Liao, M. Y. Wang, L. J. Li, R. Rallo, R. Damoiseaux, D. Telesca, L. Madler, Y. Cohen, J. I. Zink, and A. E. Nel. 2012. Use of Metal Oxide Nanoparticle Band Gap To Develop a Predictive Paradigm for Oxidative Stress and Acute Pulmonary Inflammation. *Acs Nano* 6: 4349-4368.

239. Elihn, K., and P. Berg. 2009. Ultrafine Particle Characteristics in Seven Industrial Plants. *Annals of Occupational Hygiene* 53: 475-484.

240. Donaldson, K., A. Schinwald, F. Murphy, W. S. Cho, R. Duffin, L. Tran, and C. Poland. 2013. The Biologically Effective Dose in Inhalation Nanotoxicology. *Accounts Chem Res* 46: 723-732.

241. Royal Commission on Environmental Pollution, G. B. 2008. *Novel materials in the environment : the case of nanotechnology*. TSO, Norwich.

242. Murphy, M. P. 2009. How mitochondria produce reactive oxygen species. *Biochem J* 417: 1-13.

243. Forman, H. J., J. M. Fukuto, and M. Torres. 2004. Redox signaling: thiol chemistry defines which reactive oxygen and nitrogen species can act as second messengers. *Am J Physiol-Cell Ph* 287: C246-C256.

244. Forman, H. J., M. Torres, and J. Fukuto. 2002. Redox signaling. *Molecular and Cellular Biochemistry* 234: 49-62.

245. van Klaveren, R. J., and B. Nemery. 1999. Role of reactive oxygen species in occupational and environmental obstructive pulmonary diseases. *Curr Opin Pulm Med* 5: 118-123.

246. Croft, S., B. C. Gilbert, J. R. L. Smith, and A. C. Whitwood. 1992. An Esr Investigation of the Reactive Intermediate Generated in the Reaction between Fe(II) and H2O2 in Aqueous-Solution - Direct Evidence for the Formation of the Hydroxyl Radical. *Free Radical Research Communications* 17: 21-39.

247. Donaldson, K., D. M. Brown, C. Mitchell, M. Dineva, P. H. Beswick, P. Gilmour, and W. MacNee. 1997. Free radical activity of PM10: Iron-mediated generation of hydroxyl radicals. *Environmental Health Perspectives* 105: 1285-1289.

248. Shen, H. Y., and C. Anastasio. 2012. A comparison of hydroxyl radical and hydrogen peroxide generation in ambient particle extracts and laboratory metal solutions. *Atmospheric Environment* 46: 665-668.

249. Charrier, J. G., and C. Anastasio. 2011. Impacts of antioxidants on hydroxyl radical production from individual and mixed transition metals in a surrogate lung fluid. *Atmospheric Environment* 45: 7555-7562.

250. Vidrio, E., H. Jung, and C. Anastasio. 2008. Generation of hydroxyl radicals from dissolved transition metals in surrogate lung fluid solutions. *Atmospheric Environment* 42: 4369-4379.

251. Valavanidis, A., A. Salika, and A. Theodoropoulou. 2000. Generation of hydroxyl radicals by urban suspended particulate air matter. The role of iron ions. *Atmospheric Environment* 34: 2379-2386.

252. Jung, H. J., B. Kim, M. A. Malek, Y. S. Koo, J. N. Jung, Y. S. Son, J. C. Kim, H. Kim, and C. U. Ro. 2012. Chemical speciation of size-segregated floor dusts and airborne magnetic particles collected at underground subway stations in Seoul, Korea. *J Hazard Mater* 213: 331-340.

253. Keenan, C. R., R. Goth-Goldstein, D. Lucas, and D. L. Sedlak. 2009. Oxidative Stress Induced by Zero-Valent Iron Nanoparticles and Fe(II) in Human Bronchial Epithelial Cells. *Environmental Science & Technology* 43: 4555-4560.

254. Tkaczyk, J., and M. Vizek. 2007. Oxidative stress in the lung tissue - sources of reactive oxygen species and antioxidant defence. *Prague Med Rep* 108: 105-114.

255. Li, N., C. Sioutas, A. Cho, D. Schmitz, C. Misra, J. Sempf, M. Y. Wang, T. Oberley, J. Froines, and A. Nel. 2003. Ultrafine particulate pollutants induce oxidative stress and mitochondrial damage. *Environmental Health Perspectives* 111: 455-460.

256. Di Pietro, A., G. Visalli, B. Baluce, R. T. Micale, S. La Maestra, P. Spataro, and S. De Flora. 2011. Multigenerational mitochondrial alterations in pneumocytes exposed to oil fly ash metals. *International Journal of Hygiene and Environmental Health* 214: 138-144.

257. Freyre-Fonseca, V., N. L. Delgado-Buenrostro, E. B. Gutierrez-Cirlos, C. M. Calderon-Torres, T. Cabellos-Avelar, Y. Sanchez-Perez, E. Pinzon, I. Torres, E. Molina-Jijon, C. Zazueta, J. Pedraza-Chaverri, C. M. Garcia-Cuellar, and Y. I. Chirino. 2011. Titanium dioxide nanoparticles impair lung mitochondrial function. *Toxicology Letters* 202: 111-119.

258. Kim, Y. H., F. Fazlollahi, I. M. Kennedy, N. R. Yacobi, S. F. Hamm-Alvarez, Z. Borok, K. J. Kim, and E. D. Crandall. 2010. Alveolar Epithelial Cell Injury Due to Zinc Oxide Nanoparticle Exposure. *American Journal of Respiratory and Critical Care Medicine* 182: 1398-1409.

259. Wittkopp, S., N. Staimer, T. Tjoa, D. Gillen, N. Daher, M. Shafer, J. J. Schauer, C. Sioutas, and R. J. Delfino. 2013. Mitochondrial Genetic Background Modifies the Relationship between Traffic-Related Air Pollution Exposure and Systemic Biomarkers of Inflammation. *Plos One* 8.

260. Weichenthal, S. A., K. Godri-Pollitt, and P. J. Villeneuve. 2013. PM2.5, oxidant defence and cardiorespiratory health: a review. *Environ Health-Glob* 12.

261. Halliwell, B., and M. Whiteman. 2004. Measuring reactive species and oxidative damage in vivo and in cell culture: how should you do it and what do the results mean? *Brit J Pharmacol* 142: 231-255.

262. Ohyama, M., T. Otake, S. Adachi, T. Kobayashi, and K. Morinaga. 2007. A comparison of the production of reactive oxygen species by suspended particulate matter and diesel exhaust particles with macrophages. *Inhalation Toxicology* 19: 157-160.

263. Dick, C. A. J., D. M. Brown, K. Donaldson, and V. Stone. 2003. The role of free radicals in the toxic and inflammatory effects of four different ultrafine particle types. *Inhalation Toxicology* 15: 39-52.

264. Monteiller, C., L. Tran, W. MacNee, S. Faux, A. Jones, B. Miller, and K. Donaldson. 2007. The pro-inflammatory effects of low-toxicity low-solubility particles, nanoparticles and fine particles, on epithelial cells in vitro: the role of surface area. *Occupational and Environmental Medicine* 64: 609-615.

265. Elihn, K., P. Cronholm, H. L. Karlsson, K. Midander, I. O. Wallinder, and L. Moller. 2013. Cellular Dose of Partly Soluble Cu Particle Aerosols at the Air-Liquid Interface Using an In Vitro Lung Cell Exposure System. *J Aerosol Med Pulm D* 26: 84-93.

266. Baulig, A., M. Garlatti, V. Bonvallot, A. Marchand, R. Barouki, F. Marano, and A. Baeza-Squiban. 2003. Involvement of reactive oxygen species in the metabolic pathways triggered by diesel exhaust particles in human airway epithelial cells. *American Journal of Physiology-Lung Cellular and Molecular Physiology* 285: L671-L679.

267. Riva, D. R., C. B. Magalhaes, A. A. Lopes, T. Lancas, T. Mauad, O. Malm, S. S. Valenca, P. H. Saldiva, D. S. Faffe, and W. A. Zin. 2011. Low dose of fine particulate matter (PM2.5) can induce acute oxidative stress, inflammation and pulmonary impairment in healthy mice. *Inhalation Toxicology* 23: 257-267.

268. Shukla, A., C. Timblin, K. BeruBe, T. Gordon, W. McKinney, K. Driscoll, P. Vacek, and B. T. Mossman. 2000. Inhaled particulate matter causes expression of nuclear factor (NF)-kappa B-related genes and oxidant-dependent NF-kappa B activation in vitro. *American Journal of Respiratory Cell and Molecular Biology* 23: 182-187.

269. Patel, E., C. Lynch, V. Ruff, and M. Reynolds. 2012. Co-exposure to nickel and cobalt chloride enhances cytotoxicity and oxidative stress in human lung epithelial cells. *Toxicology and Applied Pharmacology* 258: 367-375.

270. Ramesh, V., P. Ravichandran, C. L. Copeland, R. Gopikrishnan, S. Biradar, V. Goornavar, G. T. Ramesh, and J. C. Hall. 2012. Magnetite induces oxidative stress and apoptosis in lung epithelial cells. *Molecular and Cellular Biochemistry* 363: 225-234.

271. Xiao, G. G., M. Y. Wang, N. Li, J. A. Loo, and A. E. Nel. 2003. Use of proteomics to demonstrate a hierarchical oxidative stress response to diesel exhaust particle chemicals in a macrophage cell line. *Journal of Biological Chemistry* 278: 50781-50790.

272. Nel, A., T. Xia, L. Madler, and N. Li. 2006. Toxic potential of materials at the nanolevel. *Science* 311: 622-627.

273. Li, N., M. Q. Hao, R. F. Phalen, W. C. Hinds, and A. E. Nel. 2003. Particulate air pollutants and asthma - A paradigm for the role of oxidative stress in PM-induced adverse health effects. *Clinical Immunology* 109: 250-265.

274. Blake, D. J., A. Singh, P. Kombairaju, D. Malhotra, T. J. Mariani, R. M. Tuder, E. Gabrielson, and S. Biswal. 2010. Deletion of Keap1 in the Lung Attenuates Acute Cigarette Smoke-Induced Oxidative Stress and Inflammation. *American Journal of Respiratory Cell and Molecular Biology* 42: 524-536.

275. Li, N., J. Alam, M. I. Venkatesan, A. Eiguren-Fernandez, D. Schmitz, E. Di Stefano, N. Slaughter, E. Killeen, X. R. Wang, A. Huang, M. Y. Wang, A. H. Miguel, A. Cho, C. Sioutas, and A. E. Nel. 2004. Nrf2 is a key transcription factor that regulates antioxidant defense in macrophages and epithelial cells: Protecting against the proinflammatory and oxidizing effects of diesel exhaust chemicals. *Journal of Immunology* 173: 3467-3481.

276. Thimmulappa, R. K., K. H. Mai, S. Srisuma, T. W. Kensler, M. Yamamato, and S. Biswal. 2002. Identification of Nrf2-regulated genes induced by the chemopreventive agent sulforaphane by oligonucleotide microarray. *Cancer Research* 62: 5196-5203.

277. Ritz, S. A., J. X. Wan, and D. Diaz-Sanchez. 2007. Sulforaphane-stimulated phase II enzyme induction inhibits cytokine production by airway epithelial cells stimulated with diesel extract. *American Journal of Physiology-Lung Cellular and Molecular Physiology* 292: L33-L39.

278. Li, Y. J., H. Takizawa, A. Azuma, T. Kohyama, Y. Yamauchi, S. Takahashi, M. Yamamoto, T. Kawada, S. Kudoh, and I. Sugawara. 2008. Disruption of Nrf2 enhances susceptibility to airway inflammatory responses induced by low-dose diesel exhaust particles in mice. *Clinical Immunology* 128: 366-373.

279. Zhou, Y. M., C. Y. Zhong, I. M. Kennedy, V. J. Leppert, and K. E. Pinkerton. 2003. Oxidative stress and NF kappa B activation in the lungs of rats: a synergistic interaction between soot and iron particles. *Toxicology and Applied Pharmacology* 190: 157-169.

280. Dagher, Z., G. Garcon, S. Billet, A. Verdin, F. Ledoux, D. Courcot, A. Aboukais, and P. Shirali. 2007. Role of nuclear factor-kappa B activation in the adverse effects induced by air pollution particulate matter (PM2.5) in human epithelial lung cells (L132) in culture. *J Appl Toxicol* 27: 284-290.

281. Potnis, P. A., R. Mitkus, A. Elnabawi, K. Squibb, and J. L. Powell. 2013. Role of NF-kappa B in the oxidative stress-induced lung inflammatory response to iron and selenium at ambient levels. *Toxicol Res-Uk* 2: 259-269.

282. Churg, A., C. S. Xie, X. S. Wang, R. Vincent, and R. D. Wang. 2005. Air pollution particles activate NF-kappa B on contact with airway epithelial cell surfaces. *Toxicology and Applied Pharmacology* 208: 37-45.

283. Goebeler, M., J. Roth, E. B. Brocker, C. Sorg, and K. Schulzeosthoff. 1995. Activation of Nuclear Factor-Kappa-B and Gene-Expression in Human Endothelial-Cells by the Common Haptens Nickel and Cobalt. *Journal of Immunology* 155: 2459-2467.

284. Alessandrini, F., I. Beck-Speier, D. Krappmann, I. Weichenmeier, S. Takenaka, E. Karg, B. Kloo, H. Schulz, T. Jakob, M. Mempel, and H. Behrendt. 2009. Role of Oxidative Stress in Ultrafine Particle-induced Exacerbation of Allergic Lung Inflammation. *American Journal of Respiratory and Critical Care Medicine* 179: 984-991.

285. Brown, D. M., L. Hutchison, K. Donaldson, and V. Stone. 2007. The effects of PM10 particles and oxidative stress on macrophages and lung epithelial cells: modulating effects of calcium-signaling antagonists. *American Journal of Physiology-Lung Cellular and Molecular Physiology* 292: L1444-L1451.

286. Mossman, B. T., K. M. Lounsbury, and S. P. Reddy. 2006. Oxidants and signaling by mitogen-activated protein kinases in lung epithelium. *American Journal of Respiratory Cell and Molecular Biology* 34: 666-669.

287. Marano, F., S. Boland, V. Bonvallot, A. Baulig, and A. Baeza-Squiban. 2002. Human airway epithelial cells in culture for studying the molecular mechanisms of the inflammatory response triggered by diesel exhaust particles. *Cell Biol Toxicol* 18: 315-320.

288. Zelko, I. N., T. J. Mariani, and R. J. Folz. 2002. Superoxide dismutase multigene family: A comparison of the CuZn-SOD (SOD1), Mn-SOD (SOD2), and EC-SOD (SOD3) gene structures, evolution, and expression. *Free Radical Biology and Medicine* 33: 337-349.

289. Comhair, S. A., P. R. Bhathena, C. Farver, F. B. Thunnissen, and S. C. Erzurum. 2001. Extracellular glutathione peroxidase induction in asthmatic lungs: evidence for redox regulation of expression in human airway epithelial cells. *FASEB J* 15: 70-78.

290. Wu, M. L., M. D. Layne, and S. F. Yet. 2012. Heme oxygenase-1 in environmental toxin-induced lung disease. *Toxicol Mech Method* 22: 323-329.

291. Kosmider, B., E. M. Messier, H. W. Chu, and R. J. Mason. 2011. Human Alveolar Epithelial Cell Injury Induced by Cigarette Smoke. *Plos One* 6.

292. Eom, H. J., and J. Choi. 2009. Oxidative stress of silica nanoparticles in human bronchial epithelial cell, Beas-2B. *Toxicol in Vitro* 23: 1326-1332.

293. Deng, X. B., W. Rui, F. Zhang, and W. J. Ding. 2013. PM2.5 induces Nrf2-mediated defense mechanisms against oxidative stress by activating PIK3/AKT signaling pathway in human lung alveolar epithelial A549 cells. *Cell Biol Toxicol* 29: 143-157.

294. Brauner, E. V., L. Forchhammer, P. Moller, J. Simonsen, M. Glasius, P. Wahlin, O. Raaschou-Nielsen, and S. Loft. 2007. Exposure to ultrafine particles from ambient air and oxidative stress-induced DNA damage. *Environ Health Perspect* 115: 1177-1182.

295. Zielinski, H., I. S. Mudway, K. A. Berube, S. Murphy, R. Richards, and F. J. Kelly. 1999. Modeling the interactions of particulates with epithelial lining fluid antioxidants. *American Journal of Physiology-Lung Cellular and Molecular Physiology* 277: L719-L726.

296. Fujii, T., S. Hayashi, J. C. Hogg, R. Vincent, and S. F. Van Eeden. 2001. Particulate matter induces cytokine expression in human bronchial epithelial cells. *American Journal of Respiratory Cell and Molecular Biology* 25: 265-271.

297. Gilmour, P. S., I. Rahman, K. Donaldson, and W. MacNee. 2003. Histone acetylation regulates epithelial IL-8 release mediated by oxidative stress from environmental particles. *American Journal of Physiology-Lung Cellular and Molecular Physiology* 284: L533-L540.

298. Calcabrini, A., S. Meschini, M. Marra, L. Falzano, M. Colone, B. De Berardis, L. Paoletti, G. Arancia, and C. Fiorentini. 2004. Fine environmental particulate engenders alterations in human lung epithelial A549 cells. *Environ Res* 95: 82-91.

299. Lindbom, J., M. Gustafsson, G. Blomqvist, A. Dahl, A. Gudmundsson, E. Swietlicki, and A. G. Ljungman. 2006. Exposure to wear particles generated from studded tires and pavement induces inflammatory cytokine release from human macrophages. *Chemical Research in Toxicology* 19: 521-530.

300. Hetland, R. B., F. R. Cassee, M. Refsnes, P. E. Schwarze, M. Lag, A. J. F. Boere, and E. Dybing. 2004. Release of inflammatory cytokines, cell toxicity and apoptosis in epithelial lung cells after exposure to ambient air particles of different size fractions. *Toxicol in Vitro* 18: 203-212.

301. Saldiva, P. H., R. W. Clarke, B. A. Coull, R. C. Stearns, J. Lawrence, G. G. Murthy, E. Diaz, P. Koutrakis, H. Suh, A. Tsuda, and J. J. Godleski. 2002. Lung inflammation induced by concentrated ambient air particles is related to particle composition. *Am J Respir Crit Care Med* 165: 1610-1617.

302. Dominici, F., R. D. Peng, K. Ebisu, S. L. Zeger, J. M. Samet, and M. L. Bell. 2007. Does the effect of PM10 on mortality depend on PM nickel and vanadium content? A reanalysis of the NMMAPS data. *Environmental Health Perspectives* 115: 1701-1703.

303. Riley, M. R., D. E. Boesewetter, A. M. Kim, and F. P. Sirvent. 2003. Effects of metals Cu, Fe, Ni, V, and Zn on rat lung epithelial cells. *Toxicology* 190: 171-184.

304. Jalava, P. I., M. R. Hirvonen, M. Sillanpaa, A. S. Pennanen, M. S. Happo, R. Hillamo, F. R. Cassee, M. Gerlofs-Nijland, P. J. A. Borm, R. P. F. Schins, N. A. H. Janssen, and R. O. Salonen. 2009. Associations of urban air particulate composition with inflammatory and cytotoxic responses in RAW 246.7 cell line. *Inhalation Toxicology* 21: 994-1006.

305. Gerlofs-Nijland, M. E., J. A. Dormans, H. J. Bloemen, D. L. Leseman, A. John, F. Boere, F. J. Kelly, I. S. Mudway, A. A. Jimenez, K. Donaldson, C. Guastadisegni, N. A. Janssen, B. Brunekreef, T. Sandstrom, L. van Bree, and F.

R. Cassee. 2007. Toxicity of coarse and fine particulate matter from sites with contrasting traffic profiles. *Inhal Toxicol* 19: 1055-1069.

306. Gerlofs-Nijland, M. E., M. Rummelhard, A. J. Boere, D. L. Leseman, R. Duffin, R. P. Schins, P. J. Borm, M. Sillanpaa, R. O. Salonen, and F. R. Cassee. 2009. Particle induced toxicity in relation to transition metal and polycyclic aromatic hydrocarbon contents. *Environ Sci Technol* 43: 4729-4736.

307. Brown, D. M., V. Stone, P. Findlay, W. MacNee, and K. Donaldson. 2000. Increased inflammation and intracellular calcium caused by ultrafine carbon black is independent of transition metals or other soluble components. *Occupational and Environmental Medicine* 57: 685-691.

308. Boland, S., A. Baeza-Squiban, T. Fournier, O. Houcine, M. C. Gendron, M. Chevrier, G. Jouvenot, A. Coste, M. Aubier, and F. Marano. 1999. Diesel exhaust particles are taken up by human airway epithelial cells in vitro and alter cytokine production. *American Journal of Physiology-Lung Cellular and Molecular Physiology* 276: L604-L613.

309. Becker, S., S. Mundandhara, R. B. Devlin, and M. Madden. 2005. Regulation of cytokine production in human alveolar macrophages and airway epithelial cells in response to ambient air pollution particles: further mechanistic studies. *Toxicol Appl Pharmacol* 207: 269-275.

310. Gioda, A., E. Fuentes-Mattei, and B. Jimenez-Velez. 2011. Evaluation of cytokine expression in BEAS cells exposed to fine particulate matter (PM2.5) from specialized indoor environments. *Int J Environ Heal R* 21: 106-119.

311. Rice, T. M., R. W. Clarke, J. J. Godleski, E. Al-Mutairi, N. F. Jiang, R. Hauser, and J. D. Paulauskis. 2001. Differential ability of transition metals to induce pulmonary inflammation. *Toxicology and Applied Pharmacology* 177: 46-53.

312. Yu, M., X. Zheng, H. Witschi, and K. E. Pinkerton. 2002. The role of interleukin-6 in pulmonary inflammation and injury induced by exposure to environmental air pollutants. *Toxicological Sciences* 68: 488-497.

313. Sawyer, K., S. Mundandhara, A. J. Ghio, and M. C. Madden. 2010. The Effects of Ambient Particulate Matter on Human Alveolar Macrophage Oxidative and Inflammatory Responses. *J Toxicol Env Heal A* 73: 41-57.

314. Singh, N. P., M. T. Mccoy, R. R. Tice, and E. L. Schneider. 1988. A Simple Technique for Quantitation of Low-Levels of DNA Damage in Individual Cells. *Experimental Cell Research* 175: 184-191.

315. Gilmour, P. S., D. M. Brown, T. G. Lindsay, P. H. Beswick, W. MacNee, and K. Donaldson. 1996. Adverse health effects of PM(10) particles: Involvement of iron in generation of hydroxyl radical. *Occupational and Environmental Medicine* 53: 817-822.

316. Wessels, A., D. Van Berlo, A. W. Boots, K. Gerloff, A. M. Scherbart, F. R. Cassee, M. E. Gerlofs-Nijland, F. J. Van Schooten, C. Albrecht, and R. P. F. Schins. 2011. Oxidative stress and DNA damage responses in rat and mouse lung to inhaled carbon nanoparticles. *Nanotoxicology* 5: 66-78.

317. Marnett, L. J. 2002. Oxy radicals, lipid peroxidation and DNA damage. *Toxicology* 181: 219-222.

318. Romieu, I., A. Barraza-Villarreal, C. Escamilla-Nunez, A. C. Almstrand, D. Diaz-Sanchez, P. D. Sly, and A. C. Olin. 2008. Exhaled breath malondialdehyde as a marker of effect of exposure to air pollution in children with asthma. *Journal of Allergy and Clinical Immunology* 121: 903-909.

319. Karlsson, H. L., A. G. Ljungman, J. Lindbom, and L. Moller. 2006. Comparison of genotoxic and inflammatory effects of particles generated by wood combustion, a road simulator and collected from street and subway. *Toxicology Letters* 165: 203-211.

320. Jung, M. H., H. R. Kim, Y. J. Park, D. S. Park, K. H. Chung, and S. M. Oh. 2012. Genotoxic effects and oxidative stress induced by organic extracts of particulate matter (PM10) collected from a subway tunnel in Seoul, Korea. *Mutat Res-Gen Tox En* 749: 39-47.

321. Sorensen, M., R. P. F. Schins, O. Hertel, and S. Loft. 2005. Transition metals in personal samples of PM2.5 and oxidative stress in human volunteers. *Cancer Epidemiology Biomarkers & Prevention* 14: 1340-1343.

322. Prahalad, A. K., J. Inmon, A. J. Ghio, and J. E. Gallagher. 2000. Enhancement of 2 '-deoxyguanosine hydroxylation and DNA damage by coal and oil fly ash in relation to particulate metal content and availability. *Chemical Research in Toxicology* 13: 1011-1019.

323. Prahalad, A. K., J. Inmon, L. A. Dailey, M. C. Madden, A. J. Ghio, and J. E. Gallagher. 2001. Air pollution particles mediated oxidative DNA base damage in a cell free system and in human airway epithelial cells in relation to particulate metal content and bioreactivity. *Chemical Research in Toxicology* 14: 879-887.

324. Hartwig, A., M. Asmuss, I. Ehleben, U. Herzer, D. Kostelac, A. Pelzer, T. Schwerdtle, and A. Burkle. 2002. Interference by toxic metal ions with DNA repair processes and cell cycle control: molecular mechanisms. *Environ Health Perspect* 110 Suppl 5: 797-799.

325. Knaapen, A. M., T. Shi, P. J. Borm, and R. P. Schins. 2002. Soluble metals as well as the insoluble particle fraction are involved in cellular DNA damage induced by particulate matter. *Mol Cell Biochem* 234-235: 317-326.

326. Sacks, J. D., L. W. Stanek, T. J. Luben, D. O. Johns, B. J. Buckley, J. S. Brown, and M. Ross. 2011. Particulate Matter-Induced Health Effects: Who Is Susceptible? *Environmental Health Perspectives* 119: 446-454.

327. Saxon, A., and D. Diaz-Sanchez. 2005. Air pollution and allergy: you are what you breathe. *Nat Immunol* 6: 223-226.

328. Salter, H. H. 1860. *On asthma: its pathology and treatment*. Blanchard and Lea, Philadelphia,.

329. To, T., S. Stanojevic, G. Moores, A. S. Gershon, E. D. Bateman, A. A. Cruz, and L. P. Boulet. 2012. Global asthma prevalence in adults: findings from the cross-sectional world health survey. *Bmc Public Health* 12.

330. Asthma UK. 2013. Asthma facts and FAQs.

331. National Health Service UK. 2013. What is asthma?

332. Holgate, S., H. Bisgaard, L. Bjermer, T. Haahtela, J. Haughney, R. Horne, A. McIvor, S. Palkonen, D. B. Price, M. Thomas, E. Valovirta, and U. Wahn. 2008. The Brussels Declaration: the need for change in asthma management. *European Respiratory Journal* 32: 1433-1442.

333. Eder, W., M. J. Ege, and E. von Mutius. 2006. The asthma epidemic. *N Engl J Med* 355: 2226-2235.

334. Yawn, B. P. 2008. Factors accounting for asthma variability: achieving optimal symptom control for individual patients. *Primary care respiratory journal : journal of the General Practice Airways Group* 17: 138-147.

335. Taylor, D. R., E. D. Bateman, L. P. Boulet, H. A. Boushey, W. W. Busse, T. B. Casale, P. Chanez, P. L. Enright, P. G. Gibson, J. C. de Jongste, H. A. M. Kerstjens, S. C. Lazarus, M. L. Levy, P. M. O'Byrne, M. R. Partridge, I. D. Pavord, M. R. Sears, P. J. Sterk, S. W. Stoloff, S. J. Szefler, S. D. Sullivan, M. D. Thomas, S. E. Wenzel, and H. K. Reddel. 2008. A new perspective on concepts of asthma severity and control. *European Respiratory Journal* 32: 545-554.

336. Agache, I. O. 2013. From phenotypes to endotypes to asthma treatment. *Curr Opin Allergy Clin Immunol*.

337. Wenzel, S. E. 2006. Asthma: defining of the persistent adult phenotypes. *Lancet* 368: 804-813.

338. Lotvall, J., C. A. Akdis, L. B. Bacharier, L. Bjermer, T. B. Casale, A. Custovic, R. F. Lemanske, A. J. Wardlaw, S. E. Wenzel, and P. A. Greenberger. 2011. Asthma endotypes: A new approach to classification of disease entities within the asthma syndrome. *Journal of Allergy and Clinical Immunology* 127: 355-360.

339. Moore, W. C., D. A. Meyers, S. E. Wenzel, W. G. Teague, H. S. Li, X. N. Li, R. D'Agostino, M. Castro, D. Curran-Everett, A. M. Fitzpatrick, B. Gaston, N. N. Jarjour, R. Sorkness, W. J. Calhoun, K. F. Chung, S. A. A. Comhair, R. A. Dweik, E. Israel, S. P. Peters, W. W. Busse, S. C. Erzurum, E. R. Bleecker, and N. H. L. B. Inst. 2010. Identification of Asthma Phenotypes Using Cluster Analysis in the Severe Asthma Research Program. *American Journal of Respiratory and Critical Care Medicine* 181: 315-323.

340. Haldar, P., I. D. Pavord, D. E. Shaw, M. A. Berry, M. Thomas, C. E. Brightling, A. I. Wardlaw, and R. H. Green. 2008. Cluster analysis and clinical asthma phenotypes. *American Journal of Respiratory and Critical Care Medicine* 178: 218-224.

341. Green, R. H., C. E. Brightling, G. Woltmann, D. Parker, A. J. Wardlaw, and I. D. Pavord. 2002. Analysis of induced sputum in adults with asthma: identification of subgroup with isolated sputum neutrophilia and poor response to inhaled corticosteroids. *Thorax* 57: 875-879.

342. Pavord, I. D., C. E. Brightling, G. Woltmann, and A. J. Wardlaw. 1999. Non-eosinophilic corticosteroid unresponsive asthma. *Lancet* 353: 2213-2214.

343. Holgate, S. T., H. S. Arshad, G. C. Roberts, P. H. Howarth, P. Thurner, and D. E. Davies. 2010. A new look at the pathogenesis of asthma. *Clin Sci* 118: 439-450.

344. Sporik, R., S. T. Holgate, T. A. E. Plattsmills, and J. J. Cogswell. 1990. Exposure to House Dust Mite Allergen (Der p 1) and the Development of Asthma in Childhood - a Prospective Study. *New England Journal of Medicine* 323: 502-507.

345. Black, P. N., A. A. Udy, and S. M. Brodie. 2000. Sensitivity to fungal allergens is a risk factor for life-threatening asthma. *Allergy* 55: 501-504.

346. O'Driscoll, B. R., L. C. Hopkinson, and D. W. Denning. 2005. Mold sensitization is common amongst patients with severe asthma requiring multiple hospital admissions. *BMC Pulm Med* 5: 4.

347. Darrow, L. A., J. Hess, C. A. Rogers, P. E. Tolbert, M. Klein, and S. E. Sarnat. 2012. Ambient pollen concentrations and emergency department visits for asthma and wheeze. *Journal of Allergy and Clinical Immunology* 130: 630-638.

348. Dales, R. E., S. Cakmak, S. Judek, T. Dann, F. Coates, J. R. Brook, and R. T. Burnett. 2004. Influence of outdoor aeroallergens on hospitalization for asthma in Canada. *Journal of Allergy and Clinical Immunology* 113: 303-306.

349. Miller, E. K., K. M. Edwards, G. A. Weinberg, M. K. Lwane, M. R. Griffin, C. B. Hall, Y. W. Zhu, P. G. Szilagyi, L. L. Morin, L. H. Heil, X. Y. Lu, J. V. Williams, and N. V. S. Network. 2009. A novel group of rhinoviruses is associated with asthma hospitalizations. *Journal of Allergy and Clinical Immunology* 123: 98-104.

350. Papadopoulos, N. G., P. Xepapadaki, P. Mallia, G. Brusselle, J. B. Watelet, M. Xatzipsalti, G. Foteinos, C. M. van Drunen, W. J. Fokkens, C. D'Ambrosio, S. Bonini, A. Bossios, J. Lotvall, P. van Cauwenberge, S. T. Holgate, G. W. Canonica, A. Szczeklik, G. Rohde, J. Kimpen, A. Pitkaranta, M. Makela, P.

Chanez, J. Ring, and S. L. Johnston. 2007. Mechanisms of virus-induced asthma exacerbations: state-of-the-art. A GA(2)LEN and InterAirways document. *Allergy* 62: 457-470.

351. Johnston, N. W., S. L. Johnston, J. M. Duncan, J. M. Greene, T. Kebadze, P. K. Keith, M. Roy, S. Waserman, and M. R. Sears. 2005. The September epidemic of asthma exacerbations in children: A search for etiology. *Journal of Allergy and Clinical Immunology* 115: 132-138.

352. Althuis, M. D., M. Sexton, and D. Prybylski. 1999. Cigarette smoking and asthma symptom severity among adult asthmatics. *J Asthma* 36: 257-264.

353. Dykewicz, M. S. 2009. Occupational asthma: Current concepts in pathogenesis, diagnosis, and management. *Journal of Allergy and Clinical Immunology* 123: 519-528.

354. Anderson, S. D., and E. Daviskas. 2000. The mechanism of exercise-induced asthma is ... *Journal of Allergy and Clinical Immunology* 106: 453-459.

355. Stevenson, D. D., and A. Szczeklik. 2006. Clinical and pathologic perspectives on aspirin sensitivity and asthma. *Journal of Allergy and Clinical Immunology* 118: 773-786.

356. Farah, C. S., and C. M. Salome. 2012. Asthma and obesity: A known association but unknown mechanism. *Respirology* 17: 412-421.

357. Sutherland, E. R., E. Goleva, T. S. King, E. Lehman, A. D. Stevens, L. P. Jackson, A. R. Stream, J. V. Fahy, D. Y. M. Leung, and A. C. R. Network. 2012. Cluster Analysis of Obesity and Asthma Phenotypes. *Plos One* 7.

358. Fenger, R. V., A. Gonzalez-Quintela, C. Vidal, F. Gude, L. L. Husemoen, M. Aadahl, N. D. Berg, and A. Linneberg. 2012. Exploring the obesity-asthma link: do all types of adiposity increase the risk of asthma? *Clinical and Experimental Allergy* 42: 1237-1245.

359. Loerbroks, A., M. C. Gadinger, J. A. Bosch, T. Sturmer, and M. Amelang. 2010. Work-related stress, inability to relax after work and risk of adult asthma: a population-based cohort study. *Allergy* 65: 1298-1305.

360. Waldeck, B. 2002. β–adrenoceptor agonists and asthma - 100 years of development. *Eur J Pharmacol* 445: 1-12.

361. Barnes, P. J. 1998. Efficacy of inhaled corticosteroids in asthma. *Journal of Allergy and Clinical Immunology* 102: 531-538.

362. Hallstrand, T. S., and W. R. Henderson. 2010. An update on the role of leukotrienes in asthma. *Curr Opin Allergy Cl* 10: 60-66.

363. Bousquet, J., P. Cabrera, N. Berkman, R. Buhl, S. Holgate, S. Wenzel, H. Fox, S. Hedgecock, M. Blogg, and G. Della Cioppa. 2005. The effect of treatment with omalizumab, an anti-IgE antibody, on asthma exacerbations and emergency medical visits in patients with severe persistent asthma. *Allergy* 60: 302-308.

364. Walker, S., M. Monteil, K. Phelan, T. J. Lasserson, and E. H. Walters. 2006. Anti-IgE for chronic asthma in adults and children. *Cochrane Db Syst Rev*.

365. Ober, C., N. J. Cox, M. Abney, A. Di Rienzo, E. S. Lander, B. Changyaleket, H. Gidley, B. Kurtz, J. Lee, M. Nance, A. Pettersson, J. Prescott, A. Richardson, E. Schlenker, E. Summerhill, S. Willadsen, R. Parry, and C. S. G. Asthma. 1998. Genome-wide search for asthma susceptibility loci in a founder population. *Hum Mol Genet* 7: 1393-1398.

366. Harada, M., T. Hirota, A. I. Jodo, Y. Hitomi, M. Sakashita, T. Tsunoda, T. Miyagawa, S. Doi, M. Kameda, K. Fujita, A. Miyatake, T. Enomoto, E. Noguchi, H. Masuko, T. Sakamoto, N. Hizawa, Y. Suzuki, S. Yoshihara, M. Adachi, M. Ebisawa, H. Saito, K. Matsumoto, T. Nakajima, R. A. Mathias, N. Rafaels, K. C. Barnes, B. E. Himes, Q. L. Duan, K. G. Tantisira, S. T. Weiss, Y. Nakamura, S. F. Ziegler, and M. Tamari. 2011. Thymic Stromal

Lymphopoietin Gene Promoter Polymorphisms Are Associated with Susceptibility to Bronchial Asthma. *American Journal of Respiratory Cell and Molecular Biology* 44: 787-793.

367. He, J. Q., T. S. Hallstrand, D. Knight, M. Chan-Yeung, A. Sandford, B. Tripp, D. Zamar, Y. Bosse, A. L. Kozyrskyj, A. James, C. Laprise, and D. Daley. 2009. A thymic stromal lymphopoietin gene variant is associated with asthma and airway hyperresponsiveness. *Journal of Allergy and Clinical Immunology* 124: 222-229.

368. Gudbjartsson, D. F., U. S. Bjornsdottir, E. Halapi, A. Helgadottir, P. Sulem, G. M. Jonsdottir, G. Thorleifsson, H. Helgadottir, V. Steinthorsdottir, H. Stefansson, C. Williams, J. Hui, J. Beilby, N. M. Warrington, A. James, L. J. Palmer, G. H. Koppelman, A. Heinzmann, M. Krueger, H. M. Boezen, A. Wheatley, J. Altmuller, H. D. Shin, S. T. Uh, H. S. Cheong, B. Jonsdottir, D. Gislason, C. S. Park, L. M. Rasmussen, C. Porsbjerg, J. W. Hansen, V. Backer, T. Werge, C. Janson, U. B. Jonsson, M. C. Y. Ng, J. Chan, W. Y. So, R. Ma, S. H. Shah, C. B. Granger, A. A. Quyyumi, A. I. Levey, V. Vaccarino, M. P. Reilly, D. J. Rader, M. J. A. Williams, A. M. van Rij, G. T. Jones, E. Trabetti, G. Malerba, P. F. Pignatti, A. Boner, L. Pescollderungg, D. Girelli, O. Olivieri, N. Martinelli, B. R. Ludviksson, D. Ludviksdottir, G. I. Eyjolfsson, D. Arnar, G. Thorgeirsson, K. Deichmann, P. J. Thompson, M. Wjst, I. P. Hall, D. S. Postma, T. Gislason, J. Gulcher, A. Kong, I. Jonsdottir, U. Thorsteinsdottir, and K. Stefansson. 2009. Sequence variants affecting eosinophil numbers associate with asthma and myocardial infarction. *Nature Genetics* 41: 342-347.

369. Moffatt, M. F., I. G. Gut, F. Demenais, D. P. Strachan, E. Bouzigon, S. Heath, E. von Mutius, M. Farrall, M. Lathrop, W. O. C. M. Cookson, and G. Consortium. 2010. A Large-Scale, Consortium-Based Genomewide Association Study of Asthma. *New England Journal of Medicine* 363: 1211-1221.

370. Reijmerink, N. E., D. S. Postma, M. Bruinenberg, I. M. Nolte, D. A. Meyers, E. R. Bleecker, and G. H. Koppelman. 2008. Association of IL1RL1, IL18R1,

and IL18RAP gene cluster polymorphisms with asthma and atopy. *Journal of Allergy and Clinical Immunology* 122: 651-654.

371. Moffatt, M. F., M. Kabesch, L. M. Liang, A. L. Dixon, D. Strachan, S. Heath, M. Depner, A. von Berg, A. Bufe, E. Rietschel, A. Heinzmann, B. Simma, T. Frischer, S. A. G. Willis-Owen, K. C. C. Wong, T. Illig, C. Vogelberg, S. K. Weiland, E. von Mutius, G. R. Abecasis, M. Farrall, I. G. Gut, G. M. Lathrop, and W. O. C. Cookson. 2007. Genetic variants regulating ORMDL3 expression contribute to the risk of childhood asthma. *Nature* 448: 470-U475.

372. Cantero-Recasens, G., C. Fandos, F. Rubio-Moscardo, M. A. Valverde, and R. Vicente. 2010. The asthma-associated ORMDL3 gene product regulates endoplasmic reticulum-mediated calcium signaling and cellular stress. *Hum Mol Genet* 19: 111-121.

373. Carreras-Sureda, A., G. Cantero-Recasens, F. Rubio-Moscardo, K. Kiefer, C. Peinelt, B. A. Niemeyer, M. A. Valverde, and R. Vicente. 2013. ORMDL3 modulates store-operated calcium entry and lymphocyte activation. *Hum Mol Genet* 22: 519-530.

374. Wu, H., I. Romieu, J. J. Sienra-Monge, H. Li, B. E. del Rio-Navarro, and S. J. London. 2009. Genetic variation in ORM1-like 3 (ORMDL3) and gasdermin-like (GSDML) and childhood asthma. *Allergy* 64: 629-635.

375. Van Eerdewegh, P., R. D. Little, J. Dupuis, R. G. Del Mastro, K. Falls, J. Simon, D. Torrey, S. Pandit, J. McKenny, K. Braunschweiger, A. Walsh, Z. Y. Liu, B. Hayward, C. Folz, S. P. Manning, A. Bawa, L. Saracino, M. Thackston, Y. Benchekroun, N. Capparell, M. Wang, R. Adair, Y. Feng, J. Dubois, M. G. FitzGerald, H. Huang, R. Gibson, K. M. Allen, A. Pedan, M. R. Danzig, S. P. Umland, R. W. Egan, F. M. Cuss, S. Rorke, J. B. Clough, J. W. Holloway, S. T. Holgate, and T. P. Keith. 2002. Association of the ADAM33 gene with asthma and bronchial hyperresponsiveness. *Nature* 418: 426-430.

376. Puxeddu, I., Y. Y. Pang, A. Harvey, H. M. Haitchi, B. Nicholas, H. Yoshisue, D. Ribatti, G. Clough, R. M. Powell, G. Murphy, N. A. Hanley, D. I. Wilson, P. H. Howarth, S. T. Holgate, and D. E. Davies. 2008. The soluble form of a disintegrin and metalloprotease 33 promotes angiogenesis: Implications for airway remodeling in asthma. *Journal of Allergy and Clinical Immunology* 121: 1400-1406.

377. Koppelman, G. H., D. A. Meyers, T. D. Howard, S. L. Zheng, G. A. Hawkins, E. J. Ampleford, J. F. Xu, H. Koning, M. Bruinenberg, I. M. Nolte, C. C. van Diemen, H. M. Boezen, W. Timens, P. A. Whittaker, O. C. Stine, S. J. Bartons, J. W. Holloway, S. T. Holgate, P. E. Graves, F. D. Martinez, A. J. van Oosterhout, E. R. Bleecker, and D. S. Postma. 2009. Identification of PCDH1 as a Novel Susceptibility Gene for Bronchial Hyperresponsiveness. *American Journal of Respiratory and Critical Care Medicine* 180: 929-935.

378. Palmer, C. N. A., A. D. Irvine, A. Terron-Kwiatkowski, Y. W. Zhao, H. H. Liao, S. P. Lee, D. R. Goudie, A. Sandilands, L. E. Campbell, F. J. D. Smith, G. M. O'Regan, R. M. Watson, J. E. Cecil, S. J. Bale, J. G. Compton, J. J. DiGiovanna, P. Fleckman, S. Lewis-Jones, G. Arseculeratne, A. Sergeant, C. S. Munro, B. El Houate, K. McElreavey, L. B. Halkjaer, H. Bisgaard, S. Mukhopadhyay, and W. H. I. McLean. 2006. Common loss-of-function variants of the epidermal barrier protein filaggrin are a major predisposing factor for atopic dermatitis. *Nature Genetics* 38: 441-446.

379. Weidinger, S., M. O'Sullivan, T. Illig, H. Baurecht, M. Depner, E. Rodriguez, A. Ruether, N. Klopp, C. Vogelberg, S. K. Weiland, W. H. I. McLean, E. Von Mutius, A. D. Irvine, and M. Kabesch. 2008. Filaggrin mutations, atopic eczema, hay fever, and asthma in children. *Journal of Allergy and Clinical Immunology* 121: 1203-1209.

380. McLean, W. H. I., C. N. A. Palmer, J. Henderson, M. Kabesch, S. Weidinger, and A. D. Irvine. 2008. Filaggrin variants confer susceptibility to asthma. *Journal of Allergy and Clinical Immunology* 121: 1294-1295.

381. Nieminen, M. M., J. Kaprio, and M. Koskenvuo. 1991. A Population-Based Study of Bronchial-Asthma in Adult Twin Pairs. *Chest* 100: 70-75.

382. Skadhauge, L. R., K. Christensen, K. O. Kyvik, and T. Sigsgaard. 1999. Genetic and environmental influence on asthma: a population based study of 11,688 Danish twin pairs. *European Respiratory Journal* 13: 8-14.

383. von Mutius, E. 2009. Gene-environment interactions in asthma. *Journal of Allergy and Clinical Immunology* 123: 3-11.

384. Ober, C., and D. Vercelli. 2011. Gene-environment interactions in human disease: nuisance or opportunity? *Trends in Genetics* 27: 107-115.

385. Holgate, S. T. 2008. The airway epithelium is central to the pathogenesis of asthma. *Allergology international : official journal of the Japanese Society of Allergology* 57: 1-10.

386. Brown, M. S., S. E. Sarnat, K. A. DeMuth, L. A. S. Brown, D. R. Whitlock, S. W. Brown, P. E. Tolbert, and A. M. Fitzpatrick. 2012. Residential Proximity to a Major Roadway Is Associated with Features of Asthma Control in Children. *Plos One* 7.

387. Patel, M. M., S. N. Chillrud, K. C. Deepti, J. M. Ross, and P. L. Kinney. 2013. Traffic-related air pollutants and exhaled markers of airway inflammation and oxidative stress in New York City adolescents. *Environ Res* 121: 71-78.

388. Janssen, N. A. H., B. Brunekreef, P. van Vliet, F. Aarts, K. Meliefste, H. Harssema, and P. Fischer. 2003. The relationship between air pollution from heavy traffic and allergic sensitization, bronchial hyperresponsiveness, and respiratory symptoms in Dutch schoolchildren. *Environmental Health Perspectives* 111: 1512-1518.

389. Riedl, M. A. 2008. The effect of air pollution on asthma and allergy. *Curr Allergy Asthm R* 8: 139-146.

390. Watts, J. 2006. Doctors blame air pollution for China's asthma increases. *Lancet* 368: 719-720.

391. Weichenthal, S., A. Dufresne, and C. Infante-Rivard. 2007. Indoor ultrafine particles and childhood asthma: exploring a potential public health concern. *Indoor Air* 17: 81-91.

392. Hwang, B. F., Y. L. Lee, Y. C. Lin, J. J. K. Jaakkola, and Y. L. Guo. 2005. Traffic related air pollution as a determinant of asthma among Taiwanese school children. *Thorax* 60: 467-473.

393. Gowers, A. M., P. Cullinan, J. G. Ayres, H. R. Anderson, D. P. Strachan, S. T. Holgate, I. C. Mills, and R. L. Maynard. 2012. Does outdoor air pollution induce new cases of asthma? Biological plausibility and evidence; a review. *Respirology* 17: 887-898.

394. Carlsten, C., and E. Melen. 2012. Air pollution, genetics, and allergy: an update. *Curr Opin Allergy Cl* 12: 455-460.

395. Kim, B. J., J. H. Seo, Y. H. Jung, H. Y. Kim, J. W. Kwon, H. B. Kim, S. Y. Lee, K. S. Park, J. Yu, H. C. Kim, J. H. Leem, J. Y. Lee, J. Sakong, S. Y. Kim, C. G. Lee, D. M. Kang, M. Ha, Y. C. Hong, H. J. Kwon, and S. J. Hong. 2013. Air pollution interacts with past episodes of bronchiolitis in the development of asthma. *Allergy* 68: 517-523.

396. Laube, B. L., D. L. Swift, H. N. Wagner, P. S. Norman, and G. K. Adams. 1986. The Effect of Bronchial Obstruction on Central Airway Deposition of a Saline Aerosol in Patients with Asthma. *American Review of Respiratory Disease* 133: 740-743.

397. Kirkham, P., and I. Rahman. 2006. Oxidative stress in asthma and COPD: Antioxidants as a therapeutic strategy. *Pharmacol Therapeut* 111: 476-494.

398. Andreadis, A. A., S. L. Hazen, S. A. A. Comhair, and S. C. Erzurum. 2003. Oxidative and nitrosative events in asthma. *Free Radical Biology and Medicine* 35: 213-225.

399. Comhair, S. A. A., P. R. Bhathena, R. A. Dweik, M. Kavuru, and S. C. Erzurum. 2000. Rapid loss of superoxide dismutase activity during antigen-induced asthmatic response. *Lancet* 355: 624-624.

400. Kelly, F. K., J. Mudway, A. Blomberg, A. Frew, and T. Sandstrom. 1999. Altered lung antioxidant status in patients with mild asthma. *Lancet* 354: 482-483.

401. Buettner, G. R. 1993. The Pecking Order of Free-Radicals and Antioxidants - Lipid-Peroxidation, Alpha-Tocopherol, and Ascorbate. *Archives of Biochemistry and Biophysics* 300: 535-543.

402. Buettner, G. R., and B. A. Jurkiewicz. 1996. Catalytic metals, ascorbate and free radicals: Combinations to avoid. *Radiat Res* 145: 532-541.

403. Bucchieri, F., S. M. Puddicombe, J. L. Lordan, A. Richter, D. Buchanan, S. J. Wilson, J. Ward, G. Zummo, P. H. Howarth, R. Djukanovic, S. T. Holgate, and D. E. Davies. 2002. Asthmatic bronchial epithelium is more susceptible to oxidant-induced apoptosis. *Am J Respir Cell Mol Biol* 27: 179-185.

404. Lee, Y. L., T. R. Hsiue, Y. C. Lee, Y. C. Lin, and Y. L. L. Guo. 2005. The association between glutathione S-transferase P1, M1 polymorphisms and asthma in Taiwanese schoolchildren. *Chest* 128: 1156-1162.

405. Breton, C. V., M. T. Salam, H. Vora, W. J. Gauderman, and F. D. Gilliland. 2011. Genetic Variation in the Glutathione Synthesis Pathway, Air Pollution, and Children's Lung Function Growth. *American Journal of Respiratory and Critical Care Medicine* 183: 243-248.

406. Schroer, K. T., A. M. Gibson, U. Sivaprasad, S. A. Bass, M. B. Ericksen, M. Wills-Karp, T. LeCras, A. M. Fitzpatrick, L. A. S. Brown, K. F. Stringer, and G. K. K. Hershey. 2011. Downregulation of glutathione S-transferase pi in asthma contributes to enhanced oxidative stress. *Journal of Allergy and Clinical Immunology* 128: 539-548.

407. Wu, W. D., V. Doreswamy, D. Diaz-Sanchez, J. M. Samet, M. Kesic, L. Dailey, W. L. Zhang, I. Jaspers, and D. B. Peden. 2011. GSTM1 modulation of IL-8 expression in human bronchial epithelial cells exposed to ozone. *Free Radical Biology and Medicine* 51: 522-529.

408. Fitzpatrick, A. M., S. T. Stephenson, G. R. Hadley, L. Burwell, M. Penugonda, D. M. Simon, J. Hansen, D. P. Jones, and L. A. S. Brown. 2011. Thiol redox disturbances in children with severe asthma are associated with posttranslational modification of the transcription factor nuclear factor (erythroid-derived 2)-like 2. *Journal of Allergy and Clinical Immunology* 127: 1604-1611.

409. Montaser, A., J. A. McLean, H. Liu, and J.-M. Mermet. 1998. An introduction to ICP spectrometries for elemental analysis. In *Inductively coupled plasma mass spectrometry*. A. Montaser, ed. Wiley-VCH, New York ; Chichester. xxix, 964p., [968]p. of plates.

410. Olesik, J. W. 2000. Inductively coupled plasma mass spectrometry. In *Inorganic mass spectrometry : fundamentals and applications*. C. M. Barshick, D. C. Duckworth, and D. H. Smith, eds. Marcel Dekker, New York, N.Y. viii, 512 p.

411. Grecz, N., R. B. Brannon, and G. Killgore. 1987. Radiation Sterilization of Surgical-Instruments with a Consideration of Metal Shielding on Sterilization Efficiency. *Am J Infect Control* 15: 101-106.

412. Cozens, A. L., M. J. Yezzi, K. Kunzelmann, T. Ohrui, L. Chin, K. Eng, W. E. Finkbeiner, J. H. Widdicombe, and D. C. Gruenert. 1994. CFTR expression

and chloride secretion in polarized immortal human bronchial epithelial cells. *Am J Respir Cell Mol Biol* 10: 38-47.

413. Gray, T. E., K. Guzman, C. W. Davis, L. H. Abdullah, and P. Nettesheim. 1996. Mucociliary differentiation of serially passaged normal human tracheobronchial epithelial cells. *American Journal of Respiratory Cell and Molecular Biology* 14: 104-112.

414. Starnes, J. W. 2008. Effect of storage conditions on lactate dehydrogenase released from perfused hearts. *Int J Cardiol* 127: 114-116.

415. Matteucci, E., G. Gregori, L. Pellegrini, R. Navalesi, and O. Giampietro. 1991. Effects of Storage Time and Temperature on Urinary Enzymes. *Clin Chem* 37: 1436-1441.

416. Dunphy, G., and D. Ely. 1990. Decreased Storage Stability of Creatine-Kinase in a Cardiac Reperfusion Solution. *Clin Chem* 36: 778-780.

417. Reynolds, E. S. 1963. The Use Of Lead Citrate at High pH as an Electron-Opaque Stain in Electron Microscopy. *The Journal of Cell Biology* 17: 208-212.

418. Nieuwenhuijsen, M. J., J. E. Gomez-Perales, and R. N. Colvile. 2007. Levels of particulate air pollution, its elemental composition, determinants and health effects in metro systems. *Atmospheric Environment* 41: 7995-8006.

419. Midander, K., K. Elihn, A. Wallen, L. Belova, A. K. B. Karlsson, and I. O. Wallinder. 2012. Characterisation of nano- and micron-sized airborne and collected subway particles, a multi-analytical approach. *Science of the Total Environment* 427: 390-400.

420. Oberdorster, G., J. Ferin, and B. E. Lehnert. 1994. Correlation between Particle-Size, in-Vivo Particle Persistence, and Lung Injury. *Environmental Health Perspectives* 102: 173-179.

421. Loxham, M., M. J. Cooper, M. E. Gerlofs-Nijland, F. R. Cassee, D. E. Davies, M. R. Palmer, and D. A. H. Teagle. 2013. Physicochemical Characterization of Airborne Particulate Matter at a Mainline Underground Railway Station. *Environmental Science & Technology* 47: 3614-3622.

422. Sundh, J., U. Olofsson, L. Olander, and A. Jansson. 2009. Wear rate testing in relation to airborne particles generated in a wheel-rail contact. *Lubr Sci* 21: 135-150.

423. Donaldson, K., V. Stone, P. J. A. Borm, L. A. Jimenez, P. S. Gilmour, R. P. F. Schins, A. M. Knaapen, I. Rahman, S. P. Faux, D. M. Brown, and W. MacNee. 2003. Oxidative stress and calcium signaling in the adverse effects of environmental particles (PM10). *Free Radical Biology and Medicine* 34: 1369-1382.

424. Zimmer, A. T., and A. D. Maynard. 2002. Investigation of the aerosols produced by a high-speed, hand-held grinder using various substrates. *Annals of Occupational Hygiene* 46: 663-672.

425. Weckwerth, G. 2001. Verification of traffic emitted aerosol components in the ambient air of Cologne (Germany). *Atmospheric Environment* 35: 5525-5536.

426. Liljedahl Bare Wire. 2012. Contact Wire and Stranded Conductors for Overhead Catenary Systems. Liljebahl Bare Wire, Helsingborg, Sweden.

427. Lamifil. 2012. Railway Applications and Solutions.

428. Kubo, S., and K. Kato. 1998. Effect of arc discharge on wear rate of Cu-impregnated carbon strip in unlubricated sliding against Cu trolley under electric current. *Wear* 216: 172-178.

429. Kubo, S., and K. Kato. 1999. Effect of arc discharge on the wear rate and wear mode transition of a copper-impregnated metallized carbon contact strip sliding against a copper disk. *Tribol Int* 32: 367-378.

430. Dong, L., G. X. Chen, M. H. Zhu, and Z. R. Zhou. 2007. Wear mechanism of aluminum-stainless steel composite conductor rail sliding against collector shoe with electric current. *Wear* 263: 598-603.

431. World Health Organization Regional Office for Europe. 2000. *Air quality guidelines for Europe*. WHO Reg. Office for Europe, Copenhagen.

432. Olanow, C. W. 2004. Manganese-induced parkinsonism and Parkinson's disease. *Ann Ny Acad Sci* 1012: 209-223.

433. Bloemen, H. J. T., M. E. Gerlofs-Nijland, N. A. H. Janssen, T. Sandstrom, L. van Bree, and F. R. Cassee. 2005. Chemical characterization and source apportionment estimates of particulate matter collected within the framework of EU project HEPMEAP. RIVM report 863001002 ed. Rijksinstituut voor Volksgezondheid en Milieu.

434. Stohs, S. J., and D. Bagchi. 1995. Oxidative Mechanisms in the Toxicity of Metal Ions. *Free Radical Biology and Medicine* 18: 321-336.

435. Holmgren, K., and A. Gebremedhin. 2004. Modelling a district heating system: Introduction of waste incineration, policy instruments and co-operation with an industry. *Energ Policy* 32: 1807-1817.

436. Zhang, F. S., S. I. Yamasaki, M. Nanzyo, and K. Kimura. 2001. Evaluation of cadmium and other metal losses from various municipal wastes during incineration disposal. *Environ Pollut* 115: 253-260.

437. Epstein, E., and C. E. Hagen. 1952. A Kinetic Study of the Absorption of Alkali Cations by Barley Roots. *Plant physiology* 27: 457-474.

438. Furuya, K., Y. Kudo, K. Okinaga, M. Yamuki, S. Takahashi, Y. Araki, and Y. Hisamatsu. 2001. Seasonal variation and their characterization of suspended particulate matter in the air of subway stations. *J Trace Microprobe T* 19: 469-485.

439. Apeagyei, E., M. S. Bank, and J. D. Spengler. 2011. Distribution of heavy metals in road dust along an urban-rural gradient in Massachusetts. *Atmospheric Environment* 45: 2310-2323.

440. Becker, S., J. M. Soukup, and J. E. Gallagher. 2002. Differential particulate air pollution induced oxidant stress in human granulocytes, monocytes and alveolar macrophages. *Toxicol in Vitro* 16: 209-218.

441. Lin, C. C., S. J. Chen, K. L. Huang, W. I. Hwang, G. P. Chang-Chien, and W. Y. Lin. 2005. Characteristics of metals in nano/ultrafine/fine/coarse particles collected beside a heavily trafficked road. *Environmental Science & Technology* 39: 8113-8122.

442. Raut, J. C., P. Chazette, and A. Fortain. 2009. Link between aerosol optical, microphysical and chemical measurements in an underground railway station in Paris. *Atmospheric Environment* 43: 860-868.

443. Westerdahl, D., S. A. Fruin, P. L. Fine, and C. Sioutas. 2008. The Los Angeles International Airport as a source of ultrafine particles and other pollutants to nearby communities. *Atmospheric Environment* 42: 3143-3155.

444. Jung, H. J., B. Kim, J. Ryu, S. Maskey, J. C. Kim, J. Sohn, and C. U. Ro. 2010. Source identification of particulate matter collected at underground subway stations in Seoul, Korea using quantitative single-particle analysis. *Atmospheric Environment* 44: 2287-2293.

445. Samet, J. M., F. Dominici, F. C. Curriero, I. Coursac, and S. L. Zeger. 2000. Fine particulate air pollution and mortality in 20 US Cities, 1987-1994. *New England Journal of Medicine* 343: 1742-1749.

446. Klepczynska-Nystrom, A., B. M. Larsson, J. Grunewald, C. Pousette, A. Lundin, A. Eklund, and M. Svartengren. 2012. Health effects of a subway environment in mild asthmatic volunteers. *Respiratory Medicine* 106: 25-33.

447. Steenhof, M., I. Gosens, M. Strak, K. J. Godri, G. Hoek, F. R. Cassee, I. S. Mudway, F. J. Kelly, R. M. Harrison, E. Lebret, B. Brunekreef, N. A. Janssen, and R. H. Pieters. 2011. In vitro toxicity of particulate matter (PM) collected at different sites in the Netherlands is associated with PM composition, size fraction and oxidative potential - the RAPTES project. *Part Fibre Toxicol* 8: 26.

448. Keberle, H. 1964. The Biochemistry of Desferrioxamine and Its Relation to Iron Metabolism. *Ann N Y Acad Sci* 119: 758-768.

449. Soumelis, V., P. A. Reche, H. Kanzler, W. Yuan, G. Edward, B. Homey, M. Gilliet, S. Ho, S. Antonenko, A. Lauerma, K. Smith, D. Gorman, S. Zurawski, J. Abrams, S. Menon, T. McClanahan, R. de Waal-Malefyt, F. Bazan, R. A. Kastelein, and Y. J. Liu. 2002. Human epithelial cells trigger dendritic cell-mediated allergic inflammation by producing TSLP. *Nat Immunol* 3: 673-680.

450. Blank, F., B. Rothen-Rutishauser, and P. Gehr. 2007. Dendritic cells and macrophages form a transepithelial network against foreign particulate antigens. *American Journal of Respiratory Cell and Molecular Biology* 36: 669-677.

451. Kouzaki, H., K. Iijima, T. Kobayashi, S. M. O'Grady, and H. Kita. 2011. The Danger Signal, Extracellular ATP, Is a Sensor for an Airborne Allergen and Triggers IL-33 Release and Innate Th2-Type Responses. *Journal of Immunology* 186: 4375-4387.

452. Liew, F. Y., N. I. Pitman, and I. B. McInnes. 2010. Disease-associated functions of IL-33: the new kid in the IL-1 family. *Nature Reviews Immunology* 10: 103-110.

453. Ovrevik, J., M. Lag, J. A. Holme, P. E. Schwarze, and M. Refsnes. 2009. Cytokine and chemokine expression patterns in lung epithelial cells exposed to components characteristic of particulate air pollution. *Toxicology* 259: 46-53.

454. Strak, M., M. Steenhof, K. J. Godri, I. Gosens, I. S. Mudway, F. R. Cassee, E. Lebret, B. Brunekreef, F. J. Kelly, R. M. Harrison, G. Hoek, and N. A. H.

Janssen. 2011. Variation in characteristics of ambient particulate matter at eight locations in the Netherlands - The RAPTES project. *Atmospheric Environment* 45: 4442-4453.

455. Brunauer, S., P. H. Emmett, and E. Teller. 1938. Adsorption of Gases in Multimolecular Layers. *J Am Chem Soc* 60: 309-319.

456. Zhang, W. G., H. M. Jiang, C. Y. Dong, Q. Yan, L. Z. Yu, and Y. Yu. 2011. Magnetic and geochemical characterization of iron pollution in subway dusts in Shanghai, China. *Geochem Geophy Geosy* 12.

457. Matsushima, K., K. Morishita, T. Yoshimura, S. Lavu, Y. Kobayashi, W. Lew, E. Appella, H. F. Kung, E. J. Leonard, and J. J. Oppenheim. 1988. Molecular-Cloning of a Human Monocyte-Derived Neutrophil Chemotactic Factor (Mdncf) and the Induction of Mdncf Messenger-Rna by Interleukin-1 and Tumor Necrosis Factor. *Journal of Experimental Medicine* 167: 1883-1893.

458. Baggiolini, M., A. Walz, and S. L. Kunkel. 1989. Neutrophil-activating peptide-1/interleukin 8, a novel cytokine that activates neutrophils. *J Clin Invest* 84: 1045-1049.

459. Huber, A. R., S. L. Kunkel, R. F. Todd, 3rd, and S. J. Weiss. 1991. Regulation of transendothelial neutrophil migration by endogenous interleukin-8. *Science* 254: 99-102.

460. Fahy, J. V., K. W. Kim, J. Liu, and H. A. Boushey. 1995. Prominent neutrophilic inflammation in sputum from subjects with asthma exacerbation. *J Allergy Clin Immunol* 95: 843-852.

461. Devalaraja, R. M., L. B. Nanney, J. Du, Q. Qian, Y. Yu, M. N. Devalaraja, and A. Richmond. 2000. Delayed wound healing in CXCR2 knockout mice. *J Invest Dermatol* 115: 234-244.

462. Rennekampff, H. O., J. F. Hansbrough, V. Kiessig, C. Dore, M. Sticherling, and J. M. Schroder. 2000. Bioactive interleukin-8 is expressed in wounds and enhances wound healing. *J Surg Res* 93: 41-54.

463. Luppi, F., A. M. Longo, W. I. de Boer, K. F. Rabe, and P. S. Hiemstra. 2007. Interleukin-8 stimulates cell proliferation in non-small cell lung cancer through epidermal growth factor receptor transactivation. *Lung Cancer* 56: 25-33.

464. Han, X. L., R. Gelein, N. Corson, P. Wade-Mercer, J. K. Jiang, P. Biswas, J. N. Finkelstein, A. Elder, and G. Oberdorster. 2011. Validation of an LDH assay for assessing nanoparticle toxicity. *Toxicology* 287: 99-104.

465. Chen, X. P., Z. F. Zhong, Z. T. Xu, L. D. Chen, and Y. T. Wang. 2010. 2 ',7 '-Dichlorodihydrofluorescein as a fluorescent probe for reactive oxygen species measurement: Forty years of application and controversy. *Free Radical Res* 44: 587-604.

466. Bass, D. A., J. W. Parce, L. R. Dechatelet, P. Szejda, M. C. Seeds, and M. Thomas. 1983. Flow Cytometric Studies of Oxidative Product Formation by Neutrophils - a Graded Response to Membrane Stimulation. *Journal of Immunology* 130: 1910-1917.

467. Keller, A., A. Mohamed, S. Drose, U. Brandt, I. Fleming, and R. P. Brandes. 2004. Analysis of dichlorodihydrofluorescein and dihydrocalcein as probes for the detection of intracellular reactive oxygen species. *Free Radical Res* 38: 1257-1267.

468. Royall, J. A., and H. Ischiropoulos. 1993. Evaluation of 2',7'-Dichlorofluorescin and Dihydrorhodamine 123 as Fluorescent-Probes for Intracellular H2O2 in Cultured Endothelial-Cells. *Archives of Biochemistry and Biophysics* 302: 348-355.

469. Robinson, J. P., L. H. Bruner, C. F. Bassoe, J. L. Hudson, P. A. Ward, and S. H. Phan. 1988. Measurement of Intracellular Fluorescence of Human-Monocytes Relative to Oxidative-Metabolism. *J Leukocyte Biol* 43: 304-310.

470. Diabate, S., B. Bergfeldt, D. Plaumann, C. Ubel, and C. Weiss. 2011. Anti-oxidative and inflammatory responses induced by fly ash particles and carbon black in lung epithelial cells. *Anal Bioanal Chem* 401: 3197-3212.

471. Lebel, C. P., H. Ischiropoulos, and S. C. Bondy. 1992. Evaluation of the Probe 2',7'-Dichlorofluorescin as an Indicator of Reactive Oxygen Species Formation and Oxidative Stress. *Chemical Research in Toxicology* 5: 227-231.

472. Kalyanaraman, B., V. Darley-Usmar, K. J. A. Davies, P. A. Dennery, H. J. Forman, M. B. Grisham, G. E. Mann, K. Moore, L. J. Roberts, and H. Ischiropoulos. 2012. Measuring reactive oxygen and nitrogen species with fluorescent probes: challenges and limitations. *Free Radical Biology and Medicine* 52: 1-6.

473. Burkitt, M. J., and P. Wardman. 2001. Cytochrome c is a potent catalyst of dichlorofluorescin oxidation: Implications for the role of reactive oxygen species in apoptosis. *Biochem Bioph Res CO* 282: 329-333.

474. Lawrence, A., C. M. Jones, P. Wardman, and M. J. Burkitt. 2003. Evidence for the role of a peroxidase compound I-type intermediate in the oxidation of glutathione, NADH, ascorbate, and dichlorofluorescin by cytochrome c/H2O2 - Implications for oxidative stress during apoptosis. *Journal of Biological Chemistry* 278: 29410-29419.

475. Karlsson, M., T. Kurz, U. T. Brunk, S. E. Nilsson, and C. I. Frennesson. 2010. What does the commonly used DCF test for oxidative stress really show? *Biochem J* 428: 183-190.

476. Ohashi, T., A. Mizutani, A. Murakami, S. Kojo, T. Ishii, and S. Taketani. 2002. Rapid oxidation of dichlorodihydrofluorescin with heme and hemoproteins:

formation of the fluorescein is independent of the generation of reactive oxygen species. *Febs Letters* 511: 21-27.

477. Bonini, M. G., C. Rota, A. Tomasi, and R. P. Mason. 2006. The oxidation of 2 ',7 '-dichlorofluorescin to reactive oxygen species: A self-fulfilling prophesy? *Free Radical Biology and Medicine* 40: 968-975.

478. Rotoli, B. M., O. Bussolati, A. L. Costa, M. Blosi, L. Di Cristo, P. P. Zanello, M. G. Bianchi, R. Visigalli, and E. Bergamaschi. 2012. Comparative effects of metal oxide nanoparticles on human airway epithelial cells and macrophages. *J Nanopart Res* 14.

479. Mutlu, E. A., P. A. Engen, S. Soberanes, D. Urich, C. B. Forsyth, R. Nigdelioglu, S. E. Chiarella, K. A. Radigan, A. Gonzalez, S. Jakate, A. Keshavarzian, G. R. S. Budinger, and G. M. Mutlu. 2011. Particulate matter air pollution causes oxidant-mediated increase in gut permeability in mice. *Particle and Fibre Toxicology* 8.

480. Bayram, H., J. L. Devalia, R. J. Sapsford, T. Ohtoshi, Y. Miyabara, M. Sagai, and R. J. Davies. 1998. The effect of diesel exhaust particles on cell function and release of inflammatory mediators from human bronchial epithelial cells in vitro. *Am J Respir Cell Mol Biol* 18: 441-448.

481. Ghio, A. J., and R. B. Devlin. 2001. Inflammatory lung injury after bronchial instillation of air pollution particles. *American Journal of Respiratory and Critical Care Medicine* 164: 704-708.

482. Blank, F., M. Wehrli, A. Lehmann, O. Baum, P. Gehr, C. von Garnier, and B. M. Rothen-Rutishauser. 2011. Macrophages and dendritic cells express tight junction proteins and exchange particles in an in vitro model of the human airway wall. *Immunobiology* 216: 86-95.

483. Jalava, P. I., R. O. Salonen, A. S. Pennanen, M. S. Happo, P. Penttinen, A. I. Halinen, M. Sillanpaa, R. Hillamo, and M. R. Hirvonen. 2008. Effects of

solubility of urban air fine and coarse particles on cytotoxic and inflammatory responses in RAW 264.7 macrophage cell line. *Toxicology and Applied Pharmacology* 229: 146-160.

484. Bruewer, M., A. Luegering, T. Kucharzik, C. A. Parkos, J. L. Madara, A. M. Hopkins, and A. Nusrat. 2003. Proinflammatory cytokines disrupt epithelial barrier function by apoptosis-independent mechanisms. *J Immunol* 171: 6164-6172.

485. Wang, F. J., W. V. Graham, Y. M. Wang, E. D. Witkowski, B. T. Schwarz, and J. R. Turner. 2005. Interferon-gamma and tumor necrosis factor-alpha synergize to induce intestinal epithelial barrier dysfunction by up-regulating myosin light chain kinase expression. *Am J Pathol* 166: 409-419.

486. Bleck, B., D. B. Tse, M. A. C. de Lafaille, F. J. Zhang, and J. Reibman. 2008. Diesel exhaust particle-exposed human bronchial epithelial cells induce dendritic cell maturation and polarization via thymic stromal lymphopoietin. *J Clin Immunol* 28: 147-156.

487. Bleck, B., D. B. Tse, T. Gordon, M. R. Ahsan, and J. Reibman. 2010. Diesel Exhaust Particle-Treated Human Bronchial Epithelial Cells Upregulate Jagged-1 and OX40 Ligand in Myeloid Dendritic Cells via Thymic Stromal Lymphopoietin. *Journal of Immunology* 185: 6636-6645.

488. Bleck, B., G. Grunig, A. Chiu, M. Liu, T. Gordon, A. Kazeros, and J. Reibman. 2013. MicroRNA-375 Regulation of Thymic Stromal Lymphopoietin by Diesel Exhaust Particles and Ambient Particulate Matter in Human Bronchial Epithelial Cells. *J Immunol* 190: 3757-3763.

489. Inoue, K., E. Koike, R. Yanagisaw, S. Hirano, M. Nishikawa, and H. Takano. 2009. Effects of multi-walled carbon nanotubes on a murine allergic airway inflammation model. *Toxicology and Applied Pharmacology* 237: 306-316.

490. Wang, X. J., P. Katwa, R. Podila, P. Y. Chen, P. C. Ke, A. M. Rao, D. M. Walters, C. J. Wingard, and J. M. Brown. 2011. Multi-walled carbon nanotube instillation impairs pulmonary function in C57BL/6 mice. *Particle and Fibre Toxicology* 8.

491. Beamer, C. A., T. A. Girtsman, B. P. Seaver, K. J. Finsaas, C. T. Migliaccio, V. K. Perry, J. B. Rottman, D. E. Smith, and A. Holian. 2012. IL-33 mediates multi-walled carbon nanotube (MWCNT)-induced airway hyper-reactivity via the mobilization of innate helper cells in the lung. *Nanotoxicology*.

492. Totlandsdal, A. I., F. R. Cassee, P. Schwarze, M. Refsnes, and M. Lag. 2010. Diesel exhaust particles induce CYP1A1 and pro-inflammatory responses via differential pathways in human bronchial epithelial cells. *Particle and Fibre Toxicology* 7.

493. Xia, T., M. Kovochich, M. Liong, L. Madler, B. Gilbert, H. B. Shi, J. I. Yeh, J. I. Zink, and A. E. Nel. 2008. Comparison of the Mechanism of Toxicity of Zinc Oxide and Cerium Oxide Nanoparticles Based on Dissolution and Oxidative Stress Properties. *Acs Nano* 2: 2121-2134.

494. Panas, A., C. Marquardt, O. Nalcaci, H. Bockhorn, W. Baumann, H. R. Paur, S. Mulhopt, S. Diabate, and C. Weiss. 2013. Screening of different metal oxide nanoparticles reveals selective toxicity and inflammatory potential of silica nanoparticles in lung epithelial cells and macrophages. *Nanotoxicology* 7: 259-273.

495. Urbanski, N. K., and A. Beresewicz. 2000. Generation of (OH)-O-. initiated by interaction of Fe2+ and Cu+ with dioxygen; comparison with the Fenton chemistry. *Acta Biochim Pol* 47: 951-962.

496. Podmore, I. D., H. R. Griffiths, K. E. Herbert, N. Mistry, P. Mistry, and J. Lunec. 1998. Vitamin C exhibits pro-oxidant properties. *Nature* 392: 559-559.

497. Carr, A., and B. Frei. 1999. Does vitamin C act as a pro-oxidant under physiological conditions? *Faseb Journal* 13: 1007-1024.

498. Camhi, S. L., J. Alam, L. Otterbein, S. L. Sylvester, and A. M. K. Choi. 1995. Induction of Heme Oxygenase-1 Gene-Expression by Lipopolysaccharide Is Mediated by Ap-1 Activation. *American Journal of Respiratory Cell and Molecular Biology* 13: 387-398.

499. Novitsky, T. J. 1998. Limitations of the Limulus amebocyte lysate test in demonstrating circulating lipopolysaccharides. *Stress of Life* 851: 416-421.

500. Trivedi, L., C. Valerio, and J. E. Slater. 2003. Endotoxin content of standardized allergen vaccines. *Journal of Allergy and Clinical Immunology* 111: 777-783.

501. Ekstrand-Hammarstrom, B., C. M. Akfur, P. O. Andersson, C. Lejon, L. Osterlund, and A. Bucht. 2012. Human primary bronchial epithelial cells respond differently to titanium dioxide nanoparticles than the lung epithelial cell lines A549 and BEAS-2B. *Nanotoxicology* 6: 623-634.

502. Konczol, M., E. Goldenberg, S. Ebeling, B. Schafer, M. Garcia-Kaufer, R. Gminski, B. Grobety, B. Rothen-Rutishauser, I. Merfort, R. Giere, and V. Mersch-Sundermann. 2012. Cellular Uptake and Toxic Effects of Fine and Ultrafine Metal-Sulfate Particles in Human A549 Lung Epithelial Cells. *Chemical Research in Toxicology* 25: 2687-2703.

503. Konczol, M., S. Ebeling, E. Goldenberg, F. Treude, R. Gminski, R. Giere, B. Grobety, B. Rothen-Rutishauser, I. Merfort, and V. Mersch-Sundermann. 2011. Cytotoxicity and Genotoxicity of Size-Fractionated Iron Oxide (Magnetite) in A549 Human Lung Epithelial Cells: Role of ROS, JNK, and NF-kappa B. *Chemical Research in Toxicology* 24: 1460-1475.

504. Wang, Z. Y., N. Li, J. Zhao, J. C. White, P. Qu, and B. S. Xing. 2012. CuO nanoparticle interaction with human epithelial cells: cellular uptake, location, export, and genotoxicity. *Chemical Research in Toxicology* 25: 1512-1521.

505. Frohlich, E. 2012. The role of surface charge in cellular uptake and cytotoxicity of medical nanoparticles. *Int J Nanomed* 7: 5577-5591.

506. Boublil, L., E. Assemat, M. C. Borot, S. Boland, L. Martinon, J. Sciare, and A. Baeza-Squiban. 2013. Development of a repeated exposure protocol of human bronchial epithelium in vitro to study the long-term effects of atmospheric particles. *Toxicol in Vitro* 27: 533-542.

507. Pante, N., and M. Kann. 2002. Nuclear pore complex is able to transport macromolecules with diameters of similar to 39 nm. *Molecular Biology of the Cell* 13: 425-434.

508. Upadhyay, D., V. Panduri, A. Ghio, and D. W. Kamp. 2003. Particulate matter induces alveolar epithelial cell DNA damage and apoptosis - Role of free radicals and the mitochondria. *American Journal of Respiratory Cell and Molecular Biology* 29: 180-187.

509. Karlsson, H. L., A. Holgersson, and L. Moller. 2008. Mechanisms related to the genotoxicity of particles in the subway and from other sources. *Chemical Research in Toxicology* 21: 726-731.

510. Churg, A., and M. Brauer. 2000. Ambient atmospheric particles in the airways of human lungs. *Ultrastruct Pathol* 24: 353-361.

511. Cookson, W. 2004. The immunogenetics of asthma and eczema: a new focus on the epithelium. *Nat Rev Immunol* 4: 978-988.

512. Xiao, C., S. M. Puddicombe, S. Field, J. Haywood, V. Broughton-Head, I. Puxeddu, H. M. Haitchi, E. Vernon-Wilson, D. Sammut, N. Bedke, C. Cremin, J. Sones, R. Djukanovic, P. H. Howarth, J. E. Collins, S. T. Holgate, P. Monk,

and D. E. Davies. 2011. Defective epithelial barrier function in asthma. *J Allergy Clin Immunol* 128: 549-556.

513. Delfino, R. J., R. S. Zeiger, J. M. Seltzer, D. H. Street, R. M. Matteucci, P. R. Anderson, and P. Koutrakis. 1997. The effect of outdoor fungal spore concentrations on daily asthma severity. *Environ Health Perspect* 105: 622-635.

514. O'Hollaren, M. T., J. W. Yunginger, K. P. Offord, M. J. Somers, E. J. O'Connell, D. J. Ballard, and M. I. Sachs. 1991. Exposure to an aeroallergen as a possible precipitating factor in respiratory arrest in young patients with asthma. *N Engl J Med* 324: 359-363.

515. Gilleberg, S. B., J. L. Faull, and K. A. Graeme-Cook. 1998. A preliminary survey of aerial biocontaminants at six London Underground stations. *Int Biodeter Biodegr* 41: 149-152.

516. Picco, A. M., and M. Rodolfi. 2000. Airborne fungi as biocontaminants at two Milan underground stations. *Int Biodeter Biodegr* 45: 43-47.

517. Bogomolova, E., and I. Kirtsideli. 2009. Airborne fungi in four stations of the St. Petersburg Underground railway system. *Int Biodeter Biodegr* 63: 156-160.

518. Awad, A. H. A. 2002. Environmental study in subway metro stations in Cairo, Egypt. *J Occup Health* 44: 112-118.

519. Tomee, J. F., R. van Weissenbruch, J. G. de Monchy, and H. F. Kauffman. 1998. Interactions between inhalant allergen extracts and airway epithelial cells: effect on cytokine production and cell detachment. *J Allergy Clin Immunol* 102: 75-85.

520. Shen, H. D., M. F. Tam, H. Chou, and S. H. Han. 1999. The importance of serine proteinases as aeroallergens associated with asthma. *Int Arch Allergy Immunol* 119: 259-264.

521. Knight, D. A., S. Lim, A. K. Scaffidi, N. Roche, K. F. Chung, G. A. Stewart, and P. J. Thompson. 2001. Protease-activated receptors in human airways: upregulation of PAR-2 in respiratory epithelium from patients with asthma. *J Allergy Clin Immunol* 108: 797-803.

522. Sun, G., M. A. Stacey, M. Schmidt, L. Mori, and S. Mattoli. 2001. Interaction of mite allergens Der p3 and Der p9 with protease-activated receptor-2 expressed by lung epithelial cells. *J Immunol* 167: 1014-1021.

523. Kheradmand, F., A. Kiss, J. Xu, S. H. Lee, P. E. Kolattukudy, and D. B. Corry. 2002. A protease-activated pathway underlying Th cell type 2 activation and allergic lung disease. *J Immunol* 169: 5904-5911.

524. Tai, H. Y., M. F. Tam, H. Chou, H. J. Peng, S. N. Su, D. W. Perng, and H. D. Shen. 2006. Pen ch 13 allergen induces secretion of mediators and degradation of occludin protein of human lung epithelial cells. *Allergy* 61: 382-388.

525. Kobayashi, T., K. Iijima, S. Radhakrishnan, V. Mehta, R. Vassallo, C. B. Lawrence, J. C. Cyong, L. R. Pease, K. Oguchi, and H. Kita. 2009. Asthma-related environmental fungus, Alternaria, activates dendritic cells and produces potent Th2 adjuvant activity. *J Immunol* 182: 2502-2510.

526. Leino, M. S., M. Loxham, C. Blume, E. J. Swindle, N. P. Jayasekera, P. W. Dennison, B. W. Shamji, M. J. Edwards, S. T. Holgate, P. H. Howarth, and D. E. Davies. 2013. Barrier disrupting effects of alternaria alternata extract on bronchial epithelium from asthmatic donors. *Plos One* 8: e71278.

527. Blume, C., E. J. Swindle, P. Dennison, N. P. Jayasekera, S. Dudley, P. Monk, H. Behrendt, C. B. Schmidt-Weber, S. T. Holgate, P. H. Howarth, C. Traidl-Hoffmann, and D. E. Davies. 2013. Barrier responses of human bronchial epithelial cells to grass pollen exposure. *Eur Respir J* 42: 87-97.

528. Murai, H., H. B. Qi, B. Choudhury, J. Wild, N. Dharajiya, S. Vaidya, A. Kalita, A. Bacsi, D. Corry, A. Kurosky, A. Brasier, I. Boldogh, and S. Sur. 2012.

Alternaria-Induced Release of IL-18 from Damaged Airway Epithelial Cells: An NF-kappa B Dependent Mechanism of Th2 Differentiation? *Plos One* 7.

529. Boitano, S., A. N. Flynn, C. L. Sherwood, S. M. Schulz, J. Hoffman, I. Gruzinova, and M. O. Daines. 2011. Alternaria alternata serine proteases induce lung inflammation and airway epithelial cell activation via PAR(2). *American Journal of Physiology-Lung Cellular and Molecular Physiology* 300: L605-L614.

530. Yoshimura, T., K. Matsushima, S. Tanaka, E. A. Robinson, E. Appella, J. J. Oppenheim, and E. J. Leonard. 1987. Purification of a human monocyte-derived neutrophil chemotactic factor that has peptide sequence similarity to other host defense cytokines. *Proc Natl Acad Sci U S A* 84: 9233-9237.

531. Hammond, M. E., G. R. Lapointe, P. H. Feucht, S. Hilt, C. A. Gallegos, C. A. Gordon, M. A. Giedlin, G. Mullenbach, and P. Tekamp-Olson. 1995. IL-8 induces neutrophil chemotaxis predominantly via type I IL-8 receptors. *J Immunol* 155: 1428-1433.

532. Aggarwal, B. B., W. J. Kohr, P. E. Hass, B. Moffat, S. A. Spencer, W. J. Henzel, T. S. Bringman, G. E. Nedwin, D. V. Goeddel, and R. N. Harkins. 1985. Human-Tumor Necrosis Factor - Production, Purification, and Characterization. *Journal of Biological Chemistry* 260: 2345-2354.

533. Baldwin, A. S. 1996. The NF-kappa B and I kappa B proteins: New discoveries and insights. *Annu Rev Immunol* 14: 649-683.

534. Hoffmann, E., O. Dittrich-Breiholz, H. Holtmann, and M. Kracht. 2002. Multiple control of interleukin-8 gene expression. *J Leukoc Biol* 72: 847-855.

535. Li, C. X., M. M. Hao, Z. Cao, W. Ding, R. Graves-Deal, J. Y. Hu, D. W. Piston, and R. J. Coffey. 2007. Naked2 acts as a cargo recognition and targeting protein to ensure proper delivery and fusion of TGF-alpha-

containing exocytic vesicles at the lower lateral membrane of polarized MDCK cells. *Molecular Biology of the Cell* 18: 3081-3093.

536. Belham, C. M., R. J. Tate, P. H. Scott, A. D. Pemberton, H. R. Miller, R. M. Wadsworth, G. W. Gould, and R. Plevin. 1996. Trypsin stimulates proteinase-activated receptor-2-dependent and -independent activation of mitogen-activated protein kinases. *Biochem J* 320 (Pt 3): 939-946.

537. Rallabhandi, P., Q. M. Nhu, V. Y. Toshchakov, W. Piao, A. E. Medvedev, M. D. Hollenberg, A. Fasano, and S. N. Vogel. 2008. Analysis of proteinase-activated receptor 2 and TLR4 signal transduction: a novel paradigm for receptor cooperativity. *J Biol Chem* 283: 24314-24325.

538. Yike, I. 2011. Fungal Proteases and Their Pathophysiological Effects. *Mycopathologia* 171: 299-323.

539. Doherty, T. A., N. Khorram, K. Sugimoto, D. Sheppard, P. Rosenthal, J. Y. Cho, A. Pham, M. Miller, M. Croft, and D. H. Broide. 2012. Alternaria Induces STAT6-Dependent Acute Airway Eosinophilia and Epithelial FIZZ1 Expression That Promotes Airway Fibrosis and Epithelial Thickness. *Journal of Immunology* 188: 2622-2629.

540. Inoue, Y., Y. Matsuwaki, S. H. Shin, J. U. Ponikau, and H. Kita. 2005. Nonpathogenic, environmental fungi induce activation and degranulation of human eosinophils. *J Immunol* 175: 5439-5447.

541. Fekkar, A., V. Balloy, C. Pionneau, C. Marinach-Patrice, M. Chignard, and D. Mazier. 2012. Secretome of Human Bronchial Epithelial Cells in Response to the Fungal Pathogen Aspergillus fumigatus Analyzed by Differential In-Gel Electrophoresis. *Journal of Infectious Diseases* 205: 1163-1172.

542. Hanada, K., M. Tamai, M. Yamagishi, S. Ohmura, J. Sawada, and I. Tanaka. 1978. Isolation and Characterization of E-64, a New Thiol Protease Inhibitor. *Agr Biol Chem Tokyo* 42: 523-528.

543. Powers, J. C., J. L. Asgian, O. D. Ekici, and K. E. James. 2002. Irreversible inhibitors of serine, cysteine, and threonine proteases. *Chem Rev* 102: 4639-4750.

544. Barrett, A. J., and J. T. Dingle. 1972. Inhibition of Tissue Acid Proteinases by Pepstatin. *Biochem J* 127: 439-&.

545. Reese, T. A., H. E. Liang, A. M. Tager, A. D. Luster, N. Van Rooijen, D. Voehringer, and R. M. Locksley. 2007. Chitin induces accumulation in tissue of innate immune cells associated with allergy. *Nature* 447: 92-96.

546. Carmona, E. M., J. D. Lamont, A. Xue, M. Wylam, and A. H. Limper. 2010. Pneumocystis cell wall beta-glucan stimulates calcium-dependent signaling of IL-8 secretion by human airway epithelial cells. *Resp Res* 11.

547. Neveu, W. A., E. Bernardo, J. L. Allard, V. Nagaleekar, M. J. Wargo, R. J. Davis, Y. Iwakura, L. A. Whittaker, and M. Rincon. 2011. Fungal Allergen beta-Glucans Trigger p38 Mitogen-Activated Protein Kinase-Mediated IL-6 Translation in Lung Epithelial Cells. *Am J Respir Cell Mol Biol* 45: 1133-1141.

548. Esch, R. E. 2004. Manufacturing and standardizing fungal allergen products. *Journal of Allergy and Clinical Immunology* 113: 210-215.

549. Nagarkar, D. R., J. A. Poposki, M. R. Comeau, A. Biyasheva, P. C. Avila, R. P. Schleimer, and A. Kato. 2012. Airway epithelial cells activate Th2 cytokine production in mast cells through IL-1 and thymic stromal lymphopoietin. *Journal of Allergy and Clinical Immunology* 130: 225-232.

550. Cakmak, S., R. E. Dales, and F. Coates. 2012. Does air pollution increase the effect of aeroallergens on hospitalization for asthma? *Journal of Allergy and Clinical Immunology* 129: 228-231.

551. Knox, R. B., C. Suphioglu, P. Taylor, R. Desai, H. C. Watson, J. L. Peng, and L. A. Bursill. 1997. Major grass pollen allergen Lol p 1 binds to diesel exhaust

particles: Implications for asthma and air pollution. *Clinical and Experimental Allergy* 27: 246-251.

552. Becker, S., J. M. Soukup, C. Sioutas, and F. R. Cassee. 2003. Response of human alveolar macrophages to ultrafine, fine, and coarse urban air pollution particles. *Exp Lung Res* 29: 29-44.

553. Kagan, V. E., Y. Y. Tyurina, V. A. Tyurin, N. V. Konduru, A. I. Potapovich, A. N. Osipov, E. R. Kisin, D. Schwegler-Berry, R. Mercer, V. Castranova, and A. A. Shvedova. 2006. Direct and indirect effects of single walled carbon nanotubes on RAW 264.7 macrophages: Role of iron. *Toxicology Letters* 165: 88-100.

554. Weiden, M. D., B. Naveed, S. Kwon, L. N. Segal, S. J. Cho, J. Tsukiji, R. Kulkarni, A. L. Comfort, K. J. Kasturiarachchi, C. Prophete, M. D. Cohen, L. C. Chen, W. N. Rom, D. J. Prezant, and A. Nolan. 2012. Comparison of WTC Dust Size on Macrophage Inflammatory Cytokine Release In vivo and In vitro. *Plos One* 7.

555. Swindle, E. J., and D. E. Davies. 2011. Artificial airways for the study of respiratory disease. *Expert review of respiratory medicine* 5: 757-765.

556. Lesniak, A., F. Fenaroli, M. R. Monopoli, C. Aberg, K. A. Dawson, and A. Salvati. 2012. Effects of the Presence or Absence of a Protein Corona on Silica Nanoparticle Uptake and Impact on Cells. *Acs Nano* 6: 5845-5857.

557. Lesniak, A., A. Salvati, M. J. Santos-Martinez, M. W. Radomski, K. A. Dawson, and C. Aberg. 2013. Nanoparticle Adhesion to the Cell Membrane and Its Effect on Nanoparticle Uptake Efficiency. *J Am Chem Soc* 135: 1438-1444.

558. Prasad, R. Y., K. Wallace, K. M. Daniel, A. H. Tennant, R. M. Zucker, J. Strickland, K. Dreher, A. D. Kligerman, C. F. Blackman, and D. M. DeMarini. 2013. Effect of Treatment Media on the Agglomeration of Titanium Dioxide

Nanoparticles: Impact on Genotoxicity, Cellular Interaction, and Cell Cycle. *Acs Nano* 7: 1929-1942.

559. Shang, L., R. M. Dorlich, V. Trouillet, M. Bruns, and G. U. Nienhaus. 2012. Ultrasmall fluorescent silver nanoclusters: Protein adsorption and its effects on cellular responses. *Nano Res* 5: 531-542.

560. Kohli, I., S. Alam, B. Patel, and A. Mukhopadhyay. 2013. Interaction and diffusion of gold nanoparticles in bovine serum albumin solutions. *Appl Phys Lett* 102.

561. Lundqvist, M., J. Stigler, T. Cedervall, T. Berggard, M. B. Flanagan, I. Lynch, G. Elia, and K. Dawson. 2011. The Evolution of the Protein Corona around Nanoparticles: A Test Study. *Acs Nano* 5: 7503-7509.

562. Ghavami, M., S. Saffar, B. Abd Emamy, A. Peirovi, M. A. Shokrgozar, V. Serpooshan, and M. Mahmoudi. 2013. Plasma concentration gradient influences the protein corona decoration on nanoparticles. *Rsc Adv* 3: 1119-1126.

563. Vroman, L., A. L. Adams, G. C. Fischer, and P. C. Munoz. 1980. Interaction of High Molecular-Weight Kininogen, Factor-Xii, and Fibrinogen in Plasma at Interfaces. *Blood* 55: 156-159.

564. Mortensen, N. P., G. B. Hurst, W. Wang, C. M. Foster, P. D. Nallathamby, and S. T. Retterer. 2013. Dynamic development of the protein corona on silica nanoparticles: composition and role in toxicity. *Nanoscale* 5: 6372-6380.

565. Lai, S. K., D. E. O'Hanlon, S. Harrold, S. T. Man, Y. Y. Wang, R. Cone, and J. Hanes. 2007. Rapid transport of large polymeric nanoparticles in fresh undiluted human mucus. *P Natl Acad Sci USA* 104: 1482-1487.

566. Kirch, J., A. Schneider, B. Abou, A. Hopf, U. F. Schaefer, M. Schneider, C. Schall, C. Wagner, and C. M. Lehr. 2012. Optical tweezers reveal relationship

between microstructure and nanoparticle penetration of pulmonary mucus. *P Natl Acad Sci USA* 109: 18355-18360.

567. Jachak, A., S. K. Lai, K. Hida, J. S. Suk, N. Markovic, S. Biswal, P. N. Breysse, and J. Hanes. 2012. Transport of metal oxide nanoparticles and single-walled carbon nanotubes in human mucus. *Nanotoxicology* 6: 614-622.

568. Wang, Y. Y., S. K. Lai, C. So, C. Schneider, R. Cone, and J. Hanes. 2011. Mucoadhesive Nanoparticles May Disrupt the Protective Human Mucus Barrier by Altering Its Microstructure. *Plos One* 6.

569. Muller, L., P. Comte, J. Czerwinski, M. Kasper, A. C. R. Mayer, P. Gehr, H. Burtscher, J. P. Morin, A. Konstandopoulos, and B. Rothen-Rutishauser. 2010. New Exposure System To Evaluate the Toxicity of (Scooter) Exhaust Emissions in Lung Cells in Vitro. *Environmental Science & Technology* 44: 2632-2638.

570. Rothen-Rutishauser, B., R. N. Grass, F. Blank, L. K. Limbach, C. Muehlfeld, C. Brandenberger, D. O. Raemy, P. Gehr, and W. J. Stark. 2009. Direct Combination of Nanoparticle Fabrication and Exposure to Lung Cell Cultures in a Closed Setup as a Method To Simulate Accidental Nanoparticle Exposure of Humans. *Environmental Science & Technology* 43: 2634-2640.

571. Raemy, D. O., R. N. Grass, W. J. Stark, C. M. Schumacher, M. J. D. Clift, P. Gehr, and B. Rothen-Rutishauser. 2012. Effects of flame made zinc oxide particles in human lung cells - a comparison of aerosol and suspension exposures. *Particle and Fibre Toxicology* 9.

572. Lenz, A. G., E. Karg, B. Lentner, V. Dittrich, C. Brandenberger, B. Rothen-Rutishauser, H. Schulz, G. A. Ferron, and O. Schmid. 2009. A dose-controlled system for air-liquid interface cell exposure and application to zinc oxide nanoparticles. *Particle and Fibre Toxicology* 6: -.

573. Kim, J. S., T. M. Peters, P. T. O'Shaughnessy, A. Adamcakova-Dodd, and P. S. Thorne. 2013. Validation of an in vitro exposure system for toxicity assessment of air-delivered nanomaterials. *Toxicol in Vitro* 27: 164-173.

574. Savi, M., M. Kalberer, D. Lang, M. Ryser, M. Fierz, A. Gaschen, J. Ricka, and M. Geiser. 2008. A novel exposure system for the efficient and controlled deposition of aerosol particles onto cell cultures. *Environ Sci Technol* 42: 5667-5674.

575. de Bruijne, K., S. Ebersviller, K. G. Sexton, S. Lake, D. Leith, R. Goodman, J. Jetters, G. W. Walters, M. Doyle-Eisele, R. Woodside, H. E. Jeffries, and I. Jaspers. 2009. Design and Testing of Electrostatic Aerosol In Vitro Exposure System (EAVES): An Alternative Exposure System for Particles. *Inhalation Toxicology* 21: 91-101.

576. Lichtveld, K. M., S. M. Ebersviller, K. G. Sexton, W. Vizuete, I. Jaspers, and H. E. Jeffries. 2012. In Vitro Exposures in Diesel Exhaust Atmospheres: Resuspension of PM from Filters versus Direct Deposition of PM from Air. *Environmental Science & Technology* 46: 9062-9070.

577. Takenaka, S., E. Karg, W. G. Kreyling, B. Lentner, W. Moller, M. Behnke-Semmler, L. Jennen, A. Walch, B. Michalke, P. Schramel, J. Heyder, and H. Schulz. 2006. Distribution pattern of inhaled ultrafine gold particles in the rat lung. *Inhalation Toxicology* 18: 733-740.

578. Abid, A. D., D. S. Anderson, G. K. Das, L. S. Van Winkle, and I. M. Kennedy. 2013. Novel lanthanide-labeled metal oxide nanoparticles improve the measurement of in vivo clearance and translocation. *Particle and Fibre Toxicology* 10.

579. Pieters, N., M. Plusquin, B. Cox, M. Kicinski, J. Vangronsveld, and T. S. Nawrot. 2012. An epidemiological appraisal of the association between heart rate variability and particulate air pollution: a meta-analysis. *Heart* 98: 1127-1135.

580. Peters, A., M. Frohlich, A. Doring, T. Immervoll, H. E. Wichmann, W. L. Hutchinson, M. B. Pepys, and W. Koenig. 2001. Particulate air pollution is associated with an acute phase response in men - Results from the MONICA-Augsburg Study. *Eur Heart J* 22: 1198-1204.

581. Kido, T., E. Tamagawa, N. Bai, K. Suda, H. H. C. Yang, Y. X. Li, G. Chiang, K. Yatera, H. Mukae, D. D. Sin, and S. F. Van Eeden. 2011. Particulate Matter Induces Translocation of IL-6 from the Lung to the Systemic Circulation. *American Journal of Respiratory Cell and Molecular Biology* 44: 197-204.

582. Gold, D. R., A. Litonjua, J. Schwartz, E. Lovett, A. Larson, B. Nearing, G. Allen, M. Verrier, R. Cherry, and R. Verrier. 2000. Ambient pollution and heart rate variability. *Circulation* 101: 1267-1273.

583. Araujo, J. A., B. Barajas, M. Kleinman, X. P. Wang, B. J. Bennett, K. W. Gong, M. Navab, J. Harkema, C. Sioutas, A. J. Lusis, and A. E. Nel. 2008. Ambient particulate pollutants in the ultrafine range promote early atherosclerosis and systemic oxidative stress. *Circ Res* 102: 589-596.

584. Kim, J. B., C. Kim, E. Choi, S. Park, H. Park, H. N. Pak, M. H. Lee, D. C. Shin, K. C. Hwang, and B. Joung. 2012. Particulate air pollution induces arrhythmia via oxidative stress and calcium calmodulin kinase II activation. *Toxicology and Applied Pharmacology* 259: 66-73.

585. Wold, L. E., Z. Ying, K. R. Hutchinson, M. Velten, M. W. Gorr, C. Velten, D. J. Youtz, A. Wang, P. A. Lucchesi, Q. Sun, and S. Rajagopalan. 2012. Cardiovascular remodeling in response to long-term exposure to fine particulate matter air pollution. *Circulation. Heart failure* 5: 452-461.

586. Knuckles, T. L., and K. L. Dreher. 2007. Fine oil combustion particle bioavailable constituents induce molecular profiles of oxidative stress, altered function, and cellular injury in cardiomyocytes. *J Toxicol Env Heal A* 70: 1824-1837.

587. Wang, T., L. Wang, L. Moreno-Vinasco, G. D. Lang, J. H. Siegler, B. Mathew, P. V. Usatyuk, J. M. Samet, A. S. Geyh, P. N. Breysse, V. Natarajan, and J. G. N. Garcia. 2012. Particulate matter air pollution disrupts endothelial cell barrier via calpain-mediated tight junction protein degradation. *Particle and Fibre Toxicology* 9.

588. Hu, C., J. Dillon, J. Kearn, C. Murray, V. O'Connor, L. Holden-Dye, and H. Morgan. 2013. NeuroChip: A Microfluidic Electrophysiological Device for Genetic and Chemical Biology Screening of Caenorhabditis elegans Adult and Larvae. *Plos One* 8.

589. Expert Panel on Air Quality Standards. 2008. Guidelines for metals and metalloids in ambient air for the protection of human health. 14th Report of the Expert Panel on Air Quality Standards.

590. Svartengren, M., V. Strand, G. Bylin, L. Jarup, and G. Pershagen. 2000. Short-term exposure to air pollution in a road tunnel enhances the asthmatic response to allergen. *European Respiratory Journal* 15: 716-724.

591. Mushtaq, N., M. Ezzati, L. Hall, I. Dickson, M. Kirwan, K. M. Y. Png, I. S. Mudway, and J. Grigg. 2011. Adhesion of Streptococcus pneumoniae to human airway epithelial cells exposed to urban particulate matter. *Journal of Allergy and Clinical Immunology* 127: 1236-U1536.

592. Antonini, J. M., J. R. Roberts, S. Stone, B. T. Chen, D. Schwegler-Berry, and D. G. Frazer. 2009. Short-Term Inhalation Exposure to Mild Steel Welding Fume had no Effect on Lung Inflammation and Injury but did Alter Defense Responses to Bacteria in Rats. *Inhalation Toxicology* 21: 182-192.

593. Holloway, J. W., S. S. Francis, K. M. Fong, and I. A. Yang. 2012. Genomics and the respiratory effects of air pollution exposure. *Respirology* 17: 590-600.

594. Clougherty, J. E., J. I. Levy, L. D. Kubzansky, P. B. Ryan, S. F. Suglia, M. J. Canner, and R. J. Wright. 2007. Synergistic effects of traffic-related air

pollution and exposure to violence on urban asthma etiology. *Environmental Health Perspectives* 115: 1140-1146.

595. Ghio, A. J. 2009. Disruption of iron homeostasis and lung disease. *Bba-Gen Subjects* 1790: 731-739.

596. Zhang, Z., C. Kleinstreuer, J. F. Donohue, and C. S. Kim. 2005. Comparison of micro- and nano-size particle depositions in a human upper airway model. *Journal of Aerosol Science* 36: 211-233.

597. Kleinstreuer, C., and Z. Zhang. 2010. Airflow and Particle Transport in the Human Respiratory System. *Annu Rev Fluid Mech* 42: 301-334.

598. Balashazy, I., W. Hofmann, and T. Heistracher. 2003. Local particle deposition patterns may play a key role in the development of lung cancer. *Journal of Applied Physiology* 94: 1719-1725.

599. Phalen, R. F., M. J. Oldham, and A. E. Nel. 2006. Tracheobronchial particle dose considerations for in vitro toxicology studies. *Toxicological Sciences* 92: 126-132.

600. Farkas, A., and I. Balashazy. 2007. Simulation of the effect of local obstructions and blockage on airflow and aerosol deposition in central human airways. *Journal of Aerosol Science* 38: 865-884.

601. Healy, D. A., S. Hellebust, V. Silvari, J. M. Lopez, A. G. Whittaker, J. C. Wenger, J. J. A. Heffron, and J. R. Sodeau. 2012. Using a pattern recognition approach to link inorganic chemical fingerprints of ambient PM2.5-0.1 with in vitro biological effects. *Air Qual Atmos Hlth* 5: 125-147.

602. Wu, S. W., F. R. Deng, H. Y. Wei, J. Huang, H. Y. Wang, M. Shima, X. Wang, Y. Qin, C. J. Zheng, Y. Hao, and X. B. Guo. 2012. Chemical constituents of ambient particulate air pollution and biomarkers of inflammation, coagulation

and homocysteine in healthy adults: A prospective panel study. *Particle and Fibre Toxicology* 9.

603. Strak, M. M., M. Steenhof, P. H. B. Fokkens, A. J. F. Boere, D. L. A. C. Leseman, K. Meliefste, R. A. Harrison, K. J. Godri, F. Kelly, I. S. Mudway, G. Hoek, B. Brunekreef, E. Lebret, F. R. Cassee, I. Gosens, and N. A. H. Janssen. 2008. Characterization of Different Fractions of Particulate Matter at Various Locations with Contrast in Local Source Emissions: First Phase of the RAPTES Study. *Epidemiology* 19: S226-S227.

604. Strak, M., N. A. H. Janssen, K. J. Godri, I. Gosens, I. S. Mudway, F. R. Cassee, E. Lebret, F. J. Kelly, R. M. Harrison, B. Brunekreef, M. Steenhof, and G. Hoek. 2012. Respiratory Health Effects of Airborne Particulate Matter: The Role of Particle Size, Composition, and Oxidative Potential-The RAPTES Project. *Environmental Health Perspectives* 120: 1183-1189.

605. Steenhof, M., I. S. Mudway, I. Gosens, G. Hoek, K. J. Godri, F. J. Kelly, R. M. Harrison, R. H. H. Pieters, F. R. Cassee, E. Lebret, B. A. Brunekreef, M. Strak, and N. A. H. Janssen. 2013. Acute nasal pro-inflammatory response to air pollution depends on characteristics other than particle mass concentration or oxidative potential: the RAPTES project. *Occupational and Environmental Medicine* 70: 341-348.

606. Strak, M., G. Hoek, K. J. Godri, I. Gosens, I. S. Mudway, R. van Oerle, H. M. H. Spronk, F. R. Cassee, E. Lebret, F. J. Kelly, R. M. Harrison, B. Brunekreef, M. Steenhof, and N. A. H. Janssen. 2013. Composition of PM Affects Acute Vascular Inflammatory and Coagulative Markers - The RAPTES Project. *Plos One* 8.

607. Strak, M., G. Hoek, M. Steenhof, E. Kilinc, K. J. Godri, I. Gosens, I. S. Mudway, R. van Oerle, H. M. H. Spronk, F. R. Cassee, F. J. Kelly, R. M. Harrison, B. Brunekreef, E. Lebret, and N. A. H. Janssen. 2013. Components of ambient air pollution affect thrombin generation in healthy humans: the RAPTES project. *Occupational and Environmental Medicine* 70: 332-340.

608. Happo, M. S., R. O. Salonen, A. I. Halinen, P. I. Jalava, A. S. Pennanen, J. A. M. A. Dormans, M. E. Gerlofs-Nijland, F. R. Cassee, V. M. Kosma, M. Sillanpaa, R. Hillamo, and M. R. Hirvonen. 2010. Inflammation and tissue damage in mouse lung by single and repeated dosing of urban air coarse and fine particles collected from six European cities. *Inhalation Toxicology* 22: 402-416.

609. Mortazavi, A., B. A. Williams, K. Mccue, L. Schaeffer, and B. Wold. 2008. Mapping and quantifying mammalian transcriptomes by RNA-Seq. *Nature Methods* 5: 621-628.

610. Wang, Z., M. Gerstein, and M. Snyder. 2009. RNA-Seq: a revolutionary tool for transcriptomics. *Nat Rev Genet* 10: 57-63.

611. Huang, Y. C. T., E. D. Karoly, L. A. Dailey, M. T. Schmitt, R. Silbajoris, D. W. Graff, and R. B. Devlin. 2011. Comparison of Gene Expression Profiles Induced by Coarse, Fine, and Ultrafine Particulate Matter. *J Toxicol Env Heal A* 74: 296-312.

612. Pierrou, S., P. Broberg, R. A. O'Donnell, K. Pawlowski, R. Virtala, E. Lindqvist, A. Richter, S. J. Wilson, G. Angco, S. Moller, H. Bergstrand, W. Koopmann, E. Wieslander, P. E. Stromstedt, S. T. Holgate, D. E. Davies, J. Lund, and R. Djukanovic. 2007. Expression of genes involved in oxidative stress responses in airway epithelial cells of smokers with chronic obstructive pulmonary disease. *American Journal of Respiratory and Critical Care Medicine* 175: 577-586.

613. Hoogendoorn, B., K. Berube, C. Gregory, T. Jones, K. Sexton, P. Brennan, I. A. Brewis, A. Murison, R. Arthur, H. Price, H. Morgan, and I. P. Matthews. 2012. Gene and protein responses of human lung tissue explants exposed to ambient particulate matter of different sizes. *Inhalation Toxicology* 24: 966-975.

614. Bourdon, J. A., A. Williams, B. Kuo, I. Moffat, P. A. White, S. Halappanavar, U. Vogel, H. Wallin, and C. L. Yauk. 2013. Gene expression profiling to

identify potentially relevant disease outcomes and support human health risk assessment for carbon black nanoparticle exposure. *Toxicology* 303: 83-93.

615. Wallace, L. 1996. Indoor particles: A review. *J Air Waste Manage* 46: 98-126.

616. Seaton, A., A. Soutar, V. Crawford, R. Elton, S. McNerlan, J. Cherrie, M. Watt, R. Agius, and R. Stout. 1999. Particulate air pollution and the blood. *Thorax* 54: 1027-1032.

617. Harrison, R. M., C. A. Thornton, R. G. Lawrence, D. Mark, R. P. Kinnersley, and J. G. Ayres. 2002. Personal exposure monitoring of particulate matter nitrogen dioxide, and carbon monoxide, including susceptible groups. *Occupational and Environmental Medicine* 59: 671-679.

618. Chen, Y., and A. Whalley. 2012. Green Infrastructure: The Effects of Urban Rail Transit on Air Quality. *Am Econ J-Econ Polic* 4: 58-97.

Environmental Science & Technology

Article

pubs.acs.org/est

Physicochemical Characterization of Airborne Particulate Matter at a Mainline Underground Railway Station

Matthew Loxham,*[,†,⊥] Matthew J. Cooper,[‡] Miriam E. Gerlofs-Nijland,[§] Flemming R. Cassee,[§,∥] Donna E. Davies,[†,⊥] Martin R. Palmer,[‡,⊥,#] and Damon A. H. Teagle[‡,⊥,#]

[†]The Brooke Laboratory, Clinical and Experimental Sciences, Faculty of Medicine, University of Southampton, University Hospital Southampton, Tremona Road, Southampton, SO16 6YD, United Kingdom

[‡]Ocean and Earth Science, National Oceanography Centre Southampton, University of Southampton, European Way, Southampton, SO14 3ZH, United Kingdom

[§]Centre for Environmental Health, National Institute for Public Health and the Environment (RIVM), Antonie van Leeuwenhoeklaan 9, P.O. Box 1, 3721 MA Bilthoven, The Netherlands

[∥]Institute for Risk Assessment Sciences (IRAS), Utrecht University, Utrecht, Jenalaan 18d, 3584 CK, The Netherlands

[⊥]Institute for Life Sciences, Life Sciences Building, Highfield Campus, University of Southampton, Southampton, SO17 1BJ, United Kingdom

Supporting Information

ABSTRACT: Underground railway stations are known to have elevated particulate matter (PM) loads compared to ambient air. As these particles are derived from metal-rich sources and transition metals may pose a risk to health by virtue of their ability to catalyze generation of reactive oxygen species (ROS), their potential enrichment in underground environments is a source of concern. Compared to coarse (PM_{10}) and fine ($PM_{2.5}$) particulate fractions of underground railway airborne PM, little is known about the chemistry of the ultrafine ($PM_{0.1}$) fraction that may contribute significantly to particulate number and surface area concentrations. This study uses inductively coupled plasma mass spectrometry and ion chromatography to compare the elemental composition of size-fractionated underground PM with woodstove, roadwear generator, and road tunnel PM. Underground PM is notably rich in Fe, accounting for greater than 40% by mass of each fraction, and several other transition metals (Cu, Cr, Mn, and Zn) compared to PM from other sources. Importantly, ultrafine underground PM shows similar metal-rich concentrations as the coarse and fine fractions. Scanning electron microscopy revealed that a component of the coarse fraction of underground PM has a morphology indicative of generation by abrasion, absent for fine and ultrafine particulates, which may be derived from high-temperature processes. Furthermore, underground PM generated ROS in a concentration- and size-dependent manner. This study suggests that the potential health effects of exposure to the ultrafine fraction of underground PM warrant further investigation as a consequence of its greater surface area/volume ratio and high metal content.

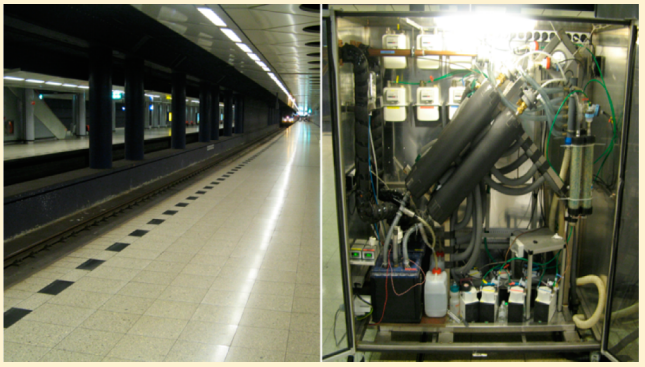

INTRODUCTION

Underground railway systems are widely used mass transit systems in many major cities, some carrying several million passengers per day.[1] High mass concentrations of respirable particulate matter (PM) with a mean aerodynamic diameter up to 10 μm (PM_{10}; coarse), 2.5 μm ($PM_{2.5}$; fine), or 0.1 μm ($PM_{0.1}$; ultrafine) have been observed in many underground railway systems.[2−4] In many cases, concentrations far exceed World Health Organization (WHO) recommended limits for 24 h average particle exposure of 50 and 25 $\mu g/m^3$ for PM_{10} and $PM_{2.5}$, respectively, presenting a potential risk for regular passengers and employees.[5] Notably, $PM_{0.1}$ levels are currently unregulated. Importantly, exposure to PM has been noted to be greater for underground journeys than for equivalent journeys made by a variety of overground modes of transport,[6] and time spent in underground railways has been suggested to be a better predictor of metal exposure than duration of exposure to traffic-derived metal pollutants.[7]

There is evidence to suggest that underground railway PM has high concentrations of Fe and other transition metals compared to ambient PM.[8−10] Transition metals are of interest as potential airborne toxicants because of their ability to generate the reactive oxygen species (ROS) superoxide ($^{\bullet}O_2^-$),

Received: November 2, 2012
Revised: March 2, 2013
Accepted: March 11, 2013
Published: March 11, 2013

hydrogen peroxide (H_2O_2) and, via the Fenton reaction, hydroxyl radical ($^{\bullet}OH$) via successive single-electron reductions of molecular oxygen.[11] It is thought that many of the toxic effects of transition metals arise from oxidative stress due to ROS generation. Defined as an excess of oxidative species that outweighs the antioxidant capacity of a system, oxidative stress can result in oxidation and functional modification of biomolecules such as lipids, proteins, and nucleic acids and can result in inflammation and tissue injury.[12] However, transition metals, and also a variety of other metals and metalloids such as lead and arsenic, can exert toxic effects via mechanisms other than direct generation of ROS; hence, study of concentrations of non-transition metals in airborne PM is also warranted.

The composition of metal-rich PM from a wide variety of sources has previously been studied, including steel mills, smelting plants, and welding fume.[13−15] However, underground PM studies generally focus on coarse and fine fractions, without parallel analysis of ultrafine PM composition.[16] Although individual ultrafine particles have a lower surface area than fine or coarse particles (0.03 vs 19.6 and 314 μm^2, respectively, for particles of 0.1, 2.5, and 10 μm diameter, assuming perfect sphericity), ultrafine PM is often present in a much greater number concentration than coarse or fine PM, and thus, their contribution to overall PM surface area has the potential to be very important, possibly being a key determinant of toxicity.[17] Furthermore, coarse and fine particles tend to accumulate in the ciliated airways by impaction and are rapidly cleared by the mucociliary escalator, whereas ultrafine particles predominantly settle by diffusion in the alveoli, from where clearance is much slower.[18] Ultrafine particles, unlike fine particles, are also able to translocate from the airway lumen to the pulmonary interstitium and potentially the systemic circulation, being detected in the liver, heart, kidneys, and brain.[19,20]

Because there is evidence that underground PM is an important potential toxicant, the aim of this study is to determine the concentration of transition and nontransition metals in respirable, size-fractionated PM collected at an underground railway station and to compare this to PM collected from other process-specific sources, namely, a woodstove, a roadwear generator, a road tunnel, and diesel exhaust.

METHODS

Acquisition of PM. Airborne PM was collected using a versatile aerosol concentration and enrichment system (VACES), with aerodynamic diameter cutpoints of 10−2.5 μm (coarse; $PM_{10-2.5}$), 2.5 μm (fine/ultrafine with no lower cutpoint, hereafter referred to as "fine"; $PM_{2.5}$), and 0.18 μm (ultrafine; $PM_{0.18}$).[21,22] Air flow was 0.9 m^3/min. PM was collected as a suspension in ultrapure water from the following:

(1) A woodstove, a portion of the exhaust smoke being diluted with filtered air, fed into a sealed chamber containing the VACES unit that sampled airborne PM at a concentration of ≈250 $\mu g/m^3$.
(2) A roadwear simulator, consisting of a circular road surface on which four wheels with studded tires rotate. Prior to operation, the chamber was flushed with filtered air, and the PM concentration was allowed to build up to a steady state of ≈5000 $\mu g/m^3$.
(3) A busy railway station located under the main departures and arrivals terminal of a major European airport, near the middle of a 5.1 km long tunnel, with further details published previously.[23] The station is used by 60 000−150 000 people per day, with three platform islands, each housing two platforms ≈400 m long. 25−30 trains per hour pass through the station during operating hours, all powered by overhead catenary. During the night, there are occasional diesel-powered freight trains passing through the station. The station is cleaned regularly during daytime hours, principally using electrically powered ride-on machines to clean the floor of dirt and dust. There is no active air ventilation/conditioning system in operation, with air exchange driven solely by "piston action" of train movement. The VACES equipment was located halfway along the central island platform, ≈3 m away from the platform edge and ≈6 m from the centers of each pair of surrounding tracks, with air intakes ≈3 m above the track level and ≈4 m below the overhead catenaries. Sampling was performed for ≈9 h between 08:30 and 17:30 on each of the three sampling days, all of which were working weekdays in July 2010.
(4) A heavily trafficked road tunnel in The Netherlands. Sampling was performed in a parking area immediately adjacent to the tunnel exit, with sampling performed in midsummer.

In addition, diesel exhaust particulate (DEP) samples from a diesel generator and exposure chamber were analyzed to provide comparison as an expected metal-poor PM.

Particulate Metal Analysis. All analysis steps were performed in a clean laboratory (class 100) environment to minimize possible contamination. PM suspensions were vortexed and bath sonicated for 30 s each. A 100 μL aliquot of suspension was reserved for anion analysis, and the remaining volume was recorded and transferred to a Teflon pot. Suspensions were evaporated to dryness at 130 °C. Three overnight digestion steps were performed: respectively, 900 μL of concentrated nitric acid (15 M, Primar Plus grade; Fisher Scientific, Loughborough, UK) with 100 μL of concentrated hydrofluoric acid (27 M, UpA grade; Romil, Cambridge, UK) pressurized at 180 °C, 1 mL of 6 M hydrochloric acid (12 M, Primar Plus grade; Fisher) at 130 °C, and 1 mL of 2% nitric acid spiked with Be, In, and Re to monitor instrument drift. Evaporation at 130 °C was performed after each of the first two steps. Hydrochloric and nitric acids were sub-boiled prior to use. Immediately prior to analysis, additional 2% nitric acid was added to produce a final mass of ≈3 g per digest. Standards were prepared using a variety of commercially available standard solutions to assess a range of metals (Table S1, Supporting Information). Blanks were prepared by performing acid digests in the absence of the PM suspension, to monitor the contribution of any contamination during the digestion process. Samples, standards, and blanks were analyzed by inductively coupled plasma mass spectrometry (ICP-MS) using a Thermofisher XSeries2 inductively coupled plasma mass spectrometer (Thermofisher Scientific, Bremen, Germany) located in the Isotope Geochemistry Instrument Suite at NOCS, Southampton.

Anion Analysis by Ion Chromatography. Concentrations of the anions NO_3^-, SO_4^{2-}, and Cl^- in the particulate samples were determined by ion chromatography. A 100 μL aliquot of each particulate suspension was vortexed for 60 s and bath-sonicated for 60 min followed by centrifugation at 20 000g for 10 min, and the supernatant was retained. Supernatants

dx.doi.org/10.1021/es304481m | Environ. Sci. Technol. 2013, 47, 3614−3622

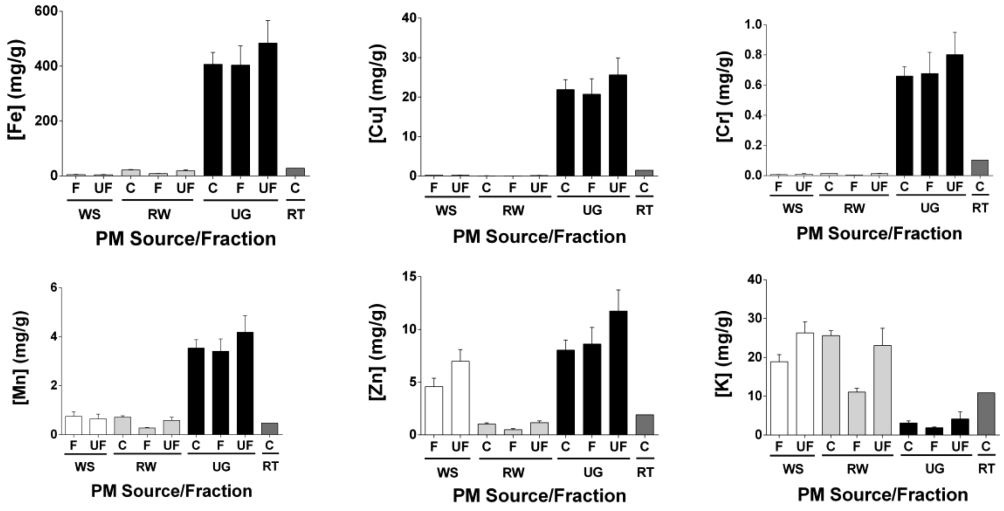

Figure 1. Concentrations of Fe, Cu, Cr, Mn, Zn, and K in PM of coarse (C), fine (F), and ultrafine (UF) fractions collected from a woodstove (WS), a roadwear generator (RW), an underground station (UG), and a road tunnel (RT). Values expressed as single values (RT) or mean ± 1 SE of two (WS, RW) or three (UG) individual samples.

were diluted in ultrapure water to a volume of ≈5 mL, before being analyzed on a Dionex ICS2500 ion chromatograph with Dionex Chromeleon software (Dionex, Sunnyvale, CA, USA). Standard solutions for NO_3^-, SO_4^{2-}, and Cl^- were prepared from serial dilutions of commercially available stock standards (Inorganic Ventures, Christiansburg, VA, USA), which were also used to monitor instrument drift.

Scanning Electron Microscopy. Underground particle suspensions were prepared for scanning electron microscopy (SEM) analysis by evaporating to dryness 100 μL of PM suspension on an aluminum stub at 50 °C overnight, followed by gold sputter coating (Hummer VI A sputter coater, Anatech, Alexandria, VA, USA) to a thickness of ≈20 nm. SEM was performed using a LEO 1450VP scanning electron microscope (Carl Zeiss Nano Technology Systems, Welwyn Garden City, UK) at 20 kV.

Measurement of ROS Generation. Primary bronchial epithelial cells (PBEC) were obtained from healthy donors by fibreoptic bronchoscopy as previously described.[24] Cells were seeded in collagen-coated 96-well plates at a density of 6000 cells per well and cultured until 80−90% confluent. Cells were then serum starved (1.5 μg/mL bovine serum albumin and 1X insulin/transferrin/sodium selenite solution (ITS) both from Sigma−Aldrich, Gillingham, UK) in bronchial epithelial basal medium (BEBM; Clonetics, San Diego, CA, USA) overnight. Cells were washed once with HBSS supplemented with Ca and Mg ($HBSS_{CaMg}$; Invitrogen, Carlsbad, CA, USA) before being loaded with 75 μL of 10 μM 2′7′-dichlorofluorescein diacetate (H_2DCF-DA; Sigma−Aldrich) at 37 °C, light excluded, for 30 min. Cells were then washed twice with $HBSS_{CaMg}$ before application of 75 μL of coarse, fine, or ultrafine underground PM in supplement-free BEBM at 6.3 or 12.5 μg/cm^2 (equivalent to 25 and 50 μg/mL, respectively). Controls comprised medium supplemented with phosphate-buffered saline to maintain osmolarity. DCF fluorescence was measured at 485 nm excitation and 530 nm emission 3 h postchallenge and calculated as the fold-change in fluorescence compared to the control.

RESULTS

Particulate Composition. Over the three sampling days at the station, the mean (±1 standard mean error (SE)) underground PM_{10} mass concentration was 287 ± 8 μg/m^3, with coarse PM at 169 ± 6 μg/m^3, fine at 75.3 ± 5.9 μg/m^3, and ultrafine at 37.7 ± 4.5 μg/m^3. Chemical analysis was carried out on underground PM as well as from the other three distinct sources and DEP. For woodstove, roadwear, and underground PM sampling, individual daily samples were analyzed separately. Road tunnel PM and DEP were analyzed in the coarse fraction only, as well-characterized references for comparison (Figure 1 and Figure S1, Supporting Information). Underground PM was the most transition-metal-rich PM, with Fe the most abundant element, comprising (mean ± 1 SE) 407 ± 43, 404 ± 70, and 484 ± 82 mg/g for coarse, fine, and ultrafine fractions, respectively. Thus, Fe comprises greater than 40% of the total mass of the PM (Figure 1). Conversely, while all other PM samples contained detectable levels of Fe, only coarse and ultrafine roadwear PM (21.5 ± 0.1 and 18.1 ± 3.5 mg/g) and road tunnel PM (27.7 mg/g) contained Fe levels greater than 1% of the total mass of the PM. Cu was also elevated in underground PM compared to PM from other sites, although the Cu concentration (21.9 ± 2.5, 20.7 ± 3.9, and 25.6 ± 4.3 mg/g for coarse, fine, and ultrafine fractions, respectively) was lower than that of Fe. As with Fe, these Cu levels were considerably higher than those seen in any other sampling locations, across all size fractions analyzed. Other transition metals that were present at high concentration in underground PM included Mn, Zr, Mo, and Sn. In addition, levels of V, Cr, Ni, Nb, and Hf were higher in underground PM than other sources, although they were found at lower absolute concentrations. Additionally, Ca was high in underground PM, particularly in the ultrafine fraction (54 ± 31 mg/g), and Mg, Ca, Zn, Ba, and Sb were also found to be elevated in underground PM, with relatively high levels of Ga and As also noted.

Woodstove PM showed a marked enrichment for K, while levels of B and Zn were similar to underground PM and in excess of levels in other PM types. Furthermore, Rb (144 ± 3.2 μg/g F, 192 ± 1.8 μg/g UF), Cd (40.4 ± 7.1 μg/g F, 58.0 ± 5.4 μg/g UF), and Pb (185 ± 43 μg/g F, 266 ± 37 μg/g UF) were

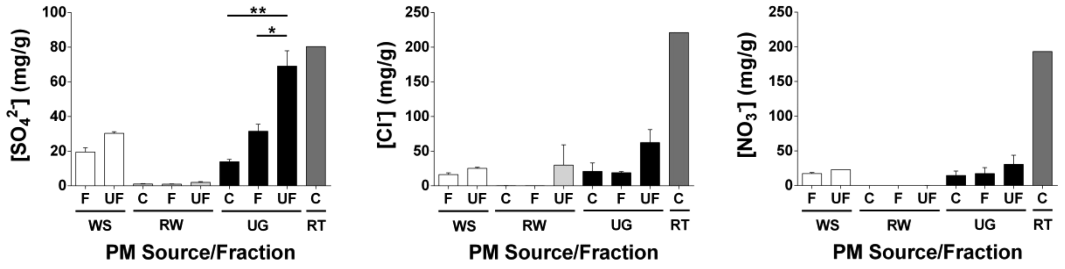

Figure 2. Concentrations of SO_4^{2-} (left panel), Cl^- (center panel), and NO_3^- (right panel) in coarse (C), fine (F), and ultrafine (UF) fractions of PM collected from a woodstove (WS), a roadwear generator (RW), an underground station (UG), and a road tunnel (RT). Values expressed as single values (RT) or mean ± 1 SE of two (WS, RW) or three (UG) individual samples. (*) $p < 0.05$ and (**) $p < 0.01$, analyzed by one-way repeated measures ANOVA.

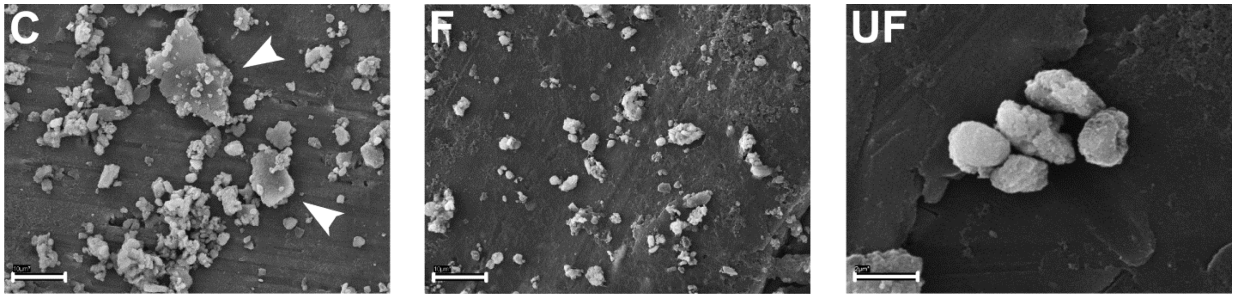

Figure 3. SEM micrographs showing morphology of coarse (C; ×5000), fine (F; ×5000), and ultrafine (UF; ×30 000) underground PM. Flakelike particulates in the coarse fraction are indicated by arrowheads. Scale bars represent 10 μm (C and F) or 2 μm (UF).

also relatively high in woodstove PM compared to other PM sources, although they were low in terms of absolute concentration. Roadwear PM possessed especially high concentrations of Al, with the three fractions showing concentrations of 71.0 ± 3.1, 27.3 ± 1.8, and 53.9 ± 7.2 mg/g, respectively. These concentrations were second only to underground PM Fe concentrations in terms of the most prevalent metals found at any site. Roadwear PM also contained notably high levels of Ti and to a lesser extent Sr, whereas levels of Sc, La, and Hg were found to be greater than other PM types, albeit at trace levels. Interestingly, roadwear PM showed generally lower metal concentrations in the fine fraction compared to the coarse and ultrafine fractions.

Road tunnel coarse PM showed relatively high levels of Li, B, and Na. Road tunnel PM also contained elevated levels of Pb relative to other PM samples at 516 μg/g. DEP was also analyzed, as a source of PM expected to be low in transition metals. As expected, the majority of elements analyzed were present in lower concentrations in DEP compared to PM from the other sources tested, and many were not detected (Table S2, Supporting Information).

Statistical analysis was performed to determine whether there was any significant difference in the concentration of any element assayed across each of the size fractions. Only B showed any pairwise difference, the ultrafine fraction being high versus coarse ($p < 0.05$) and fine ($p < 0.01$) fractions. The data were further analyzed to test for correlations between Fe and other elements across the underground PM samples, testing with Spearman's rank correlation coefficient. Sr was the element most strongly correlated with Fe ($r = 1.00$; $p < 0.0001$). However, this may be of limited importance due to the low overall concentration of Sr, generally below 100 μg/g. Indeed, 32 of the 40 elements showed concentrations correlated with those of Fe ($p < 0.05$). The strongest correlations among the abundant metals were observed for Mn, Ni, and Cu, while V was also strongly correlated with Fe (Figure S2, Supporting Information). Although no negative correlations were found, the crustal elements Na ($r = 0.517$) and K ($r = 0.433$) along with B ($r = 0.467$) showed the weakest correlation with Fe.

Particulate Anion Analysis. Ion chromatography analyses show that road tunnel PM possessed the highest concentrations of SO_4^{2-}, Cl^-, and NO_3^- (Figure 2). Roadwear PM generally showed the lowest SO_4^{2-}, Cl^-, and NO_3^- concentrations of any of the PM tested, suggesting that these anions are derived from fuel combustion rather than road and mechanical sources in the road tunnel PM. When the concentrations of each species were compared between the three size fractions of underground PM, coarse and fine fractions showed similar levels of the three anions, but ultrafine underground PM showed enrichments of SO_4^{2-}, Cl^-, and NO_3^-, and for SO_4^{2-}, this difference was of statistical significance versus coarse and fine fractions. Each anion showed only weak positive correlation with Fe concentration ($r = 0.583$, 0.483, and 0.367 for SO_4^{2-}, Cl^-, and NO_3^-, respectively).

Particulate Morphology. Examination of the coarse fraction of underground PM revealed that most particles were well below the 10 μm diameter used as a cutpoint for this fraction, with a smallest dimension of 2−3 μm or less. However, there was a clear population of particles with sizes close to the 10 μm cutpoint. The smaller particles had a nonuniform, irregular granular morphology, while the larger particles had a flakelike appearance with jagged edges (Figure 3). When examined at a greater magnification, the flat surfaces of these larger, flakelike particles were often marked by ridges or indentations. The fine fraction of underground PM contained a similar set of small particles with a largest dimension of ≈2 μm. Significantly, there was a paucity of flakelike particles compared to the coarse fraction. The ultrafine fraction of underground PM contained particles of a nonuni-

dx.doi.org/10.1021/es304481m | Environ. Sci. Technol. 2013, 47, 3614−3622

form granular shape. All fractions contained some particles of a larger size than should theoretically have been permitted by the cutpoint of the virtual impactor. These larger particles were commonly composed of 1−2 μm particles agglomerated to form a single mass, suggesting agglomeration post-collection.

ROS Generation by Underground PM. In order to measure the ROS-generating capacity of underground PM, PBEC monolayers were loaded with the oxidant sensitive dye H_2DCF-DA, which is fluorescent only after oxidation. Following 3 h exposure to underground PM, fluorescence was seen to increase in a concentration- and size-fraction-dependent manner (Figure 4), with ultrafine and fine fractions

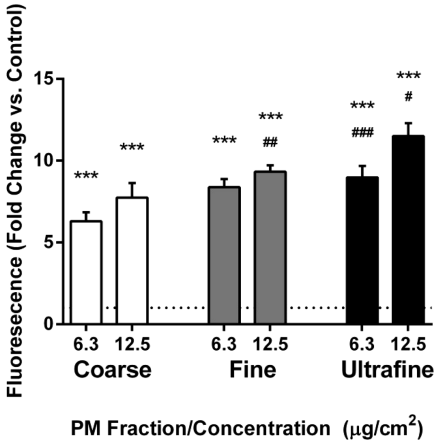

Figure 4. DCF fluorescence induced by 3 h incubation of PBECs with coarse, fine, or ultrafine underground PM. Values expressed as mean ± 1 SE, n = 3−5. (***) $p < 0.001$ vs control; (#) $p < 0.05$ for fine or ultrafine vs respective concentration of coarse PM. (##) $p < 0.01$ and (###) $p < 0.001$, analyzed by one-way repeated measures ANOVA.

generally inducing greater fluorescence than the coarse fraction (11.5 ± 0.8, 9.3 ± 0.4, and 7.7 ± 0.9 mean fold increase ± 1 SE, respectively).

DISCUSSION

This study examined the levels of transition and nontransition metals and selected metalloids in size-fractionated underground railway PM, with woodstove, roadwear, and road tunnel PM used as comparators. ICP-MS analyses of a large range of metals, especially in the rarely studied ultrafine fraction, provides new information on the chemistry of underground airborne PM. The underground railway station on which this study focused forms part of a mainline international railway. This is important because (1) the studied railway draws power from an overhead catenary, as opposed to an electrified rail, and (2) trains running on this line are larger than would generally be found on urban underground railway networks. The effects of increased load on rail wear have been detailed elsewhere.[25]

The present study showed that underground PM contained a high concentration of Fe. This observation is in agreement with other studies, which have found high Fe content in underground PM (e.g., 40−59% in Stockholm underground PM_{10},[8,26] 61% and 42% from Paris RER and Metro PM_{10}, respectively[3]). Interestingly, Stockholm underground $PM_{2.5}$ was found to contain almost undetectable levels of metal.[8] Overall, the results from underground stations are in clear contrast to samples from road traffic predominant areas, which tend to be rich in elemental carbon.[2]

Unlike the vast majority of studies of underground PM, the present study also analyzed the elemental composition of ultrafine PM ($PM_{0.1}$), which is rarely studied.[16] In urban environments, ultrafine PM is generally metal-poor[27−29] and mainly composed of elemental C along with the products of secondary reactions between gaseous pollutants that condense to form PM.[29−31] In terms of their chemistry, these secondary ultrafine particles are thought to be of little toxicological significance.[32] However, some processes involving high temperatures and resultant vaporization or combustion of substrate material have the potential to generate metal-rich ultrafine PM.[33,34] Indeed, most metals analyzed in this study were found to have higher concentrations in the ultrafine fraction compared to the coarse and fine fractions, although the differences were not statistically significant for any metal. Furthermore, our study may underestimate the relatively metal-rich nature of the ultrafine fraction compared to the fine fraction as the VACES equipment includes some ultrafine PM in the $PM_{2.5}$ fraction.[22] The majority of particles in underground PM samples are thought to be derived from interaction between wheels, rails, and brakes,[2] generating airborne particles that consist mainly of Fe but also contain among others Mn, Cr, V, Zn, and As.[35] Although abrasive forces between wheels, rails, and brakes can clearly generate coarse and fine PM due to shearing, there is evidence to suggest that ultrafine PM can be generated via the high temperatures of friction at interfaces between these components, with subsequent vaporization of the substrate.[25,34] There is also likely to be a contribution from arcing of the electrical current from the source to the contact point on the train, through which electrical current is drawn to power the train.[36,37] Crucially, however, unlike most urban underground systems that draw electric current through a third rail running parallel to the other rails, the railway in the present study is powered by an overhead catenary with the current drawn through a pantograph. Contact wires, which run above the railway line, are generally composed of Cu, alloyed with 0.1−0.5% Ag, Sn, Mg, or Cd.[38,39] The precise composition of these wires depends on the speed reached by trains drawing current. Similarly Cu or Cu−Pb−Sn alloys form the contact material of the pantograph, although in this case, it is generally as a component of a metallized carbon contact strip.[40,41] This can be contrasted with the third-rail system of power, where similar materials are used on the current-collecting component (in this case a third-rail "shoe"), but the third rail itself is an Al−stainless steel composite.[42] As such, overhead contact wire-powered underground railways may be expected to show increased airborne Cu levels compared to electrified rail-powered systems. By using the previously stated underground airborne PM mass concentrations for each size fraction described above, in conjunction with the concentration of Mn in each fraction, the mean (± 1 SE) airborne Mn concentration over the three days is calculated as 1010 ± 93 ng/m^3 well in excess of the WHO recommended limit of 150 ng/m^3 annual average and would still exceed this limit after allowing for working a 35 h exposure period per week, with zero Mn exposure outside of working hours.[43] Because Mn overexposure in welders and miners has been linked to symptoms resembling those of Parkinsonism, further study is needed of the potential effects of chronic exposure to underground dust.[44]

As the antithesis of an element found to be relatively enriched in underground PM, K was particularly high in woodstove PM. Wood combustion is a significant contributor

to airborne K,[45−47] so it is unsurprising that K was found at high levels in wood burner emissions. Interestingly, woodstove PM displayed levels of Rb, Cd, and Pb that were markedly enriched relative to other PM. Cd is a characteristic waste product of many industrial processes and is toxic to multiple organs, and it may be significant that the trees used to fuel the woodstove in this study were grown in the vicinity of a waste incinerator.[48] Waste incineration plants have been shown to release Cd as part of the incineration process,[49,50] and Pb was also enriched in woodstove PM compared to all other PM with the exception of road tunnel PM. It is well documented that the alkali metals Rb and Cs (which was also elevated in woodstove PM compared to other PM, although only at trace levels) act as analogues for K, also an alkali metal, in plant cation uptake, explaining their accumulation in plant material.[51]

Both roadwear PM and road tunnel PM have slightly raised levels of Ba but well below those seen in underground PM. Ba is also found in the brake shoes of trains; hence, brake wear is a possible source of the high Ba concentration in underground PM.[45,52] Roadwear and road tunnel PM samples also have high concentrations of Na, while roadwear PM was relatively rich in Al, K, Ti, and Sr and road tunnel PM was rich in B and Pb. These differences may reflect generation: roadwear PM is from an artificial roadwear generator while road tunnel PM is from an operational road tunnel. Ti and K are both found in brake pads,[53] while road dust contains aluminosilicates.[54] Elevated Na levels in road tunnel PM likely derive from the nearby (≈30 km) North Sea coast or from the addition of road salt. The elevated level of Pb in road tunnel PM is noteworthy as Pb is not currently used in Dutch petrol. However, Pb has been detected in road dust samples in other studies,[47,53] and probably reflects the greater volatility of Pb compared to other anthropogenically enriched toxic metals.[55]

The analyses presented here only yield the concentrations of the various elements under consideration. While this information is important, more detailed assessment of the biochemical impacts of these elevated metal levels would require information concerning their oxidation states. For example, distinction between Fe(II) and Fe(III) is important in discussing Fenton reactions and radical formation, which influences interaction with biomolecules. In addition, there is a need for study of the nature of the metal compounds in the PM. For example, environmental Fe is often found in an insoluble oxide form,[56,57] whereas metal chlorides are generally soluble. Indeed, more than one form of iron oxide has been observed in airborne PM, with urban PM Fe being mainly in the form of the hematite (Fe_2O_3), while the predominant species of underground iron has been reported for different systems as being magnetite (Fe_3O_4) or metallic iron, with minor hematite levels.[26,58] Improved identification of particular compounds could, for example, be attained by use of X-ray diffraction.[26,52]

Although metal speciation was not explicitly determined in this study, ROS generation by underground PM was investigated. Not only is ROS generation dependent upon the metal oxidation state, but it is also an intermediate step in transition-metal toxicity. In the present study, each fraction of underground PM was found to result in increased ROS generation as measured by DCF fluorescence. Furthermore, this ROS generation increased with PM concentration and was also greater for fine and ultrafine fractions compared to the coarse fraction. Considering the similarities in the metal composition of the different fractions, this effect is most likely due to the increased surface area/volume ratio as the PM size decreases. Previous studies have suggested that transition metals in lower oxidation states are better able to exert oxidative effects than those in the higher oxidation states,[59,60] which suggests that a toxicologically significant proportion of underground PM is either in a submaximal oxidation state or is able to be reduced in vitro to a state where it can further catalyze ROS generation.

Analysis of metal concentrations in all samples showed a strong correlation between different elements. Notably, Fe was positively correlated with 32 of the elements, including several of the most abundant transition metals, such as V, Cr, Mn, Co, Ni, Cu, and Zn. It is likely that these correlations are partly due to elements coming from the same source, such as Fe being alloyed with other elements to modify the properties of steel, but also partly due to the level of general mechanical activity contributing to PM load.

Ion chromatography analyses showed that road tunnel PM contained the highest concentrations of SO_4^{2-}, Cl^-, and NO_3^-. This finding is unsurprising, given that much of the PM from a road tunnel is likely to be derived from fuel combustion and thus be more representative of urban PM that is known to contain high concentrations of these anions.[47,61−63] There is also likely to be a contribution from aged PM originating from outside the tunnel, which has accumulated these anions during transport to the sampling site. Nonetheless, the lack of these anions in roadwear PM compared to other particles analyzed also accords with their predominance in environments where fuel combustion is taking place and also explains their high levels in woodstove PM. However, it may be noteworthy that, of all the PM sources, with the exception of road tunnel, underground PM showed the greatest concentration of anions. Weak correlations of SO_4^{2-}, Cl^-, and NO_3^- concentrations with Fe concentration indicates that they are unlikely to be derived from mechanical wear. One source may be motor vehicles in the vicinity. The airport is one of the busiest airports in the world, by passenger number, and there is a considerable amount of motor vehicle usage in the vicinity of the airport. The railway station lies beneath a complex of car parks and passenger drop-off/pick-up points. Thus, it is likely that PM from car exhaust is drawn into the station by the "piston action" of train movement, although the extent of this input is a matter of debate.[64−66] Additionally, contributions from aircraft particulate emissions cannot be excluded.[67] Another potential source is the diesel-powered goods trains that pass occasionally through the station at night. Although no such trains passed through the station during sampling periods, particles deposited by diesel locomotives could be re-entrained by trains passing during the day or by cleaning vehicles that are in regular use. In support of this hypothesis, the reduced levels of Cl^- and NO_3^- compared to levels of SO_4^{2-} in underground PM, especially the ultrafine fraction, suggest that the contribution of secondary species from outside is minor.

As this study focused on metals in PM, there remains a proportion of the mass of underground PM that was not identified in this study (45%, 44%, and 19% by mass for coarse, fine, and ultrafine fractions, respectively). Si was not quantified in this study as the hydrofluoric acid digestion technique precludes accurate quantification. However, Si has been found in underground PM by other groups and has been ascribed to either brake blocks or the dumping of sand to improve wheel traction under braking.[2,4] Furthermore, oxygen as found in metal oxides was not measured. Because underground PM

contains substantial levels of iron oxide, it is likely that oxygen makes up a significant proportion of the unidentified PM mass.[68] Finally, carbon, either elemental or organic, was not assayed. A wide range of organic compounds have been found in underground PM,[16] and while these may be derived from diesel train passage, it has also been noted that PM in areas located immediately below ground level, as with the station in this study, may be more influenced by above-ground sources than would be the case for deeper environments.[69] This is particularly pertinent here as the underground station lies directly beneath a large multistory car park. Indeed, underground PM is likely to contain toxicants such as polyaromatic hydrocarbons and redox-active quinones,[70] although the source of these is harder to verify. They are likely to be derived from above-ground traffic sources, and their concentrations may vary depending on the underground system (e.g., ventilation controls), above-ground urban pollution levels, and weather conditions.

This study also examined the morphology of underground PM because morphology can often serve as an indicator of the source of the particulate or at least the processes involved in its creation.[2] In terms of particle numbers, most PM of all size fractions had a granular appearance, with rough, uneven faces. No fibrous structures were observed. However, coarse PM contained a considerable number of particles of a flakelike, angular appearance, characteristic of particles created by abrasion and shearing. Such flakes may have considerably lower aerodynamic diameters than geometric diameters, resulting in an increased likelihood of deposition in the respiratory tract. Similar morphology has previously been observed in PM in other underground systems.[2,4,26] Very few flakelike particles were observed in the fine fraction, while none were seen in the ultrafine PM. Whether particulate angular shape affects uptake by cells or particle−particle interactions is not known. However, the angular nature of these particles may allow them to impinge upon the structure of the cell.[26]

Particle agglomerates were seen in all fractions, smaller structures comprising fewer than 10 individual particles, while larger structures were also observed, in excess of the respective VACES cutpoint, suggesting that the agglomerate had formed after collection. It was also observed that some particles particularly in the ultrafine ($PM_{0.18}$) fraction were larger than the stated cutpoint, although this may be reconciled by understanding that the diameter relates to the aerodynamic behavior equivalent to a sphere of unit-density of a set diameter.[71] Therefore, a particle may have an aerodynamic diameter lower than suggested by consideration of only its largest dimension.[72] Furthermore, the stated VACES cutpoint is not an absolute value but a 50% elimination value, meaning that, although 50% of particles larger than the cutpoint of 0.18 μm are eliminated, some larger particles, including up to 5% of those above 0.5 μm, may remain.[22] There also exists the possibility for smaller particles to enter larger-cutpoint fractions by adhering to larger particles.[35]

In conclusion, this study has characterized and compared size-fractionated mainline underground PM. The results show that underground PM contains a high concentration of Fe, correlated with levels of other transition metals, notably, Mn, Ni, Cu, and V, which are significantly elevated compared to PM from other sources. Crucially, ultrafine underground dust was at least as rich in metals as coarse and fine underground PM, which may have important implications for potential hazards posed by underground PM, and warrants further study of the hitherto neglected ultrafine fraction in particular.

■ ASSOCIATED CONTENT

Supporting Information

Elements analyzed by ICP-MS with sources of standards; particulate analysis results for elements not included in the main body of the paper. This material is available free of charge via the Internet at http://pubs.acs.org.

■ AUTHOR INFORMATION

Corresponding Author

*E-mail: m.loxham@soton.ac.uk.

Author Contributions

[#]These authors contributed equally to this work.

Author Contributions

The manuscript was written through contributions of all authors. All authors have given approval to the final version of the manuscript.

Notes

The authors declare no competing financial interest.

■ ACKNOWLEDGMENTS

We thank Daan L. A. C. Leseman, Paul H. B. Fokkens, and A. John F. Boere from the Centre for Environmental Health, National Institute for Public Health and the Environment (RIVM), Bilthoven, The Netherlands, for their valuable assistance with collecting size-fractionated particulate matter from the underground railway station. This work was funded by a PhD studentship to M.L. from the Medical Research Council Integrative Toxicology Training Partnership (UK).

■ ABBREVIATIONS USED

DEP	diesel exhaust particulate
PM	particulate matter
ROS	reactive oxygen species
RT	road tunnel
RW	roadwear simulator
UG	underground railway
VACES	versatile concentration and enrichment system
WS	woodstove

■ REFERENCES

(1) Nieuwenhuijsen, M. J.; Gomez-Perales, J. E.; Colvile, R. N. Levels of particulate air pollution, its elemental composition, determinants and health effects in metro systems. *Atmos. Environ.* **2007**, *41* (37), 7995−8006.

(2) Sitzmann, B.; Kendall, M.; Watt, J.; Williams, I. Characterisation of airborne particles in London by computer-controlled scanning electron microscopy. *Sci. Total Environ.* **1999**, *241* (1−3), 63−73.

(3) Bachoual, R.; Boczkowski, J.; Goven, D.; Amara, N.; Tabet, L.; On, D.; Lecon-Malas, V.; Aubier, M.; Lanone, S. Biological effects of particles from the Paris subway system. *Chem. Res. Toxicol.* **2007**, *20* (10), 1426−1433.

(4) Ripanucci, G.; Grana, M.; Vicentini, L.; Magrini, A.; Bergamaschi, A. Dust in the underground railway tunnels of an Italian town. *J. Occup. Environ. Hyg.* **2006**, *3* (1), 16−25.

(5) World Health Organization. *Air Quality Guidelines: Global Update 2005: Particulate Matter, Ozone, Nitrogen Dioxide, and Sulfur Dioxide*; World Health Organization: Copenhagen, Denmark, 2006; p 9.

(6) Adams, H. S.; Nieuwenhuijsen, M. J.; Colvile, R. N.; McMullen, M. A. S.; Khandelwal, P. Fine particle (PM2.5) personal exposure levels in transport microenvironments, London, UK. *Sci. Total Environ.* **2001**, *279* (1−3), 29−44.

(7) Crump, K. S. Manganese exposures in Toronto during use of the gasoline additive, methylcyclopentadienyl manganese tricarbonyl. *J. Exposure Anal. Environ. Epidemiol.* **2000**, *10* (3), 227−239.
(8) Klepczynska Nystrom, A.; Svartengren, M.; Grunewald, J.; Pousette, C.; Rodin, I.; Lundin, A.; Skold, C. M.; Eklund, A.; Larsson, B. M. Health effects of a subway environment in healthy volunteers. *Eur. Respir. J.* **2010**, *36* (2), 240−8.
(9) Chillrud, S. N.; Grass, D.; Ross, J. M.; Coulibaly, D.; Slavkovich, V.; Epstein, D.; Sax, S. N.; Pederson, D.; Johnson, D.; Spengler, J. D.; Kinney, P. L.; Simpson, H. J.; Brandt-Rauf, P. Steel dust in the New York City subway system as a source of manganese, chromium, and iron exposures for transit workers. *Bull. N. Y. Acad. Med.* **2005**, *82* (1), 33−42.
(10) Seaton, A.; Cherrie, J.; Dennekamp, M.; Donaldson, K.; Hurley, J. F.; Tran, C. L. The London Underground: Dust and hazards to health. *Occup. Environ. Med.* **2005**, *62* (6), 355−62.
(11) van Klaveren, R. J.; Nemery, B. Role of reactive oxygen species in occupational and environmental obstructive pulmonary diseases. *Curr. Opin. Pulm. Med.* **1999**, *5* (2), 118−23.
(12) Kelly, F. J. Oxidative stress: Its role in air pollution and adverse health effects. *Occup. Environ. Med.* **2003**, *60* (8), 612−616.
(13) Hutchison, G. R.; Brown, D. M.; Hibbs, L. R.; Heal, M. R.; Donaldson, K.; Maynard, R. L.; Monaghan, M.; Nicholl, A.; Stone, V. The effect of refurbishing a UK steel plant on PM_{10} metal composition and ability to induce inflammation. *Respir. Res.* **2005**, *6*, 43−58.
(14) Schaumann, F.; Borm, P. J. A.; Herbrich, A.; Knoch, J.; Pitz, M.; Schins, R. P. F.; Luettig, B.; Hohlfeld, J. M.; Heinrich, J.; Krug, N. Metal-rich ambient particles (particulate $matter_{2.5}$) cause airway inflammation in healthy subjects. *Am. J. Respir. Crit. Care Med.* **2004**, *170* (8), 898−903.
(15) McNeilly, J. D.; Heal, M. R.; Beverland, I. J.; Howe, A.; Gibson, M. D.; Hibbs, L. R.; MacNee, W.; Donaldson, K. Soluble transition metals cause the pro-inflammatory effects of welding fumes in vitro. *Toxicol. Appl. Pharmacol.* **2004**, *196* (1), 95−107.
(16) Midander, K.; Elihn, K.; Wallen, A.; Belova, L.; Karlsson, A. K. B.; Wallinder, I. O. Characterisation of nano- and micron-sized airborne and collected subway particles, a multi-analytical approach. *Sci. Total Environ.* **2012**, *427*, 390−400.
(17) Peters, A.; Wichmann, H. E.; Tuch, T.; Heinrich, J.; Heyder, J. Respiratory effects are associated with the number of ultrafine particles. *Am. J. Respir. Crit. Care Med.* **1997**, *155* (4), 1376−1383.
(18) Lippmann, M.; Yeates, D. B.; Albert, R. E. Deposition, retention, and clearance of inhaled particles. *Br. J. Ind. Med.* **1980**, *37* (4), 337−62.
(19) Oberdorster, G.; Ferin, J.; Lehnert, B. E. Correlation between particle-Size, in vivo particle persistence, and lung injury. *Environ. Health Perspect.* **1994**, *102*, 173−179.
(20) Nemmar, A.; Vanbilloen, H.; Hoylaerts, M. F.; Hoet, P. H. M.; Verbruggen, A.; Nemery, B. Passage of intratracheally instilled ultrafine particles from the lung into the systemic circulation in hamster. *Am. J. Respir. Crit. Care Med.* **2001**, *164* (9), 1665−1668.
(21) Kim, S.; Jaques, P. A.; Chang, M. C.; Barone, T.; Xiong, C.; Friedlander, S. K.; Sioutas, C. Versatile aerosol concentration enrichment system (VACES) for simultaneous in vivo and in vitro evaluation of toxic effects of ultrafine, fine and coarse ambient particles − Part II: Field evaluation. *J. Aerosol Sci.* **2001**, *32* (11), 1299−1314.
(22) Kim, S.; Jaques, P. A.; Chang, M. C.; Froines, J. R.; Sioutas, C. Versatile aerosol concentration enrichment system (VACES) for simultaneous in vivo and in vitro evaluation of toxic effects of ultrafine, fine and coarse ambient particles − Part I: Development and laboratory characterization. *J. Aerosol Sci.* **2001**, *32* (11), 1281−1297.
(23) Strak, M.; Steenhof, M.; Godri, K. J.; Gosens, I.; Mudway, I. S.; Cassee, F. R.; Lebret, E.; Brunekreef, B.; Kelly, F. J.; Harrison, R. M.; Hoek, G.; Janssen, N. A. H. Variation in characteristics of ambient particulate matter at eight locations in the Netherlands − The RAPTES project. *Atmos. Environ.* **2011**, *45* (26), 4442−4453.
(24) Blume, C.; Swindle, E. J.; Dennison, P. W.; Jayasekera, N. P.; Dudley, S.; Monk, P.; Behrendt, H.; Schmidt-Weber, C. B.; Holgate, S. T.; Howarth, P. H.; Traidl-Hoffman, C.; Davies, D. E.Barrier responses of human bronchial epithelial cells to grass pollen exposure. *Eur. Respir. J.* [Online early access]. DOI: 10.1183/09031936.00075612. Published Online: November 8, **2012**.
(25) Sundh, J.; Olofsson, U.; Olander, L.; Jansson, A. Wear rate testing in relation to airborne particles generated in a wheel-rail contact. *Lubr. Sci.* **2009**, *21* (4), 135−150.
(26) Karlsson, H. L.; Nilsson, L.; Moller, L. Subway particles are more genotoxic than street particles and induce oxidative stress in cultured human lung cells. *Chem. Res. Toxicol.* **2005**, *18* (1), 19−23.
(27) Li, N.; Sioutas, C.; Cho, A.; Schmitz, D.; Misra, C.; Sempf, J.; Wang, M. Y.; Oberley, T.; Froines, J.; Nel, A. Ultrafine particulate pollutants induce oxidative stress and mitochondrial damage. *Environ. Health Perspect.* **2003**, *111* (4), 455−460.
(28) Alexis, N. E.; Lay, J. C.; Zeman, K.; Bennett, W. E.; Peden, D. B.; Soukup, J. M.; Devlin, R. B.; Becker, S. Biological material on inhaled coarse fraction particulate matter activates airway phagocytes in vivo in healthy volunteers. *J. Allergy Clin. Immunol.* **2006**, *117* (6), 1396−1403.
(29) Cho, S. H.; Tong, H. Y.; McGee, J. K.; Baldauf, R. W.; Krantz, Q. T.; Gilmour, M. I. Comparative toxicity of size-fractionated airborne particulate matter collected at different distances from an urban highway. *Environ. Health Perspect.* **2009**, *117* (11), 1682−1689.
(30) Brown, D. M.; Stone, V.; Findlay, P.; MacNee, W.; Donaldson, K. Increased inflammation and intracellular calcium caused by ultrafine carbon black is independent of transition metals or other soluble components. *Occup. Environ. Med.* **2000**, *57* (10), 685−691.
(31) Peters, A. Ambient particulate matter and the risk for cardiovascular disease introduction. *Prog. Cardiovasc. Dis.* **2011**, *53* (5), 327−333.
(32) Donaldson, K.; Stone, V.; Borm, P. J. A.; Jimenez, L. A.; Gilmour, P. S.; Schins, R. P. F.; Knaapen, A. M.; Rahman, I.; Faux, S. P.; Brown, D. M.; MacNee, W. Oxidative stress and calcium signaling in the adverse effects of environmental particles (PM_{10}). *Free Radical Biol. Med.* **2003**, *34* (11), 1369−1382.
(33) Elihn, K.; Berg, P. Ultrafine particle characteristics in seven industrial plants. *Ann. Occup. Hyg.* **2009**, *53* (5), 475−484.
(34) Zimmer, A. T.; Maynard, A. D. Investigation of the aerosols produced by a high-speed, hand-held grinder using various substrates. *Ann. Occup. Hyg.* **2002**, *46* (8), 663−672.
(35) Weckwerth, G. Verification of traffic emitted aerosol components in the ambient air of Cologne (Germany). *Atmos. Environ.* **2001**, *35* (32), 5525−5536.
(36) Aarnio, P.; Yli-Tuomi, T.; Kousa, A.; Makela, T.; Hirsikko, A.; Hameri, K.; Raisanen, M.; Hillamo, R.; Koskentalo, T.; Jantunen, M. The concentrations and composition of and exposure to fine particles ($PM_{2.5}$) in the Helsinki subway system. *Atmos. Environ.* **2005**, *39* (28), 5059−5066.
(37) Pfeifer, G. D.; Harrison, R. M.; Lynam, D. R. Personal exposures to airborne metals in London taxi drivers and office workers in 1995 and 1996. *Sci. Total Environ.* **1999**, *235* (1−3), 253−260.
(38) Liljedahl Bare Wire. Contact Wire and Stranded Conductors for Overhead Catenary Systems. http://liljedahl.notitium-ipub.se/train_folder/#/12/ (accessed July 23, 2012).
(39) Lamifil. Railway Applications and Solutions. http://lamifil.be/railway/applications-and-solutions/ (accessed July 23, 2012).
(40) Kubo, S.; Kato, K. Effect of arc discharge on wear rate of Cu-impregnated carbon strip in unlubricated sliding against Cu trolley under electric current. *Wear* **1998**, *216* (2), 172−178.
(41) Kubo, S.; Kato, K. Effect of arc discharge on the wear rate and wear mode transition of a copper-impregnated metallized carbon contact strip sliding against a copper disk. *Tribol. Int.* **1999**, *32* (7), 367−378.
(42) Dong, L.; Chen, G. X.; Zhu, M. H.; Zhou, Z. R. Wear mechanism of aluminum-stainless steel composite conductor rail sliding against collector shoe with electric current. *Wear* **2007**, *263*, 598−603.
(43) World Health Organization Regional Office for Europe. *Air Quality Guidelines for Europe*, 2nd ed.; WHO Regional Office for Europe: Copenhagen, Denmark, 2000; p 273.

(44) Olanow, C. W. Manganese-induced parkinsonism and Parkinson's disease. *Ann. N. Y. Acad. Sci.* **2004**, *1012*, 209−223.
(45) Gerlofs-Nijland, M. E.; Dormans, J. A.; Bloemen, H. J.; Leseman, D. L.; John, A.; Boere, F.; Kelly, F. J.; Mudway, I. S.; Jimenez, A. A.; Donaldson, K.; Guastadisegni, C.; Janssen, N. A.; Brunekreef, B.; Sandstrom, T.; van Bree, L.; Cassee, F. R. Toxicity of coarse and fine particulate matter from sites with contrasting traffic profiles. *Inhalation Toxicol.* **2007**, *19* (13), 1055−69.
(46) Norris, G.; YoungPong, S. N.; Koenig, J. Q.; Larson, T. V.; Sheppard, L.; Stout, J. W. An association between fine particles and asthma emergency department visits for children in Seattle. *Environ. Health Perspect.* **1999**, *107* (6), 489−493.
(47) Bloemen, H. J. T.; Gerlofs-Nijland, M. E.; Janssen, N. A. H.; Sandstrom, T.; van Bree, L.; Cassee, F. R. *Chemical Characterization and Source Apportionment Estimates of Particulate Matter Collected within the Framework of EU Project HEPMEAP*, RIVM rapport 863001002; National Institute for Public Health and the Environment: Bilthoven, The Netherlands, 2005; http://www.rivm.nl/bibliotheek/rapporten/863001002.html.
(48) Stohs, S. J.; Bagchi, D. Oxidative mechanisms in the toxicity of metal ions. *Free Radical Biol. Med.* **1995**, *18* (2), 321−336.
(49) Holmgren, K.; Gebremedhin, A. Modelling a district heating system: Introduction of waste incineration, policy instruments and co-operation with an industry. *Energy Policy* **2004**, *32* (16), 1807−1817.
(50) Zhang, F. S.; Yamasaki, S. I.; Nanzyo, M.; Kimura, K. Evaluation of cadmium and other metal losses from various municipal wastes during incineration disposal. *Environ. Pollut.* **2001**, *115* (2), 253−260.
(51) Epstein, E.; Hagen, C. E. A kinetic study of the absorption of alkali cations by barley roots. *Plant Physiol.* **1952**, *27* (3), 457−74.
(52) Furuya, K.; Kudo, Y.; Okinaga, K.; Yamuki, M.; Takahashi, S.; Araki, Y.; Hisamatsu, Y. Seasonal variation and their characterization of suspended particulate matter in the air of subway stations. *J. Trace Microprobe Tech.* **2001**, *19* (4), 469−485.
(53) Apeagyei, E.; Bank, M. S.; Spengler, J. D. Distribution of heavy metals in road dust along an urban-rural gradient in Massachusetts. *Atmos. Environ.* **2011**, *45* (13), 2310−2323.
(54) Becker, S.; Soukup, J. M.; Gallagher, J. E. Differential particulate air pollution induced oxidant stress in human granulocytes, monocytes and alveolar macrophages. *Toxicol. In Vitro* **2002**, *16* (3), 209−218.
(55) Lin, C. C.; Chen, S. J.; Huang, K. L.; Hwang, W. I.; Chang-Chien, G. P.; Lin, W. Y. Characteristics of metals in nano/ultrafine/fine/coarse particles collected beside a heavily trafficked road. *Environ. Sci. Technol.* **2005**, *39* (21), 8113−8122.
(56) Pritchard, R. J.; Ghio, A. J.; Lehmann, J. R.; Winsett, D. W.; Tepper, J. S.; Park, P.; Gilmour, M. I.; Dreher, K. L.; Costa, D. L. Oxidant generation and lung injury after particulate air pollutant exposure increase with the concentrations of associated metals. *Inhalation Toxicol.* **1996**, *8* (5), 457−477.
(57) Gioda, A.; Fuentes-Mattei, E.; Jimenez-Velez, B. Evaluation of cytokine expression in BEAS cells exposed to fine particulate matter ($PM_{2.5}$) from specialized indoor environments. *Int. J. Environ. Health Res.* **2011**, *21* (2), 106−119.
(58) Jung, H. J.; Kim, B.; Malek, M. A.; Koo, Y. S.; Jung, J. N.; Son, Y. S.; Kim, J. C.; Kim, H.; Ro, C. U. Chemical speciation of size-segregated floor dusts and airborne magnetic particles collected at underground subway stations in Seoul, Korea. *J. Hazard. Mater.* **2012**, *213*, 331−340.
(59) Prahalad, A. K.; Inmon, J.; Ghio, A. J.; Gallagher, J. E. Enhancement of 2′-deoxyguanosine hydroxylation and DNA damage by coal and oil fly ash in relation to particulate metal content and availability. *Chem. Res. Toxicol.* **2000**, *13* (10), 1011−1019.
(60) Merolla, L.; Richards, R. J. In vitro effects of water-soluble metals present in UK particulate matter. *Exp. Lung Res.* **2005**, *31* (7), 671−683.
(61) Barath, S.; Mills, N. L.; Lundback, M.; Tornqvist, H.; Lucking, A. J.; Langrish, J. P.; Soderberg, S.; Boman, C.; Westerholm, R.; Londahl, J.; Donaldson, K.; Mudway, I. S.; Sandstrom, T.; Newby, D. E.; Blomberg, A. Impaired vascular function after exposure to diesel exhaust generated at urban transient running conditions. *Part. Fibre Toxicol.* **2010**, *7*, 19−29.
(62) Gomez-Perales, J. E.; Colvile, R. N.; Nieuwenhuijsen, M. J.; Fernandez-Bremauntz, A.; Gutierrez-Avedoy, V. J.; Paramo-Figueroa, V. H.; Blanco-Jimenez, S.; Bueno-Lopez, E.; Mandujano, F.; Bernabe-Cabanillas, R.; Ortiz-Segovia, E. Commuters' exposure to PM2.5, CO, and benzene in public transport in the metropolitan area of Mexico City. *Atmos. Environ.* **2004**, *38* (8), 1219−1229.
(63) Dockery, D. W.; Pope, C. A. Acute respiratory effects of particulate air-pollution. *Annu. Rev. Public Health* **1994**, *15*, 107−132.
(64) Branis, M. The contribution of ambient sources to particulate pollution in spaces and trains of the Prague underground transport system. *Atmos. Environ.* **2006**, *40* (2), 348−356.
(65) Kang, S.; Hwang, H.; Park, Y.; Kim, H.; Ro, C. U. Chemical compositions of subway particles in Seoul, Korea determined by a quantitative single particle analysis. *Environ. Sci. Technol.* **2008**, *42* (24), 9051−9057.
(66) Raut, J. C.; Chazette, P.; Fortain, A. Link between aerosol optical, microphysical and chemical measurements in an underground railway station in Paris. *Atmos. Environ.* **2009**, *43* (4), 860−868.
(67) Westerdahl, D.; Fruin, S. A.; Fine, P. L.; Sioutas, C. The Los Angeles International Airport as a source of ultrafine particles and other pollutants to nearby communities. *Atmos. Environ.* **2008**, *42* (13), 3143−3155.
(68) Karlsson, H. L.; Ljungman, A. G.; Lindbom, J.; Moller, L. Comparison of genotoxic and inflammatory effects of particles generated by wood combustion, a road simulator and collected from street and subway. *Toxicol. Lett.* **2006**, *165* (3), 203−211.
(69) Jung, H. J.; Kim, B.; Ryu, J.; Maskey, S.; Kim, J. C.; Sohn, J.; Ro, C. U. Source identification of particulate matter collected at underground subway stations in Seoul, Korea using quantitative single-particle analysis. *Atmos. Environ.* **2010**, *44* (19), 2287−2293.
(70) Ayres, J. G.; Borm, P.; Cassee, F. R.; Castranova, V.; Donaldson, K.; Ghio, A.; Harrison, R. M.; Hider, R.; Kelly, F.; Kooter, I. M.; Marano, F.; Maynard, R. L.; Mudway, I.; Nel, A.; Sioutas, C.; Smith, S.; Baeza-Squiban, A.; Cho, A.; Duggan, S.; Froines, J. Evaluating the toxicity of airborne particulate matter and nanoparticles by measuring oxidative stress potential—A workshop report and consensus statement. *Inhalation Toxicol.* **2008**, *20* (1), 75−99.
(71) Samet, J. M.; Dominici, F.; Curriero, F. C.; Coursac, I.; Zeger, S. L. Fine particulate air pollution and mortality in 20 US Cities, 1987−1994. *N. Engl. J. Med.* **2000**, *343* (24), 1742−1749.
(72) Schinwald, A.; Murphy, F. A.; Jones, A.; MacNee, W.; Donaldson, K. Graphene-based nanoplatelets: A new risk to the respiratory system as a consequence of their unusual aerodynamic properties. *ACS Nano* **2012**, *6* (1), 736−746.

OPEN ACCESS Freely available online

PLOS ONE

Barrier Disrupting Effects of *Alternaria Alternata* Extract on Bronchial Epithelium from Asthmatic Donors

Marina S. Leino[1☯], Matthew Loxham[1*☯], Cornelia Blume[1], Emily J. Swindle[1], Nivenka P. Jayasekera[1], Patrick W. Dennison[1], Betty W. H. Shamji[2], Matthew J. Edwards[2], Stephen T. Holgate[1], Peter H. Howarth[1], Donna E. Davies[1]

1 Academic Unit of Clinical and Experimental Sciences and the Southampton NIHR Respiratory Biomedical Research Unit, University of Southampton Faculty of Medicine, Sir Henry Wellcome Laboratories, South Block, University Hospital Southampton, Southampton, United Kingdom, **2** Novartis Institutes for Biomedical Research, Novartis Horsham Research Centre, Horsham, United Kingdom

Abstract

Sensitization and exposure to the allergenic fungus *Alternaria alternata* has been associated with increased risk of asthma and asthma exacerbations. The first cells to encounter inhaled allergens are epithelial cells at the airway mucosal surface. Epithelial barrier function has previously been reported to be defective in asthma. This study investigated the contribution of proteases from *Alternaria alternata* on epithelial barrier function and inflammatory responses and compared responses of *in vitro* cultures of differentiated bronchial epithelial cells derived from severely asthmatic donors with those from non-asthmatic controls. Polarised 16HBE cells or air-liquid interface (ALI) bronchial epithelial cultures from non-asthmatic or severe asthmatic donors were challenged apically with extracts of *Alternaria* and changes in inflammatory cytokine release and transepithelial electrical resistance (TER) were measured. Protease activity in *Alternaria* extracts was characterised and the effect of selectively inhibiting protease activity on epithelial responses was examined using protease inhibitors and heat-treatment. In 16HBE cells, *Alternaria* extracts stimulated release of IL-8 and TNFα, with concomitant reduction in TER; these effects were prevented by heat-treatment of the extracts. Examination of the effects of protease inhibitors suggested that serine proteases were the predominant class of proteases mediating these effects. ALI cultures from asthmatic donors exhibited a reduced IL-8 response to *Alternaria* relative to those from healthy controls, while neither responded with increased thymic stromal lymphopoietin (TSLP) release. Only cultures from asthmatic donors were susceptible to the barrier-weakening effects of *Alternaria*. Therefore, the bronchial epithelium of severely asthmatic individuals may be more susceptible to the deleterious effects of *Alternaria*.

Citation: Leino MS, Loxham M, Blume C, Swindle EJ, Jayasekera NP, et al. (2013) Barrier Disrupting Effects of *Alternaria Alternata* Extract on Bronchial Epithelium from Asthmatic Donors. PLoS ONE 8(8): e71278. doi:10.1371/journal.pone.0071278

Editor: Bernhard Ryffel, French National Centre for Scientific Research, France

Received March 20, 2013; **Accepted** June 27, 2013; **Published** August 23, 2013

Funding: This project was funded by a European Respiratory Society Long Term Fellowship to MSL, and also by the Medical Research Council, UK. The funders had no role in study design, data collection and analysis, decision to publish, or preparation of the manuscript.

Competing Interests: The authors declare that Matthew J Edwards and Betty WH Shamji are employed by Novartis plc, working at the Novartis Institutes for Biomedical Research, Horsham, UK. This does not alter the authors' adherence to all the PLOS ONE policies on sharing data and materials.

* E-mail: m.loxham@soton.ac.uk

☯ These authors contributed equally to this work.

Introduction

Asthma is a chronic inflammatory airways disease that is characterised physiologically by airway hyperresponsiveness to innocuous stimuli, and pathologically by Th2 inflammation and structural remodelling of the airways. The majority of asthma is associated with atopy, where an IgE response to specific aeroallergens has developed. The airway epithelium which forms both a physical barrier and an interface with the immune system *via* expression of adhesion molecules and secretion of a myriad cytokines, chemokines, and inflammatory mediators [1–3], is the first tissue encountered by such inhaled allergens. However, recent evidence has suggested that the asthmatic bronchial epithelium is structurally perturbed, resulting in impairment of barrier function [4].

Allergens from fungi including species of *Alternaria*, *Cladosporium*, and *Aspergillus* present a major risk factor for the development of asthma, with evidence supporting a link between sensitisation to fungi and prevalence or severity of asthma [5,6], and also between spore prevalence and asthma [7,8]. Further reports have found links between sensitivity to the common *Alternaria* species of fungi, particularly *Alternaria alternata*, and asthma [7,9–12]. Pathogenic fungi secrete a range of proteases [13], with those of the serine class being particularly associated with asthma [14]. *In vitro* studies have shown that serine proteases from *Aspergillus fumigatus* and *Alternaria alternata* induce production of IL-8 and IL-6, as well as causing epithelial cell detachment [15–17]. This action is reported to occur *via* activation of protease activated receptor (PAR)−2 [18,19], which has been observed to be up-regulated in the bronchial epithelium of asthmatic subjects [20], and can be replicated by use of a synthetic PAR-2 activating peptide [21]. Similar effects have been seen with the house dust mite (HDM) cysteine and serine protease allergens Der p 1 and Der p 3 [18,22], and also serine proteases from German cockroach extract [23]. *Alternaria*-induced PAR-2 cleavage has also been suggested to be responsible for TSLP release from epithelial cells, and the activity

of proteases as adjuvants in allergic sensitisation [24–26]. However, even though it is well recognised that the bronchial epithelium is a polarised structure, little is known about the directionality of epithelial cytokine release. Vectorial cytokine release may be critical for establishing concentration gradients of certain cytokines that play key roles in chemoattraction and immune cell recruitment.

Aside from their activity towards PARs, proteases can also perturb the epithelial barrier by directly cleaving tight junction proteins, facilitating permeation of allergens and pathogens to the underlying tissue. Der p 1 can degrade occludin and trigger ZO-1 breakdown, resulting in tight junction disassembly and increased paracellular permeability [27,28]; similar effects have also been seen with HDM serine proteases [29]. The *Penicillium* allergen Pen ch 13, a serine protease, has been reported to cleave occludin [30], and effects on occludin, ZO-1, and claudin-1 have been noted with serine and cysteine proteases in pollen from a variety of sources [31].

Previous studies have focused on use of epithelial cell lines which are not covered by a cytoprotective mucous layer that protects the airways *in vivo*, which may explain their susceptibility to the proteolytic effects of allergen-derived proteases. Furthermore, the observation that there is impaired epithelial barrier function in asthma [4] led us to investigate the effect of *Alternaria* on epithelial barrier function, and to determine whether there is a differential response to *Alternaria* extract between fully differentiated cultures of primary human bronchial epithelial cells (PBECs) from healthy donors and those from asthmatic donors. As *Alternaria* has been observed to be both pro-inflammatory [16] and to induce development of a Th2-type response [32,33], vectorial secretion of IL-8, TNFα, thymic stromal lymphopoietin (TSLP), IL-18 and IL-33 was analysed.

Methods

Ethics Statement

Ethical approval had been obtained from the Southampton local research ethics committee under the description "Pathophysiology of Airway Diseases such as Asthma and COPD", Rec. No 05/Q1702/165, code MRC0268. All volunteers had provided their written informed consent, and all samples were anonymous-linked, with access to patient-identifiable data being available only to those with prior ethical approval.

Cell Culture

The human bronchial epithelial cell-line, 16-HBE14o- (a gift from Professor D.C. Gruenert, San Francisco, USA) [34] was cultured in Minimal Essential Medium (MEM) with GlutaMax supplemented with 10% heat-inactivated FBS, 50 IU/ml penicillin and 50 μg/ml streptomycin (all Invitrogen, Paisley, UK). Cells were placed in Transwell® culture inserts (Corning, Tewkesbury, MA, USA) pre-coated with collagen I (Pure-Col, Nutacon BV, Leimuiden, The Netherlands); they were used for experiment when the transepithelial electrical resistance (TER) was >3000 Ω/cm^2. 24 h prior to challenge, 16HBE cells had the apical medium replaced with serum-free MEM.

Primary bronchial epithelial cells (PBECs) were grown from bronchial brushings obtained from non-asthmatic or severe asthmatic volunteers by fibreoptic bronchoscopy, as previously described [35] (for donor information, see Table S1). PBECs were expanded in culture and, at passage 2, were taken to an air-liquid interface (ALI) [4]. Cultures were used for assays at day 21 when the TER was >3000 Ω/cm^2. 24 h prior to challenge, the basolateral medium of ALI cultures was replaced with BEBM containing 1% ITS (Sigma-Aldrich, Gillingham, UK) and 1.5 μg/ml BSA basolaterally.

Lyophilised *Alternaria alternata* and *Cladosporium herbarum* extracts (Greer, Lenoir, NC, USA) were prepared by purification and lyophilisation of fungal culture medium according to current Good Manufacturing Practice to minimise inter-batch variability [36]. Extracts were dissolved into supplement-free medium and added apically to cultures to achieve the desired concentrations. Protein concentrations were 136 μg/mg dry weight for *Alternaria* extract and 30 μg/mg dry weight for *Cladosporium* extract. LPS content was not assayed, however, previous assays of the same product have shown minimal endotoxin activity [32]; in view of the lack of CD14 expression by epithelial cells [37], there is minimal possibility that LPS contamination contributed to responses of the BEC cultures. To assess heat-lability, fungal extracts were heat-treated at 65°C for 30 min while the contribution of serine, cysteine and aspartate protease activity was determined by pretreating *Alternaria* extracts with AEBSF, E-64, or Pepstatin A (Sigma-Aldrich, Gillingham, UK) respectively for 30 min immediately prior to stimulation. To assess the contribution of p38 MAPK, SB203580 (Sigma-Aldrich) was added apically for 30 min prior to challenge. At 24 h, apical and basolateral media were harvested and cells were fixed for immunostaining. Further details of cell culture and challenge can be found in Information S1.

Lactate Dehydrogenase (LDH) Assay

LDH release was measured using a CytoTox 96 LDH assay kit (Promega, Southampton, UK) according to the manufacturer's instructions. Total cellular LDH activity was determined by lysing cells with 1% Triton X-100 in culture medium for 60 min at 37°C.

FITC-Dextran Passage

FITC-dextran (4 kDa) was added to the apical compartment at a final concentration of 2 mg/ml, 1h after the addition of the fungal extracts. Basolateral FITC-dextran concentration at 24 h was determined against a standard curve using a Labsystems Fluoroskan FL fluorimeter (Thermo Fisher Scientific, Waltham, MA), with excitation and emission wavelengths set to 485 nm and 530 nm respectively.

Cytokine Analysis

Release of IL-8, TNFα, IL-18 and IL-33 into the apical and basolateral compartments was assayed by ELISA according to the manufacturer's instructions (R&D Systems, Abingdon, UK). For assay of TNFα release from ALI cultures, a high-sensitivity TNFα ELISA kit (R&D Systems) was used. TSLP was measured using an 'in-house' ELISA developed by Novartis Plc (Horsham, UK), which recognises both *E. coli* expressed recombinant TSLP and naturally secreted TSLP from primary lung fibroblasts.

Detection of Protease Activity

Alternaria extract protease activity was assessed using a protease fluorescent detection kit (Sigma-Aldrich) according to the manufacturer's instructions. This kit was also used to measure attenuation of *Alternaria* protease activity by prior heat-treatment of the extract or the protease inhibitors AEBSF, E-64, or Pepstatin A.

Statistical Analysis

Results were analysed by one-way repeated measures ANOVA with Bonferroni's correction for pairwise analyses, or a ranked version thereof (Friedman Repeated Measures ANOVA), with Bonferroni's or Tukey's correction for pairwise analyses, as

appropriate. All analyses were performed using SigmaPlot 11.0 (Systat Software, Hounslow, UK).

Results

The Effect of *Alternaria* Extracts on Inflammatory Mediator Release by 16HBE Cells

Polarised 16HBE cells were challenged with *Alternaria* extract, and cytokine release after 24 h stimulation was measured by ELISA. *Alternaria* induced a dose-dependent increase in apical IL-8 release (Figure 1A), with 100 μg/ml *Alternaria* (Alt100) significantly inducing IL-8 release compared with untreated controls, or cells treated with heat-treated Alt100 (Alt100HT) or 100 μg/ml *Cladosporium* extract (Clad100). While Alt100 also induced a significant increase in basolateral IL-8 release compared to control (Figure 1B), this was less marked than apical release. Clad100 did not increase basolateral IL-8 release above baseline and heat treatment of the *Alternaria* extract (Alt100HT) tended to reduce the stimulation of basolateral IL-8 release, but this failed to reach statistical significance. Analysis of TNFα release after *Alternaria* challenge revealed similar results to IL-8 analysis (Figure S1).

The Effect of *Alternaria* on 16HBE Transepithelial Electrical Resistance

We next investigated the effect of *Alternaria* on TER. A significant dose-dependent decrease in TER was observed 1h post-challenge with both Alt50 and Alt100 (Figure 1C). With Alt50, the drop in TER began to recover almost immediately, particularly from 3 h onwards, reaching control levels by 6 h (Figure S2). After challenge with Alt100, the TER remained significantly lower than control, even 24 h post-challenge (Figure 1D). As found with cytokine release, Alt100HT showed no significant effect on TER at any time point. Similarly, Clad100 did not affect TER. The dose-dependent, heat-labile increase in epithelial permeability caused by *Alternaria* extracts was confirmed by studies with FITC-labelled 4 kDa dextran (Figure S3), suggesting that *Alternaria* affects both ionic and macromolecular permeability; however the extent to which passage of the 4 kDa macromolecule was facilitated by exposure of the epithelium to *Alternaria* was small compared to the effect of the calcium chelator EGTA (50 μM). None of the challenges significantly induced LDH release compared with control cultures (data not shown).

Protease Activity of *Alternaria* Extract

To determine specific protease activity in *Alternaria* extract, a fluorescent protease assay was performed in the presence of a variety of protease inhibitors (Figure 2). The serine protease inhibitor AEBSF significantly reduced the protease activity of *Alternaria* extract whereas the aspartate protease inhibitor Pepstatin A had a small effect, and the cysteine protease inhibitor E-64 had no effect. Heat-treatment of *Alternaria* extract reduced protease activity to below the detection limit of the assay. No inhibitor possessed intrinsic proteolytic activity.

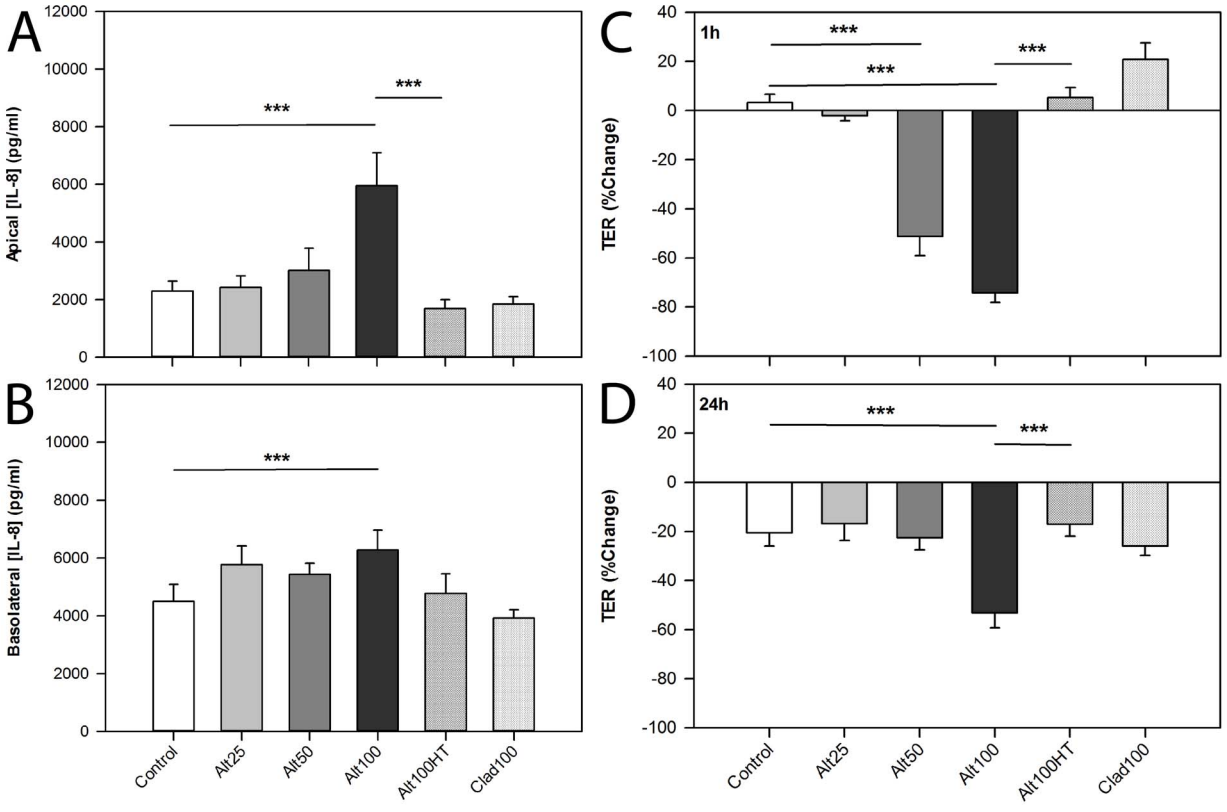

Figure 1. *Alternaria* extract induces a heat-labile increase in IL-8 release and rapid reduction in TER in polarised 16HBE cells. Polarised 16HBE cells on Transwell inserts were challenged apically with varying doses of *Alternaria* (Alt) or *Cladosporium* (Clad) fungal extracts, or heat treated fungal extract. (A) Apical and (B) basolateral supernatants were harvested 24 h post-challenge. IL-8 concentration was determined by ELISA (n = 4–9). TER was measured before challenge and at (C) 1h and (D) 24 h thereafter, and calculated as percentage change from pre-challenge readings (n = 4–15). Bars represent mean ± SEM. Analysis by one way repeated measures ANOVA with Bonferroni correction for pairwise analyses *** $p<0.001$.
doi:10.1371/journal.pone.0071278.g001

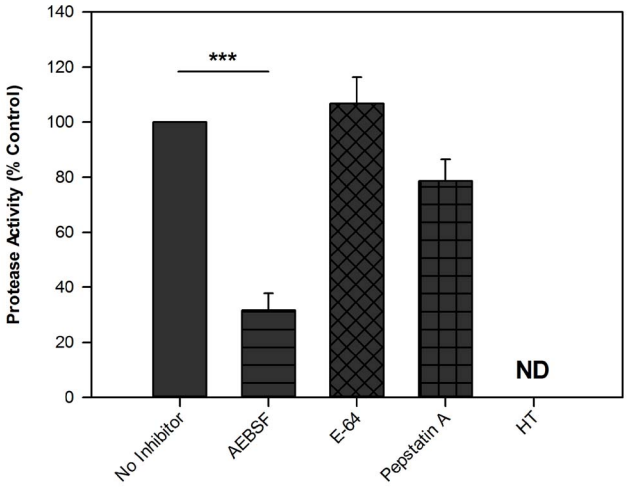

Figure 2. Protease activity of *Alternaria* extract is reduced by the serine protease inhibitor AEBSF. FITC-labelled casein was incubated with *Alternaria* extract (500 μg/ml) alone or in the presence of either AEBSF (2.5 mM), E-64 (500 μM), Pepstatin A (5 μg/ml), or heat-treated (n = 4 separate experiments measured in duplicate). Soluble fluorescence was measured after 24 h, relative to a trypsin standard. Bars represent mean fluorescence relative to inhibitor-free control ± SEM. Protease activity of 100 μg/ml Alternaria extract was equivalent to 6.7 ± 2.5 μg/ml trypsin; for comparison, Cladosporium protease activity was equivalent to 3.3 ± 0.0 μg/ml trypsin. Analysis as for Figure 1. Bars represent mean ± SEM; *** $p<0.001$.
doi:10.1371/journal.pone.0071278.g002

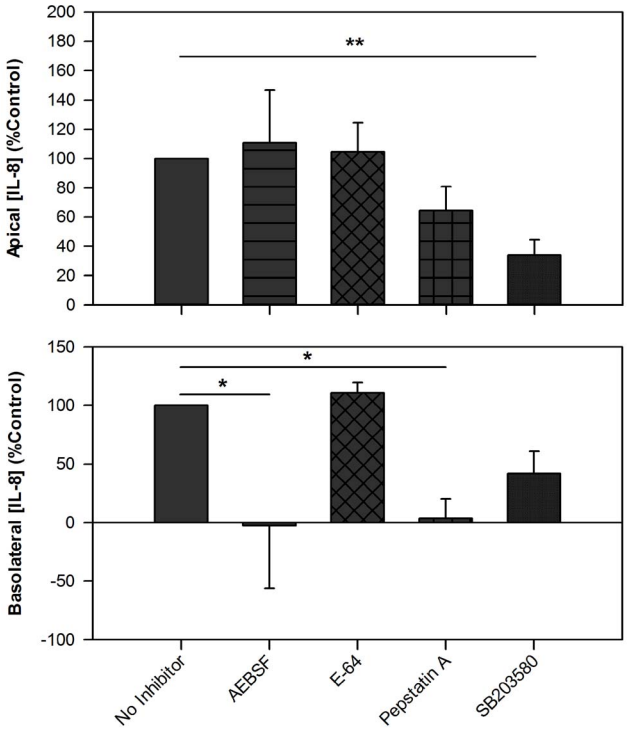

Figure 3. Inhibitors of proteases and p38 MAPK differentially inhibit apical and basolateral IL-8 release after *Alternaria* challenge. The effect of *Alternaria* extract (100 μg/ml) on 16HBE cells was tested alone or in the presence of AEBSF (250 μM), E-64 (50 μM), Pepstatin A (0.5 μg/ml) or SB203580 (25 μM) (n = 3–8). IL-8 release 24 h post-challenge was calculated as "Release (% control) = $((Alt_{INHIB} - No\ Alt_{INHIB})/(Alt_{NO\ INHIB} - No\ Alt_{NO\ INHIB})) \times 100$", to correct for any effect of the inhibitors on baseline IL-8 release without *Alternaria*. Data show mean ± SEM. Analysis as for Figure 1; * $p<0.05$, ** $p<0.01$.
doi:10.1371/journal.pone.0071278.g003

The Effect of Protease Inhibitors on Proinflammatory Cytokine Release

To examine whether protease activity contributed to the effect of *Alternaria* on the epithelial cells, Alt100 was pre-incubated with protease inhibitors prior to challenge of the epithelial cultures; control cultures were tested in the presence of inhibitor alone. Apical release of IL-8 in response to Alt100 was not significantly affected by any of the protease inhibitors; in contrast both AEBSF and Pepstatin A significantly reduced basolateral IL-8 release (Figure 3). As we failed to affect apical cytokine release with protease inhibitors, we also tested the effect of inhibiting p38 MAPK which we have previously found to inhibit pollen-induced apical IL-8 release, without affecting transcription [38]. Correspondingly, the present data shows SB203580 significantly reduced apical IL-8 release while not significantly affecting basolateral cytokine release. Neither apical nor basolateral release of TNFα were significantly affected by any of the inhibitors tested (Figure S4).

The Effect of Protease Inhibitors on the Permeabilising Activity of *Alternaria*

To further explore the effect of protease inhibition, TER changes were investigated using Alt100 pre-treated with the same inhibitors. At 1h post-challenge, either E-64 or SB203580 significantly inhibited the decrease in TER caused by *Alternaria* (Figure S5). At 24 h post-challenge, while inter-treatment differences approached significance, the significance threshold was not crossed. However, there was a notable attenuation of the effect of *Alternaria* on TER after incubation with either AEBSF or Pepstatin A.

The Effect of *Alternaria* on Polarised Cytokine Release from ALI Cultures

Having observed significant effects of *Alternaria* using the 16HBE bronchial epithelial cell line, experiments were performed using primary epithelial cells differentiated at an ALI. For these experiments, cells were derived from non-asthmatic and severe asthmatic donors allowing disease-related comparisons to be made. Preliminary studies showed that higher concentrations of *Alternaria* were required to elicit responses in ALI cultures compared to 16HBE, and therefore up to 400 μg/ml was used.

In ALI cultures from healthy donors, the highest dose of *Alternaria* (Alt400) significantly induced an approximate doubling of IL-8 release apically *versus* heat-treated *Alternaria* (Figure 4). *Alternaria* also tended to cause a dose-dependent increase in basolateral release of IL-8, significant for Alt400 with IL-8 levels eight-fold higher than control. *Cladosporium* extract had no significant effect on IL-8 release. Thus, basolateral IL-8 release tended to be more responsive to *Alternaria* than was apical IL-8 release (see Figure S6), the reverse of the situation seen in 16HBE cells, although the degree of inter-donor variability makes it difficult to draw robust conclusions regarding this directionality. When the same experiments were performed on ALI cultures from severely asthmatic donors, none of the challenges elicited a significant increase in release of IL-8 into either compartment (Figure 4). TNFα levels were generally below the lower detection limit (0.5 pg/ml) of the high-sensitivity ELISA kit.

Given the previous association of *Alternaria* with development of a Th2 phenotype [32,33,39], we also assessed release of IL-18, IL-33, and TSLP by ALI cultures after exposure to *Alternaria*. Using commercially available ELISA kits, these cytokines were undetectable (lower limit of detection = 10.2 pg/ml) in either apical or

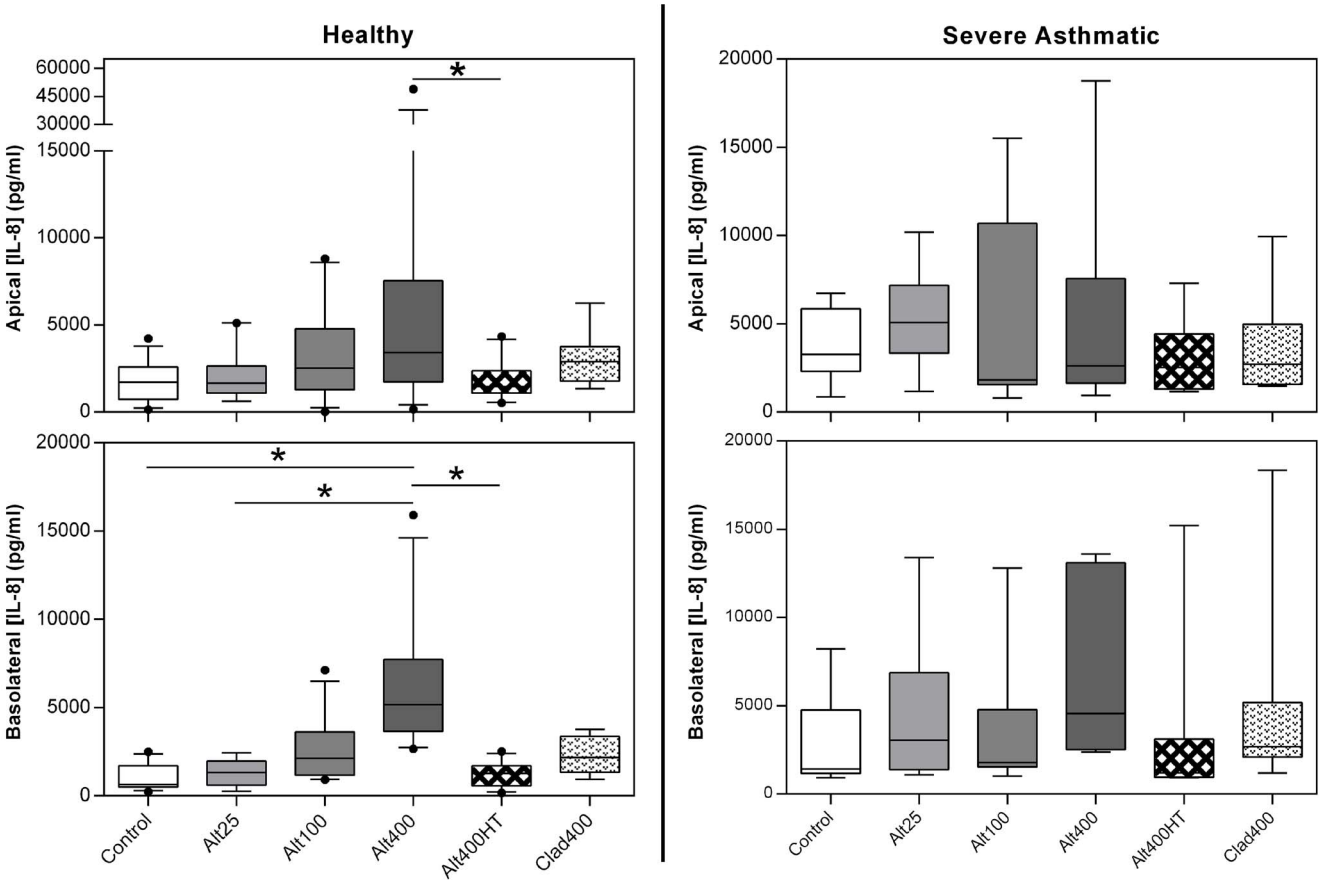

Figure 4. ALI cultures of healthy, but not severely asthmatic, donors increase IL-8 release in response to *Alternaria*. ALI cultures from healthy (n = 8–12) or severely asthmatic (n = 6–7) donors were differentiated at air-liquid interface, prior to challenge with *Alternaria* (Alt) or *Cladosporium* (Clad) fungal extracts. IL-8 release 24 h post-challenge was determined by ELISA. Box shows median and 25th/75th percentiles, and whiskers show 10th/90th percentiles. Analysis by Friedman's test with Tukey's correction for pairwise analyses; * $p<0.05$.
doi:10.1371/journal.pone.0071278.g004

basolateral supernatants across all groups. However, using an 'in-house' TSLP ELISA, basolateral TSLP release was detectable but there was no significant difference in TSLP secretion comparing untreated or *Alternaria*-stimulated ALI cultures from either healthy or severe asthmatic donors (Figure S7). No apical secretion of TSLP was detectable.

The Effect of *Alternaria* on ALI Culture Transepithelial Electrical Resistance

In ALI cultures from healthy donors, *Alternaria* had no effect on TER after 3 h (Figure 5). By 24 h, TERs in the healthy donor ALIs were all increased to 8–14% of their baseline levels, with no difference between challenges. In contrast, cultures derived from severely asthmatic donors responded to *Alternaria* challenge with a rapid dose-dependent decrease in TER at 3 h compared to control and heat-treated *Alternaria*. By 24 h post-challenge, no difference existed between treatments. These results suggest that, unlike ALI cultures from healthy donors, asthmatic donor ALI cultures are susceptible to a rapid loss of epithelial barrier function after exposure to *Alternaria*. The heat lability of this effect suggests that it is protease-mediated.

Discussion

This study investigated the potential of *Alternaria* proteases to perturb airway epithelial barrier function using cultures that are fully differentiated and covered by a layer of cytoprotective mucus as occurs *in vivo*, and to determine whether these responses are different in severe asthma. Our main findings were that ALI cultures from severely asthmatic donors exhibited a more variable IL-8 response to *Alternaria* extracts relative to those from healthy donors, while only cultures from severely asthmatic donors were susceptible to the barrier-weakening effects of *Alternaria*. Furthermore, while previous studies with cell lines have suggested that exposure to *Alternaria* extracts leads to production of cytokines that promote a Th2 response [33,39], we failed to detect any epithelial release of IL-33 or IL-18, while basolateral TSLP secretion did not change in response to *Alternaria*.

Induction of inflammation has previously been shown to occur upon challenge with serine proteases from *Aspergillus fumigatus* [15] and *Alternaria* [40,41]. However, these studies did not take into account epithelial polarisation, and were thus unable to study the directionality of cytokine release, which is important in the context of establishing a chemotactic gradient for IL-8 to act as a neutrophil chemoattractant [42–45]. The results of this study also emphasise the importance of cell differentiation since *Alternaria*-induced release of IL-8 and TNFα was predominantly apical for undifferentiated 16HBE cells, whereas for differentiated ALI cultures the greatest fold stimulation was observed for the basolateral compartment (median 2.9 fold apical *versus* 7.1 fold basolateral in healthy donor cultures). Also of note is the observation that TSLP is exclusively released into the basolateral

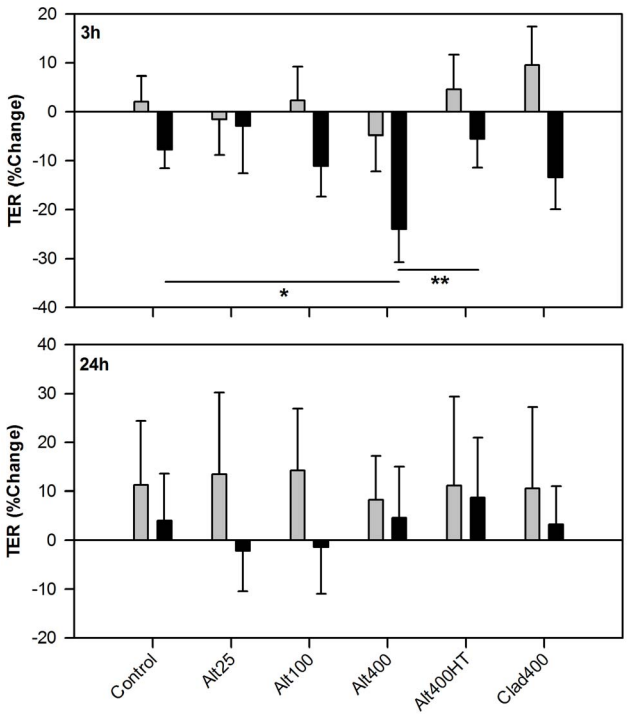

Figure 5. ALI cultures from severely asthmatic donors are sensitive to the barrier weakening effect of *Alternaria*. ALI cultures from healthy (grey bars; n = 7–9) and severely asthmatic (black bars; n = 6–7) donors were challenged with *Alternaria* (Alt) or *Cladosporium* (Clad) fungal extracts. TER was measured pre-challenge and 3 h and 24 h post-challenge. Results are expressed as percentage change in TER relative to pre-challenge and are shown as mean ± SEM. Analysis as for Figure 1; * $p<0.05$, ** $p<0.01$.
doi:10.1371/journal.pone.0071278.g005

compartment highlighting the importance of epithelial polarisation for vectorial cytokine secretion. This may be significant in terms of establishing appropriate concentration gradients for chemoattractants that direct cells to the luminal or subepithelial compartments.

Although *Alternaria*-stimulated IL-8 release into the basolateral compartment was relatively small, this stimulatory effect was greatly inhibited by AEBSF and Pepstatin A suggesting a protease-mediated effect. Conversely, protease inhibition failed to affect apical IL-8 release, which was instead sensitive to inhibition of p38 MAPK which is thought to play a role in stabilising IL-8 mRNA [46]. Although it has been well established that some growth factors are selectively sorted to the basolateral surface *via* information that usually resides in the cytoplasmic tail of the cargo [47], this does not explain how trafficking of a protein such as IL-8 is differentially regulated towards the apical or basolateral domains. Although this question has not been explored in detail, we have recently shown that trafficking of IL-8 in ALI cultures challenged with grass pollen extract is post-transcriptionally regulated with apical release being selectively regulated by p38 MAPK [38] as observed in the present study using *Alternaria*. While the PAR-2 agonist trypsin, as well as a PAR-2 activating peptide, have been shown to activate p38 MAPK expression weakly, it seems unlikely that PAR-2 activation lies upstream of p38 MAPK activation in mediating *Alternaria*-induced apical IL-8 release as this response was insensitive to protease inhibitors.

Although HDM serine and cysteine proteases have been reported to increase epithelial permeability [27,29], there is a paucity of comparative studies of fungal proteases, particularly using *Alternaria*. The present study suggests that heat labile activities in *Alternaria* extracts significantly and rapidly weaken the epithelial barrier, initially due to cysteine protease activity, and also *via* a p38 MAPK-mediated mechanism. However, both E-64 and SB203580 exhibited non-specific barrier-weakening effects at the 1h time point, and this may be a factor in the apparent reduction of activity of *Alternaria* in this respect. At 24 h a lesser degree of non-specific barrier-weakening activity was displayed by the inhibitors, and serine and aspartate protease inhibition appeared to show a trend for inhibition of the reduction in TER caused by *Alternaria*.

Fungal proteases fulfil a number of functions, particularly the external digestion of macronutrients, but are also intrinsic to the pathogenesis of diseases resulting from fungal exposure [48]. Taken together, these results suggest that the effects of *Alternaria* at the airway epithelium are due to serine and, to a lesser extent, aspartate protease activity, with the involvement of proteases in general being supported by the lack of activity of heat-treated *Alternaria* extract. Recent reports have suggested a role for serine and aspartate proteases in the cellular effects of *Alternaria* but, to our knowledge, this is the first work which suggests that both classes of protease exert significant effects. For example, it has been suggested that the active component(s) of *Alternaria* in the induction of proinflammatory responses in bronchial epithelial cells is serine protease(s) acting on PAR-2 [40], although this has not been confirmed *in vivo* [49]. In contrast, it has been suggested recently that the actions of *Alternaria* on epithelial cells and eosinophils are sensitive to aspartate protease inhibition, but not to serine protease or cysteine protease inhibition [50–52]. In our studies, serine proteases were the dominant activity in the protease assays, although inhibition of either serine or aspartate protease activity had a potent suppressive effect on IL-8 release. This discrepancy may be explained by the relative sensitivity of the fluorescent assay for serine and aspartate proteases or alternatively, it is possible that the effect of Pepstatin A on IL-8 release may be due, in part, to inhibition of endogenous proteases. For example, it has been reported that challenge of epithelial cells with *Aspergillus fumigatus* triggers release of lysosomal enzymes including the aspartate protease, cathepsin D [53], which may affect subsequent cytokine responses. In addition to proteases, other constituents of *Alternaria* extract such as β-glucans and chitin (cell wall components) have been noted to exert immunomodulatory effects [54–56]. However, the lack of residual effect after heat-treatment of *Alternaria* in the present study suggests that the effect of β-glucans was negligible in our studies, although we cannot exclude the effect of other unidentified components, either proteinaceous or small molecules, which may be affected by heat treatment.

The study was then extended to examine primary bronchial epithelial cells in ALI cultures, as a more accurate model of human airway exposure. ALI cultures from non-asthmatic donors exhibited increased IL-8 release in response to *Alternaria*, while responses of cultures from asthmatic donors exhibited a trend of being blunted and not statistically significant, although considerable inter-individual variability was observed.

ALI cultures from healthy donors were resistant to the increase in epithelial permeability seen when ALI cultures from severely asthmatic donors were challenged with *Alternaria*. To our knowledge, this is the first study which has examined differential responses to *Alternaria* between healthy and asthmatic ALI cultures. The implications are potentially significant: if the permeability of the bronchial epithelium in asthma is significantly increased by *Alternaria*, passage of inhaled allergens to the subepithelial tissue may be facilitated, and epithelial homeostasis disrupted. Since ALI

cultures from asthmatic donors also displayed a lack of response to *Alternaria* in terms of IL-8 secretion, the ability to upregulate recruitment of neutrophils and clearance of allergens and toxicants in response to *Alternaria* may be affected. This impaired response of the epithelial cells from asthmatic donors to *Alternaria* is unlikely to be due to carry-over of corticosteroids used for asthma control therapy, as we have shown that similar ALI cultures respond to pollen extract with a significant increase in IL-8 release irrespective of whether they were derived from healthy or severely asthmatic donors [38].

Using commercially available ELISA kits, we failed to detect any IL-18, IL-33 or TSLP release by the ALI cultures. IL-33 release has been shown to be increased by *Alternaria* in murine BAL fluid and in normal human bronchial epithelial cells (NHBE) [33], however in the latter case the epithelial cell cultures were undifferentiated. In contrast, others have failed to detect IL-33 or TSLP secretion from either NHBEs challenged with *Alternaria* [39] or mouse lung epithelial cells challenged with *Aspergillus fumigatus* [56]. We also failed to detect IL-18, despite a recent report of a marked rapid release of IL-18 after *Alternaria* challenge of NHBE cells [39]. However, control experiments performed in our laboratory and assayed at the same time showed IL-18 and TSLP production in response to rhinovirus challenge (data not shown), suggesting that the lack of any observable effect with *Alternaria* was not due to defective epithelial synthesis or release of these mediators. Although we initially failed to detect TSLP with a commercial ELISA (from R&D Systems), use of an alternative 'in-house' ELISA (developed by Novartis plc.) enabled detection and quantification of basolateral TSLP release, however no apical secretion was evident. We postulate that this difference in detection is due to differences in antibody recognition of recombinant and native TSLP, making the commercial ELISA kit much less sensitive for detection of the naturally produced protein. Having observed such a large difference in sensitivity for detection of TSLP, it is possible that the ELISAs employed for measurement of IL-33 and IL-18 may also be similarly compromised.

TSLP is secreted by epithelial cells and potently activates human dendritic cells to release a battery of cytokines which results in Th2-skewing of naïve CD4+ T cells [57]. *Alternaria* has been shown to increase TSLP expression and release from airway epithelial cells *in vitro via* PAR-2 activation [26]. However, even though we were confident in our ability to detect TSLP reliably, we found no significant change in TSLP release in response to *Alternaria*. One likely explanation is the use of fully differentiated ALI cultures in the present work, as opposed to undifferentiated monolayers in the previous studies, emphasising the importance of using models that closely mimic the *in vivo* state. While there is strong evidence to suggest that *Alternaria* exposure can induce Th2-type responses *in vivo*, and that TSLP released from structural cells can act as a potent mediator for Th2 skewing [58], it is possible that epithelial cells require the presence of other cell types or multiple stimuli for *Alternaria* to have such an effect. For example, IL-4 and double-stranded RNA potently synergise to stimulate TSLP release from bronchial epithelial cells *in vitro* [59].

In summary, this study demonstrates that *Alternaria* extract is able to significantly induce release of inflammatory cytokines and to increase the permeability of a polarised airway epithelial cell line. These effects were attributed to a heat-labile component of the *Alternaria*, identified as being serine and possibly aspartate protease mediated. Crucially, this study is the first to demonstrate that fully differentiated epithelial cultures from asthmatic donors appear to have a blunted IL-8 response to high levels of *Alternaria*, while at the same time being more susceptible to the barrier-weakening effect of *Alternaria*, than those from healthy donors.

Supporting Information

Figure S1 Alternaria extract induces a heat-labile increase in TNFα release from polarised 16HBE cells. Polarised 16HBE cells on Transwell inserts (n = 3–9) were challenged apically with *Alternaria* (Alt) or *Cladosporium* (Clad) fungal extracts. Apical and basolateral supernatants were harvested 24 h post-challenge. TNFα concentration was determined by ELISA. Analysis by one way repeated measures ANOVA with Bonferroni correction for pairwise analyses. Bars represent mean ± SEM; ** $p<0.01$; *** $p<0.001$.
(TIF)

Figure S2 *Alternaria* extract induces a dose-dependent decrease in 16HBE TER. TER was measured before fungal challenge of polarised 16HBE cells, and at regular intervals up to 24 h thereafter (n = 4–15). Graph shows TER of polarised 16HBE cultures in medium alone (▲), or with *Alternaria* extract at 50 (•) and 100 μl/ml (♦), expressed as percentage change from pre-challenge value. Points represent mean ± SEM.
(TIF)

Figure S3 *Alternaria* extract increases epithelial macromolecular permeability. Polarised 16HBE cells on Transwell inserts were challenged with medium, Alt50, Alt100 (all n = 4), Alt100HT, Clad100, or EGTA (n = 2) 1 h before addition of 2 mg/ml 4 kDA FITC-dextran. After 24 h challenge, basolateral FITC-dextran concentration was determined fluorimetrically. Analysis as for Figure S1 Bars represent mean ± SEM; ** $p<0.01$.
(TIF)

Figure S4 Inhibitors of proteases and p38 MAPK have no significant effect on apical or basolateral TNFα release after fungal challenge. The effect of *Alternaria* (100 μg/ml) on 16HBE cells was tested alone or in the presence of AEBSF (250 μM), E-64 (50 μM), Pepstatin A (0.5 μg/ml) or SB203580 (25 μM) (n = 3–8). TNFα release 24 h post-challenge was calculated as "Release (% control) = $((Alt_{INHIB} - \text{No } Alt_{INHIB})/(Alt_{NO\ INHIB} - \text{No } Alt_{NO\ INHIB})) \times 100$", to correct for any effect of the inhibitors on baseline TNFα release without *Alternaria*. Analysis as for Figure S1. Data show mean ± SEM.
(TIF)

Figure S5 *Alternaria*-induced drop in TER is sensitive to inhibition of cysteine protease and p38 MAPK. The effect of *Alternaria* (100 μg/ml) on 16HBE cells was tested alone or in the presence of AEBSF (250 μM), E-64 (50 μM), Pepstatin A (0.5 μg/ml) or SB203580 (25 μM) (n = 3–6). TER was measured at 1 h and 24 h post-challenge, calculated as percentage change from pre-challenge, and corrected for any effect of the inhibitor alone by subtracting the percentage change in TER in the absence of Alternaria from the percentage change in TER in the presence of Alternaria, with each respective inhibitor or inhibitor-free condition. Bars represent mean change ± SEM; ** $p<0.01$.
(TIF)

Figure S6 The increase in IL-8 release in healthy donor ALI cultures is driven by increased basolateral release of IL-8. ALI cultures from healthy (n = 8–12) or severely asthmatic (n = 6–7) donors were differentiated at air-liquid interface, prior to challenge with Alternaria (Alt) 400 μg/ml. IL-8 release 24 h post-challenge was determined by ELISA. Lines represent difference in individual donor cultures between control and Alt400-stimulated IL-8 release. Analysis by Wilcoxon Matched Pair test. *** $p<0.001$.
(TIF)

Figure S7 Alternaria challenge does not affect basolateral release of TSLP in healthy or severely asthmatic donor ALI cultures. ALI cultures from healthy (n = 7–12) or severely asthmatic (n = 6–7) donors were differentiated at air-liquid interface, prior to challenge with *Alternaria* (Alt) or *Cladosporium* (Clad) fungal extracts. TSLP release 24 h post-challenge was determined by ELISA. TOP: Boxes show median and $25/75^{th}$ percentiles, and whiskers show $10^{th}/90^{th}$ percentiles. Analysis by Friedman's test. BOTTOM: Lines represent difference in individual donor cultures between control and Alt400-stimulated TSLP release.
(TIF)

Information S1
(DOCX)

Table S1 PBEC donor information. Clinical characterisation of the donors of the bronchial epithelial cells used in this work. FEV_1% – forced expiratory volume in 1 second, as a percentage of predicted value; ICS – inhaled corticosteroid (dose as equivalent to micrograms per day Beclometasone dipropionate); LABA = long acting β_2-adrenoceptor agonist; anti-leuk = anti-leukotriene.
(DOCX)

Author Contributions

Conceived and designed the experiments: MSL ML CB EJS MJE STH DED. Performed the experiments: MSL ML CB BWHS. Analyzed the data: MSL ML DED. Contributed reagents/materials/analysis tools: NPJ PWD MJE DED. Wrote the paper: ML DED. Performed bronchoscopies to obtain primary cells: NPJ PWD PHH.

References

1. Cookson W (2004) The immunogenetics of asthma and eczema: a new focus on the epithelium. Nat Rev Immunol 4: 978–988.
2. Bals R, Hiemstra PS (2004) Innate immunity in the lung: how epithelial cells fight against respiratory pathogens. Eur Respir J 23: 327–333.
3. Knight DA, Holgate ST (2003) The airway epithelium: structural and functional properties in health and disease. Respirology 8: 432–446.
4. Xiao C, Puddicombe SM, Field S, Haywood J, Broughton-Head V, et al. (2011) Defective epithelial barrier function in asthma. J Allergy Clin Immunol 128: 549–556.
5. Denning DW, O'Driscoll BR, Hogaboam CM, Bowyer P, Niven RM (2006) The link between fungi and severe asthma: a summary of the evidence. Eur Respir J 27: 615–626.
6. Kauffman HF, van der Heide S (2003) Exposure, sensitization, and mechanisms of fungus-induced asthma. Curr Allergy Asthma Rep 3: 430–437.
7. O'Driscoll BR, Hopkinson LC, Denning DW (2005) Mold sensitization is common amongst patients with severe asthma requiring multiple hospital admissions. BMC Pulm Med 5: 4.
8. Delfino RJ, Zeiger RS, Seltzer JM, Street DH, Matteucci RM, et al. (1997) The effect of outdoor fungal spore concentrations on daily asthma severity. Environ Health Perspect 105: 622–635.
9. Black PN, Udy AA, Brodie SM (2000) Sensitivity to fungal allergens is a risk factor for life-threatening asthma. Allergy 55: 501–504.
10. Zureik M, Neukirch C, Leynaert B, Liard R, Bousquet J, et al. (2002) Sensitisation to airborne moulds and severity of asthma: cross sectional study from European Community respiratory health survey. BMJ 325: 411–414.
11. O'Hollaren MT, Yunginger JW, Offord KP, Somers MJ, O'Connell EJ, et al. (1991) Exposure to an aeroallergen as a possible precipitating factor in respiratory arrest in young patients with asthma. N Engl J Med 324: 359–363.
12. Neukirch C, Henry C, Leynaert B, Liard R, Bousquet J, et al. (1999) Is sensitization to Alternaria alternata a risk factor for severe asthma? A population-based study. J Allergy Clin Immunol 103: 709–711.
13. Monod M, Capoccia S, Lechenne B, Zaugg C, Holdom M, et al. (2002) Secreted proteases from pathogenic fungi. Int J Med Microbiol 292: 405–419.
14. Shen HD, Tam MF, Chou H, Han SH (1999) The importance of serine proteinases as aeroallergens associated with asthma. Int Arch Allergy Immunol 119: 259–264.
15. Tomee JF, Wierenga AT, Hiemstra PS, Kauffman HK (1997) Proteases from Aspergillus fumigatus induce release of proinflammatory cytokines and cell detachment in airway epithelial cell lines. J Infect Dis 176: 300–303.
16. Kauffman HF, Tomee JFC, van de Riet MA, Timmerman AJB, Borger P (2000) Protease-dependent activation of epithelial cells by fungal allergens leads to morphologic changes and cytokine production. Journal of Allergy and Clinical Immunology 105: 1185–1193.
17. Borger P, Koeter GH, Timmerman JA, Vellenga E, Tomee JF, et al. (1999) Proteases from Aspergillus fumigatus induce interleukin (IL)-6 and IL-8 production in airway epithelial cell lines by transcriptional mechanisms. J Infect Dis 180: 1267–1274.
18. Asokananthan N, Graham PT, Stewart DJ, Bakker AJ, Eidne KA, et al. (2002) House dust mite allergens induce proinflammatory cytokines from respiratory epithelial cells: the cysteine protease allergen, Der p 1, activates protease-activated receptor (PAR)-2 and inactivates PAR-1. J Immunol 169: 4572–4578.
19. Adam E, Hansen KK, Astudillo Fernandez O, Coulon L, Bex F, et al. (2006) The house dust mite allergen Der p 1, unlike Der p 3, stimulates the expression of interleukin-8 in human airway epithelial cells via a proteinase-activated receptor-2-independent mechanism. J Biol Chem 281: 6910–6923.
20. Knight DA, Lim S, Scaffidi AK, Roche N, Chung KF, et al. (2001) Protease-activated receptors in human airways: upregulation of PAR-2 in respiratory epithelium from patients with asthma. J Allergy Clin Immunol 108: 797–803.
21. Asokananthan N, Graham PT, Fink J, Knight DA, Bakker AJ, et al. (2002) Activation of protease-activated receptor (PAR)-1, PAR-2, and PAR-4 stimulates IL-6, IL-8, and prostaglandin E2 release from human respiratory epithelial cells. J Immunol 168: 3577–3585.
22. Sun G, Stacey MA, Schmidt M, Mori L, Mattoli S (2001) Interaction of mite allergens Der p3 and Der p9 with protease-activated receptor-2 expressed by lung epithelial cells. J Immunol 167: 1014–1021.
23. Bhat RK, Page K, Tan A, Hershenson MB (2003) German cockroach extract increases bronchial epithelial cell interleukin-8 expression. Clin Exp Allergy 33: 35–42.
24. Kheradmand F, Kiss A, Xu J, Lee SH, Kolattukudy PE, et al. (2002) A protease-activated pathway underlying Th cell type 2 activation and allergic lung disease. J Immunol 169: 5904–5911.
25. Ebeling C, Lam T, Gordon JR, Hollenberg MD, Vliagoftis H (2007) Proteinase-activated receptor-2 promotes allergic sensitization to an inhaled antigen through a TNF-mediated pathway. J Immunol 179: 2910–2917.
26. Kouzaki H, O'Grady SM, Lawrence CB, Kita H (2009) Proteases induce production of thymic stromal lymphopoietin by airway epithelial cells through protease-activated receptor-2. J Immunol 183: 1427–1434.
27. Wan H, Winton HL, Soeller C, Gruenert DC, Thompson PJ, et al. (2000) Quantitative structural and biochemical analyses of tight junction dynamics following exposure of epithelial cells to house dust mite allergen Der p 1. Clin Exp Allergy 30: 685–698.
28. Wan H, Winton HL, Soeller C, Tovey ER, Gruenert DC, et al. (1999) Der p 1 facilitates transepithelial allergen delivery by disruption of tight junctions. J Clin Invest 104: 123–133.
29. Wan H, Winton HL, Soeller C, Taylor GW, Gruenert DC, et al. (2001) The transmembrane protein occludin of epithelial tight junctions is a functional target for serine peptidases from faecal pellets of Dermatophagoides pteronyssinus. Clin Exp Allergy 31: 279–294.
30. Tai HY, Tam MF, Chou H, Peng HJ, Su SN, et al. (2006) Pen ch 13 allergen induces secretion of mediators and degradation of occludin protein of human lung epithelial cells. Allergy 61: 382–388.
31. Runswick S, Mitchell T, Davies P, Robinson C, Garrod DR (2007) Pollen proteolytic enzymes degrade tight junctions. Respirology 12: 834–842.
32. Kobayashi T, Iijima K, Radhakrishnan S, Mehta V, Vassallo R, et al. (2009) Asthma-related environmental fungus, Alternaria, activates dendritic cells and produces potent Th2 adjuvant activity. J Immunol 182: 2502–2510.
33. Kouzaki H, Iijima K, Kobayashi T, O'Grady SM, Kita H (2011) The Danger Signal, Extracellular ATP, Is a Sensor for an Airborne Allergen and Triggers IL-33 Release and Innate Th2-Type Responses. Journal of Immunology 186: 4375–4387.
34. Cozens AL, Yezzi MJ, Kunzelmann K, Ohrui T, Chin L, et al. (1994) CFTR expression and chloride secretion in polarized immortal human bronchial epithelial cells. Am J Respir Cell Mol Biol 10: 38–47.
35. Bucchieri F, Puddicombe SM, Lordan JL, Richter A, Buchanan D, et al. (2002) Asthmatic bronchial epithelium is more susceptible to oxidant-induced apoptosis. Am J Respir Cell Mol Biol 27: 179–185.
36. Esch RE (2004) Manufacturing and standardizing fungal allergen products. Journal of Allergy and Clinical Immunology 113: 210–215.
37. Pugin J, Schurermaly CC, Leturcq D, Moriarty A, Ulevitch RJ, et al. (1993) Lipopolysaccharide Activation of Human Endothelial and Epithelial-Cells Is Mediated by Lipopolysaccharide-Binding Protein and Soluble Cd14. Proceedings of the National Academy of Sciences of the United States of America 90: 2744–2748.
38. Blume C, Swindle EJ, Dennison PW, Jayasekera NP, Dudley S, et al. (2012) Barrier responses of human bronchial epithelial cells to grass pollen exposure. Eur Respir J E-pub ahead of print; doi: 10.1183/09031936.00075612.
39. Murai H, Qi HB, Choudhury B, Wild J, Dharajiya N, et al. (2012) Alternaria-Induced Release of IL-18 from Damaged Airway Epithelial Cells: An NF-kappa B Dependent Mechanism of Th2 Differentiation? Plos One 7.
40. Boitano S, Flynn AN, Sherwood CL, Schulz SM, Hoffman J, et al. (2011) Alternaria alternata serine proteases induce lung inflammation and airway epithelial cell activation via PAR(2). American Journal of Physiology-Lung Cellular and Molecular Physiology 300: L605–L614.

41. Shin SH, Lee YH, Jeon CH (2006) Protease-dependent activation of nasal polyp epithelial cells by airborne fungi leads to migration of eosinophils and neutrophils. Acta Oto-Laryngologica 126: 1286–1294.
42. Yoshimura T, Matsushima K, Tanaka S, Robinson EA, Appella E, et al. (1987) Purification of a human monocyte-derived neutrophil chemotactic factor that has peptide sequence similarity to other host defense cytokines. Proc Natl Acad Sci U S A 84: 9233–9237.
43. Baggiolini M, Walz A, Kunkel SL (1989) Neutrophil-activating peptide-1/interleukin 8, a novel cytokine that activates neutrophils. J Clin Invest 84: 1045–1049.
44. Huber AR, Kunkel SL, Todd RF 3rd, Weiss SJ (1991) Regulation of transendothelial neutrophil migration by endogenous interleukin-8. Science 254: 99–102.
45. Hammond ME, Lapointe GR, Feucht PH, Hilt S, Gallegos CA, et al. (1995) IL-8 induces neutrophil chemotaxis predominantly via type I IL-8 receptors. J Immunol 155: 1428–1433.
46. Hoffmann E, Dittrich-Breiholz O, Holtmann H, Kracht M (2002) Multiple control of interleukin-8 gene expression. J Leukoc Biol 72: 847–855.
47. Li CX, Hao MM, Cao Z, Ding W, Graves-Deal R, et al. (2007) Naked2 acts as a cargo recognition and targeting protein to ensure proper delivery and fusion of TGF-alpha-containing exocytic vesicles at the lower lateral membrane of polarized MDCK cells. Molecular Biology of the Cell 18: 3081–3093.
48. Yike I (2011) Fungal Proteases and Their Pathophysiological Effects. Mycopathologia 171: 299–323.
49. Doherty TA, Khorram N, Sugimoto K, Sheppard D, Rosenthal P, et al. (2012) Alternaria Induces STAT6-Dependent Acute Airway Eosinophilia and Epithelial FIZZ1 Expression That Promotes Airway Fibrosis and Epithelial Thickness. Journal of Immunology 188: 2622–2629.
50. Matsuwaki Y, White T, Hotta K, Inoue Y, Lawrence CB, et al. (2007) Aspartate protease from Alternaria induced cytokine production, and calcium signaling in human airway epithelial cells through a protease-activated receptor-2 (PAR-2). Journal of Allergy and Clinical Immunology 119: S137.
51. Inoue Y, Matsuwaki Y, Shin SH, Ponikau JU, Kita H (2005) Nonpathogenic, environmental fungi induce activation and degranulation of human eosinophils. J Immunol 175: 5439–5447.
52. Matsuwaki Y, Wada K, White TA, Benson LM, Charlesworth MC, et al. (2009) Recognition of fungal protease activities induces cellular activation and eosinophil-derived neurotoxin release in human eosinophils. J Immunol 183: 6708–6716.
53. Fekkar A, Balloy V, Pionneau C, Marinach-Patrice C, Chignard M, et al. (2012) Secretome of Human Bronchial Epithelial Cells in Response to the Fungal Pathogen Aspergillus fumigatus Analyzed by Differential In-Gel Electrophoresis. Journal of Infectious Diseases 205: 1163–1172.
54. Reese TA, Liang HE, Tager AM, Luster AD, Van Rooijen N, et al. (2007) Chitin induces accumulation in tissue of innate immune cells associated with allergy. Nature 447: 92–96.
55. Carmona EM, Lamont JD, Xue A, Wylam M, Limper AH (2010) Pneumocystis cell wall beta-glucan stimulates calcium-dependent signaling of IL-8 secretion by human airway epithelial cells. Respiratory Research 11.
56. Neveu WA, Bernardo E, Allard JL, Nagaleekar V, Wargo MJ, et al. (2011) Fungal Allergen beta-Glucans Trigger p38 Mitogen-Activated Protein Kinase-Mediated IL-6 Translation in Lung Epithelial Cells. Am J Respir Cell Mol Biol 45: 1133–1141.
57. Soumelis V, Reche PA, Kanzler H, Yuan W, Edward G, et al. (2002) Human epithelial cells trigger dendritic cell-mediated allergic inflammation by producing TSLP. Nature Immunology 3: 673–680.
58. Hammad H, Lambrecht BN (2008) Dendritic cells and epithelial cells: linking innate and adaptive immunity in asthma. Nature Reviews Immunology 8: 193–204.
59. Nagarkar DR, Poposki JA, Comeau MR, Biyasheva A, Avila PC, et al. (2012) Airway epithelial cells activate T(H)2 cytokine production in mast cells through IL-1 and thymic stromal lymphopoietin. Journal of Allergy and Clinical Immunology 130: 225–232.